Universität Ulm
Institut für Anatomie und Zellbiologie
Direktor: Prof. Dr. med. T. M. Böckers

Spar3, a novel protein of the postsynaptic density

Dissertation

zur Erlangung des Doktorgrades der Humanbiologie
der Medizinischen Fakultät der Universität Ulm

vorgelegt von:

Anna Dolnik

aus Sankt Petersburg

2008

Amtierender Dekan: Prof. Dr. Klaus–Michael Debatin

1. Berichterstatter: Prof. Dr. Tobias M. Böckers

2. Berichterstatter: Prof. Dr. Holger Lerche

Tag der Promotion: 28. November 2008

Contents

1 Introduction **1**

1.1 Synapses − the connections between neuronal cells 1
1.2 The dendritic spine 2
1.3 Spine organization 4
1.4 Actin cytoskeleton 6
1.5 Postsynaptic density 6
1.5.1 The receptor apparatus 7
1.5.2 Protein composition of the PSD 8
1.6 Fezzin family 11
1.7 Rap GTPases 12
1.8 Proteins downregulating Rap activation 14
1.8.1 SPA–family 15
1.9 Aim of the work 19

2 Materials **21**

2.1 Chemicals 21
2.2 Buffers and solutions 23
2.3 Kits 24
2.4 Antibiotics, stock solutions 25
2.5 Culture media for bacteria 25
2.6 Culture media for yeast 26
2.7 Culture media and buffers for cell lines and primary hippocampal culture 27
2.8 Transfection reagents 27
2.9 Biological material 27
2.9.1 Bacterial strains 27
2.9.2 Yeast strains 28

2.9.3 Cell lines 28
2.9.4 Primary antibodies (AB) 29
2.9.5 Secondary antibodies (AB) 30
2.9.6 Enzymes 30
2.10 Markers 31
2.11 Primers 31
2.12 Plasmids 32
2.13 Additional materials 32
2.14 Equipment 32

3 Methods **35**
3.1 Microbiological methods 35
3.1.1 Cultivation of bacterial strains 35
3.1.2 Production and transformation of competent bacteria 35
3.1.3 Cultivation of yeast 36
3.1.4 Production and transformation of competent yeast 37
3.2 Isolation and purification of DNA 37
3.2.1 Rapid extraction of plasmid DNA from *E.coli* 37
3.2.2 Mini–, Midi– and Maxi–extraction of plasmid DNA from E.coli with anion exchange columns 38
3.2.3 Rapid extraction of plasmid DNA from *S. cerevisiae* 38
3.2.4 Isolation and purification of DNA from agarose gels 39
3.2.5 DNA extraction from mouse tail biopsies 39
3.2.6 Estimation of DNA concentration 40
3.3 Work with recombinant DNA 40
3.3.1 Restriction of DNA 40
3.3.2 Ligation 41
3.3.3 Polymerase chain reaction (PCR) 42
3.3.4 DNA agarose gel electrophoresis 42
3.3.5 Sequencing of DNA 43
3.4 RNA methods 43
3.4.1 Isolation of RNA 43
3.4.2 Reverse transcription 44
3.5 Cultivation of eucaryotic cell lines 44
3.5.1 Cultivation of cells 45
3.5.2 Freezing of cells 45

3.5.3 Thawing of cells . . . 46
3.5.4 Primary culture of hippocampal neurons . . . 46
3.6 Transfection of cells . . . 47
3.6.1 Transfection of cell lines . . . 47
3.6.2 Transfection of primary hippocampal neurons . . . 47
3.7 Preparation of protein extracts from cells and tissues . . . 48
3.7.1 Preparation of protein lysates from cultured cells . . . 48
3.7.2 Preparation of protein extracts from tissue . . . 48
3.7.3 Isolation of subcellular protein fractions . . . 49
3.7.4 Protein expression in bacteria . . . 50
3.7.5 Induction of protein expression in bacteria . . . 51
3.7.6 Purification of GST–tagged protein . . . 51
3.8 Biochemical assays revealing protein–protein interactions . . . 52
3.8.1 GST–pulldown–assay . . . 52
3.8.2 Coimmunoprecipitation . . . 52
3.8.3 Overlay technique . . . 53
3.9 Analysis of proteins . . . 54
3.9.1 Bicinchoninic acid (BCA) protein assay . . . 54
3.9.2 SDS–polyacrylamide gel electrophoresis (SDS–PAGE) . . . 54
3.9.3 Staining of proteins in acrylamide gels . . . 56
3.9.4 Western Blot . . . 56
3.9.5 Preincubation of AB with antigen . . . 57
3.9.6 Dialysis . . . 57
3.10 Immunostaining of cultured cells and sections . . . 58
3.10.1 Immunostaining of primary hippocampal neurons . . . 58
3.10.2 Immunohistochemistry . . . 60
3.10.3 $\beta-$galactosidase reaction on brain cryosections . . . 61
3.11 Electron microscopy . . . 61
3.12 *In situ* hybridization . . . 62
3.12.1 Radioactive labeling of oligonucleotides . . . 62
3.12.2 *In situ* hybridization on tissue sections . . . 63
3.13 Yeast–two–hybrid system . . . 63
3.13.1 Principle of a yeast–two–hybrid screen . . . 63
3.13.2 Screen of a brain cDNA-library . . . 64
3.13.3 Estimation of transformation efficiency by mating . . . 65
3.13.4 Colony–lift filter assay . . . 65

3.13.5 Analysis of positive clones 65
3.14 Statistical evaluations 66

4 Results **67**
4.1 Identification of Spar3 67
4.2 Gen and protein structure of Spar3 67
4.3 Spar3: a member of the SPA–family of proteins 70
4.4 Characterization of Spar3 antibodies (AB) 70
4.5 Expression of Spar3 in tissues 72
4.6 Developmental profile of Spar3 gene expression in rat brain 73
4.7 Immunohistochemical staining reveals Spar3 expression in cortex, hippocampus and cerebellum 74
4.8 Spar3 protein expression in various brain regions 74
4.9 Spar3 is enriched in the postsynaptic density 76
4.10 Electron microscopy studies confirm the localization of Spar3 in dendritic spines and PSDs 77
4.11 Spar3 associates with F-actin in Cos–7 cells 77
4.12 The level of Spar3 protein decreases during postnatal development . . . 82
4.13 Spar3 is expressed in cultured rat hippocampal neurons 83
4.14 Spar3 localizes at the dendritic spines in cultured neurons 84
4.15 When overexpressed in hippocampal neurons, Spar3–GFP is targeted to dendrites 84
4.16 Overexpressed Spar3–GFP colocalizes with postsynaptic markers 85
4.17 Effect of Spar3 on the spine morphology *in vitro* 88
4.18 Influence of Spar3 truncated variants on spine morphology *in vitro* . . . 90
4.19 Targeting of Spar3 to spines in hippocampal neurons 91
4.20 Identification of putative interaction partners for Spar3 94
4.21 Spar3 interacts with ProSAPiP1 96
4.22 Spar3 interacts with LAPSER1, another member of Fezzin family . . . 99
4.23 Coexpression of LAPSER1 and ProSAPiP1 in hippocampal neurons . . 102
4.24 Spar3 is in a complex with $\beta-$catenin 102
4.25 Spar3 interacts with another component of Wnt-pathway − GSK3α . . 105
4.26 Spar3 is a constituent of the cell adhesion complex 106
4.27 The Spar3 knock–out mouse 106

4.27.1 Mapping of the position of the gene trap vector in the mouse genome . . . 108
4.27.2 Genotyping of Spar3 knock–out mice . . . 110
4.27.3 Analysis of mRNA expression in Spar3 knock–out mouse . . . 110
4.28 An unexpected splice event . . . 114
4.28.1 Control of the Spar3 gene expression by *in situ* hybridization in Spar3 knock–out mice . . . 116
4.28.2 Visualization of the β–galactosidase expression in brains of Spar3–knock–out mice . . . 118
4.28.3 Detection of the Spar3 truncated protein . . . 118
4.29 Spar3 knock–out mice display cataract . . . 119

5 Discussion 121
5.1 Characterization of Spar3 adds a new member to the SPA–family . . . 122
5.2 Spar3 mRNA is widely expressed in brain . . . 122
5.3 Thw peak of the Spar3 expression coincides with the active spino– and synaptogenesis . . . 123
5.4 Regulation of the Spar3 protein level . . . 124
5.5 Spar3 is a component of the PSD . . . 125
5.6 Domains of Spar3 that are required for spine targeting . . . 126
5.7 Spar and Spar3 are recruited to the spines in a different way . . . 127
5.8 Association with the actin cytoskeleton . . . 128
5.9 Association of the C'terminus of Spar3 with intermediate filaments . . . 129
5.10 Overexpression of Spar3 in neurons . . . 129
5.11 ProSAPiP1, a PSD scaffold protein, interacts with Spar3 . . . 131
5.12 Spar3 interacts with LAPSER1 . . . 132
5.13 PSD–Zip70 is a possible interaction partner of Spar3 . . . 133
5.14 Spar3 and the Wnt pathway . . . 134
5.15 Spar3 knock–out mouse . . . 136
5.16 Model of the PSD with a newly characterized Spar3 . . . 137

6 Summary 139

A Alignment of the SPA–family 141

Abbreviations

Aminoacids

Aminoacid	Triple code abbrevation	Abbrevation
Alanine	Ala	A
Asparagine	Asn	N
Aspartic acid	Asp	D
Arginine	Arg	R
Cysteine	Cys	C
Glutamine	Gln	Q
Glutamic acid	Glu	E
Glycine	Gly	G
Histidine	His	H
Isoleucine	Ile	I
Leucine	Leu	L
Lysine	Lys	K
Methionine	Met	M
Phenylalanine	Phe	F
Proline	Pro	P
Serine	Ser	S
Threonine	Thr	T
Tryptophan	Trp	W
Tyrosine	Tyr	Y
Valine	Val	V

Abbreviations

A

3–AT	3–amino–1,2,4–triazole
A	adenine
A	ampere
aa	amino acid
AB	antibodies
Abp1	amiloride binding protein 1
abs.	absolut
Act1(2)	actin–binding domain 1(2)
AD	activating domain
AF–6	afadin
AHS	adenine hemisulfat
amp	ampicillin
AMPA	α–amino–3–hydroxy–5–methyl–4–isoxazolepropionic acid
AP	adaptor protein
APQ2	aquaporin 2
approx.	approximately
APS	ammoniumpersulfat
Arp 2/3	actin related protein 2/3
as	anti–sense
ATP	adenosine triphosphate

B

bp	pair base
BD	binding domain
β-Pix	PAK–interacting exchange factor beta
Brd4	bromodomain protein
BSA	bovine serum albumin

C

°C	grad Celsius
ca.	circa
CaMKII	calcium/calmodulin dependent protein kinase
CASK	calcium/calmodulin–dependent serine protein kinase
CC	coiled coil domain
cdc42	cell division cycle 42
cDNA	complementary desoxyribonucleic acid
cfu	colony forming units (number of colonies)
Ce	cerebellum
CKI	casein kinase I
Co	cortex
CoIP	co–immunoprecipitation
CREB	cAMF responsive element binding protein

D

d	day
DAB	3,3'–diaminobenzidine hydrochloride
DAPI	4,6'–diamidino–2–phenylindole
deion.	deionized
DIV	day *in vitro*
DG	gyrus dentatus
DMEM	modified eagle medium according Dulbecco
DMF	N,N–dimethylformamide
DMSO	dimethyl sulfoxid
DNA	deoxyribonucleic acid
DOC	desoxycholat
DTT	dithiothreitol

E

E18	embryonic day 18
E6TP1	HPV E6–targeted protein 1
E.coli	*Escherichia coli*
EDTA	ethylenediaminetetraacetic acid
EGFP	enhanced green fluorescent protein
EMT	epithelial–mesenchymal transition
EphA4	ephrin A4 receptor
ER	endoplasmatic reticulum
ERK 1/2	extracellular signal–regulated kinase 1/2
et al.	et altera

F

F–actin	actin filaments
FEZ	fasciculation and elongation protein zeta
FBS	fetal bovine serum
FCS	fetal calf serum

G

G	guanine
g	gravitational acceleration
g	gramme
GABA	$\gamma-$amino butyric acid
GAP	GTPase activating protein
GDP	guanosindiphosphat
GEF	guanine nucleotide exchange factor
GFP	green fluorescent protein
GK	guanilate kinase
GKBD	guanylate kinase binding domain
GluR	glutamate receptor
GSK3α	glycogen synthase kinase alpha
GST	glutathion–S–transferase
GTP	guanosine triphosphate
GTPases	low molecular weight guanine nucleotide–binding proteins

H

h	hour
Hc	hippocampus
He	heart
HPV	human papillomavirus
HRP	horse raddish peroxidase
HT	hypothalamus

I

Ig	immunoglobulin
IP3R	inositol–1,2,5,–triphosphate receptor
IPTG	isopropyl β–D–thiogalactopyranoside

K

kan	kanamycin
kb	kilo base
KCNQ3	potassium voltage-gated channel KQT-like protein 3
kDa	kilo Dalton
Ki	kidney
conc.	concentrated

L

l	liter
LAPSER1	Leucine (L) Alanine (A) Proline (P) Serine (S) Glutamic acid (E) Arginine (R)
LFA-1	leukocyte function associated antigene–1
Li	liver
LTD	long term depression
LTP	long term potentiation
LRP	low density lipoprotein related protein 1
LZ	leucin zipper motif
LZTS	leucine zipper tumor supressor protein

M

M	mole
M	month
m	milli
μ	micro
mAB	monoclonal antibodies
MAGUK	membrane associated guanylate kinase
MAP2	microtubuli associated protein 2
MAPK	mitogen activated protein kinase–1

mGluR	metabotropic glutamate receptor
min	minute
mRNA	messenger ribonucleic acid

N

n	nano
N4BP3	Nedd4 binding protein 3
Nedd4	neural precursor cell expressed developmentally downredulated 4
Neo	neomycin
NES	nuclear export sequence
NMDA	N–methyl–D–aspartate
NP40	nonyl phenoxylpolyethoxylethanol

O

OD	optical density, absorbancy
oligo	oligonucleotide
ON	overnight
ORF	open reading frame

P

P	pellet
p	pico
p.a.	pro analyse
pAb	polyclonal antibodies
PAGE	polyacrylamide gel electrophoresis
PBS	phosphate buffered saline
PCR	polymerase chain reaction
PDZ	PSD–95/Discs Large/Zona occludens domain
PFA	paraformaldehyde
pI	isoelectric point
PI	protease inhibitor
PLL	poly–L–lysine
ProSAP	proline rich synapse associated protein
ProSAPiP1	ProSAP interacting protein 1
PSD	postsynaptic density
PSD–95	postsynaptic density protein–95

R

Rap	Ras related protein
RapGAP	Rap GTPase activating protein
R. norvegicus	*Rattus norvegicus*
Ras	roux avian sarcoma
Rho	Ras homologous member
RIPA	radio immunoprecipitation buffer
RNA	ribonucleic acid

RNase	ribonuclease
rpm	rotation pro minute
RT	room temperature
RT–PCR	reverse transcriptase polimerase chain reaction

S

S	supernatant
s	second
s.	see
S.cerevisiae	*Saccharomyces cerevisiae*
SAM	sterile alpha motif
SAP–90	synapse associated protein 90
SAPAP	synapse associated protein 90–associated protein
SD	synthetic dropout
sds	sodium dodecylsulfat
SER	smooth endoplasmic reticulum
SH3	src homology 3 domain
SIGTR	Sanger Institute Gene Trap Resource
SIPA1L1	signal induced proliferation associated protein 1 like 1
Shank	SH3 and multiple ankyrin repeats containing protein
SNK	serum–inducible kinase
Sp	spleen
SPA–1/SIPA-1	signal induced prolifiration associated protein–1
SPAR	spine associated GTPase–activating protein for Rap
SynGAP	synaptic Ras GTPase activating protein

T

T	thymine
TAE	Tris–acetat–EDTA buffer
TE	Tris–EDTA buffer
Te	testis
TEMED	N,N,N',N'–tetramethylethylendiamin
Tcf	T–cell factor
Th	thalamus
TGF	transforming growth factor
Tris	Tris–hydroxymethyl–aminomethane

U

UV	ultraviolet

V

V	volt
vol.	volume
v/v	volumeric content

W

W	week
Wnt	wingless
w/v	mass ratio (weight proportion)

X

X–Gal	5–bromo–4–chloro–3–indolyl–β–D–galactopyranoside

Y

Y	year

Z

ZO1	zonula occludens–1

Chapter 1

Introduction

The nervous system consists of neurons, these are specialized cells that receive, conduct and transmit signals. To accomplish these functions, neurons form extended branches and build contacts, which possess a specialized signal processing machinery. A typical neuron elaborates a complex dendritic arbor and an axon. The axon conducts the nerve impulses to the target cells. The dendrites receive and integrate incoming signals from axons of other neurons (Alberts et al., 1991). The human brain contains approx. 10^{11} neurons and they form about 10^{15} connections. The connections between neurons should be stable enough to create a network with functional circuits. On the other hand, the contacts should be flexible to support the formation of the new circuits and remodeling of the old ones by learning and memory formation (Gundelfinger and tom Dieck, 2000).

1.1 Synapses – the connections between neuronal cells

The specialized sites of contact between neuronal cells are called synapses. Synapses are polarized structures, which consist of two compartments divided by a cleft: the pre- and postsynapse. The accepted classification describes two types of synapses in nervous system: electrical and chemical. Electrical synapses are found in minority in the brain. Formed symmetrically by the membranes of communicating neurons as a gap junction, the electrical synapses enable bidirectional transmission. This close contact allows the ionic current to flow passively through pores in gap junction from one neuron to another. This mechanism mediates an immediate transmission. Electrical synapses lack a postsynaptic thickening and are morphologically and functionally symmetric

(Alberts et al., 1991).

Chemical synapses constitute the majority of connections in the central nervous system. In the chemical synapses, the presynaptic terminal is filled with vesicles that contain specific neurotransmitters. The electrical signal conducted by the axon triggers the fusion of docked vesicles with the presynaptic membrane. This results in a neurotransmitter release into the synaptic cleft and its binding to receptors on the postsynaptic side. Depending on the type of receptor, the neurotransmitter activates the opening of channels and an ion influx or triggers intracellular signaling cascades in the postsynaptic neuron. Thus, the chemical synapses have a polarized and asymmetric structure: the presynaptic part specializes in exocytosis of neurotransmitter and the postsynaptic part − in receiving and processing of the chemical signals.

The chemical synapses are subdivided into excitatory and inhibitory types depending on neurotransmitter type. The common inhibitory neurotransmitters, *e.g.*, γ-amino butyric acid (GABA) and glycine, primarely open Cl^- or K^+ channels to prevent depolarization of postsynaptic membrane and to suppress firing. The prevalent excitatory neurotransmitter, glutamate, opens Na^+ and Ca^{2+} channels or activates signaling cascades. This leads to depolarization and firing of neurons (Moss and Smart, 2001; Schoch and Gundelfinger, 2006).

The neurotransmitter release is limited to a special site of the presynaptic terminal − the active zone. The active zone is a subcellular compartment enriched with cytoskeletal and scaffold proteins and with proteins regulating docking and fusion of vesicles (Schoch and Gundelfinger, 2006; Zhai and Bellen, 2004). The classical cytoskeletal proteins *e.g.*, actin, myosin, spectrin, β−catenin are the fundamental components of the cytomatrix in the active zone. The specific and organizing components of the active zone are scaffold molecules, *e.g.*, calcium/calmodulin-dependent serine protein kinase (CASK), Rab3-interacting molecule (RIM), piccolo and bassoon. The strictly restricted location of bassoon in the active zone of the presynaptic terminal makes this molecule a good marker for presynapses. The size and width of the active zone is precisely opposed and adjusted to the postsynaptic site (Schoch and Gundelfinger, 2006).

1.2 The dendritic spine

The postsynaptic part of most excitatory synapses is located on morphological specializations of dendrites − spines. More than 100 years ago, Ramon y Cajal observed and described that the surface of dendrites of Purkinje cells is covered by spines. He

suggested that spines were points, where electrical charge or current is received. This was later confirmed by many investigators (Ethell and Pasquale, 2005). Usually spines are sites for excitatory synaptic input. Most chemical excitatory synapses in the mature mammalian brain are located on spines, tiny protrusions on dendrites of neurons. A typical mature dendritic spine accommodates a single synapse (Hering and Sheng, 2001).

Interestingly, this morphological aspect of investigation, despite of development of molecular methods in biology, remained current in this area: spines are classified by shape. The shape of the spines relates directly to the synaptic transmission. The common classification subdivides spines into filopodia–like, thin, stubby and mushroom–like types (Fig. 1.1) (Sorra and Harris, 2000; Hering and Sheng, 2001; Ethell and Pasquale, 2005). A filopodia–like spine has a total length greater than its neck diameter. A thin spine is similar to filopodia–like spine except for its tiny head ($< 0.6\,\mu$m in diameter). The stubby spine is typically a short protrusion with a formed head, but with a wide and short neck. The mushroom–like or "mature" spine has a large round or irregular head $\approx 2\,\mu$m in diameter connected to the dendrite with a thin neck (Fig. 1.1). Some authors distinguish branched or cup-shaped spines, but some argue that this form of spines might reflect the spine division (Sorra and Harris, 2000).

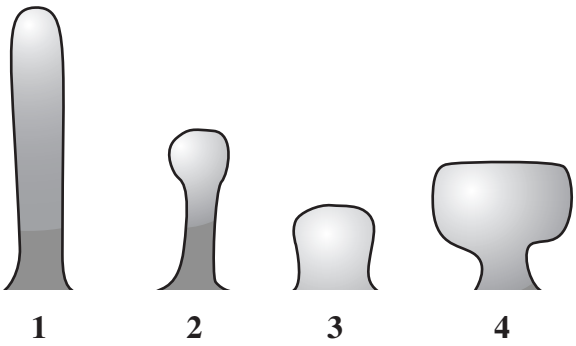

Figure 1.1: Morphological classification of spines. Representation of filopodium (1), thin (2), stubby (3) and mushroom-like (4) spine shapes. Adapted from Ethell and Pasquale (2005).

The classification of spine shapes is a result of static observation of neurons, obtained by studies of fixed electron-microscopic or fluorescent samples. Most spines change shape and show rapid motility in time–scale of seconds to minutes in cell culture, slices and in developing brain (Ethell and Pasquale, 2005).

The spines are formed during development. In *R. norvegicus* spinogenesis occurs in parallel with synaptogenesis in the middle of the first postnatal week (data for neocortical pyramidal neurons) (Yuste and Bonhoeffer, 2004). Spine density increases

continually during the first four weeks after birth with prevalence of spine population of thin, elongated and highly motile filopodia and, later, stubby spines. Simultaneously, with maturation, the spine density decreases and stabilizes at a definite level: 1–10 spines per 1 μm of dendritic length in mature neurons, depending on neuron type and brain region (Sorra and Harris, 2000). The spine density reduction coincides with a refinement of neuronal circuits. Concomitantly, the filopodia–like and stubby protrusions are replaced by thin or mushroom spines, which have more prominent necks and heads. By a number of neurodevelopmental disorders (*e.g.*, X–linked mental retardation, William's syndrome, Down's syndrome) the dendritic spines are irregularly shaped or have abnormal densities. This illustrates the importance of spine as a compartment of the neuron (Ethell and Pasquale, 2005).

Separated from the dendrite by a thin neck, spines create a synapse–specific compartment, that segregates postsynaptic chemical response. All biochemical changes in one individual spine are isolated from other spines on the same neuron. Spines have their own regulated membrane–trafficking events. The small volume of spine head allows large changes in Ca^{2+} concentration in response to the opening of small numbers of channels (Hering and Sheng, 2001). The extent of Ca^{2+} compartmentalization is dependent on the morphology of spines and is better in mature mushroom spines. Locally Ca^{2+} influx activates the signaling pathways and the protein synthesis, that makes the molecular composition of every spine to some extent individual. Many spines share the same core components, but display variable level of signaling molecules (Calabrese et al., 2006).

1.3 Spine organization

A typical mature spine includes a postsynaptic density (PSD), actin filaments (F–actin), elements of endoplasmic reticulum and polyribosomes (Fig. 1.2). The PSD is a complex matrix of proteins which builds an electron–dense structure or "an electron dense web" that is juxtaposed to the active zone of a presynaptic terminal. The PSD is characteristic of glutamatergic synapses and present in nearly all dendritic spines (Boeckers, 2006; Gundelfinger and tom Dieck, 2000).

Another characteristic component of spines is the actin cytoskeleton. Spines are highly dynamic structures and the network of actin fibers provides a framework for the spine shape and stability. Rearrangement of the actin fibers underlies changes of spine shape and spine motility (Calabrese et al., 2006; Sorra and Harris, 2000).

A smooth endoplasmic reticulum (SER) belongs to organelles present in 20% of

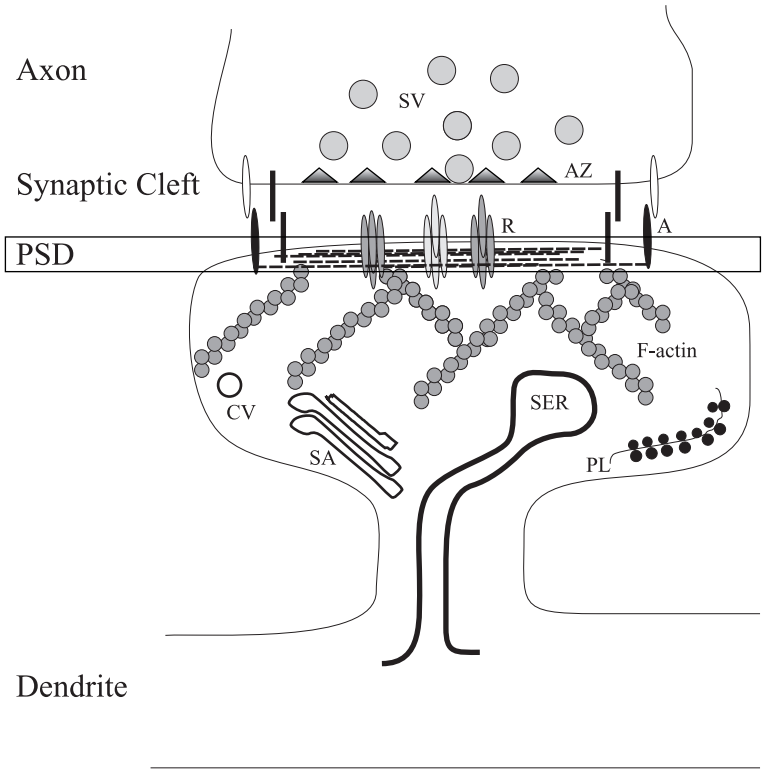

Figure 1.2: Organization of dendritic spine. The presynaptic part contains synaptic vesicles (**SV**) with neurotransmitter, dense material of active zone (**AZ**) and adhesion molecules (**A**), which hold pre- and postsynapse together. Beneath the postsynaptic membrane lies a compact matrix of proteins, the postsynaptic density (**PSD**). The PSD positions and organizes receptors (**R**), channels and adhesion molecules (**A**). Filamentous actin (**F–actin**) determines the shape and stability of a spine. Some spines contain smooth endoplasmic reticulum (**SER**), or SER, organized in stacks – spine apparatus (**SA**). Polyribosomes (**PL**) and coated vesicles are frequently present in big spines. Adapted from Hering and Sheng (2001); Ethell and Pasquale (2005).

the spines. In the large mushroom–like spines, cisternae of SER build a specialized compartment, the so–called spine apparatus. The stacks of SER function as a storage of calcium and participate in synaptic plasticity. Often, the spine apparatus is located in the vicinity of the PSD. Frequently a subset of mRNA and polyribosomes, which carry out the local protein synthesis, are also present in spines with a spine apparatus (Sheng and Hoogenraad, 2007).

Up to 36% spines in the hippocampus contain endosomes. This compartment participates in the recycling of AMPA receptors and, thus, contributes to the synaptic plasticity. The endosomal compartments also play a role in sorting synaptic proteins for degradation (Sorra and Harris, 2000).

1.4 Actin cytoskeleton

F–actin is a major component of spines. Actin fibers consist of globular actin (G–actin). Forms of G–actin (β and γ), expressed in neurons, are specifically targeted to spines where they build a network of longitudinal bundles of filaments in core and fine meshwork on the periphery of the spine. High resolution live imaging revealed that F–actin undergoes rapid continuous rearrangement in spines. G–actin polymerizes on one end of the filament, the leading edge of structure, and undergoes disassembly on the opposite end, in cytosol. The polymerization and the depolymerization of actin leads to a constant actin cycling or "treadmilling" effect, which is well described for non-neuronal cells (Alberts et al., 1991). The most recent investigation of neurons in hippocampal slices of $6-8$ days old rats and neurons in hippocampal culture of $16-24$ DIV (day *in vitro*) revealed that all actin in a resting spine was in a dynamic state. Two different pools of fibers with different dynamics were found experimentally in spines (Honkura et al., 2008; Star et al., 2002). The base of a spine is filled with filaments with a slow rate of treadmilling. The spine tip contains filaments with a very high turnover. The filaments of the slow pool turn over in ≈ 17 min and provide mechanical resistance for stability or expansion of dynamic pool. The turn-over time of the dynamic part of F–actin averages $40\,\mathrm{sec}-1\mathrm{min}$ (Honkura et al., 2008). The kinetics of actin-treadmilling is changed under conditions of synaptic transmission. The maintenance of spine volume on a dynamic basis allows the fine and rapid regulation of spine volume, depending on current conditions. Numerous actin–binding proteins and particularly the small GTPases control actin cytoskeleton dynamic and rearrangement in spines (Takai et al., 2001).

1.5 Postsynaptic density

The typical PSD consists of glutamate receptors, ion channels, adhesion molecules, elements of cytoskeleton, signaling proteins and scaffold molecules, which build a platform for interaction of all these heterogenous components (Boeckers, 2006). The PSD is proportional to the total spine volume. Depending on the spine size, the PSD dimensions varies between $200-800\,\mathrm{nm}$ of width and $30-50\,\mathrm{nm}$ of depth (Hering and Sheng, 2001). Small spines contain small PSDs, mature larger spines contain larger PSDs. In some cases, spines contain fenestrated (discontinuous, perforated) PSDs, which reflects the growth of synapses and may represent the beginning of spine division (Gundelfinger and tom Dieck, 2000).

1.5.1 The receptor apparatus

The primary function of the PSD is to build a set-up for the postsynaptic neurotransmitter reception apparatus (Gundelfinger and tom Dieck, 2000). The main excitatory transmitter, glutamate, activates metabotropic (G–protein coupled) and ionotropic (ligand-gated ion channels) receptors. To the metabotropic glutamate receptors (mGlu) belong eight different subtypes, mGlu1-mGlu8. Three subclasses of ionotropic glutamate receptors are known and named after their selective agonists: kainate receptors, N-methyl-D-aspartate (NMDA) receptors and γ–amino–3-hydroxy–5-methyl–4–isoxazolepropionic acid (AMPA) receptors. AMPA and NMDA receptors are enriched in the PSD. Physiologically AMPA and NMDA receptors are the dominant contributors to excitatory synaptic currents and synaptic transmission is mostly carried out by activation of both receptor types (Lujan et al., 2005).

In response to glutamate, AMPA receptors allow Na^+ ion influx which generate a rapid excitatory postsynaptic current and causes a partial depolarization of the postsynaptic membrane. NMDA receptors remain silent at the resting membrane potential. Only if the membrane is concomitantly depolarized (by AMPA receptors) NMDA receptors open in response to glutamate and allow a Ca^{2+} ion influx. After birth most excitatory synapses in the brain contain only NMDA receptors (referred to as silent synapses), and content of AMPA receptors increases gradually during postnatal development. A rise in the number of AMPA receptors in the PSD characterizes the maturation of neuronal contacts (Esteban, 2003).

The most remarkable property of synapses is their ability to alter the efficiency of synaptic transmission. Enhancement or weakening of synaptic transmission is referred to as synaptic plasticity. The events of synaptic plasticity were first described for the hippocampus, but later on were seen on many synapses throughout the brain. Brief, but intensive neuronal activity leads to the activation of NMDA receptors and the influx of Ca^{2+} . The strong and rapid rise in Ca^{2+} within a spine activates intracellular cascades which results in dynamic controlled insertion of AMPA receptors into the PSD. This causes a long–lasting increase in synaptic strength, or a long-term potentiation (LTP). Prolonged and weak synaptic stimulation leads to activation of NMDA receptors, followed by a slow and moderate increase in Ca^{2+}. This results in the activation of other biochemical sensors for Ca^{2+} and, in turn, in the removal of AMPA receptors from the postsynaptic membrane. This phenomenon is called long–term depression (LTD) and is characterized by long-lasting decrease in synaptic strength. Although LTP and LTD are persistent, the changes in synaptic transmission are reversible. The return of

increased synaptic strength by LTP to the "basal", "normal", non–potentiated state is called depotentiation (Malenka and Bear, 2004; Collingridge et al., 2004).

Synaptic plasticity is accompanied by a number of changes. So, LTP causes enlargement of existing PSDs and spines and splitting of existing PSDs and spines in two functional synapses. LTD leads to spine destabilization and even to spine elimination. Moreover, changes in synaptic plasticity are coupled with changes in behavior. Genetically modified mice with changed LTP or LTD also showed changes in learning or memory. Both forms of plasticity are important during development and in mature brain for strengthening or weakening of neuronal connections (Malenka and Bear, 2004; Lynch, 2004).

1.5.2 Protein composition of the PSD

The complex of proteins building the PSD is so stable, that it is possible to isolate the PSD biochemically by many centrifugation steps in sucrose gradients (Cotman and Taylor, 1972). Analysis of such fractions by quantitative mass spectrometry methods revealed the most abundant constituents of the PSDs.

The postsynaptic density-95/synapse associated protein 90 (PSD–95/SAP–90) was found to be abundant in the PSD. PSD–95 is the best studied member of the membrane associated guanylate kinase (MAGUK) protein family. PSD–95 constitutes about 1% of the PSD by mass, which is equivalent to approx. 300 molecules in an average PSD (Sheng and Hoogenraad, 2007). PSD–95 is an adaptor molecule that harbors mediating protein–protein interactions domains: three PSD-95/Discs Large/Zona occludens (PDZ) domains, src homology 3 (SH3) domain and guanylate kinase (GK) homology domain. The GK domain of PSD–95 and PSD–95–related proteins does not exhibit GK activity, but functions as a site of interaction with other proteins (*e.g.* with synapse associated protein 90–associated protein (SAPAP)). The PDZ domains of PSD–95 interact with C–termini of a variety of transmembrane proteins in the postsynaptic site. One of the most important interactions is the binding of the NR2 subunit of NMDA receptor. PSD–95 also stabilizes AMPA receptors in the PSD: PSD–95 binds the C'terminus of stargazin, a protein, regulating delivery of AMPA receptor subunits to cell surface (Fig. 1.3). Another essential binding partner of PSD–95 is the adhesion molecule, that is a part of a complex holding pre- and postsynapse together, neuroligin. PSD–95 also couples to NMDA receptor a number of signaling molecules, *e.g.*, Spar (s. section 1.8.1), receptor tyrosine kinase Erb4, SynGAP (synaptic Ras and Rap GTPase activating protein), Kalirin-7 (guanine nucleotide exchange factor (GEF) for Rac1),

neuronal nitric oxide synthase (Boeckers, 2006). Overexpression of PSD–95 leads to an increase of the number of dendritic spines, spine enlargement and increase in AMPA receptor content. PSD–95 mutant mice showed enhanced LTP and severely impaired spatial learning (Migaud et al., 1998; Boeckers, 2006).

ProSAP/Shank (Prolin rich synapse associated protein/SH3 and multiple ankyrin repeats domains protein) proteins, a family of multidomain scaffold molecules, constitute a substantial proportion of a total protein mass of the PSD. This family of proteins is encoded by three genes (ProSAP1/Shank2, ProSAP2/Shank3, ProSAP3/Shank1), which are alternatively spliced, so the family consists of eight members. The ProSAP/-Shank proteins are located deeper in the PSD, approx. 30 nm beneath the postsynaptic membrane, in comparison to PSD–95, which is mapped to $5 - 10$ nm under the membrane. The full-size 200 kDa ProSAP/Shank molecules contain ankyrin repeats, an SH3 domain, a PDZ domain, a prolin–rich region and a sterile alpha motif (SAM) domain (Boeckers, 2006).

ProSAP proteins directly or indirectly interact with a variety of receptor complexes in the PSD. The NMDA receptor–PSD–95 complex is connected to ProSAPs via the linker molecule SAPAP (synapse associated protein 90). Dimers of another linker molecule, Homer, attach mGluR receptors to the ProSAP scaffold. In addition, dimers of Homer link inositol–1,2,5,–triphosphate receptor (IP3R) to ProSAP/Shank. This interaction couples ER cisternae spatially and functionally to the PSD (Fig. 1.3). Recently reported direct interaction between expressed in cerebellum subunit GluRδ2 and PDZ domain of ProSAP2/Shank3 adds AMPA receptors to the list of ProSAP interactors.

ProSAP/Shank molecules are connected to the cytoskeleton. ProSAP/Shank proteins interact with cortactin, a protein, which facilitates the nucleation of new actin branches by binding Arp2/3 complex and F–actin. Abp1 and α-fodrin are other molecules linking ProSAP and dynamic F–actin structures. ProSAP proteins also directly recruit players of different signaling cascades. To this group belong phospholipase Cβ3, GTPase dynamin, β-Pix (a GEF for small GTPases Rac and cdc42). This is, however, not a complete list of molecules associated with ProSAP/Shank (Boeckers et al., 2002; Sheng and Kim, 2000).

The SAM domain of ProSAP/Shank proteins can bind to each other, which leads to multimerization of those large molecules in sheet-like structures. The sheets of ProSAP form a platform, which brings receptor complexes, signaling molecules, other scaffold molecules and cytoskeleton together (Fig. 1.3). For the construction of a higher order PSD structure ProSAP/Shank proteins have been postulated to be "master organizing"

molecules of the PSD (Baron et al., 2006; Boeckers, 2006).

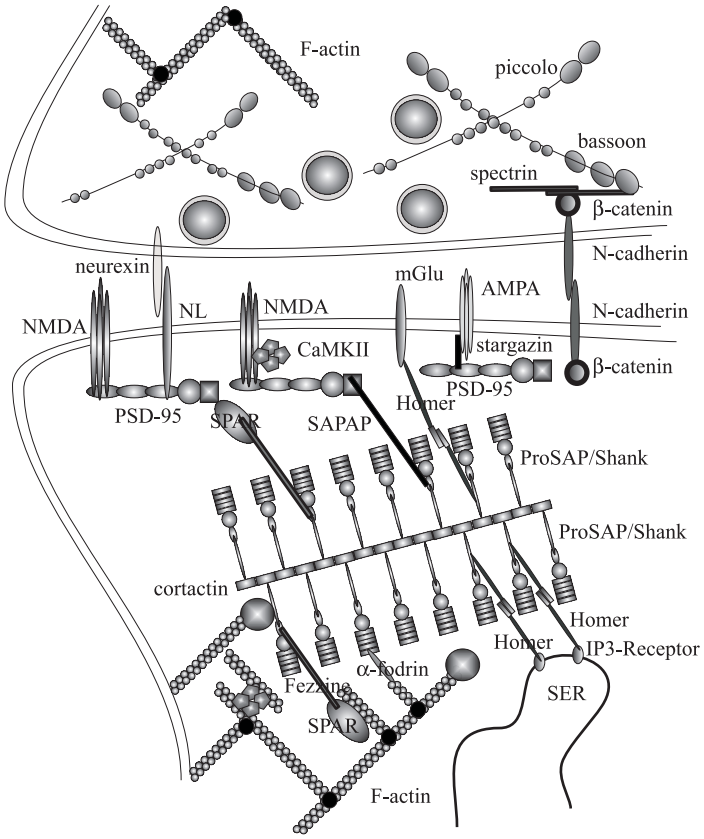

Figure 1.3: Model of the organization of the PSD, adapted from Boeckers (2006); Ziv and Garner (2004). Only some important components of the typical PSD and very few of the presynaptic part are depicted. The presynapse contains vesicles with glutamate, scaffold proteins (*e.g.* bassoon, piccolo) and cytoskeletal proteins. The adhesion molecules align pre- and postsynapse together. Postsynaptically scaffold proteins, such as PSD–95 build specialized protein complexes around the glutamate receptors and some adhesion molecules. ProSAP/ Shank molecules, present in the deeper layer of the PSD, assemblies in regular stacks via its C'terminal SAM domain. The platform of ProSAP/Shank proteins clusters the receptor complexes and links PSD components to the actin cytoskeleton.
AMPA, α–amino–3–hydroxy–5–methyl–4–isoxazoleproprionic acid receptor, CaMKII, Ca^{2+}/calmodulin dependent protein kinase, F–actin, filamentous actin, IP3-Receptor, inositol–1, 4, 5–triphosphate receptor, mGlu, metabotropic glutamate receptor, NMDA, N–methyl–D–aspartate receptor, NL, neuroligin, ProSAP/Shank, prolin rich synapse associated protein/SH3 and multiple ankyrin repeats domains protein, PSD–95, postsynaptic density–95 protein, SAPAP, synapse associated protein 90–associated protein, SER, smooth endoplasmic reticulum, SPAR, spine associated RapGAP.

In agreement with this concept, the mutation or deletion of different members of the ProSAP family leads to changes in synaptic function. The Shank1/ProSAP3 knock–out mice have an improved spatial learning, but show an impairment in long-term retention of spatial memory (Hung et al., 2008). In humans, ProSAP2/Shank3 significantly

contributes to cognitive development. A deletion or disruption of the ProSAP2/Shank3 gene (22q13.3) causes profound mental retardation. Transgene expression of ProSAP2-/Shank3 lead to induction of functional dendritic spines in normally aspiny cerebellar neurons, showing, that ProSAP can orchestrate a program of spinogenesis (Boeckers, 2006; Roussignol et al., 2005).

Except for scaffold molecules, a significant part of the PSD consists of cytoskeletal proteins. Analysis of the PSD fraction by mass spectrometry revealed that 12% of the PSD represented actin, and actin–binding proteins such as Arp2/3 complex, α-actinin, drebrin and spectrin (fodrin). Additionally, motor proteins, such as dynein and different isoforms of myosin (4% by mass) were found in the PSD. This group of proteins contributes to structural remodeling and transport processes in the PSD (Sheng and Hoogenraad, 2007).

The next group of proteins, which is abundant in the PSD, are signaling molecules. To this group belong kinases, phosphorylases, small GTPases and their regulators. All these molecules are assembled in complexes and associated with scaffold or cytoskeletal components of the PSD. Calcium/calmodulin dependent kinase II (CaMKII), α and β, constitutes 8.7% mass of the PSD. By stimulation of neurons in culture, the CaMKII content in the PSD transiently increases up to five–fold. CaMKII isoforms directly bind to the subunits of NMDA receptors. CaMKII molecules are the primary mediators of Ca^{2+} influx: they phosphorylate a number of downstream effectors. In addition to enzymatic function CaMKII plays a structural role in the PSD. The monomeric isoforms of kinase associate with each other and form large clusters. They bind and stabilize F–actin bundles (Okabe, 2007).

The synaptic GTPase activating protein, SynGAP, is the next signaling protein which is enriched in the PSD. First identified as Ras–specific GAP, SynGAP was also shown to stimulate the intrinsic GTPase reaction of Rap (Pena et al., 2008). SynGAP is a constituent of NMDA receptor complexes, via interaction with PSD–95. SynGAP regulates glutamate receptor transport and induction of LTP. The knock–out of SynGAP leads to premature synapse formation and enlargement of spines in cultured hippocampal neurons. It remains unclear why a signaling molecule as SynGAP is so abundant in the PSD (Sheng and Hoogenraad, 2007; Vazquez et al., 2004).

1.6 Fezzin family

Recently a novel family of scaffold molecules localized in dendritic spines, Fezzins, was discovered. The family consists of four homologous proteins: ProSAP-interacting

protein 1/leucine zipper tumor suppressor 3 (ProSAPiP1/LZTS3), LAPSER1/LZTS2, PSD-Zip70/LZTS1 and Nedd4 Binding Protein 3 (N4BP3). First described as cell growth modulators and tumor suppressor proteins Fezzins LZTS 1–3 were lost in several tumor tissues and cell lines. Overexpression of cDNA of these Fezzins in transformed cell lines inhibited cell growth and colony–forming efficiencies of the cancer cells. All Fezzin family members except N4BP3 are characterized by a coiled coil domain with a leucine zipper, a fasciculation and elongation protein zeta 1 (FEZ)–domain and a C'terminal PDZ–binding motif. All these domains act as sites for specific protein–protein interactions. The three most related members of this family ProSAPiP1, LAPSER1 and PSD–Zip70 are expressed in brain and enriched in the PSD (Wendholt et al., 2006; Konno et al., 2002; Schmeisser, 2007). ProSAPiP1 and LAPSER1 were shown to interact with the PDZ domain of ProSAP2/Shank3 via their PDZ-binding domain. The Fezzins can also form homo- and heterodimers via coiled coil domains and additionally contribute to the formation of the PSD platform of scaffold molecules. Simultaneously, Fezzins interact with several signaling molecules. LAPSER1 binds armadillo repeats of $\beta-$catenin and negatively regulates $\beta-$catenin-mediated transcription in several human cancer cell lines. The C'terminus of LAPSER1 contains the leucine rich CRM/exportin-regulated nuclear export sequence (NES), through which LZTS2 regulates the nuclear trafficking of $\beta-$catenin and increases $\beta-$catenin level in the cytoplasm (Thyssen et al., 2006). Interaction of $\beta-$catenin with LAPSER1 was also confirmed for neurons in our group (Schmeisser, 2007). Recently it was shown, that Fezzins PSD–Zip70, ProSAPiP1 and LAPSER1 interact with and recruit Spar, a regulator of Rap GTPases, to spines (Wendholt et al., 2006; Schmeisser, 2007; Maruoka et al., 2005).

1.7 Rap GTPases

The low molecular weight guanine nucleotide–binding proteins (small GTPases) are components of signaling pathways, which mediate and direct the signal transduction from receptors to effector proteins. The GTPases exist in two forms: active GTP–bound and inactive GDP–bound. Since GTPases are the key regulators of many cellular events, the activation of this group of proteins is strictly controlled. The guanine nucleotide exchange factors (GEF) induce a conversion of the inactive, GDP-bound form into the active, GTP–bound protein. Inactivation of GTPases, accompanied by hydrolysis of GTP to GDP, is mediated by GTPase–activating proteins (GAP).

The GTPases constitute a superfamily, consisting of over 100 members. The follow-

ing groups of GTPases with different functions belong to this superfamily: Ras, Rho, Rab, Sar1/Arf and Ran. The Ras family of GTPases was discovered in the context of cancer research. It was shown, that Ras GTPases regulate cell proliferation, differentiation and cell survival. The Ras family consists of a number of subfamilies and among them Rap.

The Rap group contains five GTP-binding proteins: Rap1A, Rap1B and Rap2A, Rap2B, Rap2C. Rap1 and Rap2 differs significantly (approx. 60% identity at protein level). Isoforms of Rap A and B share 95% identities to each other in case of Rap1, and 90% for Rap2. Rap1 is ubiquitously expressed, with a particularly high level of expression in platelets, neutrophils and brain. First characterized as an anti-oncogenic protein, Rap1 in culture reverted a phenotype of *K–Ras* transformed cells and antagonized Ras signaling. Rap inhibited Ras induced signal transmission by binding but not activating the Ras effectors (Bos, 1998). However, Rap has other, Ras–independent functions. The Rap 1 GTPase regulates proliferation and differentiation of cells. Another important role of Rap is the regulation of the cell adhesion. It was shown that Rap1 regulates E–cadherin in different cellular context (in *Drosophila* imaginal disk cells, mammalian epithelial cells, primary osteoblasts, endothelial cells). Rap1 was required during the initial formation of cell–cell junctions and was down–regulated when the junctions maturated. Prevention of Rap1 activation resulted in the disruption of cell–cell adhesion. Furthermore, both Rap1 and Rap2 are involved directly in inside–out activation of $\beta 1$ and $\beta 2$ integrins and integrin–mediated adhesion. In leukocytes, T- and B–lymphocytes Rap GTPases were shown to regulate cell spreading and chemokine-induced migration (Takai et al., 2001; Kooistra et al., 2007). In T–cells Rap1 was activated in an antigene-dependent manner and accumulated at the contact site of T–lymphocyte with an antigene presenting cell. Rap1 mediated the convertion of integrin LFA–1 (leukocyte function–associated antigen 1) to a high affinity state, which was essential for immunological synapse formation between lymphocytes and antigen-presenting cell (Katagiri et al., 2002; de Bruyn et al., 2002).

Recently, the Rap GTPases were shown to play a role in different processes in the nervous system. Rap1 is activated in cortical, but not in hippocampal neurons by calcium influx and mediates via ERK1/2 CREB–dependent transcription (Chen et al., 2005). Rap1B, and not Rap1A is involved in the establishment of the polarity of neurons and differentiation one of the neurits to an axon. Rap1B acts upstream of cdc42 and the localization of this GTPase in the tip of one extension is crucial for axon formation. Overexpression of the constitutively active Rap1B 2h after plating led to the induction of supernumerary axons at the expense of dendrites (Schwamborn

and Pueschel, 2004). An overexpression of the other member of Rap family, Rap2 in mature cultured neurons, leads to a retraction of axon and dendrites, accompanied by an increase in filopodia–like structures and a loss of dendritic spines (Fu et al., 2007). In hippocampal cultures, the overexpression of Rap1 induced the formation of thin and filopodia–like spines. The effect of spine elongation was mediated by a profilin binding protein, afadin (AF–6), which was recruited by Rap1 to the spines (Xie et al., 2005). The activation of Rap GTPases also caused functional changes in neurons. In hippocampal slices Rap1 via p38 MAPK mediated activity induced LTD by removing AMPA receptors from synaptic sites. Rap2 via JNK triggered removal of AMPA receptors from synapses during depotentiation (Zhu et al., 2005, 2002). Knock–in mice, which expressed a dominant negative Rap1, demonstrated a lack of spatial memory and a deficit in remembering of the temporal context of events. Concomitantly the mice exhibited a reduction in some types of LTP (Morozov et al., 2003).

1.8 Proteins downregulating Rap activation

Only a few GTPase activating proteins are described for the subfamily of Rap GTPases. Due to structural and functional similarity the GAP specific for Rap are subdivided in two families. The first family, RapGAP, consists of two members Rap1GAP1 and Rap1GAP2. Both have also splice isoforms. (Schultess et al., 2005). The second group of proteins, SPA–like, includes signal–induced proliferation associated protein 1 (SPA–1/SIPA1), Spine associated RapGAP (Spar), Spar2 and a novel protein characterized in this work, Spar3 (Kurachi et al., 1997; Pak et al., 2001; Spilker et al., 2008). Spar has been found and independently characterized in several groups. Therefore Spar is known under other names as E6TP1 (E6 targeted protein 1), SPAL1 (SPA 1–like protein 1) or SIPA1L1 (SPA–1 like protein 1) (Gao et al., 1999; C. Roy et al., 2002). From this point on, the SPA–like family will be denoted as SPA–family.

Tuberin belongs to a group of proteins which downregulate Rap in brain, but can downregulate also other small GTPases. Tuberin is specific to Rap1 and Rheb GTPases and it is not affiliated to any group (Zhang et al., 2003). Recently several proteins downregulating Ras GTPase were shown to have the same specificity for Rap. SynGAP, a signaling molecule, which is present in the PSD at the same level as CaMKII, belongs to bifunctional Ras-Rap-specific GAP (Pena et al., 2008).

1.8.1 SPA–family

All members of the SPA-family share the same domain structure: a RapGAP, a PDZ and a coiled coil. Spar, the best characterized protein of the SPA–1 family, contains Act1 and Act2 domains, responsible for association with actin fibers. Additionally, the guanylate kinase binding domain (GKBD) mediating interactions with scaffold proteins of MAGUK family was mapped in the Spar C'terminus (Fig. 1.4)(Pak et al., 2001).

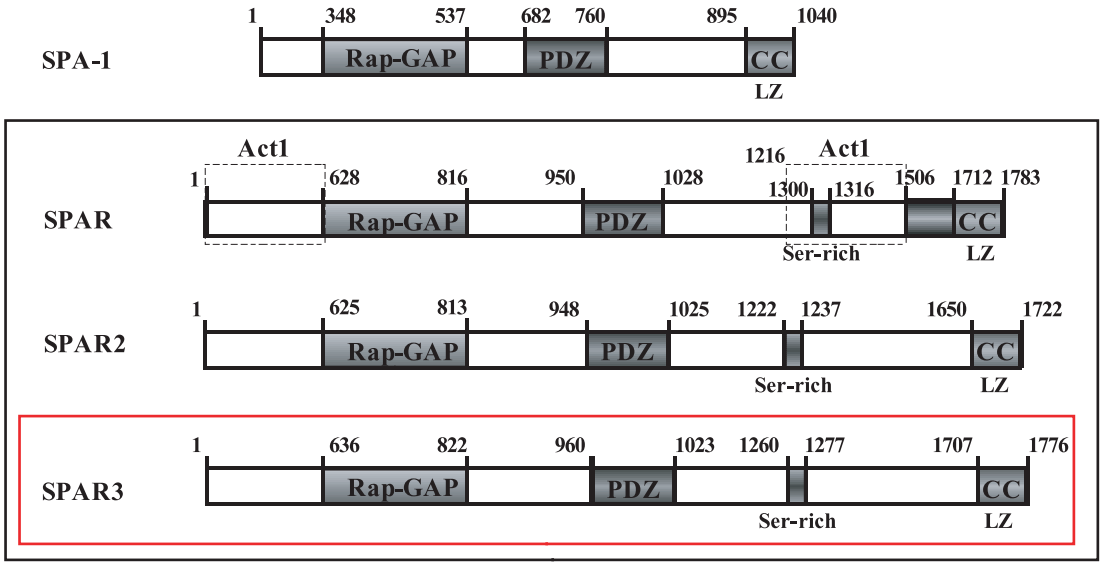

Figure 1.4: Domain organization of the SPA-family of proteins. Each member contains a Rap-GAP domain, a PDZ domain, a coiled coil domain with a leucine–zipper motif. The Spar proteins expressed in brain contain a serine–rich region. In the black frame are the Spar proteins, expressed in brain. Spar3, characterized in this work, is highlighted in the red frame. Act domain, responsible for association with actin, GKBD, guanylate kinase binding domain, RapGAP, Rap GTPase activating domain, PDZ, (PSD–95/Discs Large/Zona occludens) – domain, Ser-rich, serine rich motif, CC, coiled coil, LZ, leucine zipper. Adapted from Spilker et al. (2008)

SPA–1, the smallest protein of the family, migrates at 130 kDa. It is widely expressed: high levels of protein were found in peripheral blood leukocytes, lymphocytes and lymphoid organs, such as spleen or thymus. Moderate level of SPA–1 was revealed in prostate, kidneys, liver, lungs. No expression of SPA–1 was observed in adult or fetal brain (Kurachi et al., 1997).

The Spar and Spar2 proteins are larger than SPA–1, with a calculated molecular weight of about 190 kDa. Both proteins, Spar and Spar2, are mostly described as brain proteins, although Spar was first detected in epithelial cells. The expression of Spar was also found in cardiac muscle (Singh et al., 2003; Roy et al., 1999). Spar2 (on mRNA level) was detected in heart, testis, liver and lungs. No Spar2 transcripts were

revealed in kidney, muscle and spleen. It is not known, if Spar and Spar2 are expressed in other tissues (Pak et al., 2001; Spilker et al., 2008).

Non-neuronal SPA–1

The first described member of the SPA-family of proteins, SPA–1, was identified in a lymphoid cell line as a protein which was induced in lymphocytes after mitogenic stimulation by Il-2. (Kurachi et al., 1997).

SPA–1 displays a GAP activity against cytoplasmic Rap1 and Rap2 *in vitro*. (Hattori et al., 1995; Kurachi et al., 1997). However, only GAP activity against Rap1 was confirmed *in vivo*: SPA–1 knock–out mice revealed a marked accumulation of Rap1GTP in immature hematopoetic progenitors (Kooistra et al., 2007).

SPA–1 downregulates Rap1 and thus negatively regulates integrin-mediated adhesion. By overexpression of SPA–1 in the cell lines, the cells become rounded and detach from the matrix (Tsukamoto et al., 1999). The specific location of SPA–1 in the cells is mediated by the actin cytoskeleton. SPA–1 was shown to bind the actin-bundling protein α-actinin and the cytoskeletal protein afadin (AF-6) (Su et al., 2003; Harazaki et al., 2004).

Interestingly, the bone marrow cells express several GAP for Rap, but their expression is temporary segregated. The hematopoetic progenitors express a high level of SPA–1 and by maturation SPA–1 is gradually replaced by Rap1GAP. In SPA–1 knock–out animals the unregulated activation of Rap1 in blood progenitors leads to increased cell expansion and survival via ERK activation. The animals developed a spectrum of myeloid disorders such as chronic myelogenous leukemia and myelodisplastic syndrome (Kooistra et al., 2007).

In kidneys, SPA–1 regulates the translocation and fusion to the apical membrane of the water channel aquaporin 2 (AQP2). AQP2 is the only known water channel in kidneys regulated by vasopressin. Insertion of AQP2 into the apical membrane in renal principle cells brings them into a water permeable state and leads to water reabsorbsion. Downregulation of AQP2 leads to diabetes insipidus, characterized by massive loss of water through kidney. SPA–1 via its PDZ domain binds directly to the C'terminus of AQP2 and triggers translocation of the channel to the membrane. As it was verified in the SPA–1 knock–out mouse, GAP activity of SPA–1 is necessary for the regulation of channel positioning (Noda et al., 2004; Noda and Sasaki, 2005).

In cell lines (HeLa and NIH 3T3) SPA–1 was shown to interact with a DNA-binding bromodomain protein (Brd4). Brd4 binding to SPA–1 increased its GAP function for

Rap1 and Rap2. Brd4 was able to recruit transiently a pool of SPA–1 to the nucleus (Farina et al., 2004).

Spar and Spar2 – GAP for Rap, expressed in brain

The next member of the family E6TP1 was first reported as an anti-oncogenic protein in humans. E6TP1 was targeted for ubiquitin-mediated degradation by the viral E6 oncoprotein. This leads to an accumulation of Rap1–GTP and to the transformation of human mammary and cervical epithelial cells. Human E6TP1 has a 95% amino acid identity to the recently described rat Spar (Singh et al., 2003).

Spar was characterized as a 200 kDa protein, which is expressed in brain and regulates spine morphology. Spar interacts directly via GKBD with PSD–93/chapsin and with PSD–95 and is a constituent of the PSD–95-NMDA receptor complex (C. Roy et al., 2002; Pak et al., 2001). Several Fezzins PSD–Zip70, ProSAPiP1, LAPSER1 were demonstrated to interact with Spar and bring it in complex with a master scaffold molecule of the PSD ProSAP2/Shank3 (Maruoka et al., 2005; Schmeisser, 2007; Wendholt et al., 2006). In cell lines overexpressed Spar is associated with actin cytoskeleton. Moreover, by cotransfection PSD–95 was recruited by Spar to F–actin. *In vitro*, Spar displayed specific GAP activity to Rap1A and Rap2A, but not to other tested GTPases (H-Ras, RhoA, Rac1 and cdc42). In cultured hippocampal neurons Spar was not present in all spines: almost half of the small spines (with PSD–95 staining intensity below average) did not contain Spar. In neurons, overexpressed Spar accumulated in spines, induced spine enlargement and the formation of large spines of irregular shape. The changes in spine morphology were mediated by down–regulation of Rap–GTPases and interaction with actin. Expression of dominant negative constructs of Spar, lacking RapGAP or actin-interacting domains, caused spine destabilization and formation of filopodia–like protrusions (Pak et al., 2001).

The level of Spar in spines was regulated by the neuronal activity, via upregulation of the serum-inducible kinase (SNK). The basal level of this activity-inducible kinase is very low in the cultured neurons under normal conditions. By excitatory synaptic transmission SNK is synthesized in the cell body and targeted to spines, where it binds to the Act2 domain of Spar and phosphorylates it. This results in Spar degradation via the ubiquitin-proteosome pathway, which is accompanied by weakening the synaptic strength and transformation of mature spines in immature filopodia. Loss of Spar and transformation of spines were most pronounced in the proximal dendrites near the cell body, where the concentration of SNK was the highest (Pak and Sheng, 2003; Seeburg

and Sheng, 2008).

Recent study on 2 DIV cultured neurons revealed, that Spar is a downstream mediator of signaling from EphA4 receptor. In young neurons, EphA4 is found in growth cones. Receptor activation causes growth cone collapse and neurite retraction. This mechanism is utilized for the topographic organization of neuronal connections: the axons with high receptor expression avoid regions with high ephrin expression. The C'terminus of EphA4 interacts with the PDZ domain of Spar, which leads to the ephrin dependent Rap1 inactivation. This results in decreased integrin-dependent adhesion and growth cone collapse (Richter et al., 2007).

Spar2 was described as a Spar–homologous protein, expressed in brain. In spite of the similar structure and high homology to Spar, Spar2 seems to have other, unknown, functions in neurons. By overexpression in neurons Spar2 did not influence the spine morphology. In cell lines Spar2 did not associate with actin fibers. Spar2 displayed equal GAP activity to all five Rap GTPases, which was 20% lower as downregulation of the same GTPases by Spar (Spilker et al., 2008).

1.9 Aim of the work

Synapse associated RapGAP protein 3 is a novel protein which has not been investigated before. A clone of Spar3 was obtained as the result of a yeast–two–hybrid screen of a rat brain cDNA library with a Fezzin molecule ProSAPiP1 as bait. The objective of this work was to characterize Spar3. This has included the generation of Spar3–specific antibodies, the analysis of Spar3 expression in rat brain on mRNA and protein level, the investigation of the cellular location of Spar3 in the primary hippocampal culture, the detection of the Spar3 presence in different neuron compartments by biochemical fractionation and by electron microscopy. A matter of particular interest was the identification of elements in Spar3 responsible for synaptic targeting and a study of the Spar3 overexpression effects on spine morphology in the cultured neurons.

The interaction of ProSAPiP1 with Spar3 was to be confirmed biochemically and in cell culture (hippocampal neurons). Further investigations were conducted to understand the function of Spar3. For this purpose, a yeast–two–hybrid screen had to be performed to identify new interaction partners of Spar3. Found interactions had to be verified by coimmunoprecipitation, in cell lines and in hippocampal neurons.

To investigate the role of Spar3 *in vivo*, a Spar3 knock–out mouse had to be generated and initially characterized. That included mapping of the targeting vector in genome and on RNA level, development of mice genotyping, verification of truncated protein expression by staining of sections and Western blot.

Chapter 2

Materials

2.1 Chemicals

Chemical substances from AppliChem, Calbiochem, Fluka, Merck, PeqLab, Roth, Serva and Sigma used in this work were of analytical purity.

Acetic acid	Fluka/Sigma, Deisenhofen
Acrylamide–N'N'–methylenebisacrylamide mix	Serva, Heidelberg
Adenine hemisulfate	Sigma, Deisenhofen
Agar	Roth, Karlsruhe
Agarose	PeqLab, Erlangen
Albumin from chicken egg	Sigma, Deisenhofen
3–amino–1,2,4–triazole	Sigma, Deisenhofen
Ammonium persulfate (APS)	Sigma, Deisenhofen
Ampicillin sodium salt	Roth, Karlsruhe
B 27 Supplement	Gibco/Invitrogen, Karlsruhe
5–brom–4–chlor–3–indoxyl–β-D– –galactopyranoside (X–gal)	AppliChem, Darmstadt
Bromphenol blue	Sigma, Deisenhofen
Bovine Serum Albumin (BSA)	PAA Laboratories, Austria
Chloroform	Roth, Karlsruhe
Denhardt's solution	Sigma, Deisenhofen
Dextransulfate	Fluka/Sigma, Deisenhofen
Diaminobenzidine tetrahydrochloride (DAB)	Sigma, Deisenhofen
N,N-dimethylformamide (DMF)	Sigma, Deisenhofen
Dimethyl sulfoxide (DMSO)	Sigma, Deisenhofen
Disodium hydrogen phosphate	Merck, Darmstadt
Dithiothreitol (DTT)	Fluka/Sigma, Deisenhofen
EDTA-free protease inhibitor	Roche, Mahnheim
Ethanol	Fluka/Sigma, Deisenhofen

Ethidium bromide	Roth, Karlsruhe
Ethylene diamine tetraacetat (EDTA)	AppliChem, Darmstadt
Fetal bovine serum (FBS)	HyClone, USA
Fetal calf serum (FCS)	Biochrom, Berlin
Fish–gel	Sigma, Deisenhofen
Formamide deionized	Sigma, Deisenhofen
Formalin	Merck, Darmstadt
Gelatin for EM	Serva, Heidelberg
Gel Code Blue Stain Reagent	Pierce, Bonn
Glass beads	Sigma, Deisenhofen
D(+)–Glucose	Sigma, Deisenhofen
L-Glutamine	Gibco/Invitrogen, Karlsruhe
Glutaraldehyde	Biochemika/Sigma, Deisenhofen
Glutathione	Serva, Heidelberg
Glutathione-sepharose	Amersham Biosciences, Freiburg
Glycerol	Roth, Karlsruhe
Glycine	AppliChem, Darmstadt
Hepes	Roth, Karlsruhe
High Fidelity PCR Supermix	Invitrogen, Karlsruhe
Hybridization cocktail	Sigma, Deisenhofen
Hydrochloric acid	Merck, Darmstadt
Hydrogen peroxide	Sigma, Deisenhofen
Igepal CA–830 (NP–40)	Sigma, Deisenhofen
Isopropyl–β–D–1–thiogalactoside (IPTG)	AppliChem, Darmstadt
Isopropanol	Fluka/Sigma, Deisenhofen
Kanamycin	Roth, Karlsruhe
Lead citrate	Merck, Darmstadt
LR–Gold	London Resin Ltd, London
N–lauryl–sarcosin	Sigma, Deisenhofen
Magnesium chloride	Roth, Karlsruhe
Magnesium sulfate	Merck, Darmstadt
2-mercaptoethanol	Fluka/Sigma, Deisenhofen
Methanol	Fluka/Sigma, Deisenhofen
Methylbenzoat	Merck, Darmstadt
Milk powder (blotting grade)	Roth, Karlsruhe
μMACS Protein A conjugated microbeads	Mitenyi Biotech, Bergisch Gladbach
Monopotassium phosphate	Merck, Darmstadt
Monosodium phosphate	Merck, Darmstadt
Mounting medium	Sigma, Deisenhofen
Mowiol 4–88	Calbiochem, USA
Ovalbumin	Sigma, Deisenhofen
Paraformaldehyde (PFA)	Merck, Darmstadt
Paraplast	Sigma, Deisenhofen

peqGOLD RNAPure Solution	PeqLab, Erlangen
Penicillin–Streptomycin	Gibco/Invitrogen, Karlsruhe
Picric acid	Merck, Darmstadt
Poly–L–lysin	Sigma, Deisenhofen
Ponceau S Red	Serva, Heidelberg
Potassium acetate	Merck, Darmstadt
Potassium chloride	Roth, Karlsruhe
Propanol	Fluka/Sigma, Deisenhofen
^{32}S – ATP	GE Healthcare, Munich
D(+)–Saccharose	Roth, Karlsruhe
Salmon testis DNA	Sigma, Deisenhofen
Sodium acetate	Merck, Darmstadt
Sodium bicarbonate	Sigma, Deisenhofen
Sodium citrate	Merck, Darmstadt
Sodium chloride	AppliChem, Darmstadt
Sodium deoxycholate	Merck, Darmstadt
Sodium dodecyl sulfate (SDS)	Roth, Karlsruhe
Sodium hydroxide solution (1N)	Merck, Darmstadt
D–Sorbitol	Sigma, Deisenhofen
N'N'N'N',–Tetramethylethylenediamin (TEMED)	Sigma, Deisenhofen
Tris (ultrapure)	USB corporation, USA
Triton–X100	Roche, Mahnheim
Tryptone	Sigma, Deisenhofen
tRNA	Sigma, Deisenhofen
Tween–20	Roth, Karlsruhe
Uranilacetate	Merck, Darmstadt
Xylol	Prolabo, France
Yeast extract	Merck, Darmstadt

2.2 Buffers and solutions

6× **DNA loading buffer**, pH 8.0:	0,25% [w/v] bromphenol blue 30% [v/v] glycerol 50 mM EDTA
Mowiol	10% [w/v] Mowiol 4-88 25% [v/v] glycerol 0.1 M Tris–HCl pH 8.5
PBS, pH 7.4	137 mM NaCl 2.7 mM KCl 10 mM Na_2HPO_4 2 mM KH_2PO_4

Phosphate buffer, pH 7.2:	0.2 M NaH_2PO_4 0.2 M Na_2HPO_4
RIPA buffer	50 mM Tris–HCl, pH 8.0 150 mM NaCl 1% [w/v] NP-40 1% [w/v] sodium deoxycholate 0.1% [w/v] SDS
20×**SSC buffer**	0.3 M NaCl 0.3 M sodium citrate
TBS, pH 7.6	150 mM NaCl 50 mM Tris–HCl
TAE buffer, pH 8.5	40 mM Tris–HCl 1.14 ml/l acetic acid 2 mM EDTA
TE buffer, pH 7.4-8.0	10 mM Tris–HCl, pH 8.0 1 mM EDTA
1 M **Tris**–HCl, pH 6.8; 8.0	
1.5 M **Tris**–HCl, pH 8.8	
X–gal stock solution	20 mg/ml X–gal 99% DMF
X–gal in Z-buffer	1 mg/ml X–gal 39 mM 2–mercaptoethanol Z-buffer
Z buffer	60 mM Na_2HPO_4 40 mM NaH_2PO_4 10 mM KCl 1 mM $MgSO_4$

2.3 Kits

Kits with prefabricated solutions were used for following appilications:

Application	Kit	Producer
DNA extraction from agarose gel	JETQUICK Gel Extraction Spin Kit	GENOMED, Bad Oeynhausen
Purification of PCR products from agarose gel	JETQUICK PCR Purification Kit	GENOMED, Bad Oeynhausen
Plasmid DNA isolation in mini scale	JETQUICK Plasmid Miniprep Spin Kit	GENOMED, Bad Oeynhausen
Plasmid DNA isolation in midi scale	JETSTAR 2.0 Midi Plasmid Purification Kit	GENOMED, Bad Oeynhausen
Endotoxin free plasmid DNA isolation in maxi scale	NucleoBond PC 500 EF	MACHEREY–NAGEL GmbH& Co KG., Dueren
Western Blot Signal Detection	ECL Plus Western Blotting Detection Reagents Kit	Amersham Biosciences, Freiburg
Measurement of protein concentration	BCA Protein Assay Kit	Pierce, USA
Rapid cloning of PCR Products	Zero Blunt TOPO PCR Cloning Kit	Invitrogen, USA
Immunohistochemistry	Vectastain ABC kit	Jackson Immunoresearch, USA

2.4 Antibiotics, stock solutions

Ampicillin
50 mg/ml ampicillin–sodium salt
50% [v/v] ethanol

Kanamycin

525 mg/ml kanamycin

Antibiotics were added to autoclaved and approx. 55°C warm medium or agar. The working dilution of ampicillin was 100 μg/ml. Kanamycin was added to a concentration of 50 μg/ml.

2.5 Culture media for bacteria

LB medium
1% [w/v] tryptone
0.5% [w/v] yeast extract
1% [w/v] NaCl

LB-Agar
LB Medium
1.5% agar

SOB Medium
2% [w/v] tryptone
0.5% [w/v] yeast extract
0.5% [w/v] NaCl

2YT–Medium
2% [w/v] tryptone
1% [w/v] yeast extract
0.5% [w/v] NaCl

2.6 Culture media for yeast

Complete medium:

YPD medium
5% [w/v] YPD
0.01% [w/v] adenine hemisulfate (AHS)
12 μg/ml Kanamycin

YPD Agar
6.7% [w/v] YPDA
0.01% [w/v] AHS
12 μg/ml Kanamycin

Selection medium:

SD medium
2.7% [w/v] DOB

one of the following dropout supplement, in concentration:

0.74 g/l	CSM–Trp (pAS 2–1 vector, "bait")
0.69 g/l	CSM–Leu (pACT2 vector, "prey")
0.64 g/l	CSM–Leu/–Trp (yeast, containing both pACT2 and pAS 2–1)
0.62 g/l	CSM–His/–Leu/–Trp
0.01% [w/v]	AHS
12 μg/ml	Kanamycin

SD Agar
43.7 g/l DOBA

one of the following dropout supplement, in concentration:

0.74 g/l	CSM–Trp (pAS 2–1 vector, "bait")
0.69 g/l	CSM–Leu (pACT2 vector, "prey")
0.64 g/l	CSM–Leu/–Trp (yeast, containing both pACT2 and pAS 2–1)
0.01% [w/v]	AHS

12 μg/ml	Kanamycin

SD Agar for selection colonies, expressing HIS3 reporter:

43.7 g/l	DOBA
0.62 g/l	CSM–His/–Leu/–Trp
0.01% [w/v]	AHS
5 nM	3–amino–1,2,3–triazol
12 μg /ml	Kanamycin

2.7 Culture media and buffers for cell lines and primary hippocampal culture

Dulbecco's PBS	PAA Laboratories, Austria
Dulbecco's Modified Eagle Medium (DMEM)	Gibco/Invitrogen, Karlsruhe
HBSS (Hank's BSS)	PAA Laboratories, Austria
Neurobasal medium	Gibco/Invitrogen, Karlsruhe

DMEM+	10% [v/v] FBS
	2 mM glutamine
	1% [v/v] Penicillin-Streptomycin

Neurobasal medium+	50× B27 Supplement
	2 mM glutamine
	100× Penicillin-Streptomycin

2.8 Transfection reagents

OPTIFECT Reagent (Invitrogen, USA) was used to transfect the primary cultures of hippocampal neurons. FuGENE (Roche, Mannheim) was applied for transfection of cell lines.

2.9 Biological material

2.9.1 Bacterial strains

The bacterial strains with following genotypes were supplied from Stratagene, Heidelberg:

E.coli XL–1 Blue	recA1 end A1 gyrA96 thi–1 hsdR17 relA1 lac [F' proAB $lacI^q$ Z ΔM15 Tn10(Tet^R)] (Bullock et al., 1987)
E.coli BL21	F^- dcm ompT hsdS(r_{B^-} m_{B^-}) gal (Studier et al., 1990)

2.9.2 Yeast strains

The yeast strains with following genotype were supplied from Clontech, USA:

S. cerevisiae Y187	MATα ura3–52 his3–200 ade2–101 trp1–901 leu2–3 112 met^- gal4Δ gal80Δ URA3::$GAL1_{UAS}$–$GAL1_{TATA}$–lacZ (Harper et al., 1993)
S. cerevisiae AH109	MATa trp1–901 leu2–3 112 ura3–52 his 3–200 gal4Δ gal80Δ LYS2 ::$GAL1_{UAS}$–$GAL1_{TATA}$–HIS3 MEL1 $GAL2_{UAS}$–$GAL2_{TATA}$–ADE URA3::$MEL1_{UAS}$–$MEL1_{TATA}$–lacZ (James et al., 1996)

2.9.3 Cell lines

Cell line	Cell type	Company	Reference
Cos–7	Kidneys of african velvet monkey	DSMZ, Braunschweig	(Gluzman, 1981)
HeLa	Human cervix carcinoma	DSMZ, Braunschweig	(Scherer et al., 1953)
ES XT0120	Mouse embryonic stem cells, modified with an insertion of pGT0Ixf RC gene trap vector. Insertion:7:29029138–29214220.	Sanger Institute Gene Trap Resource, England	(Skarnes et al., 2004)

2.9.4 Primary antibodies (AB)

Designation	Origin	Clonality	Application	Dilution	Company
Bassoon	rabbit	pAB	IF	1:500	BD Biosciences,USA
$\beta-$catenin (N'terminus)	mouse	mAB	IF Western	1:100 1:1000	Upstate, USA
$\beta-$galactosidase	mouse	mAB	Western	1:1000	Chemicon/Millipore, USA
GFP	mouse	mAB	Western	1:3000	Clontech, Heidelberg
mGluR1	mouse	mAB	IF	1:500	Clontech, Heidelberg
GSKα/β	mouse	pAB	IF Western	1:100 1:500	Sigma, Deisenhofen
GST	rabbit	pAB	Western	1:5000	PINEDA, Berlin
KCNQ3	rabbit	pAB	IF	1:500	Alomone Labs, Munich
LAPSER1	rabbit	pAB	Western	1:500	PINEDA, Berlin
Neuroligin 1–3	mouse	mAB	Western	1:1000	Synaptic systems, Göttingen
Phalloidin alexa 568-conjugated	*Amanita phalloides*	–	IF	1:50	Invitrogen, Karlsruhe
ProSAP2	guinea pig	pAB	IF Western	1:400 1:1000	PINEDA, Berlin
ProSAPiP1 SA7461	rabbit	pAB	IF Western	1:100 1:2000	Eurogentec, Cologne
PSD–Zip70 (LZTS1)	rabbit	pAB	Western	1:100	Gen Way Biotech, USA
Spar (E6TP1)	goat	pAB	IF	1:100	Santa Cruz, USA
Spar3 (to GST tagged protein)	rabbit	pAB	IF Western	1:300 1:500	PINEDA, Berlin
Spar3 (to peptide)	rabbit	pAB	EM Immuno-histochem. Western	1:10 1:500 1:1000	Eurogentec, Cologne
Synaptophysin	mouse	mAB	IF	1:400	Sigma, Deisenhofen
α–tubulin	mouse	mAB	IF	1:1000	Sigma, Deisenhofen
Vimentin	mouse	pAB	IF	1:1000	Chemicon/Millipore, USA

2.9.5 Secondary antibodies (AB)

Designation	Application	Dilution	Company
anti–guinea pig–IgG, horse raddish peroxidase (HRP) conjugated	Western	1:2000	DAKO Cytomation, Denmark
anti–guinea pig–IgG, Alexa Fluor 488 conjugated	IF	1:1000	Invitrogen, Karlsruhe
anti–guinea pig–IgG, Alexa Fluor 555 conjugated	IF	1:1000	Invitrogen, Karlsruhe
anti–mouse–IgG, HRP conjugated	Western	1:2000	DAKO Cytomation, Denmark
anti–mouse-IgG, Alexa Fluor 488 conjugated	IF	1:1000	Invitrogen, Karlsruhe
anti–mouse–IgG, Alexa Fluor 555 conjugated	IF	1:1000	Invitrogen, Karlsruhe
anti–rabbit 10 nm gold conjugated	EM	1:50	Aurion, Netherlands
anti–rabbit–IgG, HRP conjugated	Western	1:2000	DAKO Cytomation, Denmark
anti–rabbit–IgG, Alexa Fluor 488 conjugated	IF	1:1000	Invitrogen, Karlsruhe
anti–rabbit–IgG, Alexa Fluor 555 conjugated	IF	1:1000	Invitrogen, Karlsruhe
anti–rabbit–IgG, biotin conjugated	Immunohistochemistry	1:200	Jackson Immunoresearch, USA
anti–goat-IgG, HRP conjugated	Western	1:2000	DAKO Cytomation, Denmark
anti–goat–IgG Alexa Fluor 488 conjugated	IF	1:1000	Invitrogen, Karlsruhe
anti–goat–IgG Alexa Fluor 555 conjugated	IF	1:1000	Invitrogen, Karlsruhe

2.9.6 Enzymes

Desoxyribonuclease (DNase)	Roche, Mahnheim
DNase, cell culture	Invitrogen, Karlsruhe
Lysozyme	Serva, Heidelberg
M–MVL reverse transcriptase	Invitrogen, Karlsruhe
Proteinase K	Sigma, Munich
Ribonuclease A (RNase A)	Quagen, Hilden
T4–Ligase	Invitrogen, Karlsruhe
Terminal transferase	Sigma, Deisenhofen
Trypsin	Gibco/Invitrogen, Karlsruhe
Trypsin 2.5% in PBS w/o Ca^{2+}, Mg^{2+}	Biochrom, Berlin

For DNA restriction, enzymes and their appropriate buffers were supplied from Invitrogen, Karlsruhe and applied according producer's instructions.

Enzyme stock solutions:

Lysozyme	10 mg/ml lysozyme 10 mM Tris–HCl, pH 8.0
Trypsin	0.125% Trypsin 0.5 mM EDTA 1×PBS

2.10 Markers

DNA

1 Kb DNA ladder	Invitrogen, Karlsruhe
100 bp DNA	Invitrogen, Karlsruhe

Protein

Prestained Protein Marker	Fermentas, Canada
Prestained Protein Marker Broad Range	BioLabs, England

2.11 Primers

The primers were supplied from Operon, Cologne. Restriction sites are shown in bold. The primer sequences used for analysis of the gene trap vector insertion in mouse genome are documented in the section 4, together with schemas of corresponding reactions.

Primer	$5' -$ Sequence $-' 3$	Amplification
sense	GAATTCACCATGAGTGAGGAGTCACCGCTG	C'–terminus–Spar3 (3903 – 5780 bp of Spar3)
anti–sense	GTCGACTCAGAGTTCCTTCTTCTCCCTGCT	C'–terminus–Spar3
sense	GAATTCACCATGAGTGAGGAGTCACCGCTG	Coiled coil of Spar3 (5104 – 5337 bp of Spar3)
anti–sense	GTCGACTCAGAGTTCCTTCTTCTCCCTGCT	Coiled coil of Spar3
sense	GAATTCTCGAGTGACAGTGGCATC	C'term–Δcoil–Spar3 (3903 – 5130 bp of Spar3)
anti–sense	GTCGACATCCAGCGGTGACTCCTC	C'term–Δcoil–Spar3

2.12 Plasmids

Plasmid	Application	Selection	Promoter	Company
pGEX–4T–1	Expression of GST–tagged protein in bacteria	amp	tac	GE–Healthcare, Munich
pCR 2.1 (TOPO–Blunt Kit)	Cloning and amplification of PCR products	amp/kan	T7	Invitrogen, Karlsruhe
pACT2	Expression of GAL4–AD-fused protein (yeast two–hybrid screen)	amp	ADH1	Clontech, Heidelberg
pAS 2–1	Expression of GAL4–BD–fused protein (yeast two–hybrid screen)	amp	ADH1	Clontech, Heidelberg
pDsRed2–C1–2	Expression of RFP–tagged protein in mammalian cells	kan	CMV	Clontech, Heidelberg
pEGFP–C1–3	Expression of GFP–tagged protein in mammalian cells	kan	CMV	Clontech, Heidelberg

2.13 Additional materials

Cell scraper	BD Falcon, Heidelberg
13 mm ⌀ coverslips	Glaswarenfabrik Karl Hecht, Sondheim
Electroporation cuvette	BioRAD, Munich
Hyperfilm ECL	Amersham Biosciences, Freiburg
Gelatine capsules	Capsuline, USA
Glass beads (plasmid isolation from yeast)	Sigma, Deisenhofen
Grids (electron microscopy)	Plano, Wetzlar
Membrane (dialysis)	Roth, Karlsruhe
Micro Bio–Spin P–30 Tris chromatography columns	BioRad, Munich
Neubauer chamber	Brand, Wertheim
Nylon sieves	BD Falcon, Heidelberg
24–well plates	BD Falcon, Heidelberg
Petri dishes	NUNC, Danmark
Poly–Prep chromatography column	BioRAD, Munich
45 μm filters	Schleicher & Schuell, Dassel
Nitrocellulose membrane (Western blot)	Schleicher & Schuell, Dassel
Secure clamps for dialysis	Roth, Karlsruhe
Whatman paper (Western blot)	Schleicher & Schuell, Dassel
Whatman # 5 filters (filter-lift assay)	Schleicher & Schuell, Dassel

2.14 Equipment

Cell bench Hera Safe	Heraeus, Hanau
Centrifuges:	
5804 R (cell culture)	Eppendorf, Wesseling-Berzdorf
Multifuge 3 S–R	Heraeus, Hanau
Avanti J–25	Beckman, Krefeld
Ultracentifuge LB–55M	Beckman, Krefeld
Cryocontainer	Nalgene, UK
Cryotom Leica CM3050S	Leica, Wetzlar
Film developer Curix 60	AGFA, Schrobenhausen
Freezer −80°C	Forma Scientific, USA
Homogenizator Potter S	B.Braun Biotech International, Melsungen
Incubators:	
Bacteria and yeast: Binder	Binder, Tuttlingen
cell cultures: Hera Cell	Heraeus, Hanau
Microscopes:	
Axioscope	Zeiss, Oberkochen
EM10 transmission electron microscope	Zeiss, Oberkochen
PCR Mastercycler gradient	Eppendorf, Wesseling-Berzdorf
Pulser	BioRAD, Munich
Scanner MIRAX	Zeiss, Oberkochen
Software:	
Axiovision 4.7	Zeiss, Oberkochen
Adobe Photoshop CS2	Adobe Systems, USA
MatLab 12	The MathWorks, Munich
Thermomixer comfort	Eppendorf, Wesseling-Berzdorf
UV spectrophotometer DU 530	Beckman, Krefeld
Vortex Reax Top	Heidolf, Schwabach

Chapter 3

Methods

3.1 Microbiological methods

3.1.1 Cultivation of bacterial strains

Three basic types of medium for bacteria were used in this work: LB, SOB and 2YT. All three are a mix of tryptone, yeast extract and sodium salt in different proportions. LB medium was used for selective growth of plasmid containing bacteria with an appropriate selection factor (an antibiotic), SOB − for recovery of freshly electroporated bacteria, 2YT − for production of competent bacteria. All media were autoclaved before usage. The appropriate antibiotic was added to the LB medium or LB-agar, when necessary.

For the cultivation of *E.coli* strains, the medium was inoculated with bacterial material (colony from plate, glycerol-culture or preparatory culture) and agitated. Agitation was performed with 200 rpm at 37°C, unless otherwise stated. The bacteria were kept as colonies on agar plates at 4°C up to 8 weeks. Glycerol stock cultures were made for long term–storage. 300 μl of sterile 87% glycerol were added to 700 μl of bacterial suspension of an optical density (OD_{600}) $0.600 - 0.900$ and thoroughly mixed. Such glycerol cultures were stored at −80°C.

3.1.2 Production and transformation of competent bacteria

Competence is the ability of bacteria to take up extracellular "naked" DNA from its environment. The natural competence of bacteria is low. Under certain conditions an artificial competence can be induced. The application of an electrical field on a bacterial culture makes bacteria briefly permeable to DNA. The transfer of external

DNA in bacterial cells is called 'transformation'.

For preparation of electro-competent *E.coli*, the bacterial material was inoculated in 50 ml YT medium and agitated overnight. The preparatory culture was then diluted with fresh YT medium to $OD_{600} = 0.3$ and a final volume of 300 ml. The culture was incubated by agitation up to $OD_{600} = 0.6$. The bacterial suspension was placed on ice for 20 min and then harvested for 10 min at 2000 *g* and 4°C. The pellet was resuspended in 50 ml of deion. water and centrifuged again. The wash–step was repeated three times. The final pellet of bacteria was resuspended in the same volume of 10% [v/v] sterile glycerol and aliquoted in 50 μl. The aliquots were stored at −80°C for several months.

For transformation, an aliquot of competent bacteria was thawed on ice. 25 ng of plasmid DNA or ligation product were added to the bacteria and mixed. The DNA-bacteria blend was placed into the electroporation cuvette, to the Pulser, and a potential of 1.8 kV was briefly applied. The bacteria were resuspended in 800 μl in SOB medium containing 2 mM $MgCl_2$ and incubated 60 min at 37°C by agitation in a 2 ml tube. After centrifugation for 30 sec at 1000 *g*, the bacteria were plated on agar with the appropriate antibiotic. The plate was incubated at 37°C overnight.

3.1.3 Cultivation of yeast

An enriched non–selective yeast growth medium, YPD, was used for cultivation of *S. cerevisiae* cultures. YPD was inoculated with yeast material (a colony from plate, glycerol-culture or preparatory culture) and agitated overnight. The yeast was agitated at 200 rpm and 30°C, unless otherwise stated. For temporary use, *e.g.*, for production of competent yeasts for transformation, strains were kept as colonies on YPD–agar plates at 4°C up to 8 weeks. The glycerol stock cultures were made for long term–storage (the same recipe as in section 3.1.1). The glycerol culture was stored at −80°C.

A selection medium, a Minimal Synthetic Dropout (SD) Base was utilized to select yeast transformants. Dropout supplements were added to the Minimal SD Base to make a synthetic, defined medium lacking the specified nutrients for selecting yeast transformants: SD Leu–, SD Trp–, SD Leu–/Trp– and SD Leu–/Trp–/His–. Adenine-hemisulfate (AHS) was always added to the agar plates with a selection medium to reduce the rate of reversion of *ade2–101* mutation, which leads to the synthesis of red pigment and is therefore unwanted.

3.1.4 Production and transformation of competent yeast

Eucaryotic cells such as yeast can also be made competent for transformation. The yeast material was inoculated in 25 ml YPD–medium and agitated overnight. Then, the preparatory culture was mixed with fresh YPD medium to $OD_{600} = 0.3$, to 50 ml volume and agitated to $OD_{600} = 0.6$. The cells were harvested 5 min at 1000 g and 4°C. The yeast were resuspended in 25 ml ice cold deion. water and pelleted again. The wash–step was repeated twice. After the last washing step, the pellet was resuspended in the same volume of 1 M sorbitol and aliquoted in 50 μl. The competent yeast were stored up to one week at 4°C. For the best results the competent yeast were transformed the same day or the day following the preparation.

For transformation, 0.1 μg of plasmid DNA was added to an aliquot of competent yeast. The DNA-yeast mix was placed in the ice–cold electroporation cuvette to a Pulser. A 2.5 kV potential was shortly applied and yeast were transferred to 2 ml tube filled with 1 ml YPD medium. The tube was incubated by agitation for 2 h. The yeast were pelleted 30 sec at 2000 g and plated on appropriate selection agar. The plates were incubated 3 to 7 days at 30°C.

3.2 Isolation and purification of DNA

Plasmids are non-obligate, circular, extrachromosomal bacterial replicons, which are used for cloning DNA fragments. The cultivation of bacteria leads to the amplification of plasmid DNA in a large scale for cloning, transformation and transfection of the cells. For DNA isolation bacteria are lysed by strong alkali (Birnbaum and Doly, 1979). Proteins are denatured by strong alkali (NaOH) and strong detergent (SDS). The small plasmids are stable in alkali and therefore remain free in the solution, and are separated from proteins and chromosomal DNA. The plasmid solution can then be purified in anion-exchange columns. For rapid extraction, the plasmids are precipitated by ethanol.

3.2.1 Rapid extraction of plasmid DNA from *E.coli*

Rapid DNA extractions were performed to reveal recombinant clones from *E.coli* containing plasmids. This method was used for the quick analysis of transformants, when the yield and purity of DNA was not crucial.

The material of one colony was inoculated in 1 ml of LB medium with antibiotic and grown overnight. The bacteria were centrifuged for 1 min at 12000 g and the medium

was discarded. The pellet was resuspended in 200 μl of **Solution 1** by vortexing. An equal volume of alkalic lysis buffer (**Solution 2**) was added to the suspension and mixed by inverting the tube. The mix was incubated 5 min at RT. 200 μl of the neutralization buffer (**Solution 3**) and 200 μl of chloroform were immediately added to the lysed bacteria and intensively mixed. After 10 min centrifugation at 12000 g and RT the upper phase (approx. 600 μl) was transferred to a fresh tube and the DNA was precipitated with 40 μl of 3 M sodium acetate and 1 ml of 100% ethanol. The DNA was pelleted by a 10 min centrifugation at 12000 g. The DNA pellet was washed with 1 ml of 70% ethanol. The DNA was dried for 10 min at RT and resuspended it in 30 μl of deion. water containing 1 μg/μl RNase A.

Solution 1 (resuspension buffer)	50 mM glucose 25 mM Tris–HCl, pH 8.0 10 mM EDTA
Solution 2 (alkalic lysis buffer)	200 mM NaOH 1% [w/v] SDS
Solution3 (neutralization buffer)	3 M potassium acetate 11.5% [v/v] acetic acid

3.2.2 Mini–, Midi– and Maxi–extraction of plasmid DNA from E.coli with anion exchange columns

When higher purity and concentration of DNA were needed, the DNA was extracted with *JETQUICK Plasmid Miniprep Spin Kit* or *JETSTAR Plasmid Midi/Maxi Kit* according to the instructions of the company. For transfection of hippocampal primary culture endotoxin-free plasmid DNA was isolated with *NucleoBond PC 500 EF Kit* according to the reference book provided by the manufacturer.

3.2.3 Rapid extraction of plasmid DNA from *S. cerevisiae*

Rapid DNA extraction is used for isolation of both plasmids (section 3.13) from yeast colonies obtained by a yeast–two–hybrid screen. The yield and purity of DNA is not crucial since DNA is used for transformation in bacteria.

The material of one yeast colony was inoculated in 2 ml of YPD medium and agitated overnight at 30°C with 200 rpm. The yeast culture was pelleted for 1 min at 12000 g and the medium was discarded. 200 μl of lysis solution, 200 μl of glass beads

and 200 μl of chloroform were added to the yeast pellet. The mixture was vortexed vigorously for 2 min. After 5 min centrifugation at 12000 g and RT, the upper phase was transferred to a new tube. 3 M sodium acetate (pH 5.2, 1/10 vol. of upper phase) and 96% ethanol (2.5 vol. of upper phase) were added to the tube. The mixture was centrifuged for 30 min at 12000 g, RT. The obtained pellet containing the DNA was washed with 1 ml of ice–cold 70% ethanol, dried at RT 10 min and resuspended in 30 μl of deion. water. $1-2$ μl of the isolated DNA was used for transformation of competent bacteria.

Yeast Lysis Solution
2% [v/v] Triton X–100
1% [w/v] SDS
100 mM NaCl
10 mM Tris–HCl, pH 8.0
1 mM EDTA

3.2.4 Isolation and purification of DNA from agarose gels

DNA purified by separation in agarose gels is frequently used for many molecular techniques, *e.g.*, sequencing or ligation. To obtain the DNA, the band of interest was cut out with a sterile scalpel. The DNA was then extracted with JETQUICK Gel Extraction Spin Kit according to the instructions of the manufacturer.

3.2.5 DNA extraction from mouse tail biopsies

DNA extracted from tail tissue was used for genotyping of animals by PCR. The tail biopsies were performed by qualified staff of the animal facility. The animals were older than 21 day.

The tail biopsies (approx. 5 mm of tail) were shortly frozen for $15-30$ min at -80°C. After that, the tails were placed at RT and 700 μl of tissue lysis buffer was pipetted to each tail. The tail was agitated in the buffer at 56°C for 2 h. The unsolved remains of tissue (mostly hairs) were pelleted by centrifugation (10 min, 13000 g, RT). The supernatant was placed into 1.5 ml tube and an equal volume of isopropanol was added. The mixture was incubated for 10 min at RT to precipitate DNA from the solution and then pelleted for 10 min by centrifugation at 13000 g and RT. The DNA-containing pellet was washed with 1 ml of cold 70% ethanol and centrifuged again (10 min, 13000 g, RT). The ethanol was discarded and the DNA was dried at 60°C in a thermomixer. 100 μl of Tris-EDTA (TE) buffer were pipetted to the DNA. To bring the DNA pellet into solution the cap was vortexed intensively and incubated 10 min

by agitation at 65°C. The obtained DNA was diluted 1:20 in TE buffer and set as a template for PCR.

Tissue lysis buffer
10 mM Tris–HCl pH 8.0
100 mM EDTA
0.5% [w/v] SDS
0.5 mg/ml proteinase K
0.2 mg/ml RNase

3.2.6 Estimation of DNA concentration

The concentration and quality of a DNA or RNA sample were measured with a UV spectrophotometer. DNA in solution has an absorption peak at 260 nm. The measurement requires a control (100 μl of solvent, normally distilled water). Simultaneously, it was possible to assess the purity of DNA. Evaluation of the DNA quality is based on the fact that the OD at 260 nm is twice that at 280 nm if the solution contains pure DNA. If there is any contaminant, the OD ratio between 260 and 280 nm will be affected. Clean DNA has an OD_{260}/OD_{280} between 1.8 and 2.0. If the measured value is lower, it indicates a contamination (Sambrook et al., 1989). The concentration of double stranded DNA is calculated as follows:

1. measurement of absorbancy A_{260} after dilution of DNA sample
2. sample containing 50 μg/ml DNA has an OD of 1.0 at a wave length of 260 nm; $A_{260} \times 50 \times \text{DILUTION FACTOR} = [\text{c DNA}]$ μg/ml (in undiluted sample)

3.3 Work with recombinant DNA

3.3.1 Restriction of DNA

There are three main groups of restriction endonucleases: Type I, II and III. Only type II endonucleases recognize specific DNA sequences and cleave at constant positions at or in the vicinity to that sequence. Usually they require Mg^{2+} ions as a cofactor. More than 3500 endonucleases of type II are characterized and many are commercially available. The enzymes of Type II (Invitrogen, Karlsruhe) were used in this work. For analysis of plasmids on a small scale, $0.2 - 1\,\mu$g of DNA (or approx. 6 μl DNA from a probe of a rapid extraction, section 3.2.3) were pipetted to a 1.5 ml tube. 1.5 μl of 10× endonuclease–specific buffer (provided by the manufacturer) were added. 3 units (U) of enzyme or 2 U each of two different enzymes (when restriction in one buffer was

possible) were added to the DNA mix. The probe was filled to a final volume of 15 μl with deion. water and incubated for 1 h at the optimal temperature (usually 37°C). The efficiency of a restriction was verified on agarose gel (section 3.3.4).

For the restriction in a preparative scale $5 - 10\,\mu$g of DNA were mixed with 8 μl of 10× endonuclease-specific buffer (Invitrogen, Karlsruhe). 1 μl of enzyme (10 U/ μl) or 1 μl of two different enzymes, if necessary, were added to the probe. Deion. water was pipetted to a final volume of 80 μl. The restriction occurred for $1 - 2$ h as described above. The DNA–loading buffer was added to the probe and the DNA was loaded onto the agarose gel. After separation the DNA fragments were cut out of the gel and processed as described in section 3.2.4.

3.3.2 Ligation

Ligation with T4–DNA–ligase

The connecting of ends of linear DNA fragments together by covalent bonds is called ligation. DNA ligation involves the creation of a phosphodiester bond between the 3' hydroxyl group of one nucleotide and the 5' phosphate group of another nucleotide. The enzyme is derived from the T4 bacteriophage (T4 DNA ligase) is used to ligate DNA fragments. This enzyme ligates DNA fragments with sticky or blunt ends in the plasmid DNA. The reaction requires $0.25 - 1$ mM ATP.

For the ligation $50 - 100$ ng DNA of digested vector and DNA–fragment were pipetted in a tube. 1 μl of 5× ligase-buffer (Invitrogen, Karlsruhe) and 1 U of T4–DNA–Ligase were added to DNA. The probe was filled with distilled water to a final volume of 5 μl. The ligation was carried out 1 h at RT or overnight at 16°C.

TOPO-Cloning

The PCR–products were cloned into the TOPO–vector by the Zero Blunt TOPO PCR Cloning Kit. The method enables direct cloning of the PCR product into the vector without additional procedures. The basis of TOPO cloning is the enzyme DNA topoisomerase I from the *Vaccinia virus*, which functions both as a restriction enzyme and a ligase. Its biological role is to cleave and rejoin DNA during replication. Invitrogen (Karlsruhe) provides a linearized vector with topoisomerase I covalently bound to each 3' phosphate. By addition of the PCR–product the enzyme religates the ends of fragment and vector and is released from the DNA.

3.3.3 Polymerase chain reaction (PCR)

The PCR is an *in vitro* technique for exponential amplification of a DNA fragment via enzymatic replication without using a living organism. It relies on the ability of DNA-copying enzymes to remain stable at high temperatures (*e.g.*, Taq–polymerase from ***T****hermus* ***aq****uaticus* or Pfu–polymerase from ***P****yrococcus* ***fu****rosius*). To copy DNA, the polymerase requires two other components: a supply of the four nucleotides and a short sequence of $20-30$ nucleotides, a primer, to initiate the process. Two different primer sequences are used to bracket the target region to be amplified.

One PCR cycle consists of three steps:

- denaturation of DNA: $1-10$ min at $94-96$°C, DNA is denatured into single strands;
- annealing the primer: one to several minutes at $50-65$°C, the primers hybridize or "anneal" by hydrogen bonds to their complementary sequences of the target DNA strand (template);
- synthesis: one to several minutes at 72°C, the polymerase binds and extends a complementary DNA strand from each primer.

The cycle is repeated 30 times or more. The amplification is selective – only the DNA sequence located between the primers is amplified exponentially. Each newly synthesized DNA piece acts as a new template. Following amplification, the PCR products can be easily analyzed by agarose gel.

The exact schedule of the reaction (temperature and duration of three steps of reaction) was specific to each experiment, depending on properties of the template DNA and of the primers. A DNA thermal cycler was used to program the reaction. For a typical reaction 1.5 ng of template DNA was pipetted together with 10 ng of sense primer and 10 ng of antisense primer and filled to a final volume of 25 μl with a High fidelity PCR Supermix. The Supermix contained Taq polymerase (produces sticky ends) and Pfu–polymerase (makes blunt ends).

3.3.4 DNA agarose gel electrophoresis

Electrophoresis is a technique that results in the separation of charged molecules by weight. It is used for analysis and purification of PCR products or digested DNA. DNA is a negatively charged molecule in solution, therefore it is moved by electric potential through an agarose matrix. Higher concentrations of agarose facilitate separation of

small DNA fragments and low agarose concentrations allow resolution of larger pieces of DNA. Agarose was mixed with TAE buffer to the concentration of 1%. The agarose suspension was heated in a microwave oven until the agarose was completely melted. To visualize the DNA after electrophoresis, ethidium bromide was added to the melted agarose to a final concentration of $0.2\,\mu$g/ml. The solution was poured into a casting tray containing a sample comb. After solidification at RT, the gel was inserted into the electrophoresis chamber filled with TAE buffer. The DNA samples mixed with a $6\times$ DNA loading buffer were loaded into gel wells. A field strength of $5-8\,$V/cm was applied to the gel for $40\,\text{min}-1\text{h}$ to separate the DNA fragments. Electrophoresis chambers, power supplies, gel casting trays, sample combs were supplied by BioRad Laboratories, USA.

3.3.5 Sequencing of DNA

The principle of DNA sequencing is based on the same principles as PCR reaction (section 3.3.3): DNA denaturation, annealing and replication. The reaction mix includes the template DNA, free nucleotides and an enzyme (Taq polymerase). Additionally it contains only one primer that hybridizes to one strand of the template DNA and fluorescent dideoxyribonucleotides (ddNTP) without 3' hydroxyl group. Once ddNTP is added to the end of a DNA strand, there is no way to continue elongation. The most of the nucleotides are regular, and just a part of them ($\approx 5\%$) are ddNTP, so that 5% of the time the enzyme will get a modified nucleotide and the reaction in this case will be terminated. For example, in case of ddT the strand will be terminated at all possible positions of T. In an automated DNA sequencer, truncated fragments of all possible sizes are separated by size and are monitored by a laser for the four different colors. The color information is decoded into files with information about the position of the nucleotides. The sequencing allows to get an information about the exact sequence of DNA up to $700-1200\,$bp. In this work $1\,\mu$g of DNA and specific primers ($10\,\text{ng}/\mu\text{l}$) were sent for sequencing to MWG-Biotech AG, Ebersberg.

3.4 RNA methods

3.4.1 Isolation of RNA

A $100-200\,$mg piece of brain tissue was homogenized by a syringe in 1 ml of peqGOLD RNAPure solution. $200\,\mu$l of chloroform were pipetted to the probe and vortexed for

10 sec. The mixture was incubated at RT for 10 min and then centrifuged for 30 min at 4°C and 6000 g. The aqueous phase containing RNA was transferred to a new cup. 1 ml of isopropanol was added to the solution and RNA was precipitated by incubation for 10 min at RT. The precipitate was pelleted by a 30 min centrifugation step at 4°C and 6000 g. The pellet was washed twice with 1 ml of 75% ethanol. The pellet was dried at RT and then dissolved in 22 μl of water. To bring RNA into solution the cup was agitated at 60°C for $5 - 10$ min.

3.4.2 Reverse transcription

For the analysis of gene expression, the RNA was reverse transcribed in complementary DNA (cDNA). The cDNA was then used as a template for PCR. The first strand synthesis was carried out with a M–MVL (Moloney murine leukemia virus) reverse transcriptase. 1 μg RNA was diluted in 27 μl of water. Secondary structures were denaturated at 65°C for 5 min followed by a quick cooling on ice. To 1μg of denaturated RNA the following components of the reaction were added: 5× standard buffer (Invitrogen, Karlsruhe), 1 mM DTT, 0.5 mM dNTP-Mix, 400 units of M–MVL reverse transcriptase and 4 μg of random hexamere primers. In some cases, 2 pM of Spar3–specific anti–sense primer were pipetted instead of the random hexamere primers. The annealing of primers occurred at 25°C for 10 min. Then the cDNA synthesis was carried out at 37°C for 50 min and the reaction was stopped by a 5 min incubation at 97°C. 1.5 μl of cDNA mixture was pipetted for an analysis by PCR.

3.5 Cultivation of eucaryotic cell lines

Cell cultures can be subdivided into primary cultures and immortalized cell lines. Primary cells are explanted directly from a donor organism. In culture they survive for some time, then they age and die. Some cell types can undergo several but strictly limited number of divisions (*e.g.* blood cells, fibroblasts, glia). The growth properties of immortalized or so–called transformed cell lines have been altered. They grow and divide indefinitely *in vitro* under the correct cultivation conditions. By now a lot of immortalized eucaryotic cell lines of different origin have been obtained, characterized and are commercially available. It is possible to find lines with definite growth properties to overexpress a protein or coexpress several proteins in different "cell contexts". The correct folding of overexpressed protein and specific posttranslational modification is an advantage of the animal cell lines over bacteria. The ease of transfection and cul-

tivation in comparison to the primary cultures make them an essential instrument for the investigations of protein–protein interactions and for the overexpression of proteins in a small scale. All cells were cultivated at 37°C with 5% CO_2 in an incubator. All working media were stored at 4°C. Before application to the cells, all media or enzymes were preheated to 37°C.

3.5.1 Cultivation of cells

The cultivation of immortalized cell lines begins with the thawing of the cells in a low passage (section 3.5.3). A passage is a transfer of a small number of cells in a new flask. Cells were split regularly to avoid senescence associated with prolonged high cell density. The old medium was discarded and the cells were rinsed with calcium– and magnesium–free PBS. 1 ml of 0.5 mM EDTA and 0,125% trypsin solution in PBS was added to the cells and incubated at 37°C, until the cells began to detach. The detached cells were resuspended in 5 ml of serum–containing medium. The number of cells was defined in a Neubauer cell counting chamber. The cells were diluted for cultivation to a concentration of 2.8×10^6 cells per 100 cm^2. For transfection the cells were split 0.7×10^7 cells per 100 cm^2.

3.5.2 Freezing of cells

Cryogenic preservation (storage at −196°C) of immortalized cell lines is necessary to maintain reserves of cells in a low passage. The supply can be used in case of morphological and physiological changes of cells during cultivation or in case of contamination.

The cells chosen for storage were healthy and in a log phase of growth. The cells were rinsed with PBS and trypsinized as described above (section 3.5.1). The detached cells were resuspended in serum containing medium and pelleted by centrifugation for 3 min at 600 g. The cells were diluted with a cooled (4°C) cryoprotectant solution of 10% DMSO in 90% FCS to a final concentration of $1 - 5 \times 10^6$ cells per ml. The cell suspension was aliquoted into cryovials and placed into a cryocontainer filled with isopropanol. The vials with cells were incubated for 24 h in −70°C freezer and then transferred to liquid nitrogen ($T \approx -196$°C). The number of holder, cell line, passage of the cells, date were documented in a card file.

3.5.3 Thawing of cells

Immortalized cell lines were stored in liquid nitrogen at $T \approx -196°C$. For cultivation the cells were thawed. The vial with cells was transferred from liquid nitrogen to a 37°C water bath. The content of the vial was resuspended in 10 ml of DMEM with 10% FBS and 2 mM glutamine. The cells were pelleted by centrifugation for 5 min at 600 g. The supernatant still containing the cryoprotector, which is toxic for the cells, was immediately discarded. 10 ml of fresh DMEM with 10% FBS and 2 mM glutamin was added to the pellet and the cells were pipetted into a Petri dish. The next day the cells were washed and the old medium was replaced by a fresh one. The culture was split when the cells formed a confluent layer. Further on, the cells were cultivated as described in a section 3.5.1.

3.5.4 Primary culture of hippocampal neurons

The primary culture system provides a powerful model for the study of hippocampal neurons *in vitro*. The neurons were cultivated on glass coverslips in 24–well–plates. Before the cell preparation, the coverslips were coated 1 h at 37°C with 0.05 mg/ml poly–L–lysin and the wells were washed with sterile water. The cells were extracted from the hippocampi of rat embryos on embryonic day 18 (E18). The pregnant rat was killed by an overdosis of CO_2. The uterus containing the embryos was removed with forceps. The heads of the embryos were dissected with scissors and placed in a petri-dish with ice–cold HBSS. Each head was fixed with forceps through the eyes, the skin peeled off with other forceps and the skull was opened with scissors. The brain was taken out and put in ice–cold HBSS. The hemispheres were opened, the *pia mater* and *arachnoid* were removed, and the hippocampus was cut out of the brain. All hippocampi were collected to a 15 ml tube with ice–cold HBSS. After all embryos were preparated the 15 ml tube with tissue pieces was transferred to a clean bench. The hippocampi were washed three times with 8 ml of HBSS. The last portion of HBSS was taken off to 1.8 ml and 200 μl of 2.5% trypsin were pipetted to the final concentration of 0.25%. The tissue was incubated with trypsin for 20 min at 37°C. After incubation the supernatant was removed. The hippocampi were washed five times with 5 ml HBSS. The last aliquot of HBSS was taken off to the volume of 1.6 ml. 400 μl of DNase I in HBSS were added to the tissue to a final concentration of 0.01%. The whole volume was pipetted up and down until the cells were dispersed. The suspension was filtered though a nylon sieve of an aperture of 125 μm. The sieve was washed with 18 ml of DMEM+. The cells were counted in a Neubauer chamber and diluted with DMEM+

to an appropriate concentration for seeding. Per well 4×10^4 cells per ml were plated for immunostaining and 8×10^4 cells per ml - for transfection. After 24 h DMEM+ was replaced for neurobasal medium+. The culture of primary neurons remained stable up to 6 weeks.

3.6 Transfection of cells

Transfection is a method by which plasmid DNA is delivered into cultured mammalian cells. The transfection is mostly carried out chemically by mixing cationic lipids with the DNA to produce liposomes, which fuse with the cell plasma membrane and release DNA into the cell. Immortalized cell lines were transfected with FuGENE. The transfection efficiency was at least above 30%. $24 - 48$ h after transfection the cells were fixed for immunofluorescence or collected for Western blotting (sections 3.9.2, 3.9.4). Primary cell cultures were transfected with Optifect. The efficiency of transfection was under 1%. It was, however, sufficient to obtain results for immunostaining.

3.6.1 Transfection of cell lines

3 μl of FuGENE 6 Transfection Reagent were combined with 75 μl of DMEM and 1μg of DNA. After 15 min incubation the mix was applied to the cultures of Cos–7 or HeLa cells, split one day before transfection.

3.6.2 Transfection of primary hippocampal neurons

In order to increase the survival rate of transfected cells, the neurons were washed twice with 600 μl of neurobasal medium. Before transfection the antibiotic–containing medium was changed for 500 μl neurobasal medium supplemented with B27 and glutamine but lacking antibiotic. The amount of transfection reagent, media and DNA was optimized for hippocampal cells in 24 well plates. For each well, 3 μl of Optifect were mixed with 50 μl of neurobasal medium and incubated 5 min at RT. At that time 1 μg of DNA was pipetted to 50 μl of neurobasal medium in another cup. Both mixtures were mixed together and incubated for 30 min at RT. The resulting 100 μl mixture of DNA and transfection reagent were added into the well. The cells were placed in the incubator. The fluorescence of EGFPC1–3 vectors was visible after $6 - 10$ h of transfection. The cells were fixed $24 - 48$ h after transfection.

3.7 Preparation of protein extracts from cells and tissues

To prevent unwanted degradation of proteins during protein extraction, EDTA–free complete protease inhibitor (PI) was added to all solutions except to PBS and SDS–PAGE probe buffer. All buffers, centrifuges and centrifuge tubes were cooled to 4°C before the experiments.

3.7.1 Preparation of protein lysates from cultured cells

The cultured cells were washed 3 times with cold PBS. The cells were collected with a cell scraper in 150 μl of 1× loading buffer for SDS–PAGE (section 3.9.2). Before applying to the gel the probe was incubated 5 min at 95°C.

For extraction of proteins associated to the cytoskeleton, the cells were collected in 150 μl of RIPA buffer, which contains a composition of detergents for optimal protein extraction. The cells were agitated in a 1.5 ml tube at 4°C. The extraction time was defined empirically and varied from 1 to 24 h. After 15 min of centrifugation at 4°C and 12000 g, the supernatant was mixed with 2× loading buffer for SDS–PAGE (section 3.9.2) and incubated 5 min at 95°C.

3.7.2 Preparation of protein extracts from tissue

The preparation of brain extracts was most often practiced. The same procedure was used for protein extraction from other tissue with insignificant modifications. The rat was sacrificed by an overdosis of CO_2 . The head was cut off and the skin removed. The skull was opened with scissors and the brain was taken out. The brain was placed in cold buffer A (section. 3.7.3, 10 ml per 1 g of tissue) and homogenized with 12 strokes of 900 rpm in a potter S on ice. After 10 min of centrifugation at 1000 g the supernatant (S1) was collected in a beaker and another portion of buffer A was added to the pellet (P1). The pellet P1 was homogenized with another 12 strokes. The centrifugation step was repeated and the supernatant (S1') was poured to S1. Both supernatants (S1+S1') were centrifuged for 15 min at 12000 g. The resulting supernatant was discarded. The pellet (P2) was resuspended either in the same volume of RIPA buffer for protein extraction or in 1 ml of 50 mM Tris–HCl, pH 8.0 for following processing with SDS–PAGE probe buffer.

The extraction with RIPA buffer was necessary for most applications, *e.g.*, coim-

munoprecipitation and pull–down assay. The extraction time (at 4°C, under rotation) varied from 1 to 24 h. After incubation, the probe was centrifuged for 15 min at 4°C and 12000 g. The supernatant was processed for SDS–PAGE or used for other applications.

3.7.3 Isolation of subcellular protein fractions

The excitatory synapses display a prominent structure on the surface of postsynaptic membrane called the postsynaptic density (PSD). The series of centrifugation steps in combination with Triton X–100 extraction allow to separate fractions with different cell organelles, compartments and a PSD fraction (Carlin et al., 1985). The experiment allows to locate proteins in neurons "biochemically". Centrifugations were held in the rotor SS–34 (Sorvall), JA25.50, unless otherwise stated. During fractionation the weight of pellets was controlled at each step. Aliquots of all fractions, whose abbreviations are designated in bold, were collected and analyzed by Western blotting. The blot illustrated the subcellular distribution of target proteins in neurons.

Brains of three adult rats (approx. 6 g of tissue) were isolated as described in section 3.7.2. The tissue was homogenized in buffer A (10 ml/g) with 12 strokes by 900 rpm. An aliquot of "total homogenate" at this step (**H**) was taken for analysis. Then the homogenate was centrifuged twice for 10 min at 1000 g with a further homogenization step between the centrifugations (section 3.7.2). The supernatants S1 and S1' were collected and centrifuged for 15 min at 12000 g. The centrifugation resulted in supernatant **S2** (soluble fraction) and pellet **P2** (crude membrane fraction). The pellet P2 was resuspended in 10 ml/g of buffer A and homogenized with 6 strokes at 900 rpm. After 20 min of centrifugation at 12000 g the supernatant S2' was discarded and the pellet P2' was resuspended in buffer B (1.5 ml per g of pellet). Three different concentrations of sucrose were poured in tubes for the L7 SW–28 Beckmann rotor building up gradients of sucrose: 9.3 ml of 0.85 M sucrose on the top, 1 M in the middle and 1.2 M at the bottom. 2.5 ml of resuspended P2' in buffer B was gently applied to each sucrose gradient. After 2 h of centrifugation at 85000 g the myelin probe (**My**) was harvested at the top of the upper gradient, the mitochondria (**Mi**) in the $0.85 - 1.0$ M gradient boundary and the synaptosome fraction (**Sy**) in $1.0 - 1.2$ M interphase. Five volumes of 1 mM Tris–HCl (pH8.1) were added to one volume of synaptosome fraction to create an osmotic shock. The mix was agitated 30 min on ice and then centrifuged for 30 min at 33000 g. The supernatant S3 was discarded. The pellet P3 containing synaptosomes was resuspended in 5 mM Tris–HCl (pH8.1), 1.5 ml per g of pellet. The sucrose gradients ($0.85 - 1.0 - 1.2$ M) were made as previously described and 2.5 ml

of P3 in 5 mM Tris was applied to each gradient (typically only to one, due to continuous material reduction). The centrifugation occurred for 2 h at 85000 g in a L7 SW–28 Beckmann rotor. The fraction "synaptic junctions" (**SJ**) was collected in the $1.0 - 1.2$ M interphase. 6 ml of buffer B and 6 ml of buffer C were added per 1 g of synaptic junctions. The mixture was agitated for 15 min on ice and centrifuged for 30 min at 33000 g. The supernatant S4 was discarded. The pellet P4 contained the PSD I fraction. Buffer B and C were added in the same proportion per g of pellet. The following extraction for 15 min was carried out on ice. The extract was centrifuged for 30 min at 33000 g. The supernatant S5 was discarded. The pellet P5 contained the **PSD II** fraction.

Buffer A	0.32 M sucrose 5 mM HEPES, pH 7.4
Buffer B	0.32 M sucrose 5 mM Tris–HCl, pH 8.1
Buffer C	0.32 M sucrose 12 mM Tris–HCl, pH 8.1 1% [v/v] Triton X–100

Solutions for the gradients	0.85 M/1.0 M/1.2 M sucrose	0.85 M (1.0 M, 1.2 M) sucrose 5 mM Tris–HCl, pH 8.1

3.7.4 Protein expression in bacteria

The glutathione S–transferase (GST) Gene Fusion System is utilized for the controlled expression of foreign proteins at high levels in *E. coli*. The pGEX–T1–3 vector contains the *tac* hybrid promotor and the lac Iq repressor. In the absence of the inductor the gene product of the lac Iq repressor binds at the operator of the *tac* promotor and blocks the expression. After addition of the inductor, isopropyl–β–D–1–thiogalactoside (IPTG), the *tac* promoter is derepressed and activated. The best results were obtained, when the pGEX vectors were transformed in the strain BL21. This strain is deficient in the OmpT and Lon proteases which are the major sources of protein degradation in bacteria. These mutations increase the yield of protein. Up to several mg of overexpressed protein can be obtained and purified at glutathione-sepharose column. GST–tagged proteins were used for pull–down experiments to confirm protein–protein interactions, for immunization of animals and for assays, illustrating the specificity of AB.

3.7.5 Induction of protein expression in bacteria

E.coli BL21 was transformed with pGEX–4T–1 vector, containing the specific DNA fragment. A small volume of LB medium containing 100 μg/ml ampicillin was inoculated with a bacterial colony from an agar plate. The culture was grown overnight at 200 rpm at 37°C. 5 ml of the overnight culture were added to 295 ml of fresh LB–ampicillin medium. The culture was incubated by agitation at 37°C up to an $OD_{600} = 0.4$. IPTG was added to a final concentration of 1 mM and the culture was agitated for additional 2 h. The bacteria were placed on ice for 15 min and then harvested by centrifugation for 15 min at 4°C and 2000 g. The pellet was frozen at −20°C overnight.

3.7.6 Purification of GST–tagged protein

The principle of purification is based on glutathione affine chromatography. The N-terminal part of the GST-fusion proteins binds to glutathione-sepharose. The column is washed intensively. GST–tagged proteins are eluted with glutathione.

The bacterial pellet (section 3.7.5) was resuspended in 12 ml of ice–cold PBS. Lysozyme was added to the suspension to a final concentration of 1 mM. After incubation for 1 h on ice the bacteria were lysed. 10 ml of 0.2% Triton–X100 were mixed in the viscous solution of lysed bacteria. This step prevents aggregation of proteins. The enzymes DNase and RNase were added to the final concentration of 5 μg/ml each. The mixture was incubated by agitation 20 min at 4°C and then centrifuged 30 min at 3000 g in an SS34 Sorvall Rotor. The supernatant was collected in a precooled tube and mixed with 1 mM DTT. The solution was filtered through a 0.45 μm filter. In the meantime, 500 μl of glutathione–sepharose slurry was washed three times with 20 ml cold PBS. The filtered supernatant was poured into a tube containing glutathione–sepharose. The suspension was incubated by rotation at 4°C overnight. The beads and protein solution were applied to a Poly–Prep chromatography column. The column was washed with several bed volumes of cold PBS until the $OD_{280} = 0.02$ (usually $20 - 25$ times with 1 ml of PBS). The GST–tagged protein was eluted with repeated application of 300 μl of elution buffer (up to 12 times). All aliquots were collected and placed on ice. The OD_{280} of the aliquots was examined. The aliquots containing a high concentrations of overexpressed protein were pooled and frozen at −80°C or subjected to dialysis (section 3.9.6). The concentration of overexpressed protein was controlled on SDS–PAGE, using Gel Code Blue Stain Reagent (section 3.9.3).

Elution buffer, pH 8.0 30 mM glutathione

50 mM Tris–HCl

3.8 Biochemical assays revealing protein–protein interactions

3.8.1 GST–pulldown–assay

The pull–down assay is an *in vitro* method used to determine interaction between two or more proteins. The requirement for an assay is the availability of a purified and tagged protein, which is used to capture and 'pull–down' a protein-binding partner. The beads with tagged protein are incubated with brain lysate and non-interacting proteins are washed out. The bound proteins are analyzed by Western blotting.

50 μl of the glutathione–sepharose beads were pipetted into a 1.5 ml tube and washed three times with 1 ml of cold PBS. 100 μg of dialysed GST–tagged protein (section 3.9.6) were filled up to 500 μl with PBS and mixed with the beads. The GST-protein and sepharose suspension was agitated for 1 h at 4°C. The beads were centrifuged for 1 min at 2000 g and the supernatant was discarded. 1 ml of brain extract (extraction with RIPA buffer, section 3.7.2) was added to the beads, mixed by vortexing and incubated overnight at 4°C by agitation. Then the sepharose was centrifuged for 1 min at 12000 g and the supernatant was discarded. The beads were washed five times with 1 ml of RIPA buffer. For the last washing step was performed by applying 1 ml of 50 mM Tris–HCl pH 8.0. The sepharose was resuspended in 30 μl of 2× SDS–PAGE loading buffer and processed as described in sections 3.9.2, 3.9.3 for analysis by Western blotting.

To control of the non–specific binding of proteins to the beads, 50 μl of glutathione–sepharose were incubated with the brain lysate only, without coupling GST–tagged protein.

3.8.2 Coimmunoprecipitation

Coimmunoprecipitation aims at the investigation protein–protein interactions *in vivo*. The principle of coimmunoprecipitation is based on the ability of the bacterial protein A and G to bind the Fc region of immunoglobulin class G antibodies (AB). The binding of the Fc region orients the antigen binding domains of AB away from the beads, making them available for binding to their respective target epitope. AB are able to precipitate not only target protein, but also target protein in complex together with interacting

partners. All components of bound immune complex (AB, antigen and interacting proteins) are eluted from the support and analyzed on Western blot with AB against possible interacting partners.

μMACS Protein A conjugated MicroBeads and columns (*Mitenyi Biotech, Bergisch Gladbach*) were used for coimmunoprecipitation. MACS microbeads are extremely small magnetic particles, which are used in combination with columns containing a special matrix. The holder generating a strong magnetic field allows to wash beads without centrifugation. All buffers used for coimmunoprecipitation contained EDTA–free PI. 50 μl of the magnetic beads conjugated with protein A were pipetted into a 1.5 ml tube. 10 μl of polyclonal AB, 5 μl of monoclonal or affinity purified AB were added to the beads and incubated for 40 min on ice to enable the binding of AB to the protein A. 500 μl of the brain extract (in RIPA buffer, section 3.7.2) were added. The mixture was incubated overnight at 4°C by agitation. The column was attached to the magnetic holder and rinsed once with cold RIPA buffer. Then the mixture was applied to the column. The column was rinsed six times with 200 μl of cold RIPA buffer,followed by washing with 200 μl of cold 20 mM Tris–HCl. For elution of proteins the column was incubated for 5 min with 20 μl of preheated to 95°C elution buffer. Afterwards another 50 μl of buffer (95°C) were applied to the column and the eluate was collected. The elution buffer was simultaneously the 1× SDS–PAGE loading buffer. The probe was directly placed to an acrylamide gel for subsequent analysis on Western blot (sections 3.9.2, 3.9.3).

Elution buffer

50 mM Tris–HCl pH6.8
50 mM DTT
1% [w/v] SDS
1 mM EDTA
0.005% [w/v] bromphenol blue
10% [v/v] glycerol

3.8.3 Overlay technique

An overlay assay is based on the incubation of labelled (*e.g.*, GFP tagged) immobilized on the membrane proteins with a tissue lysate. The interaction partners from the tissue lysate are precipitated to the labelled protein on the membrane and can be later detected by specific AB. Individual domains of proteins can be overexpressed as GFP–constructs in cells and examined for the ability to interact with proteins from the tissue lysate. Overexpressed GFP is used as a control of unspecific precipitation.

Cos–7 cells were transfected with GFP constructs (section 3.6.1). After 24 h cells

were harvested and a protein lysate was made as described in section 3.7.1. The probes were applied onto acrylamide gel, so that at least two probes of each GFP–construct were present on one gel.

The lysates of GFP-tagged proteins were separated by SDS–PAGE (section 3.9.2) and transferred to a nitrocellulose membrane (section 3.9.3). The membrane with immobilized proteins was cut into two pieces. The first piece was placed in PBS. The second was blocked for 1 h at RT in 3% milk. The brain extract (in RIPA buffer, section 3.7.2), was added to the blocked membrane and incubated by agitation at 4°C overnight. After incubation with the lysate, the membrane was washed for 1 h with 6 changes of cold PBS. The appropriate 1.AB were applied for detection of proteins precipitated with GFP–constructs. In the meantime the second membrane was taken from PBS and placed in 3% milk for 1 h at RT. The second membrane was incubated with anti–GFP AB. The membranes were incubated with the 1.AB in milk overnight at 4°C. Then, the membranes were rinsed for 20 min with four changes of PBS. Both membranes were incubated for 1 h with respective 2.AB in 3% milk. The membranes were washed again with PBS. The blot was developed as described in section 3.9.3.

3.9 Analysis of proteins

3.9.1 Bicinchoninic acid (BCA) protein assay

The concentration of protein in samples is measured by the BCA protein assay. This is a two–step process, in which Cu^{2+} first forms a complex with protein amide bonds and is reduced to Cu^{+} (biuret reaction). Then BCA forms a detectable purple complex with Cu^{+}, which exhibits a linear absorbance at 562 nm with increasing protein concentrations (Smith et al., 1985). The measurement of protein concentrations was performed with the BCA protein assay kit (Pierce, Bonn) according to the instructions of the producer.

3.9.2 SDS–polyacrylamide gel electrophoresis (SDS–PAGE)

The migration of charged molecules in solution in an electric field is called electrophoresis. Sodium dodecyl sulfate (SDS) is an anionic detergent which denatures proteins by "wrapping around" the polypeptide backbone. Disulphide bridges in proteins are reduced by 2–mercaptoethanol or DTT. All proteins become linear and are coated in a uniform negatively charged cloud. Therefore, on SDS–PAGE migration of proteins

is determined by molecular weight (Laemmli, 1970). The equipment for SDS–PAGE was supplied from BioRAD, Munich.

A gel cassette was assembled from two glass plates with spacers in a casting frame. The resolving gel mix was pipetted to a beaker and poured into a gel cassette. A layer of isopropanol was applied to the acrylamide solution and removed after gel polymerization. The stacking gel solution was poured over the resolving gel. The comb was immediately inserted into the frame and removed after gel polymerization. The protein concentration of the samples for SDS–PAGE was evaluated by the method described in section 3.9.1. The samples were mixed with an equal volume of 2× loading buffer and heated to 95°C for 5 min. For comparative or quantitative analysis of protein expression the same protein concentration was applied to each lane. The gel was put in a electrophoresis chamber filled with running buffer. The molecular weight marker and samples were loaded in wells and a voltage of 100 V was applied. The run time of proteins was monitored by separation of a prestained protein marker. The time of separation was dependent on the percentage of the gel and the molecular weight of proteins to be detected. The gel was stained (section 3.9.3) or used for Western blot (section 3.9.4).

Resolving gel	8% or 10% [v/v] acrylamide–N'N'–methylenebisacrylamide mix 375 mM Tris–HCl, pH8.8 0.1% [w/v] SDS 0.1% [w/v] ammonium persulfate 0.08% [v/v] TEMED
Stacking gel	5% acrylamide–N'N'–methylenebisacrylamide mix 125 mM Tris–HCl, pH 6.8 0.1% [w/v] SDS 0.1% [w/v] ammonium persulfate 0.2% [v/v] TEMED
1×**loading buffer**	100 mM Tris–HCl pH 6.8 4% [w/v] SDS 20% [v/v] glycerol 0.006% [w/v] bromphenol blue 200 mM 2–mercaptoethanol
Running buffer	25 mM Tris 250 mM glycine 0.1% [w/v] SDS

3.9.3 Staining of proteins in acrylamide gels

For detection of proteins acrylamide gels were stained with Gel Code Blue Stain Reagent (Pierce, Bonn). The gels were washed with three changes of deion. water for 15 min. The water was changed for Gel Code Blue Stain and the gel was agitated in the dye solution for 1 h at RT. The washing–steps with water were repeated.

3.9.4 Western Blot

The transfer of proteins from a gel to a membrane and their subsequent detection on the membrane is called Western blot. The method relies on the ability of AB to specifically detect one protein out of a complex protein mixture and allows to obtain semiquantitative data about its molecular weight and expression. The proteins are separated by molecular weight using SDS–PAGE (section 3.9.2) and transferred to a nitrocellulose membrane. The membrane is blocked to quench non–specific binding sites for AB. After the membrane blocking the primary AB are applied to detect the antigen. This is followed by an application of enzyme labelled secondary AB directed against primary. An appropriate substrate is added to the AB-bound enzyme, together they produce a detectable product. In this work, horseradish peroxidase (HRP) labelled secondary AB were used in combination with the ECL Plus Western Blotting Detection Reagents kit as a chemiluminescent substrate for HRP. Light as a product of the enzyme–substrate reaction was detected by Hyperfilm ECL.

The proteins were separated by SDS–PAGE as described in section 3.9.2. The nitrocellulose membrane, gel sized Whatman papers and 2 fiber pads were wet in transfer buffer. The nitrocellulose membrane and gel were sandwiched between 2 Whatman papers and put between two fiber pads. The resulting "pad, papers, gel, membrane, papers, pad" stack was moved to the assembly tray with membrane oriented to positive pole. The gel was closer to the negative pole. The transfer of negatively charged SDS-coated proteins occurred to the membrane placed at positive pole. The assembly tray was closed and put in a blot tank keeping the polarity. The ice-block container was inserted into blot tank for optimal cooling. The tank was filled with transfer buffer. For uniform cooling during transfer a magnet tube was put in a tank for mixing the buffer and tank was placed at 4°C at the magnet plate. The current 1 mA/cm^2 was applied for 90 min. After transfer the membrane was stained with Ponceau S Red solution. Ponceau reversibly binds to proteins and is used as a control of protein transfer. After 5 min incubation with Ponceau, the membrane was washed with water, the blot, was stripped, if necessary.

All incubations were carried out at RT, when not otherwise stated. The non–specific binding sites were quenched by immersing the membrane in 3% [w/v] non–fat milk in TBS for 1 h. The membrane was briefly rinsed with TBS and incubated overnight at 4°C with primary AB diluted in TBS or 3% [w/v] milk and 0.01% [v/v] Tween–20 in TBS. The membrane was washed with three changes of 0.01% Tween–20 [v/v] in TBS for 15 min. HPR labelled secondary AB in 3% milk were incubated for 90 min by agitation. The membrane was rinsed with three changes of 0.01% Tween–20 [v/v] in TBS for 15 min. In the meantime the detection reagents of ECL Plus System were equilibrated to RT. The solutions A and B were mixed in ratio 40:1 and the mix was applied to the membrane (0.1 ml/cm^2). After 5 min of incubation the membrane was put in a film cassette. The next steps were carried out in the dark room. The membrane was exposed to the film for 30 sec −10 min and the film was developed in the machine Curix 60.

Transfer buffer

25 mM Tris
192 mM glycine
20% [v/v] methanol
0.1% [w/v] SDS

3.9.5 Preincubation of AB with antigen

The preincubation of AB with antigen is a control experiment for the specificity of AB in Western Blotting, experimentally leading to the elimination of specific bands on the membrane. 300 μg of purified GST–tagged C'terminus of Spar3 (1300 − 1776 aa) were pipetted to 200 μl TBS. 6 μl of anti–Spar3 (generated against 1300 − 1776 aa) AB were added to the cup and incubated overnight by agitation at 4°C. The incubation was followed by a 15 min centrifugation step at 2000 g and 4°C. The supernatant was added to TBS to a final dilution of preincubated AB (1:500). One part of the blot was placed in TBS with preincubated AB. As a control the second part of the blot with identical SDS–PAGE probes was incubated with anti–Spar3 AB diluted 1:500. The blot was developed as described in section 3.9.4.

3.9.6 Dialysis

Dialysis is a technique that enables the removal of small unwanted compounds from solutions containing macromolecules by selective diffusion through a semi-permeable membrane. The sample is pipetted in the membrane and placed in a large volume

($\times 500 - 1000$ volumes of sample) of dialysis buffer. Differences in the composition between the sample and the dialysis buffer lead to an adjustment of the concentration of the buffer compounds. Molecules that are larger than the membrane pores are retained in the sample, small molecules diffuse through the membrane. The permeability of the membrane depends on the molecular weight cut–off index (MWCO). The concentration of contaminants in the sample is decreased to an acceptable level for usage in some ion-sensitive applications (*e.g.*, GST–pull–down assay).

The tubular membranes for dialysis with a MWCO $8.000 - 10.000$ were soaked for 20 min in deion. water. They were then heated to 80°C in 1 l of 1 mM EDTA in 2% [w/v] sodium bicarbonate for 30 min. The membranes were rinsed in distilled water and transferred into 1 mM EDTA. The tubes were boiled for 10 min. The membranes were stored in 1 mM EDTA at 4°C up to several months or immediately used for dialysis. Before use, the membranes were washed inside and outside with distilled water. Secure clamps were applied to ends of the tubular membrane. $1 - 2$ ml of the sample were loaded into the "tube". The membrane was placed in 4 l of dialysis buffer (0.2 M $NaHCO_3$ in 0.5 M NaCl, pH 8.0). The sample was dialyzed by agitation overnight at 4°C.

3.10 Immunostaining of cultured cells and sections

Immunostaining is an AB-based method, which enables the visualization of specific proteins in sample. Immunostaining consists of several basic steps: fixation (for the preservation of cell morphology and tissue architecture), blocking (for preventing of non–specific AB binding), staining (visualization of specific proteins), washing (washing out unbound or unspecifically bound AB). Each step is optimized empirically, depending on specificity of AB (*e.g.*, background staining or loss of antigenic reactivity in the fixative).

3.10.1 Immunostaining of primary hippocampal neurons

Specific AB that are conjugated with a fluorescent dye (*e.g.*, Alexa-fluor family), are used to perform an immunofluorescence (IF). There are two types of IF staining methods: (1) direct, when the primary AB are labeled with a fluorescent dye; (2) indirect, when secondary AB labeled with fluorochrome are applied to the primary AB. More often double indirect IF is carried out to determine colocalization of protein with some marker proteins. By double IF AB derived from different animal species are mixed

and incubated as a "cocktail" (*e.g.*, rabbit anti-antigen A and mouse anti–antigen B). The corresponding secondary AB (*e.g.*, goat anti-rabbit alexa 488 and goat anti-mouse alexa 648) were mixed in the same way. The secondary AB must be controlled for cross-reaction and for reactivity to other antigens on sample then the primary AB.

If not otherwise stated, the steps of IF were carried out at RT. For the fixative, paraformaldehyde (PFA) was dissolved at temperature lower than 57°C. The fixative, 4% PFA with 2% sucrose in PBS, pH 7.4, was stored as frozen aliquots at −20°C. The mounting medium, Mowiol, was dissolved overnight in a Tris-glycerol solution pH 7.4 and then centrifuged 30 min at 12000 *g*. The aliquots of PFA and Mowiol were thawed shortly before use.

The culture medium was discarded and the cells on coverslips were shortly washed with PBS. For 24–well–plate 1 ml of cold fixative was carefully given to each well. The fixation occurred for 20 min. The PFA solution was replaced with PBS and the cells were washed with three changes of PBS for 15 min. For a better antigen accessibility, the cells were permeabilized 5 min with 0.05% Triton X–100 on ice. To quench unspecific binding sites the coverslips were incubated for 1 h with a blocking solution. Alternatively, blocking solution "A" was used, when AB produced a high background. The primary AB were applied in blocking solution for 2 h at RT or overnight at 4°C. The cells were rinsed for 15 min with three changes of PBS and incubated for 90 min with the secondary AB in blocking solution. The washing step with PBS was repeated. To prevent the building of crystals in the mounting medium, the coverslips were immersed in distilled water for 1 min. The drops of Mowiol were placed to the slides. The coverslips were laid on the mounting medium with the cell layer faced to the drop. The staining was documented using an Axioscope microscope equipped with a Zeiss CCD camera (16 bits; 1280 × 1024 pixels per image). The images were analyzed with the Axiovision and Adobe Photoshop software.

Blocking solution	1 × PBS 0.1% [w/v] ovalbumin 0.5% [v/v] FISH-gel 0.01% [v/v] Tween-20
Blocking solution "A"	50 mM Tris–HCl pH 7,4 150 mM NaCl 5% [v/v] FCS 0.3% [v/v] Triton-X100

3.10.2 Immunohistochemistry

Staining of tissue sections, immunohistochemistry, is often performed using non–fluorescent methods, *e.g.*, with peroxidase coupled secondary AB. This enzyme catalyzes reaction with diaminobenzidine tetrahydrochloride (DAB) that results in a colored product.

The rat was sacrificed and the brain was isolated as described in section 3.7.2. The tissue was immersed for 24 h in Bouin solution. After fixation, the brain was rinsed overnight in flowing water. The tissue was consequently dehydrated in 70% ethanol for 24 h, in 80% ethanol for another 24 h, in 96% ethanol for 2 h and, finally, in ethanol abs. for the next 2 h. The brain was placed in methylbenzoat and incubated for 48 h, using two changes. The methylbenzoat was changed for preheated paraplast and the sample was incubated overnight at 60°C. The brain was embedded in fresh paraplast. The block containing the sample was left to indurate overnight at RT. 8 μm thick sections were cut and immobilized on object plate for immunostaining.

Before staining the sections were deparaffinized for 15 min in three changes of xylol. The sections were hydrated in isopropanol, ethanol abs., 96% ethanol and, finally, in 70% ethanol, for 5 min each incubation. After a short immersion in distilled water sections were incubated for 10 min in a hydrogen peroxide solution. This step is necessary to suppress the activity of endogenous peroxidase. The specimen was rinsed for 15 min with three changes of PBS.

The following incubations were carried out in a humidified chamber at RT unless otherwise stated. The unspecific binding sites were blocked by incubation with 1% bovine serum albumin (BSA) in PBS for 1 h. The 1.AB were applied to the sections in 0.5% BSA in PBS and incubated overnight at 4°C. After washing with three changes of PBS, 5 min each, the sample was transferred into biotin–conjugated 2.AB for 2 h. The washing step with PBS was repeated. In the meantime, the solutions A and B of the ABC Vectastain kit, were pipetted together and left for 30 min at RT before application to the section. The preincubation is necessary for the formation of peroxidase conjugated avidin–biotin complexes. The ABC mix was applied to the section and incubated for 2 h. The sample was rinsed with 2 changes of PBS, 5 min each. For pH equilibration the sections were placed in 5 mM Tris–HCl, pH 7.4 for 5 min. The developing solution was mixed with a substrate for peroxidase, DAB, and incubated with the sections for $5 - 10$ min. When the colour was intensively brown, the reaction was stopped by washing. The sample was rinsed for 10 min with two changes of distilled water and dehydrated. The dehydration occurred in five steps, 5 min each, in

70% ethanol, 96% ethanol, isopropanol and two changes of xylol. The sections were embedded in mounting medium and documented on the MIRAX scanner.

Bouin fixative	75 ml picric acid (saturated) 25 ml 37% formalin 5 ml acetic acid
Hydrogen peroxide solution	0.1% [v/v] hydrogen peroxide 5 mM Tris–HCl, pH 7.4 130 mM NaCl
ABC solution (ABC Vectastain kit)	1.0 ml PBS 20 μl solution A 20 μl solution B
Developing solution	5 mM Tris–HCl, pH 7.4 0.1% [v/v] hydrogen peroxide 0.6 mg/ml DAB

3.10.3 $\beta-$galactosidase reaction on brain cryosections

To test knock–out mice for expression of the reporter gene $\beta-$galactosidase, the brains of knock–out animals were isolated (as in section 3.7.2) and shock–frozen in liquid nitrogen. If stored for several days the brains were transferred to $-80°$C freezer. 8 μm thick sections were cut at a cryotom and immobilized to an object plate. The substrate for $\beta-$galactosidase, 1 mg/ml X–gal solution and 39 mM 2–mercaptoethanol in Z–buffer, were applied to fresh cryosections. The sections were placed in a humidified chamber and incubated at 30°C up to 2 h. The samples were shortly rinsed in water, embedded in mounting media and documented on the MIRAX scanner.

3.11 Electron microscopy

Small pieces of rat brain (cortex) were immersed in 4% PFA and 0.1% glutaraldehyde in 0.1 M phosphate buffer pH 7.3 and incubated for 3 h. The tissue was washed in five changes of 0.1 M phosphate buffer, 10 min each. The samples were dehydrated by 15 min incubations in 30%, 50%, 70%, 90%, 100% propanol and incubated in 1:1 LR-Gold:propanol for 2 h. Then the tissue was transferred into 100% LR–Gold and incubated for 1h. After polymerization for 48 h under UV light, the samples were cut on a Reichert ultramicrotome. Ultrathin sections ($70-80$ nm) were collected on grids.

All solutions used for electron microscopy were centrifuged before application. The sample was blocked for 10 min in 0.2% gelatine and 0.5% BSA in PBS. The grids were shortly dried by a touch of a filter paper, placed onto a drop of Spar3 AB and incubated for 15 min. The grids were consequently immersed in four vials with blocking buffer, for 30 sec each. This was followed by a 15 min incubation with gold-conjugated second AB directed against rabbit. The grids were rinsed by immersion for 30 sec in blocking buffer, PBS, and distilled water. The grids were dried and contrasted with 2% uranyl acetate for 4 min and then with 0.3% lead citrate for 1 min. The sections were examined using an EM10 transmission electron microscope at 80 kV.

3.12 *In situ* hybridization

In situ hybridization is a method that uses a labeled complementary DNA (cDNA) probe to localize a specific mRNA sequence in a section of tissue (*in situ*). The hybridization is performed on 8 μm thick cryosections of unfixed tissue. The probe is labelled by radioactivity. It hybridizes to the target sequence at an elevated temperature, and then the excess of probe is washed away.

All incubations were carried out in a humidified chamber. Two different complimentary antisense oligonucleotides (oligos) were applied to detect Spar3 mRNA:

$$5' - \text{GCACCTCCAGCACCGAGATGCTGGCATTTGTACGGT} - 3'$$

and

$$5' - \text{ATTGCGGACTGAAACATGCCAGAAATCTCAAGACAG} - 3'.$$

3.12.1 Radioactive labeling of oligonucleotides

The oligonucleotides were radioactively labelled with $^{32}S - ATP$. 40 ng of oligos were pipetted to 1 μl of 10× Terminal Transferase buffer (Sigma, Deisenhofen) and 2 μl deion. water. 45 μl of $^{32}S - ATP$ and 1,5 μl of terminal transferase were added. The mix was incubated for 4 h at 37°C and centrifuged for 1 min at 2000 g. 38 μl of deion. water was pipetted to the mix. The oligos were purified from unbound $^{32}S - ATP$ on Micro Bio–Spin P–30 Tris chromatography columns.

3.12.2 *In situ* hybridization on tissue sections

The protocol was developed for 20 object plates with sections, 60 µl of hybridization cocktail was applied to a pair of object plates faced to each other. 10 µl of radioactive labelled oligonucleotides and 60 µl of salmon testis DNA were mixed and incubated for 5 min at 80°C. The sample was placed on ice for 3 min. 200 mM DTT in 600 µl of hybridization cocktail (Sigma, Deisenhofen) and 30 µl of tRNA were added to the sample. 60 µl of hybridization solution was applied to the section and covered with another section-containing object plate. The incubation occurred overnight at 42°C and followed by a 15 min wash–step in 1× sodium chloride–sodium citrate buffer (SSC) at RT. Then the samples were rinsed in five changes of 0.1% [v/v] 2–mercaptoethanol in 1 × SSC (washing buffer), 15 min each, at 50°C. The samples were cooled in washing buffer for 15 min at RT and were washed at RT with three changes of 1 × SSC, 2 min each. This was followed by a short immersion (15 s) in 50%, 70%, 96% ethanol and then in ethanol abs. at RT. The sections were dried, placed into a film cassette and exposed to the film in the dark room. The exposure time was about 20 days. The film was developed in the Curix 60 machine.

Hybridization cocktail
50% [v/v] formamide deion.
4 × SSC
1 × PBS
0.5% [v/v] Denhardt's solution
1% [w/v] N–lauryl sarcosine
10% [w/v] dextransulfate

3.13 Yeast–two–hybrid system

Most biological processes such as signal transduction, enzymatic reactions or the formation of cellular structures rely on non-covalent interactions between proteins. The two–hybrid screen is a method of detecting protein–protein interactions in yeast cells (*S. cerevisiae*). The system is often used to find novel interacting partners.

3.13.1 Principle of a yeast–two–hybrid screen

The method is based on the reconstitution of an artificially split transcription factor by a non-covalent protein interaction (Fields and Song, 1989). Transcription factors contain DNA–binding (BD domain) and transactivation domains (AD), which allow the factor to bind DNA, and recruit RNA polymerase. In the case of the yeast transcription

factor GAL4, the two domains are artificially separated, which results in a loss of GAL4 transcription factor activity. The truncated transcription factor can activate the transcription of a reporter gene, in both fragments are indirectly connected. Using recombinant DNA techniques it is possible to generate cDNA molecules encoding the BD or AD domains of GAL4 in–frame with another cDNA. In the two-hybrid system, a non-covalent protein–protein interaction between protein A coupled to BD domain ("bait" construct) and protein B coupled to AD–domain ("prey" construct) causes the two hybrid proteins to interact and reconstitute GAL4 transcription factor function, which leads to the activation of the reporter gene, lac Z. $\beta-$galactosidase, the gene product of lacZ, converts the colorless substrate X–Gal to a colored product that is easily detected.

The physical interaction of two proteins must be confirmed by other methods, *e.g.*, coimmunoprecipitation and immunofluorescence, in order to demonstrate that proteins can form complex *in vivo*.

3.13.2 Screen of a brain cDNA-library

The rat brain cDNA-library was transformed into the strain AH109 and stored at $-20°$C. The strain Y190 was chosen for transformation with a bait plasmid, coding for the GAL4–BD–C'term Spar3 ($3903 - 5780$ bp of Spar3 in pAS2–1). The transformed yeast was incubated on the selection agar SD plates lacking tryptophan (–Trp) for 5–7 days at 30°C. The material of one yeast colony was inoculated in 15 ml of SD medium –Trp and agitated overnight at 200 rpm and 30°C. 55 ml of fresh SD medium –Trp were added to the culture and incubated for $8 - 10$ h at 200 rpm and 30°C to an OD $= 0.8$. The culture was centrifuged for 5 min at 2500 g and the pellet was resuspended in 50 ml of YPD medium. The AH109 strain containing the cDNA of the rat brain library (in pACT2) was added to the tube containing the Y190 strain. 50 ml of fresh YPD medium were added to the mixture. The yeast suspension was mixed and divided in two equal volumes and filled in two separate 2l jars. The mating of the strains occurred at 40 rpm and 30°C for $18 - 20$ h. The yeast was plated on selection plates containing 3–AT and lacking histidine (His), leucine (Leu) and Trp (SD –His/–Leu/–Trp +3–AT). Only double transformed yeast with reconstituted function of GAL4 transcription factor grew on selection plates. 100 μl of 1:10, 1:100, 1:1 000 and 1:10 000 dilutions of yeast suspension were plated on selection plates with SD lacking Leu and Trp (SD–Leu/–Trp) to control the mating efficiency. The plates were incubated for 5–7 days at 30°C up–side–down until the colonies appeared. The colonies were transferred

to a fresh selection plate (SD –His/–Leu/–Trp + 3–AT) and incubated overnight at 30°C. The colony lift filter assay was performed to verify the activity of the reporter gene (section 3.13.4). $\beta-$galactosidase producing colonies were chosen for subsequent analysis (section 3.13.5).

3.13.3 Estimation of transformation efficiency by mating

The colonies on the plates with dilutions of yeast, 1:10-1:10 000, grown on SD-Leu/-Trp, were counted. The number of grown colonies was designated as cfu (colony forming unit). The efficiency of the mating was calculated using the formula:

$$\frac{\text{cfu} \times \text{total volume of suspension } \mu\text{l}}{\text{volume of plated suspension } (\mu\text{l}) \times \text{dilution factor}} = \text{number of screened colonies}$$

3.13.4 Colony–lift filter assay

The assay is used to measure the $\beta-$galactosidase activity in a screen of cotransformants that survive –His growth selection in GAL4 two–hybrid library screening. The freeze–thaw cycle in liquid nitrogen is a rapid and effective cell lysis method for monitoring of $\beta-$galactosidase activity.

The fresh colonies grown at 30°C for 4 days, $3-5$ mm in diameter, were taken for an assay. A substrate for β–galactosidase, X–gal, was diluted in 39 mM 2–mercaptoethanol and Z–buffer to the concentration of 1 mg/ml. A sterile Whatman #5 filter was soaked in 4 ml of X–gal solution in a clean 150 mm Petri-dish. The second clean dry filter was placed over the surface of the plate with yeast colonies and slightly pressed with the side of forceps to help colonies cling to the filter. The orientation of the filter was marked to identify the β–galactosidase producing colonies later. The filter was immersed into liquid nitrogen for 10 sec. The completely frozen filter was placed at RT and thawed. The filter with colonies side up was placed onto the X–gal pre–soaked Whatman paper. The Petri dish was closed and incubated at 30°C. Periodically, the filters were checked for the appearance of blue staining (typically the time of incubation was 30 min – 2h to avoid false positive results). The $\beta-$galactosidase producing colonies were identified by aligning the filter to the agar plate and analyzed as described in section 3.13.5.

3.13.5 Analysis of positive clones

The plasmid DNA was isolated from $\beta-$galactosidase positive colonies (see section 3.2.3). To identify the pACT vector with the "prey", the plasmids were transformed

in bacteria for the rapid DNA isolation and following restriction. The combination of restriction enzymes Eco RI and XhoI cut both pAS 2.1 and pACT2 vectors in fragments of a defined size. Empty pAS2.1 and pACT were digested with Eco RI and XhoI and loaded on a gel as controls. The colonies containing pACT with a cDNA fragment from the rat brain library were identified. The bacteria were inoculated for the extraction of high purity DNA with JETQUICK Plasmid Miniprep Spin Kit. The DNA probe was sent for sequencing (3.3.5). A search of the databases was performed with the resulting sequence. The possible interaction of "prey" and "bait" proteins was later confirmed in other systems (*e.g.*, in cell culture, by coimmunoprecipitation, in a pull–down assay).

3.14 Statistical evaluations

The number of mature, stubby, filopodia–like spines (**M**, **S**, **F**) were counted for $6-8$ neurons per transfection type. Images of neurons were chosen randomly amongst experiment series which document the results of at least two indepentent transfection experiments. A paired t–test was performed to evaluate the distributions of spines.

The paired t–test was conducted to evalate the hypothesis that the control series (GFP) and the transfected series (*e.g.*, Spar3) were drawn from normal distributions with equal expectation values. The level of rejection of this hypothesis was graded with *, **, *** corresponding to a significance levels exceeding $\alpha = 0.01$, 0.001 and 0.0001.

Chapter 4

Results

4.1 Identification of Spar3

A rat brain cDNA library was screened using the yeast two–hybrid system with 286 – 475 aminoacids (aa) of ProSAPiP1 (ProSAP Interacting Protein 1) containing a coiled coil domain with leucine–zipper motif. As a result, 50 clones were obtained including 28 clones of NM_139390, previously identified as Spar protein (Wendholt, 2006). Using a sequence analysis and a BLAST search, two other members of the SPA family, namely Spar2 (Spilker et al., 2008) and Spar3, were identified in *Rattus norvegicus*: NM_001009704 and NM_001013066 (EDM07825).

In this study we focused on the characterization of Spar3, a novel molecule and a putative new member of the postsynaptic assembly.

4.2 Gen and protein structure of Spar3

The chromosomal location of the Spar3 gene in the genome of *Rattus norvegicus* is 1q21. The gene consists of 20 exons and 21 introns of different lengths. Most exons are small and separated by small introns (Fig. 4.1). The rat cDNA has an open reading frame (ORF) of 5331 base pair (bp) and encodes 1776 aa (Fig. 4.1). In the genome of *Mus musculus*, Spar3 is located on chromosome 7a2 and has the same number of exons and introns. The size of exons and intron–exon boundaries are conserved, *i.e.*, do not differ between rat and mouse. Similarly the cDNA of *Mus musculus* has an ORF of 5331 bp and encodes 1776 aa. The rat and mouse coding DNA sequences are 94% identical.

The human Spar3 gene (NM_015073) is on chromosome 19q13.13. The human

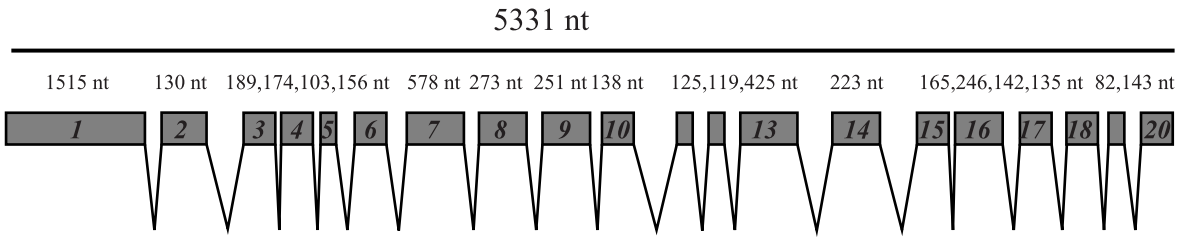

Figure 4.1: The exon-intron structure of Spar3 in the rat genome. Spar3 consists of 20 exons, separated by introns of different lengths.

cDNA has an ORF of 5346 bp, codes for 1781 aa and contains additional 5 aa in the N'terminus compared to the rat. The gene structure is slightly different – the gene consists of 22 exons, with two small initial exons belonging to an untranslated region (UTR). The human sequence is 85% identical to the rat cDNA. Comparison of rat-mouse and rat–human aa sequences reveals 97% and 90% identities, respectively.

Based on motif analysis, the molecular structure of Spar3 includes a predicted Rap–GAP domain (636-822 aa), a PDZ domain (960-1023 aa), a serine rich region (1260–1277 aa), a coiled coil (CC) domain (1707–1776 aa) containing a leucine-rich zipper motif (1709–1751 aa) and four predicted nuclear targeting signals (277–280, 615–618, 708–711, 1350–1356 aa), Fig 2 **A**, **B**.

It has been shown that the coiled coil domains and the leucine–rich repeats are involved in protein–protein interactions and play a role in di– and multimerization of molecules (Wendholt et al., 2006). The PDZ domain was first described in three different proteins **P**SD–95/**D**iscs Large/**Z**ona occludens and named accordingly. This is a structural domain that is highly characteristic for proteins in the postsynaptic density and may specifically recruit adhesion molecules or receptors with a corresponding C'terminal PDZ–interacting motif. The serine rich region might be a target for phosphorylation by the casein kinase 1 (CK1) or glycogen synthase kinase 3 (GSK3) kinases (predicted by The Eukaryotic Linear Motif Resource for Functional Sites in Proteins). The predicted Rap–GAP domain might be responsible for the downregulation of one or several GTPases (Mackay and Hall, 1998). Thus, Spar3 contains a RapGAP domain, which is characteristic for signaling molecules and several structural domains which may provide a platform for the assembly of signaling complexes.

A

```
    1               16              31              46              61
    0 MTTYRPLPNDGVDLATSCGARSTDILPGPHPGDYTPMGFWAQSGSMSQPLGESPAAATTRPSPTTPAMPKMGVRA
   75 RVADWPPKRDALREQSNPSPSQDTDGVKTTKVAHSMRNLQNGQLPSSTPASSGSRAFHRLSRRRSKDVEFQDGWP
  150 RSPGRAFLPLRHRSSSEITLSECDVEEPGDPRGTRHPGVLPLFREYGSTSSIDVQGVPEQSFFDILNEFRSEQPE
  225 ARGSQNLGELLRVDPGALSGGSCGAKGDPRNGQPTKDSLQSLQPLKEKEKARKKPVRGLGSGDTVDSSIFRKLRS
  300 SKPEGEVGRPLGETEEGRSPPEASRPWVCQKSFAHFDVQSMLFDLNESAANRVSVAQRRNTTTGASAASAASAMV
  375 ALTASRAHSLGTLDPTFTSTEDLNCKENLEQDLGDDNSNDLLLSCPHFRNEIGGERERNVSFSRASVGSPGGSSE
  450 AHMAEPALSTHRTNASISVLEVPKEQQRTQSRPRQYSIEHVDLSARYYQDYFVGKEHANYFGVDEKLGPVAVSIK
  525 REKLEDHKDHGPQYQYRIIFRTRELITLRGSILEDATPTATKHGTGRGLPLKDALEYVIPELNIHCLRLALNTPK
  600 VTEQLLKLDEQGLCRKHKVGILYCKAGQSSEEEMYNNEEAGPAFEEFLDLLGDKVCLKGFTKYAAQLDVKTDSTG
  675 THSLYTTYQDYEIMFHVSTLLPYTPNNRQQLLRKRHIGNDIVTIIFQEPGALPFTPKNIRSHFQHVFIIVRVHNP
  750 CTENVCYSMAVTRSKDAPPFGPPIPNGTTFRKSDVFRDFLLAKVINAENAAHKSDKFHTMATRTRQEYLKDLAEN
  825 CVSNTPIDSSGKFNLISLTSKKKEKTKARAGAEQHSAGAVAWRVAAQDYAQGSEIDCILGISNEFVVLLDLRTKE
  900 VVFNCYCGDVIGWTPDSSTIKIFYGRGDHIFLQAAEGSVEDIRDIVQRLKVMTNGWETVDMTLRRNGLGQLGFHV
  975 KYDGTVAEVEDYGFAWQAGLRQGSRLVEICKVAVVTLSHDQMIDLLRTSVTVKVVIIPPFEDGTPRRGWPETYDM
 1050 AATPGGRPPYRSNAPWQWSGPASHNSLPATKWTTPATPGHAQSLSRLPKHTSTSEPKMESEPGVPFRESQPLHSK
 1125 RPVSFPETPFAASPAGADRVPPYRQPSGSFSTPGSATYARYKPSPERYAAAPHPLLSFDPHFIHDGMSSGDSSSG
 1200 GLTSQESTMERPKPEPLWHVPAQARLSAMTGSMGSKHPSRQDAAGKDSPNRHSKGEPQYSSHSSSNTLSSNASSS
 1275 HSDDRWFDPLDPLEPEPDPFSKGGSSDSGIDTTLYTSSPSCMSLAKTPRPTKPHKPPGSIGLCGGGRESAGRPHP
 1350 ADRRREVSPAPAVAAQNKGYRPKMYSSGSSTPPGLVGGSRDPPRQASDMGSRTGYPTQVYKTTSAETPRPSQLSQ
 1425 CSPFQLSTSVPKSFFSKQPAHNKHSTGWKRADEPPPRPLPFTESKKQVDTNAKNVFGQPRLRASLRDLRSPRKNY
 1500 KSTIEDDLKKLIIMDNLGPEQDRDTGQSPQKSLQRTLSDESLCSGRREPSYASPTSLEPGLPSDVLFTSTCTFPS
 1575 STLPARRQHQHSHPPSGAPNTIPATGNGFPEKKSAISASELSLADGRDRPLRRLDPGMMPLPDTAAGLEWSSLVN
 1650 AAKAYEVQRAVSLFSLNDPALSPDIPPAHSPVHSHLSLERGPQTPRTTPTMSEESPLDLTGKVYQLEVMLKQLHT
 1725 DLQKEKQDKVVLQSEVASLRQNNQRLQEESQAASEQLRKFAELFSREKKEL*
```

B

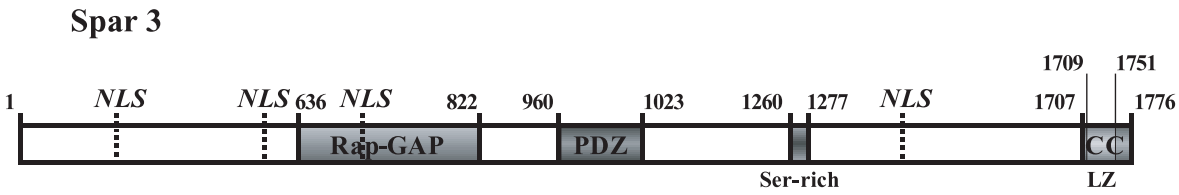

Figure 4.2: The domain structure of Spar3 at the amino acid (aa) level, based on a motif analysis. **A**. aa sequence with domains marked in color. Following domains are designated: a Rap–GTPase activating protein domain (Rap–GAP) in red, a PDZ (**P**SD–95/**D**iscs Large/**Z**ona occludens) – domain in blue, a serine–rich motif (Ser-rich) in green, a coiled coil (CC) in yellow, with leucine-zipper motif (LZ), LLL–E–LLL, conserved for all members of SPA family – in dark red. Four nuclear localization signals are shown in dark grey (NLS). The aa sequences (1471 – 1485 aa and 1695 – –1709 aa) chosen for generating of AB to peptides are highlighted in black. **B**. Schematic depiction of the Spar3 domain structure.

4.3 Spar3: a member of the SPA–family of proteins

Spar 3 constitutes, together with SPA–1, Spar and Spar2, the SPA family of proteins. SPA–1, is the only member of this family, which is not expressed in the brain. The aa sequence identity among other SPA family members ranges from 49% to 54% by comparing the entire sequence and up to 91% by comparing separated domains (Appendix A, Spilker et al. (2008)). The phylogenic tree, composed with the GENEDOC multiple sequence alignment program (NRBSC Software) indicates that Spar3 has the closest homology to the non–neuronal SPA–1 among the other Spar proteins expressed in the brain (Fig. 4.3).

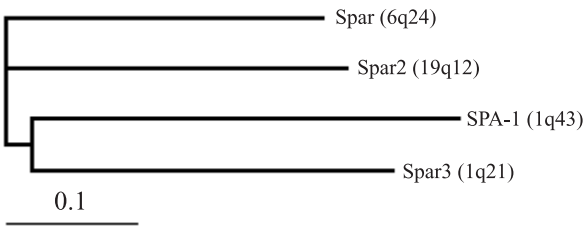

Figure 4.3: The phylogenic tree of the SPA family analysed by the GENDOC program, illustrates the homology of SPA–family members. The locations of the sequences in the rat genome are indicated in parenthesis. The branch lengths are proportional to the inferred evolutionary change. The bar 0.1 has a relative value.

4.4 Characterization of Spar3 antibodies (AB)

Two types of corresponding AB were generated to investigate Spar3. AB against two peptides in the C'terminus of protein, 15 aa each, and AB against the C'terminal Spar3–GST fusion protein. The peptide sequences used for generating the peptide AB are

$$[NH_2]\,-\text{KQVDTNAKNVFGQPRC}-\,[\text{COOH}]$$

and

$$[NH_2]\,\text{-PRATPTMSEESPLDLC-}\,[\text{COOH}]$$

(Fig. 4.2, **A**). Both peptides are chosen from regions which are not highly conserved among the different members of the SPA family. The peptides were synthesized by EUROGENTEC and injected into two rabbits as a mix, according to the standard immunization protocol. The serum, generated against the peptides, was mostly used for immunofluorescent stainings and was only partially applicable for Western blot analy-

sis. Hence, another type of serum to the Spar3–GST–fusion protein was generated. The C'terminus of Spar3 (3903 – 5337 bp corresponding to 1300 – 1776 aa) was cloned in the pGEX–4T–1 vector for expression of the Spar3–GST tagged protein. 1.5 mg of protein extracted from bacterial lysate were purified on glutathione–sepharose. The quality of the protein expression and purification was confirmed by SDS–PAGE (Fig.4.4 **A**, **B**) and Western blot (Fig. 4.4, **C**). The purified protein was sent to PINEDA (Berlin), where one rabbit and two guinea pigs were immunized with the protein.

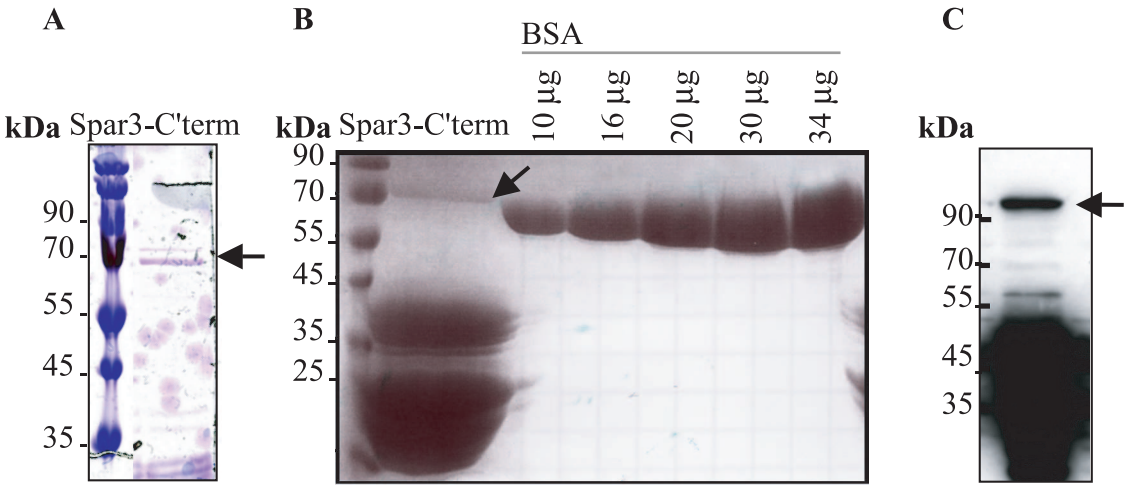

Figure 4.4: Detection of overexpressed C'term-Spar3-GST-fusion protein (1300 – 1776 aa) on SDS-PAGE and on Western blot. **A**. Coomassie staining. **B**. Gel Code Blue Stain Reagent staining. The BSA standard was applied to confirm the concentration of the C'term–Spar3–GST–fusion protein. **C**. Verification of the overexpressed C'term–Spar3–GST on blot. The band migrates at 70 kDa, as expected (s. arrows). The numerous bands below correspond to degraded or truncated, not fully translated protein.

To ensure the absence of crossreactivity of the generated anti-Spar3-AB to other Spar proteins, all the members of the SPA family expressed in brain, were overexpressed as GFP–tagged proteins in Cos–7 cells and tested on Western blot with AB generated against GST–fusion protein (Fig. 4.5, **A**) and against peptides (Fig. 4.5, **B**). The GFP–Spar –1, –2, –3 expression level was examined with anti–GFP AB. On Western blot AB against Spar3 detected several bands in both Spar-3 transfected Cos–7 cells and in brain extract co–migrating at 219 kDa. Neither AB directed against GST–tagged Spar3 nor AB specific for peptides within Spar3 recognized overexpressed Spar or Spar2 proteins. They did, however, show high specificity for Spar3 (Fig. 4.5 **A**, **B**). The predicted molecular weight of the Spar3 protein is 194 kDa. Surprisingly, the

Spar3 band detected in the brain homogenate, migrated at the same level as Spar3–GFP, 25 kDa heavier than expected.

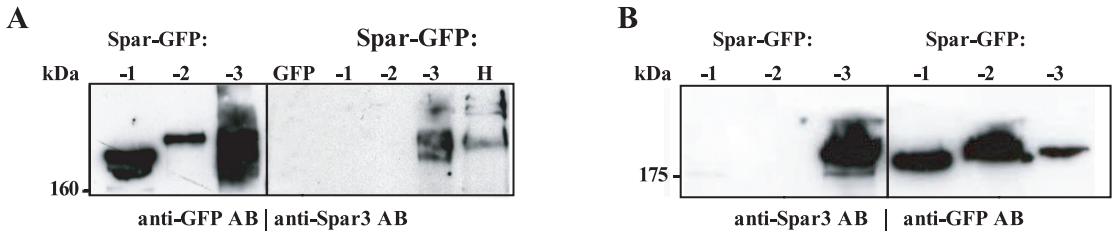

Figure 4.5: Specificity of Spar3 AB. **A**. On the left panel the GFP-constructs of Spar–1,–2,–3 overexpressed in Cos–7 are detected with anti–GFP AB, 1:3000. On the right the same protein probes of constructs, GFP overexpressed in Cos–7 cells, and brain homogenate (**H**) are exposed to AB specific for the C'term-Spar3–GST-fusion protein (PINEDA), 1:500. Anti-Spar3 AB specifically recognize Spar3 and not other members of the SPA family. **B**. On the left GFP–Spar–1,–2,–3 overexpressed in Cos–7 cells are probed with AB to two peptides indicated above (EUROGENTEC), 1:1000. On the right, the same probes are subjected to anti–GFP AB, 1:3000.

Therefore, another experiment illustrating the specificity of the obtained anti-Spar3 AB was performed: preincubation of the AB with the specific antigen. The GST–tagged $1300 - 1776$ aa of Spar3 was overexpressed in bacteria, purified and dialyzed as described in material and methods. The concentration of the protein was defined by BCA-assay after dialysis. $6\,\mu$l of the Spar3 AB were mixed with $100\,\mu$g of GST-C'terminus Spar3 in TBS buffer and incubated by agitation overnight at 4°C. The control aliquot of Spar3 AB was mixed with TBS buffer and agitated under the same conditions. The AB detected Spar3 in brain homogenate and the GFP–tagged C–terminus of Spar3 in Cos–7 lysate (left panel of Fig. 4.6). Serum, preincubated with the antigen, did not reveal a signal in brain and did not detect the GFP–tagged antigen (right panel). This additionally illustrates the specificity of the obtained AB. The migration of Spar3 wild-type protein at 219 kDa might indicate post–translational modifications, such as phosphorylation or ubiquitination of protein. In case of Spar, the same phenomenon of co-migration of GFP–tagged and "wild type" brain protein was observed (Pak et al., 2001).

4.5 Expression of Spar3 in tissues

By analysis of various tissue homogenates on Western blot, specific anti–Spar3 AB detect the 220 kDa band in brain homogenate, skeletal muscle, testis and retina homogenate (Fig. 4.7). In the brain and the retina a minor band co–migrates at about

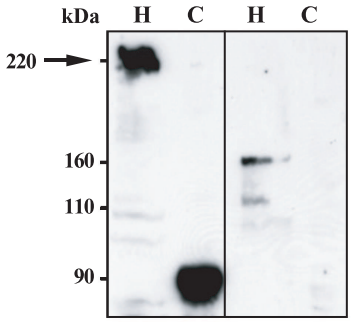

Figure 4.6: Specificity of Spar3 AB shown after pre–incubation of the AB with the antigen. On the left panel a homogenate (**H**) and a probe of the C'terminus 1300 – 1776 aa–Spar3–GFP overexpressed in Cos–7 cells (**C**) are detected with anti-Spar3 AB, 1:500. On the right panel the same concentration of AB preincubated with 100 μg of the C'terminus–Spar3–GST (1300 – 1776 aa) was applied to the blot. The signal disappeared after preincubation of AB with the specific antigen.

190 kDa and may correspond to the pool of a non–modified protein (predicted weight of Spar3 is 194 kDa).

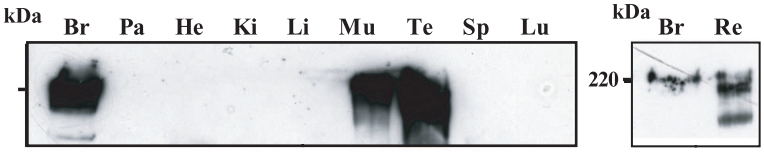

Figure 4.7: Expression of Spar3 in various rat tissues. Homogenates from the indicated rat tissues: brain (Br), pancreas (Pa), heart (He), kidney (Ki), liver (Li), skeletal muscle (Mu), testis (Te), spleen (Sp), lung (Lu), retina (Re); 20 μg of total protein per lane were analysed by immunoblotting with AB against Spar3, 1:500. Spar3 is highly expressed in brain, skeletal muscle, testis and retina.

4.6 Developmental profile of Spar3 gene expression in rat brain

The distribution of Spar3 mRNA was visualized by *in situ* hybridization in rat brain throughout development. The cryosections of rat brain were hybridized with Spar3 specific oligos. The Spar3 transcript is already present at day 1 in hippocampus, cortex and to a minor extent in cerebellum (Fig. 4.8). With time, Spar3 expression increases over the next three weeks and then slightly decreases by the third month. One year old animals only showed high level of Spar3 transcript in hippocampus. Cerebellum and cortex of adult animals contained less transcript than cerebellum and cortex of 1–3 weeks old young animals.

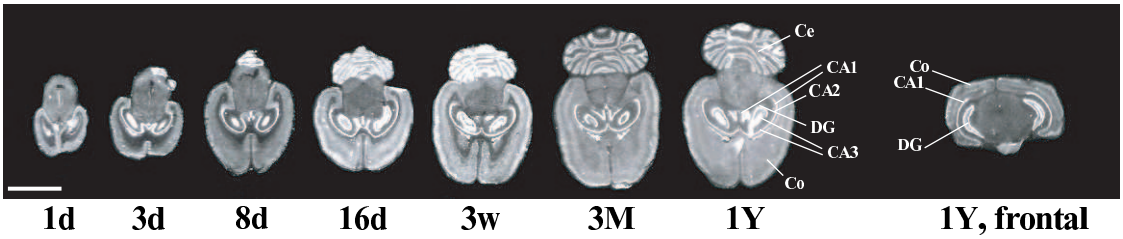

Figure 4.8: The pattern of Spar3 gene expression in a rat brain during development obtained by *in situ* hybridization. The horizontal and frontal sections of the rat brain on postnatal day 1, 3, 8, 16, 21 (**d1-21**), 3 monthes (**3M**), 1 year (**1Y**) old animals were hybridized with Spar3-specific oligos. The mRNA of Spar3 is expressed in cortex (**Co**), cerebellum (**Ce**) and in all regions of the hippocampus: dendate gyrus (**DG**), cornu ammonis 1-3 (**CA1-3**). Scale bar 7 mm.

4.7 Immunohistochemical staining reveals Spar3 expression in cortex, hippocampus and cerebellum

The pattern of Spar3 AB immunohistochemical stainings of adult rat brain sections confirms the results of *in situ* hybridization. In contradiction to the results of mRNA expression, the signal at the protein level in the adult brain is weaker than expected (Fig 4.9, **B**, **C**).

At higher magnification it is seen, that Spar3 is expressed in the cortex, especially in the large pyramidal cells, in the hippocampus and in the cerebellum. In the cerebellum, only Purkinje cells, the sole "output cells" of the cerebellar cortex, express Spar3 and display strong staining of the dendritic arbor and the soma.

In the retina, a highly anatomically and functionally differentiated structure, Spar3 is expressed in two layers: the ganglion cell layer and inner nuclear layer consisting of horizontal, bipolar, amacrine cells (Fig. 4.10, **A**). Interestingly, Spar is identified on the same layers as Spar3, but the Spar staining is more intensive, especially in the ganglion cells, where protein decorates the dendritic arbor and fills the soma (Fig. 4.10, **B**).

4.8 Spar3 protein expression in various brain regions

In adult animals the comparison of the Spar3 expression in different brain regions in Western blotting experiments showed remarkable differences on the protein level (Fig. 4.11). The protein is highly expressed in the hippocampus, thalamus and hypothalamus. Less protein is found in the cortex. Lower, but still detectable, expression is present in the cerebellum.

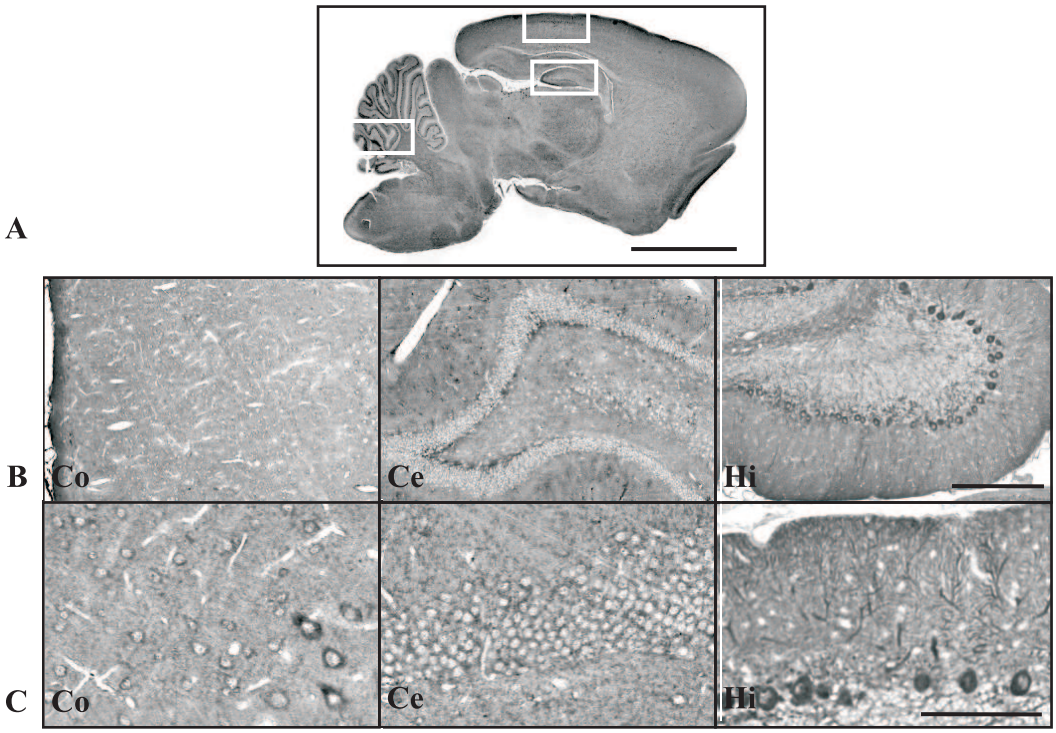

Figure 4.9: Immunohistochemical staining of different brain regions. **A**. Section of the brain. The frames show the cortex, hippocampus, cerebellum, represented as enlarged sections below. **B**, **C**. Sections of the cortex (**Co**), hippocampus (**Hi**) and cerebellum (**Ce**) and their enlarged view of each section stained with Spar3 AB, 1:500. Note the intensive staining of large pyramidal cells in the cortex. Spar3 is expressed throughout the hippocampus. The soma and the dendrites of Purkinje cells display Spar3 expression in the cerebellum. Scale bar 7 mm (**A**), 250 μm (**B**), 100 μm (**C**).

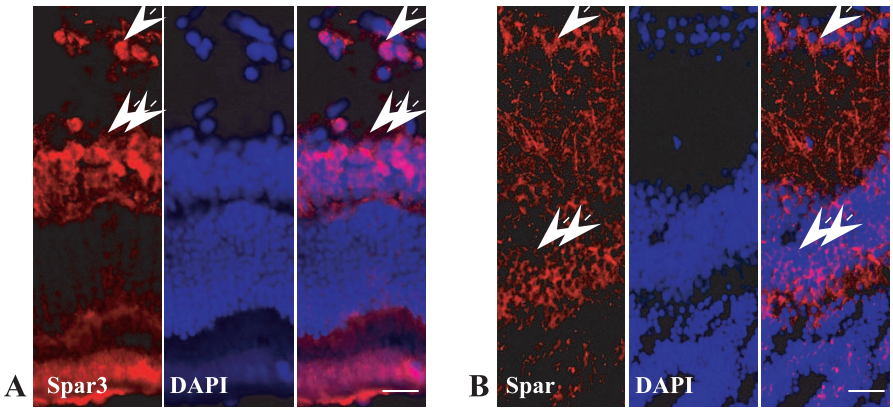

Figure 4.10: Immunohistochemical staining of Spar3 and Spar protein in the rat retina. The cryosections of retina were fixed in methanol and stained for Spar3, 1:300 (**A**) and Spar, 1:100 (**B**). **A**. The Spar3 staining is intensive in the ganglion cell layer (arrow) and in the inner nuclear layer (double arrows). **B**. The Spar expression has the same pattern as Spar3 and is even more distinct in the ganglion cells, where protein decorates the dendritic arbor. Scale bar 10 μM.

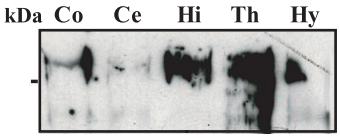

Figure 4.11: Different brain regions of adult rats (20 μg total protein per lane) show various protein levels of Spar3. The protein is highly expressed in the cortex (Co), hippocampus (Hi), thalamus (Th) and hypothalamus (Hy). Only a minor expression is found in cerebellum (Ce).

4.9 Spar3 is enriched in the postsynaptic density

A series of centrifugations of adult rat brain homogenate in density gradients and application of detergent allows the separation of PSD, compounds of the presynaptic compartment, mitochondria and myelin (Cotman and Taylor, 1972). As a control all fractions were probed for ProSAP2/Shank3, a well characterized protein of PSDs (Fig.4.12, **A**). As expected ProSAP2 was detected in the whole brain homogenate H. It was slightly enriched in the crude membrane fraction P2. The highest level of protein was found in the PSD fraction. Some ProSAP2 was detectable in the soluble fraction (S2), which contained cytoplasmic compounds. This might illustrate a slight contamination of the soluble fraction from the insoluble components (PSD matrix) through preparation. It might also reflect a local dynamic "shared" pool of ProSAP2 exchanging between PSDs (Tsuriel et al., 2006). As the S2 fraction contains the Golgi apparatus some proteins of PSD may be found there.

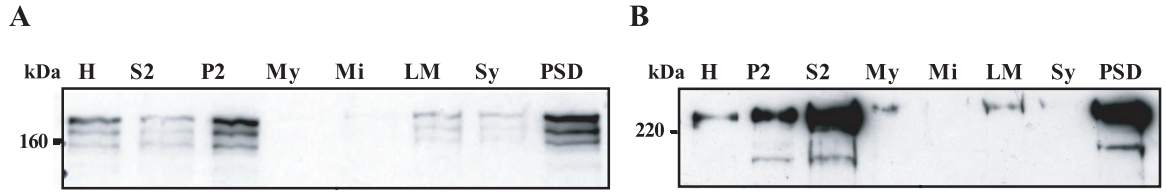

Figure 4.12: Spar3 is highly concentrated into the PSD fraction along with ProSAP2. Various subcellular fractions (20 μg total protein pro lane) are analysed by immunoblotting with ProSAP2 (**A**) and Spar3 AB (**B**). **A**. ProSAP2 AB staining (1:1000) was performed to control the fractionation. As expected ProSAP2 is present in the homogenate (**H**) and enriched in the insoluble protein fraction **P2** and the **PSD**. **B**. Spar3 compartmentalization was visualized with Spar3 AB (1:500). The Spar3 is detected in the brain homogenate (**H**), the insoluble protein fraction (**P2**) and enriched in the soluble protein fraction (**S2**) and in **PSD**. As controls myelin (**My**) and mitochondria fractions (**Mi**) display no Spar3 signal.

Spar3 was detected in the brain homogenate H, the insoluble protein fraction P2 and enriched in the soluble protein fraction S2. The biochemical fractionation revealed that Spar3 is highly concentrated in the PSD fraction along with ProSAP2 (Fig. 4.12,

B). No signal was detected in the myelin My and mitochondrial fraction Mi (applied as a control). A minor signal was present in the light membrane fraction (LM) and no signal was detected in synaptosomal fraction (Sy). The analysis shows, that Spar3 is a compound of PSDs, but a pool of protein is also present beyond PSDs in the spines, which is also confirmed by EM (section 4.10).

4.10 Electron microscopy studies confirm the localization of Spar3 in dendritic spines and PSDs

The PSD was discovered and described by electron microscopy analysis. This method allows to visualize presynaptic compartments and PSDs, spines, elements of cytoskeleton with high resolution. Immunostaining of ultra-thin sections revealed specific immunoreactivity for Spar3 in dendritic spines and PSDs of cortical neurons. No staining was observed in presynaptic terminals (Fig. 4.13, **A**, **B**).

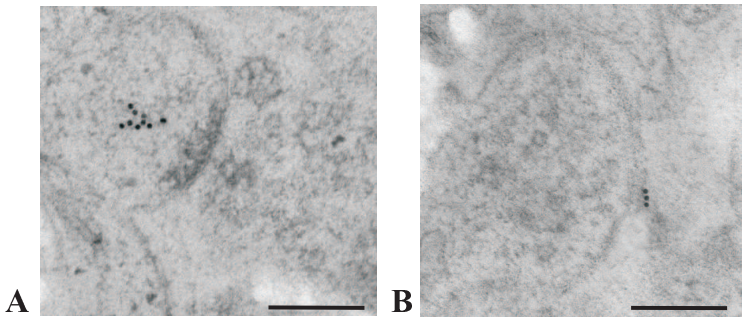

Figure 4.13: Subcellular localization of Spar3 in dendritic spines and PSDs. Ultra-thin sections of cortex were stained with anti-Spar3 AB (1:10). Spar3 is found in the spines (**A**) and the PSD (**B**). Scale bar is 1 μm.

4.11 Spar3 associates with F-actin in Cos–7 cells

Previous studies revealed that Spar binds to and reorganizes F–actin in Cos–7 cells (Pak et al., 2001). Cos–7 cells were transfected with GFP–tagged constructs and stained with alexa–568-conjugated phalloidin to visualize actin filaments. In order to compare Spar3 with the well-described Spar, Spar–GFP was transfected in Cos–7 cells. In our hands the full length Spar also binds to the actin cytoskeleton and reorganizes it to a different extent (Fig. 4.14, **A**, **B**). The full size Spar3 binds to actin fibrilles at the periphery of the cells and tends to form conglomerates around the nucleus (Fig. 4.14, **C**). To

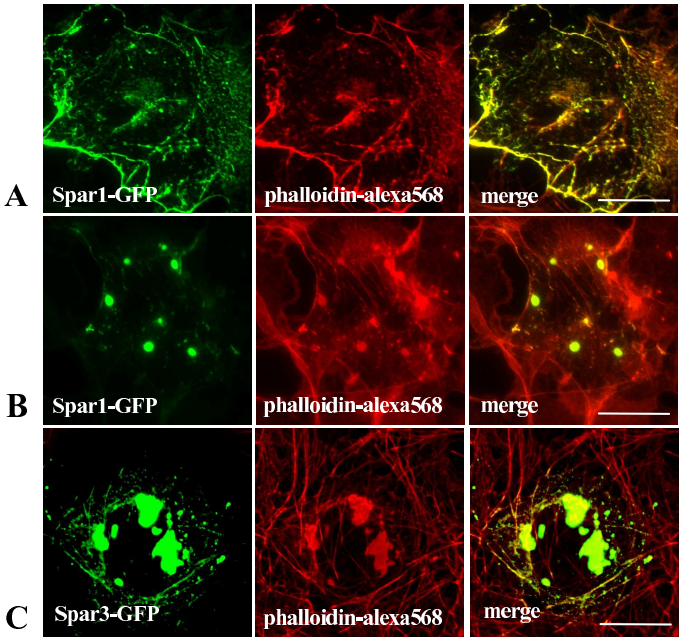

Figure 4.14: Spar molecules and the actin cytoskeleton. Spar and Spar3 were transfected into Cos–7 cells. The actin cytoskeleton was visualized with alexa-568-conjugated-phalloidin, 1:50. **A**. Spar-GFP binds with high affinity to the actin filaments. **B**. An example of the actin reorganization in the Spar1–GFP transfected cells. **C**. Spar3–GFP forms large clusters around the cell nucleus and binds to actin fibers at the cell periphery. Scale bar 20 μm.

identify the parts of Spar3 responsible for the association with actin cytoskeleton the different domains of Spar3 were cloned separately in EGFPC1-3 vectors. The following GFP–tagged constructs were generated for experiments (Fig. 4.15, **A**): Spar3, lacking C'terminus, 1−1300 aa (Spar3–ΔC); C–terminus of Spar3 1300−1776 aa containing the coiled coil domain (C'–term–Spar3); N'terminus of Spar3 1 − 500 aa (N'term-Spar3); Spar3, lacking the N' and C'terminus 548 − 1300 aa(ΔNΔC-Spar3). All constructs were verified by sequencing. Additionally, GFP–tagged truncated forms of Spar3 were transfected in Cos–7 cells and probed with anti–GFP AB to verify the molecular weight of the truncated Spar3 proteins (Fig. 4.15, **B**). The C'terminus–Spar3 was also detected by anti–Spar3 AB. When transfected in Cos–7 cells the full size Spar3–GFP forms large clusters of protein around the nucleus. Possibly, this effect is mediated in part by multimerization via the coiled coil domain. Spar3 molecules lacking the coiled coil domain containing the leucine–zipper (Spar3–ΔC) form small grains around the nuclei (Fig. 4.16, **A**). This truncated form of Spar3 associates with the actin cytoskeleton at the cell periphery in the same manner as the full size protein. In cells transfected with the first 500 aa of the N'terminus of Spar3, the actin cytoskeleton is considerably reorganized and aggregated in clumps, whereas the N' terminus–GFP colocalizes with

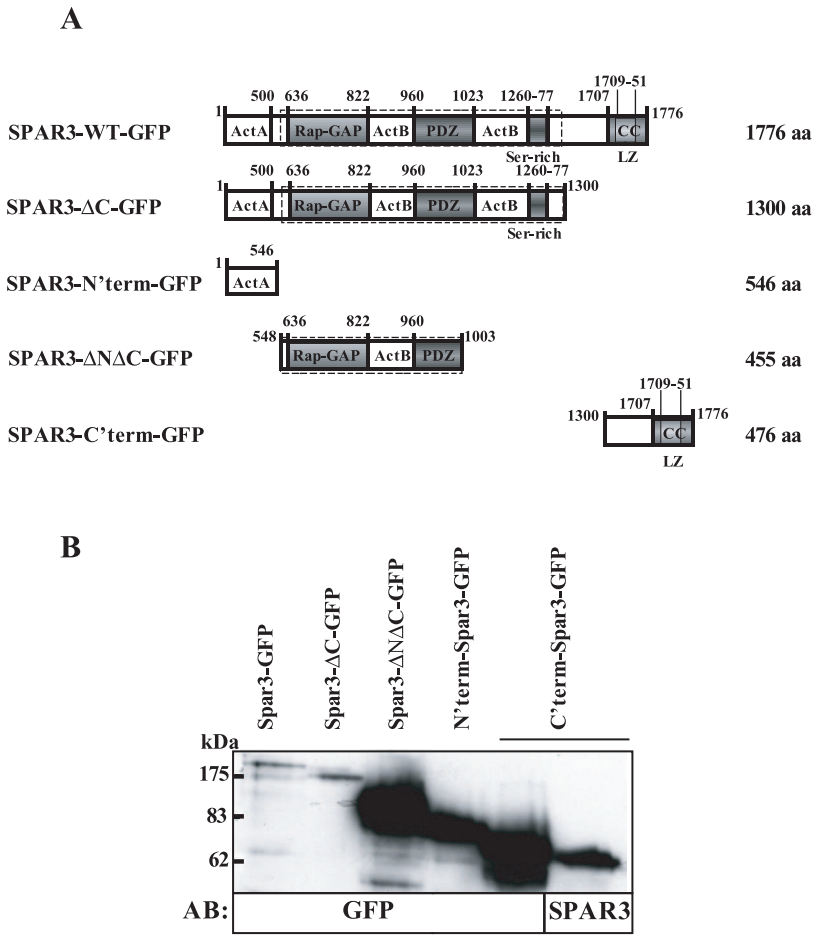

Figure 4.15: Domain organization of truncated Spar3–GFP constructs used in this study (**A**). The expression of truncated forms of Spar3 was controlled on Western blot (**B**). **A**. The depicted domains are: actin–binding region (Act), Rap-GTPase activating domain (Rap–GAP), PDZ (**P**SD–95/**D**iscs Large/**Z**ona occludens) – domain, serine–rich motif (Ser–rich), coiled coil (CC) with leucine-zipper motif (LZ). **B**. The GFP–tagged truncated forms of Spar3 were overexpressed in Cos–7 cells and detected with anti–GFP AB. The C'terminus of Spar3 contains the epitope, recognized by Spar3 AB. Therefore it was additionally probed with anti–Spar3 AB.

the altered actin structures (Fig. 4.16, **B**). The part of Spar3 lacking the N' and C'terminus ($548-1300$ aa, Rap–PDZ–Ser–GFP) binds to the F–actin with a very high affinity, as does Spar. The overexpressed truncated protein is completely recruited with high specificity to the actin fibers, without reorganizing them (Fig. 4.16, **C**). The C'terminus alone, containing the last 476 aa of Spar3, fills the cell by transfection with an independent network of filaments, which does not coincide with actin fibers (Fig. 4.16, **D**).

Since the Spar3–ΔNΔC–GFP ($548-1300$ aa) is associated with the highest affinity to the actin fibers without reorganizing them, it was chosen for the subsequent analysis

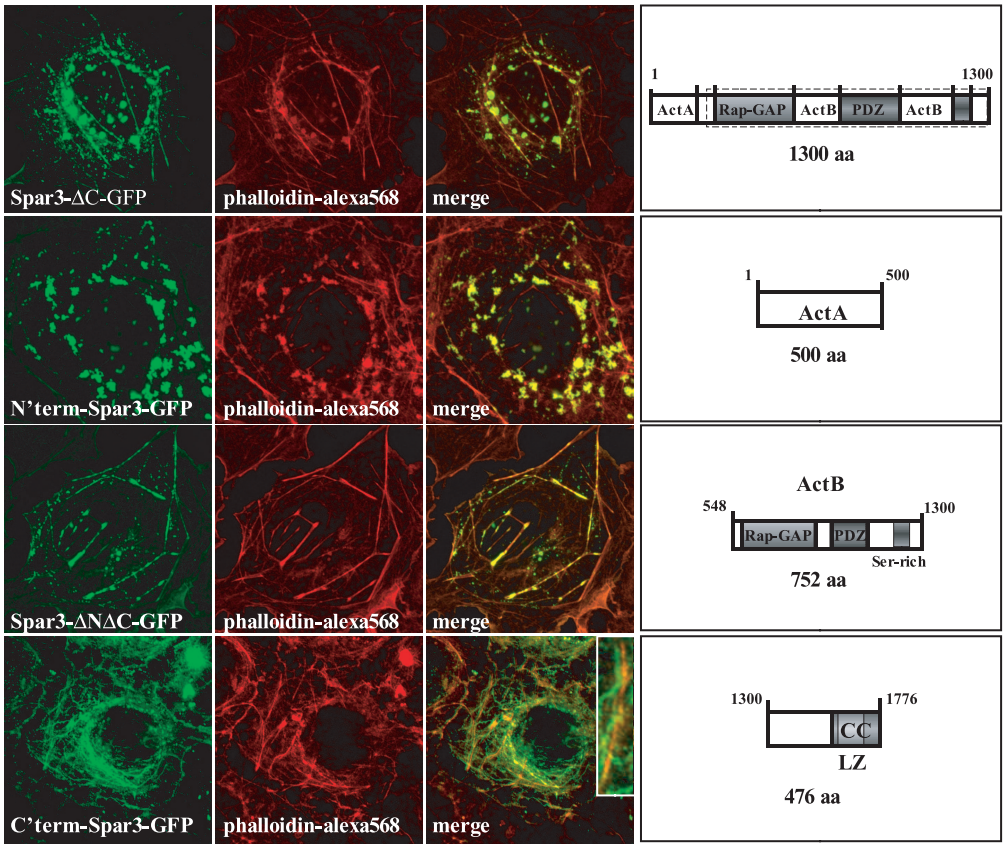

Figure 4.16: Truncated forms of Spar3 and the actin cytoskeleton. The Spar3-truncated GFP–tagged constructs were transfected into Cos–7 cells, the actin cytoskeleton was visualized with alexa–568-conjugated–phalloidin, 1:50. **A**. Spar3, lacking C'terminus (Spar3–ΔC–GFP) forms the smaller clusters in the center of the cell and still binds to actin at the cell periphery. **B**. N'term–Spar3–GFP ($1 - 500$ aa) reorganizes the actin cytoskeleton in clumps, in the same manner as Spar. **C**. Spar3, lacking N' and C' termini, is fully recruited to F–actin and shows the highest affinity when compared to all constructs and to full size Spar3. **D**. C'terminus Spar3 (C'–term–Spar3) forms its own network of filaments, which does not coincide with the actin fibers. Scale bar 20 μm.

(Fig. 4.16, **C**, Fig. 4.17, **A**). This form of the truncated protein consisted of a Rap–GAP, a PDZ and a serine–rich region. To identify which fragment is responsible for the affine association with actin, the construct was subdivided into a Rap–GAP–PDZ containing part ($548 - 1003$ aa) and a part containing the serine–rich motif ($1003 - 1300$ aa). Both were cloned into the EGFPC1 vector and the sequences were verified by sequencing and on Western blot (Fig. 4.16, **AA**). Surprisingly, the splitting of the Spar3–ΔNΔC–GFP construct into two parts led to a considerable loss of affinity of actin binding (Fig. 4.17, **B**, **C**).

To clarify which structures are formed by the C'terminus of Spar3, the intermediate filaments and microtubuli were visualized by anti-vimentin and anti–α–tubulin AB

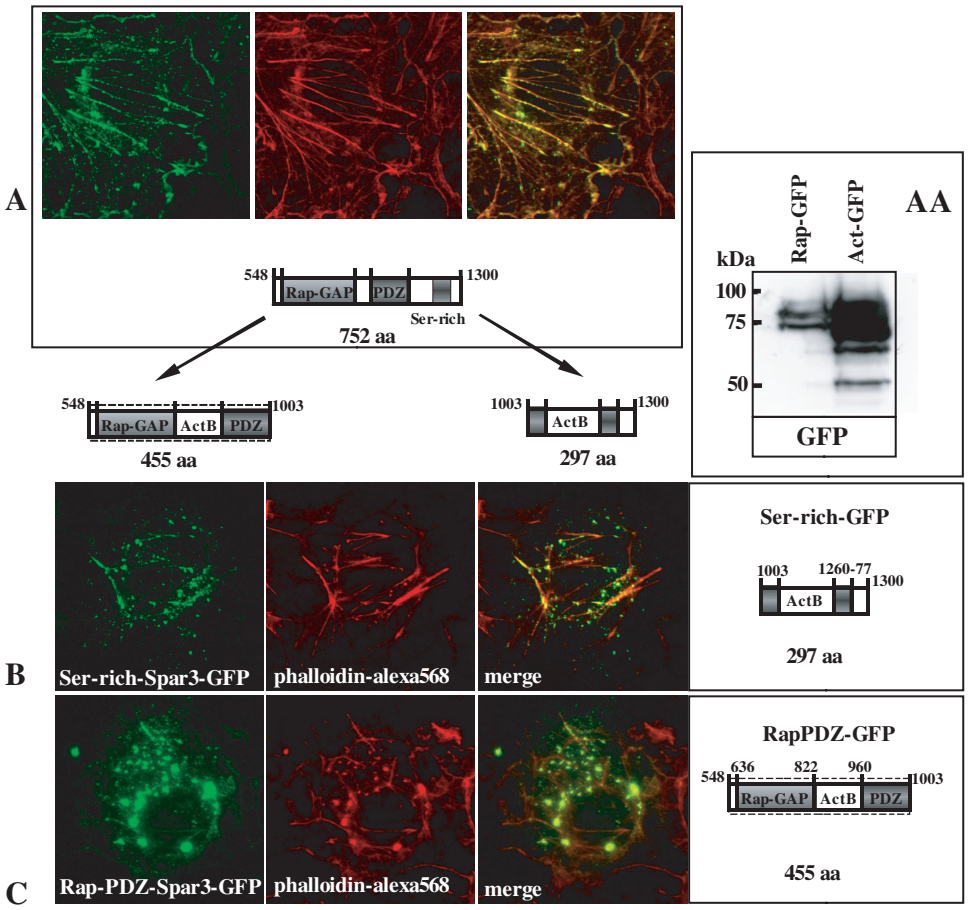

Figure 4.17: Truncated forms of Spar3 and the actin cytoskeleton. The GFP–tagged truncated forms of Spar3 were transfected into Cos–7 cells and stained with phalloidin–alexa-568 for the actin cytoskeleton. Spar3–ΔNΔC–GFP associates with actin fibers with high affinity (**A**). The Ser-rich domain alone (**B**) or the Rap-PDZ domains (**C**) associate with actin fibers with less affinity and tend to form grains in the Cos–7 cells. **AA**. Control of expression of the GFP–tagged Ser-rich and Rap-PDZ domains in Cos–7 cells on Western blot. Scale bar 20 μm.

(Fig. 4.18, **A**, **B**). Staining of the intermediate filaments revealed a complete overlap of vimentin with the network, formed by the transfected C'terminus. It is not clear if the C'terminus forms the fibers by building multimeres via the coiled coil domain or if it is able to bind to vimentin in HeLa cells. Unlike the intermediate filaments the tubulin meshwork did not reveal any similarity to the C'–term–Spar3-structures.

Thus, full size Spar3 is associated with the actin cytoskeleton, but this association is not as strong as in the case of Spar. The only part of the protein, which does not show any actin–binding properties is the C'terminus (1300 – 1776 aa).

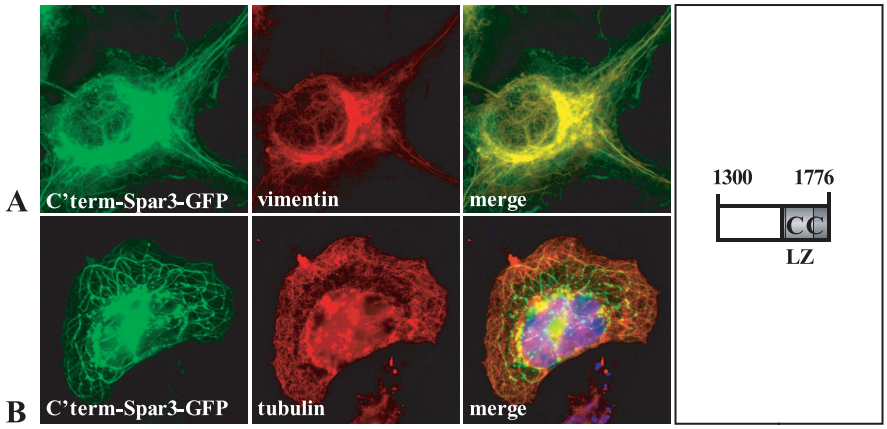

Figure 4.18: Visualization of intermediate filaments (**A**) with anti–vimentin AB and microtubuli (**B**) with anti–α–tubulin in C'terminus–Spar3 transfected HeLa cells. The staining of vimentin, 1:500, overlaps with the fluorescent structures built by the C'term-Spar3, while no signal–colocalization is observed in the case of C'term-Spar3–GFP and $\alpha-$tubulin staining, 1:1000. Scale bar 20 μm.

4.12 The level of Spar3 protein decreases during postnatal development

Protein lysates were prepared from rat hippocampus, cerebellum or cortex at various ages and analyzed by immunoblotting. In all the investigated brain regions, expression of Spar3 is high at embryonic day 18 and in newborn animals (Fig. 4.19).

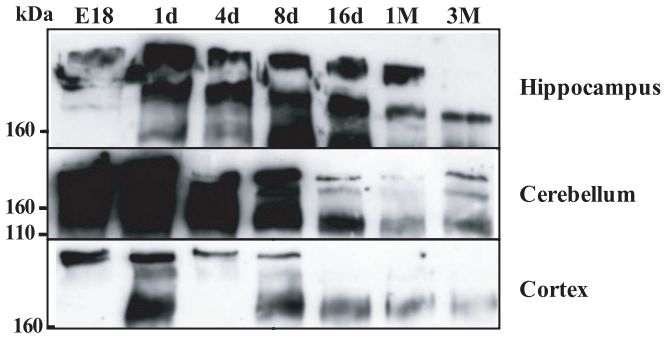

Figure 4.19: The developmental expression pattern of Spar3 in hippocampus, cerebellum and cortex of rat brain. The expression of proteins is traced with anti–Spar3 AB (1:500) on embryonic day 18 (**E18**), during postnatal development on days 1–16 (**d1–16**) and in one and three months old animals (**1 M**, **3 M**). The concentration of the total protein is 27 μg per line. Spar3 is highly expressed in hippocampus, cerebellum and cortex at **E18** up to **P8** and in hippocampus up to **1M**. The Spar3 protein level decreases in **3 M** old animals.

The level of Spar3 remains high during the first postnatal week, up to day 8 in all regions and up to 1 month in the hippocampus. Then the level of Spar3 recedes to

a low, but detectable level. The protein is detected as a pattern of multiple bands in the molecular mass range of $190 - 220$ kDa. The similar multiple–band pattern is also observed on the developmental profile of protein expression in the hippocampal cell culture. The Spar3 level in hippocampus, cerebellum and cortex is developmentally regulated and the protein might play a role especially in the first week of development by establishing synaptic connections.

4.13 Spar3 is expressed in cultured rat hippocampal neurons

The primary hippocampal culture of neurons is a well established model for the differentiation of neurons *in vitro*. The synapses start to form at day 7 *in vitro* (DIV) and cells differentiate to functionally mature neurons at 14 DIV. From day 14 to 21 the neuronal network continues its maturation (Verderio et al., 1999). To examine whether Spar3 is expressed in the hippocampal culture, the cells from the same culture preparation were harvested at different times and analysed on Western blot (Fig. 4.20). Spar3 expression began at day 3, and then, *in vitro*, its expression increased as neurons maturated. Notably, at the diverse time points Spar3 was migrating slightly differently in gel, as a multiple band pattern, which might point to modifications of the protein during the maturation of spines in the hippocampal neurons. To understand if the possible modifications are mediated by the neuronal activity (*e.g.* Ca^{2+} influx) a 21 DIV old hippocampal culture was stimulated with N–methyl–D–aspartic acid (NMDA, $100\,\mu$M, 30 min). The control cells were collected in probe buffer without any treatment. After stimulation of the hippocampal culture with NMDA, the Spar3 band is shifted at the upper limit, which might point to activity–induced modifications of the protein. Interestingly, the increase in Spar3 level in the hippocampal culture is not consistent with the expression profile of the protein in hippocampus *in vivo* (section 4.12). This discrepancy might be the result of environmental differences in the culture and brain.

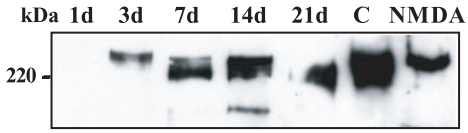

Figure 4.20: Time course of Spar3 expression in primary hippocampal cultures. The lysates of hippocampal neurons DIV 1, 3, 7, 14 and 21 after plating (10 μg total protein per lane) were analysed on Western blot. Lane C and lane NMDA are the 21 DIV cells from the other preparation (25 μg total protein per lane). NMDA – the culture was stimulated with NMDA (100 μM, 30 min); C – unstimulated neurons. The expression level of Spar3 in a hippocampal culture is increasing along with the maturation of neurons. Note the multiple band pattern of Spar3 migration. NMDA stimulation causes a shift of the protein migration in gel.

4.14 Spar3 localizes at the dendritic spines in cultured neurons

For the detection of the endogenous Spar3 protein in neurons the hippocampal culture was fixed at 21 DIV, stained with Spar3 and co–stained with synaptophysin AB. Synaptophysin is a major membrane protein of transmitter containing vesicles and is considered to be a marker of the presynaptic compartment (El Far and Betz, 2002). The staining of Spar3 was punctate and mostly opposed to the synaptophysin signals. On a high magnification view of the hippocampal cells (Fig. 4.21), the signals from the stained proteins formed a row "green–yellow–red": green for the presynaptic synaptophysin, yellow for the area of close contact of pre- and postsynaptic compartments and red for Spar3, which is localized to the dendritic spines.

4.15 When overexpressed in hippocampal neurons, Spar3–GFP is targeted to dendrites

To further characterize Spar3, Spar3–GFP was overexpressed in the cultured hippocampal neurons. The cells were transfected at DIV 15 and fixed the next day. The culture of transfected neurons was stained with AB, which are specific to the voltage gated potassium channel KCNQ3. In neurons, KCNQ3 is exclusively found in the axon and it can be used as an axonal marker (Jung Chung et al., 2006). GFP alone fills the dendrites and the axon with fluorescence of an equal intensity when overexpressed in the neurons (Fig. 4.22, **A**). Spar–GFP is mostly targeted to the dendrites, as previously described (Pak et al., 2001) and as it is documented on Fig. 4.22, **B**.

Overexpressed Spar3–GFP is mainly directed to the dendrites (Fig. 4.22, **C**). A

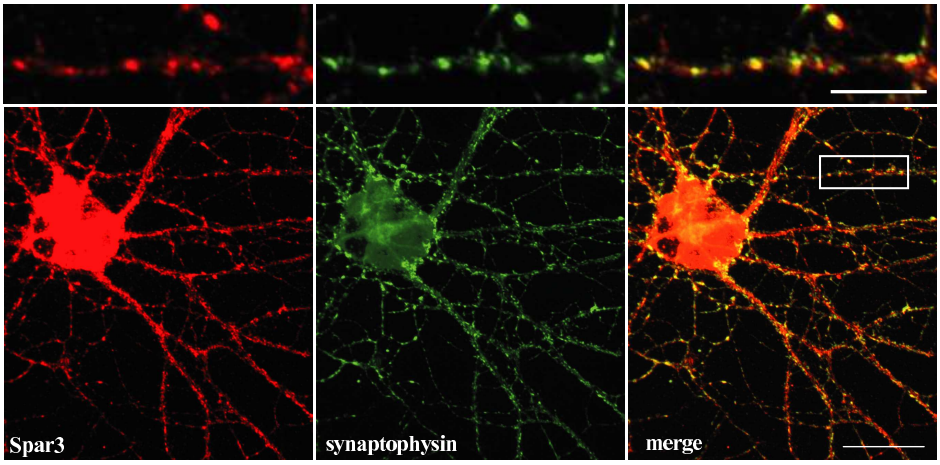

Figure 4.21: In the cultured hippocampal neurons, Spar3 localizes at the dendritic spines. The Spar3 staining is juxtaposed to that of the synaptophysin, which is the marker of presynaptic vesicles. The hippocampal neurons at 21 DIV are fixed and immunostained with anti–Spar3 AB, 1:500, and anti–synaptophysin AB, 1:400, as a presynaptic marker. Scale bar 30 μm (overview), 10 μm (insert).

weak GFP fluorescence is, however, observed in axon. The truncated Spar3, C'terminus 1300 − 1776 aa, is equally distributed to the axon and the dendrites (Fig. 4.22, **D**). This data shows that Spar3 is mainly targeted to the dendritic arbor and the N'terminus or the middle part of the protein is responsible for this sorting.

4.16 Overexpressed Spar3–GFP colocalizes with post-synaptic markers

Filamentous actin represents the major component of dendritic spines (Schubert and Dotti, 2007). The transfected neurons were incubated with alexa–568–labelled phalloidin to visualize the actin cytoskeleton. The phalloidin staining reveals punctate, actin-rich structures − the dendritic spines, in red (Fig. 4.23, **A**). The staining of actin–rich structures completely overlaps with the signal from Spar3–GFP, which indicates that Spar3 is targeted to the dendritic spines. Note that in Spar3–transfected neurons there are also some thin, filled with actin filopodia–like structures among the mature, mushroom–like spines (Fig. 4.23, **A**, s. asterisks). ProSAP2 is a key molecule of the PSD and unlike actin, a marker of spine protrusions, ProSAP2 is specifically targeted to the PSD, where it builds huge macromolecular complexes, the scaffold of the PSD (Boeckers, 2006). The ProSAP2 signal considerably overlaps with the puncta formed by Spar3–GFP (Fig. 4.23, **B**). If ProSAP2 staining highlights most of the

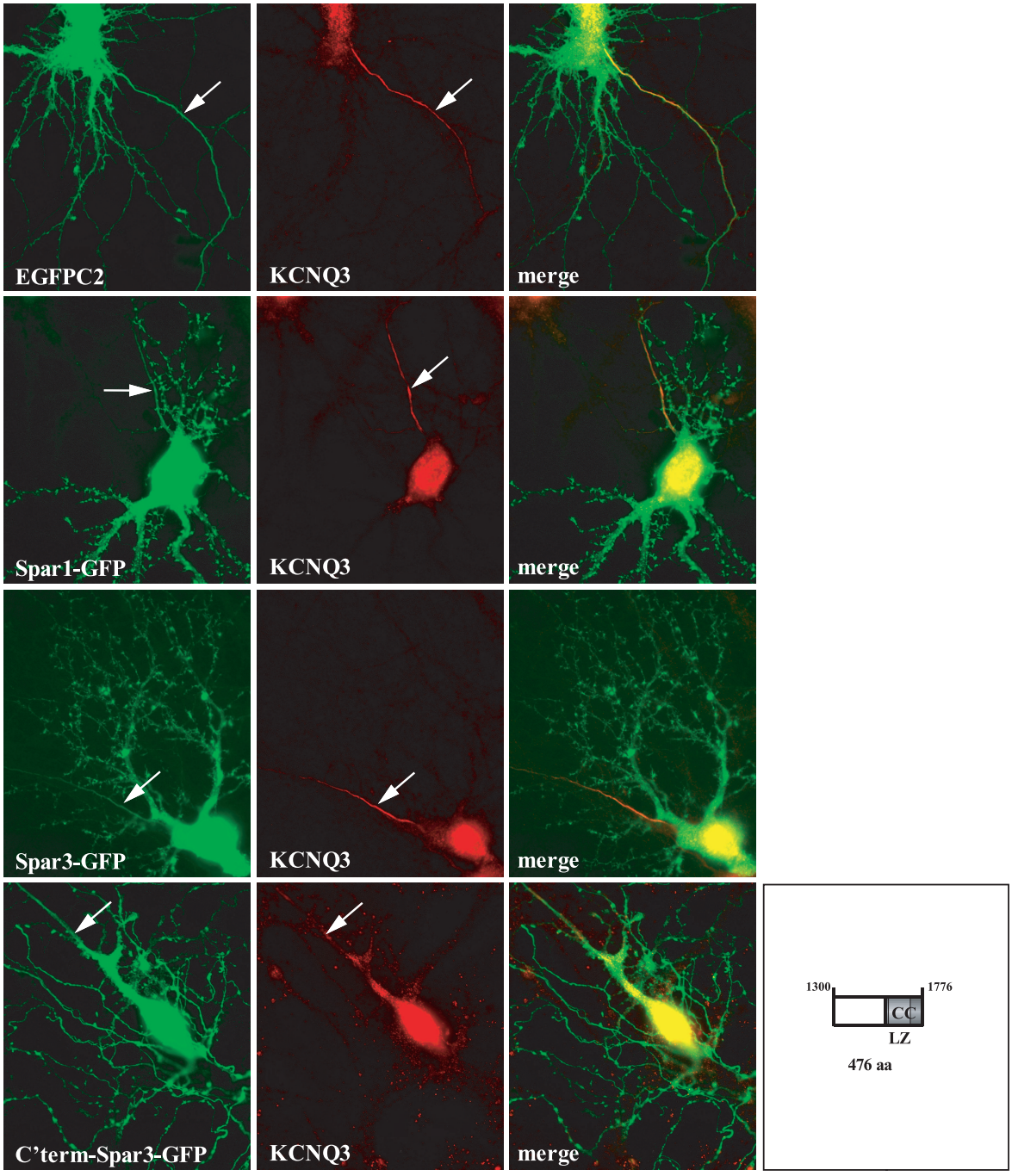

Figure 4.22: Staining of transfected neurons DIV16 with an axonal marker KCNQ3. **A**. The EGFPC2 transfected neurons were used as reference: the GFP is equally directed to the dendrites and the axon. **B**. Spar–GFP is mostly targeted to the dendritic arbor. The red axon, marked with KCNQ3 AB, does not show significant green fluorescence. **C**. Spar3–GFP localizes to the dendrites. Note the intensive fluorescence of dendrites and spines in comparison to axonal structure, marked with KCNQ3. **D**. The truncated form of Spar3, C'terminus (1300 – 1776 aa), is directed equally to the dendrites and axon. The arrows point at the axon. KCNQ3 AB were applied 1:500. Scale bar 30 μm.

PSDs, a visualization of GluR1, a major subunit of ionotropic glutamate receptor in hippocampal neurons, marks solely the active synapses. Many spines containing Spar3–GFP display the GluR1 signal (Fig. 4.23, **C**). Thus, by transfection in hippocampal neurons Spar3 is targeted to the dendritic arbor where it accumulates in the dendritic spines and colocalizes with the synaptic markers.

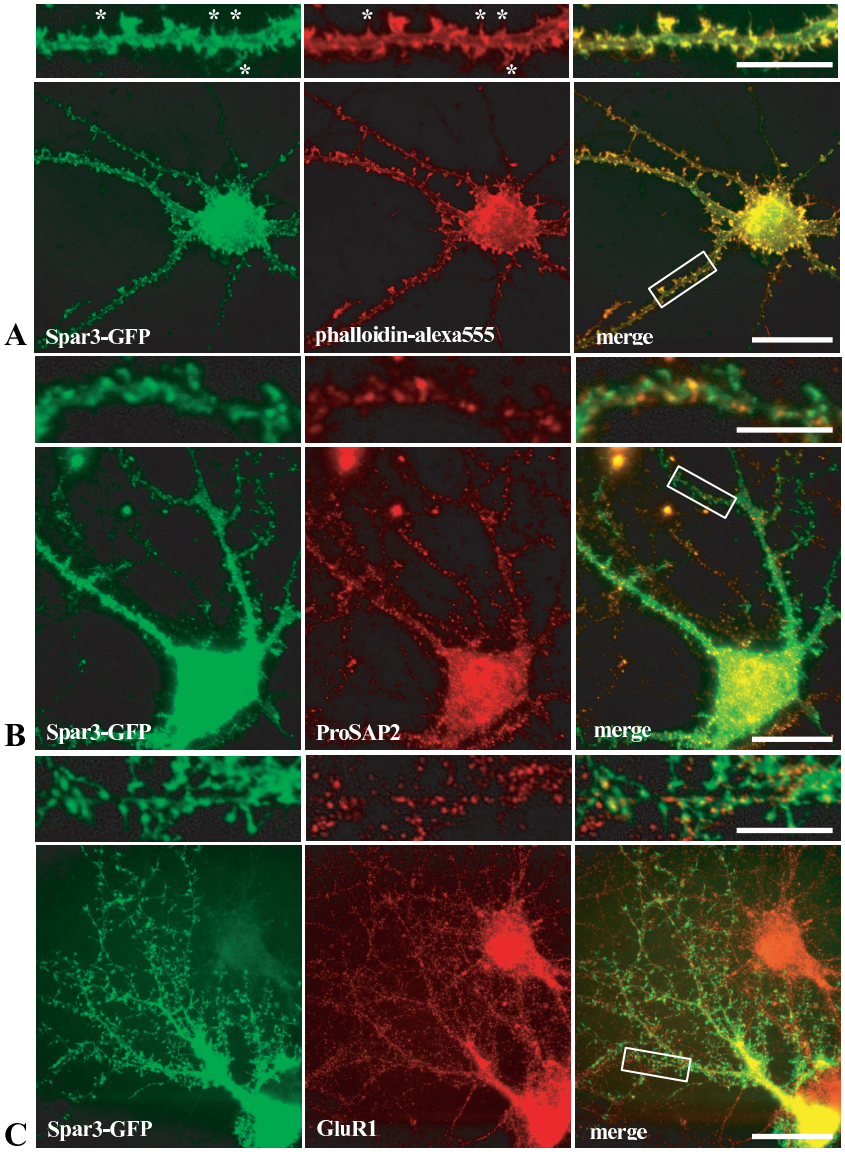

Figure 4.23: Actin (**A**), ProSAP2 (**B**) and GluR1 (**C**) staining of Spar3–GFP transfected hippocampal neurons, DIV 16. The transfected neurons were incubated with phalloidin-alexa–568, 1:50, for the visualization of F–actin, a marker of dendritic protrusions (**A**) or stained with AB against ProSAP2, 1:400, (**B**) or against GluR1, 1:500, (**C**) to highlight the marker proteins of PSD. The filopodia-like actin–rich structures are marked with asterisks on the figure with phalloidin staining. Scale bar 30 μm (overview), 10 μm (insert).

4.17 Effect of Spar3 on the spine morphology *in vitro*

Spar–GFP, transfected into hippocampal neurons, causes a decrease of the filopodia–like spines concomitant with an enlargement of the mature spine heads and formation of irregular spines (Pak et al., 2001). The other members of the SPA–family have a similar domain structure and a high identity with Spar within Rap–GAP, PDZ and coiled coil domains (Spilker et al., 2008). Therefore, the neurons transfected with Spar2 and Spar3 were documented and the spine morphology of neurons was analyzed with Adobe Photoshop CS. The transfection with Spar–GFP was repeated as a control. The shape classification described in the publication of Tyler and Pozzo-Miller (2003) was taken as a basis for the analysis. The spines were divided into three groups: mature, stubby and filopodia–like, depending on the ratio of the length (L) to the diameter of the spine neck (Dn) and the diameter of the spine head (Dh)(Fig.1.1). In mature spines Dh $\gg$ Dn, stubby type has L = Dh = Dn and by filopodia–like L $\gg$ Dh. Only spines opposed to bassoon, a marker of the active presynapses, were counted and statistically evaluated using the software MatLab 3.14. The GFP transfected control group of neurons (n = 8, 895 spines, DIV16) exhibited 58.1±3.8% of mature, 33.5±4.9% of stubby and 8.4±3.0% of filopodia–like spines (Fig. 4.24, **A**). This result is presented in each graphic, Fig. 4.24 **B**, **C**, **D** as reference, in grey. The overexpression of Spar1–GFP led to a statistically significant decrease of filopodia–like spines, $2.1 \pm 2.0\%$, which is in agreement with the results of Pak D et al (2001). The number of mature and stubby spines was almost not changed and showed only a statistically insignificant tendency to increase: stubby $39.3 \pm 1.5\%$ and mature $58.6 \pm 1.5\%$ (Fig. **B**, $n = 6$, 633 spines, 16 DIV). Spar2–GFP overexpressing neurons did not display any changes in morphology after transfection. The evaluation confirmed, that the spine ratio in Spar2–GFP expressing neurons was not significantly different from the GFP–expressing controls ($n = 6$, 610 spines, 16 DIV). Spar3–GFP transfected neurons displayed $50.6 \pm 4.4\%$ mature spines, $34.9 \pm 2.1\%$ stubby spines and $14.6 \pm 4.3\%$ filopodia–like spines ($n = 6$, 631 spines, 16 DIV). By counting only bassoon–associated spine protrusions the observed difference between Spar3–GFP and GFP transfected control neurons was not significant.

But it was obvious, that Spar3 transfected neurons formed more filopodia–like structures, which were not always opposed to the bassoon staining (Fig. 4.25 **A**, **B**). The evaluation of filopodia–like structures, not associated with bassoon, veils, in both GFP- and Spar3–GFP–transfected neurons showed considerable difference in phenotype: neurons overexpressing Spar3 exhibited 10.2±2.3 filopodia per dendrite of the second order in comparison to the control group 2.6 ± 1.2 ($n = 18$ cells per construct). Thus, Spar3

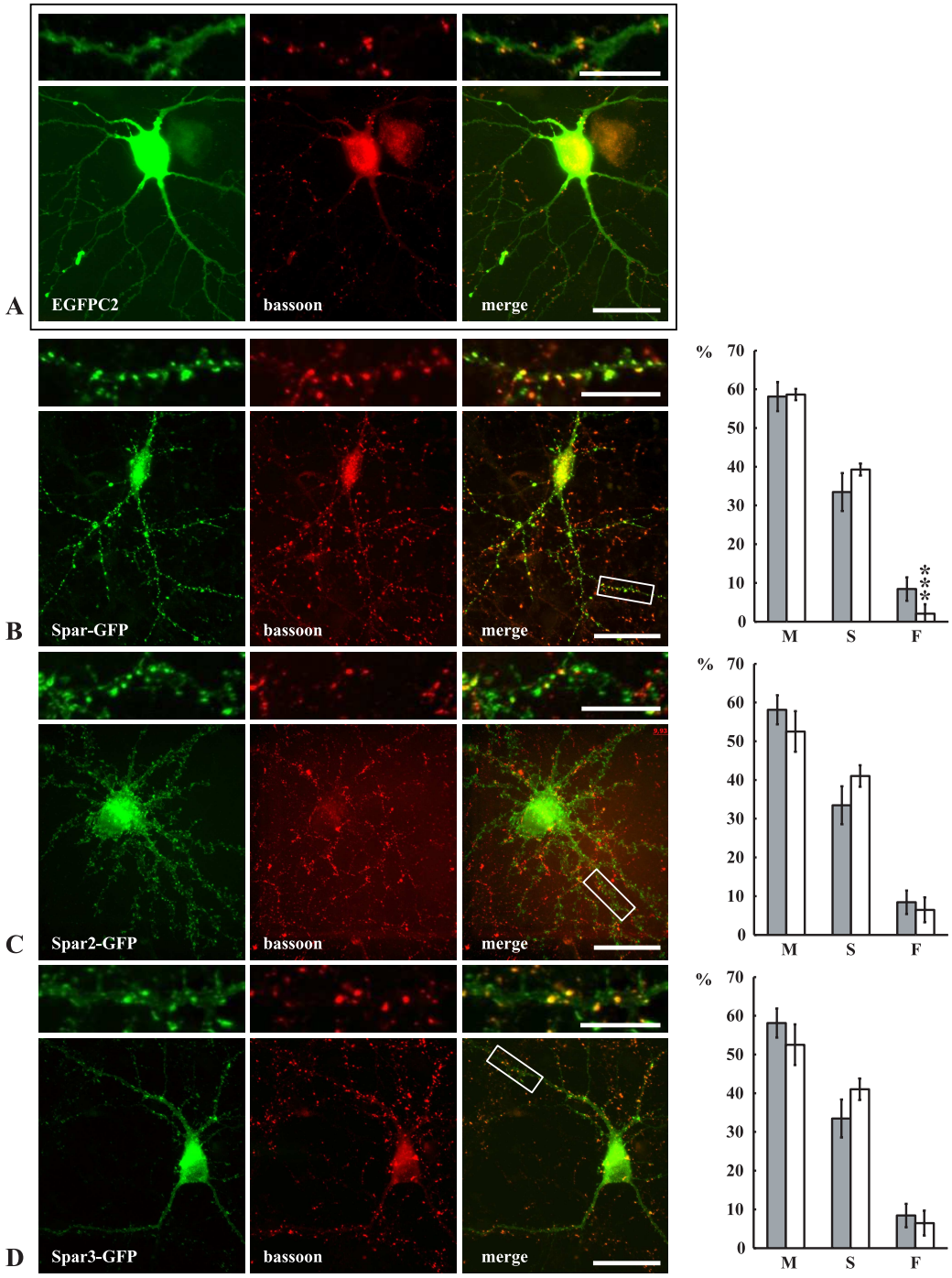

Figure 4.24: Quantification of the number of mature, stubby and filopodia–like spines in the bassoon stained neurons DIV16 overexpressing GFP (**A**), Spar–GFP (**B**), Spar2-GFP (**C**), Spar3–GFP (**D**). The neurons were transfected at DIV 15, fixed at DIV 16 and stained with bassoon, 1:500. The graphic on the right represents the statistical evaluation of the spine types by overexpression of the corresponding Spar proteins (in white) in comparison to the control GFP- expressing group (in grey). Three types of spines opposed to the bassoon staining have been evaluated: mature (**M**), stubby (**S**) and filopodia–like (**F**). Scale bar 30 μm (overview), 10 μm (insert).

produces an opposite effect on neurons by overexpression in the culture as Spar.

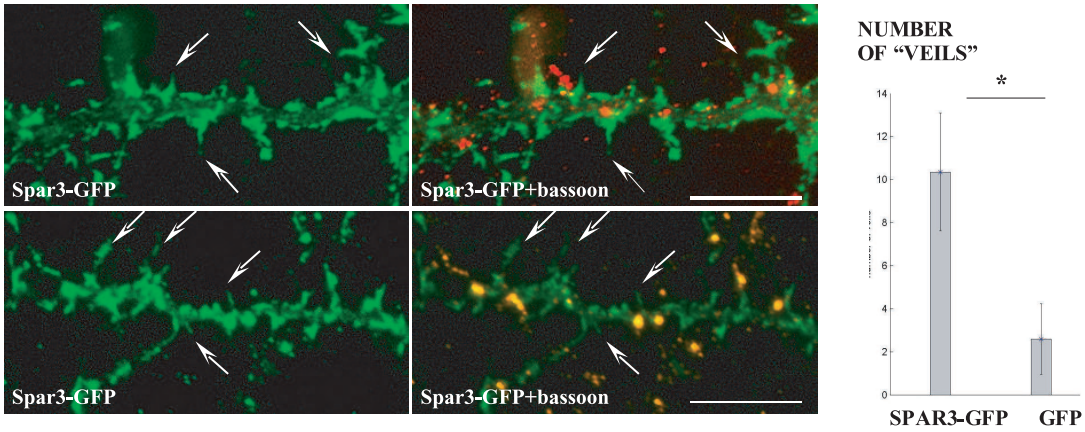

Figure 4.25: Spar3–GFP transfected neurons display filopodia–like structures, which are not opposed to the bassoon staining. Hippocampal Spar3–GFP transfected neurons DIV 16 from different preparations stained with bassoon, 1:500: **A**, **B**. The filopodia–like structures, which are not opposed to the bassoon staining (veils), are marked with arrows. As seen at the diagram on the right Spar3–GFP neurons diplay 10 ± 2.3 veils pro dendrite second order versus 2.6 ± 1.2 veils in the GFP–expressing control group of neurons. Scale bar 10 μm.

4.18 Influence of Spar3 truncated variants on spine morphology *in vitro*

The first N' terminal 500 aa of Spar3 reorganize the actin cytoskeleton by transfection in Cos–7 cells. The C'terminal part, 476 aa, is the only domain of Spar3, which is unable to associate with actin. To analyze the effects of those truncated forms of Spar3 on spine morphology, the neurons DIV 14 were transfected with the N'terminus Spar3–GFP or with the C'terminus Spar3–GFP. The cells were fixed at DIV 16 and stained with the bassoon AB. The neurons transfected with N'terminus displayed a remarkable increase in filopodia–like spines ($31.8 \pm 4.3\%$) concomitant with a decrease in mushroom–like protrusions ($33.9 \pm 3.6\%$), in comparison to GFP-expressing neurons (Fig. 4.26, **A**). The double reduction in mature spines and correspondent increase of immature spines illustrates that the N'terminus has a dominant-negative effect on spine maturation. In contrast, the C'terminus does not affect spine morphology by overexpression (Fig. 4.26, **B**). There are $52.4 \pm 7.4\%$ mature, $38.6 \pm 6.0\%$ stubby and $9.1 \pm 1.5\%$ filopodia–like spines. Hence, a ratio of spines in the C'terminus-expressing neurons remains unchanged in comparison to GFP–transfected neurons.

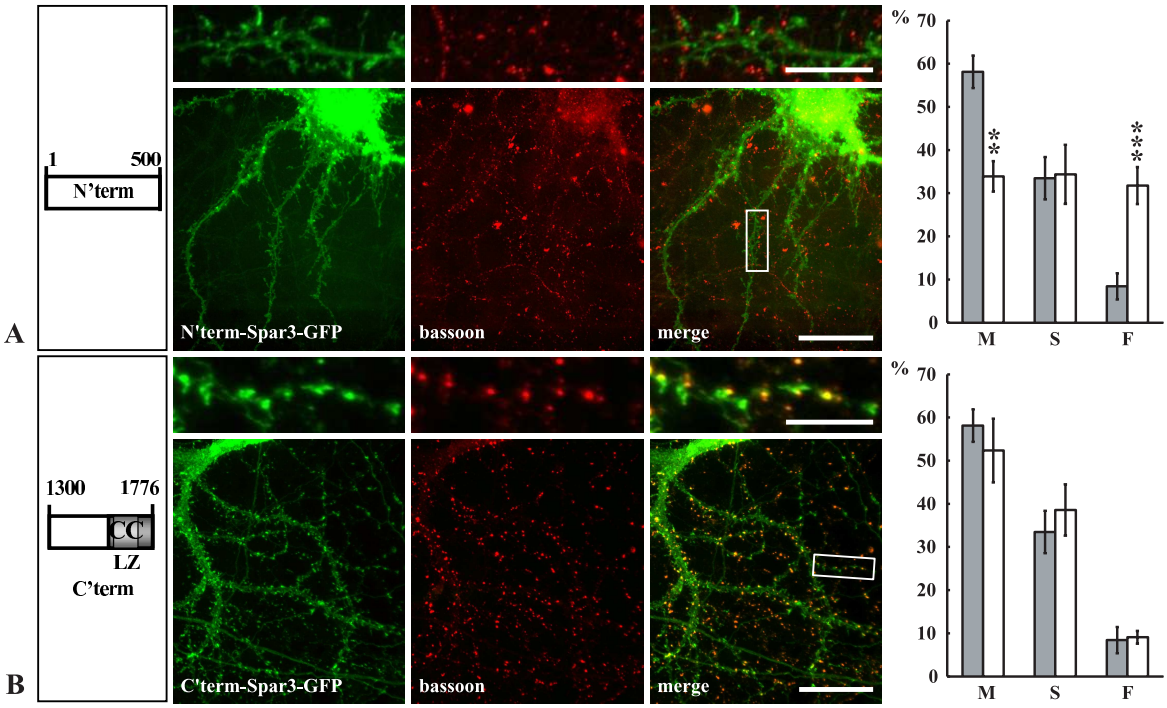

Figure 4.26: Effect of the overexpression of the truncated Spar3 forms on spine morphology. Quantification of the number of mature, stubby and filopodia–like spines in bassoon-stained DIV16 neurons transfected with truncated Spar3: the N'term-Spar3–GFP ($1-500$ aa) and the C'term-Spar3–GFP ($1300-1776$ aa). The neurons were transfected at DIV 14, fixed at DIV 16 and stained with bassoon, 1:500. The N'term-Spar3–GFP has a dominant negative effect on the spine maturation. On the contrary, the C'term-Spar3–GFP does not change spine morphology. Scale bar 30 μm (overview), 10 μm (insert).

4.19 Targeting of Spar3 to spines in hippocampal neurons

The staining with the pre- and postsynaptic markers showed that both endogenous and overexpressed Spar3 is targeted to the dendritic spines (sections 4.14, 4.16). To clarify, which domain of Spar3 is responsible for targeting of the protein to spines, cultured hippocampal neurons at day 14 were transfected with the truncated Spar3 constructs. The transfected neurons were stained with AB to a presynaptic marker bassoon at day 16 and documented. The distribution of GFP–tagged constructs in neuron was analyzed with Adobe Photoshop CS. The evaluation method of the construct targeting described in the publication Boeckers T.M. et al. was taken as a basis for the analysis (Boeckers et al., 2005). The method is based on the comparison of the average pixel intensity of the selected area in the green channel in spine and in the adjacent dendrite. The calculated ratio of average pixel intensity in dendrites/spines is called the synap-

tic clustering ratio (SCR). It reflects the distribution of a construct: by SCR > 0.8 construct is not targeted to spines and present with nearly equal probability in the spines and the dendrites. Additionally, the counterstaining of spines with bassoon was evaluated (Boeckers et al., 2005). 200 spines per construct from 7 different cells were analyzed.

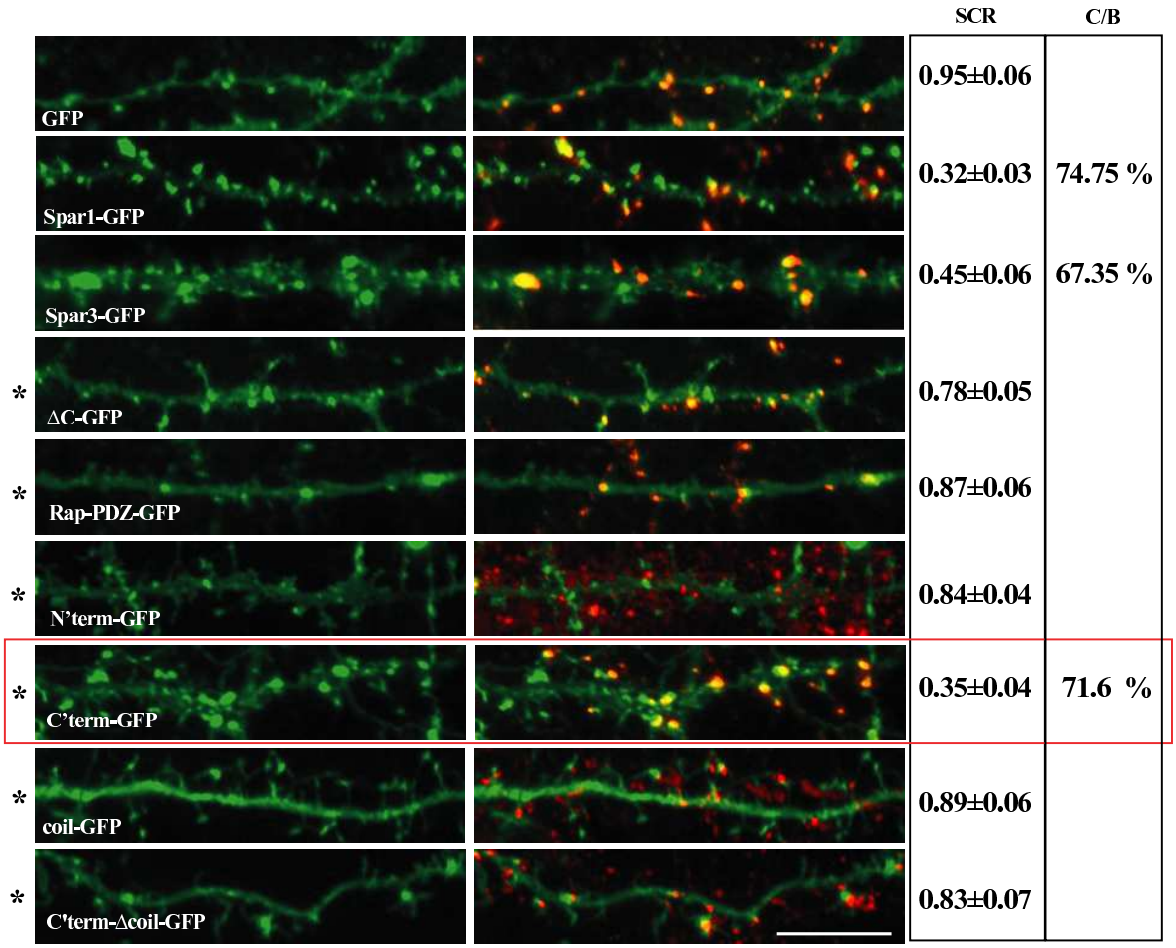

Figure 4.27: Targeting of Spar3 to spines. The hippocampal neurons were transfected at DIV14 with GFP as a control, Spar–GFP, Spar3–GFP and following **GFP–tagged Spar3 truncated forms** (marked with asterisk): ΔC (1 – 1300 aa), Rap–PDZ (548 – 1003 aa), N'term (1 – 500 aa), C'term (1300 – 1776 aa), coil (1700 – 1776 aa), C'term-Δcoil (1300 – 1708 aa). The left row represents in the green channel the dendrites of neurons, transfected with corresponding constructs. The middle row shows a merge with a bassoon staining of the same images. The third row represents the synaptic clustering ratio (SCR) for each construct. The fourth row shows the association of overexpressed construct (Spar, Spar3 or C'term-Spar3) with the presynaptic marker bassoon, **C**/**B** ratio. The only Spar3 truncated construct targeted to spines is marked with a red frame. Scale bar 10 μm.

GFP alone, when overexpressed in neurons, was diffusely distributed to spines and dendritic shafts as expected (SCR = 0.95 ± 0.06, Fig. 4.27). Spar–GFP was enriched in spines (SCR = 0.32 ± 0.03) and 74.75% of the Spar signal was juxtaposed

to the bassoon staining (this parameter was designated as C/B and illustrates construct/bassoon association). This result was consistent with the observations of Pak D. (Pak et al., 2001). The evaluation of spines in Spar3–GFP transfected neurons showed that Spar3 is also targeted to spines (SCR $= 0.45 \pm 0.06$, C/B 67.35%). Interestingly, the SCR value of Spar3 differs from Spar and indicates that Spar3 is targeted to the spines with different effectivity (Fig. 4.27). The Spar3 lacking C'terminus (ΔC, $1 - 1300$ aa) looses its synaptic localization and is diffusely distributed in the neurons (SCR $= 0.78 \pm 0.05$). Similarly, the Rap–PDZ–Spar3 truncated construct (Rap–PDZ, $548 - 1003$ aa) and N'terminus of Spar3 (N'term, $1 - 500$ aa) show no synaptic targeting, with SCR $= 0.87 \pm 0.06$ and SCR $= 0.84 \pm 0.04$, respectively.

In contrast, the C'terminus of Spar3 (C'term, 1300-1776aa) is highly accumulated in spines and even better targeted to spines as the full size protein (SCR $= 0.35 \pm 0.04$, C/B $71,6\%$). To examine whether the coiled coil domain is responsible for the spine targeting, the coiled coil alone (coil, $1700 - 1776$ aa) and the C'terminus lacking the coiled coil domain (C'term–Δcoil, $1300 - 1708$ aa) were subcloned as two different constructs, sequenced and checked on Western blot for expression (Fig. 4.28 **A**, **B**). Surprisingly, after overexpression in hippocampal neurons both constructs were uncapable to accumulate in the spines (SCR $= 0.89 \pm 0.06$ for coil alone and SCR $= 0.83 \pm 0.07$ for C'term–Δcoil, Fig. 4.27). Thus, both the coiled coil domain $1707 - 1776$ aa and the C'terminal part $1300 - 1708$ aa are essential for the targeting of Spar3 to the spines and form the so called bipartite targeting signal.

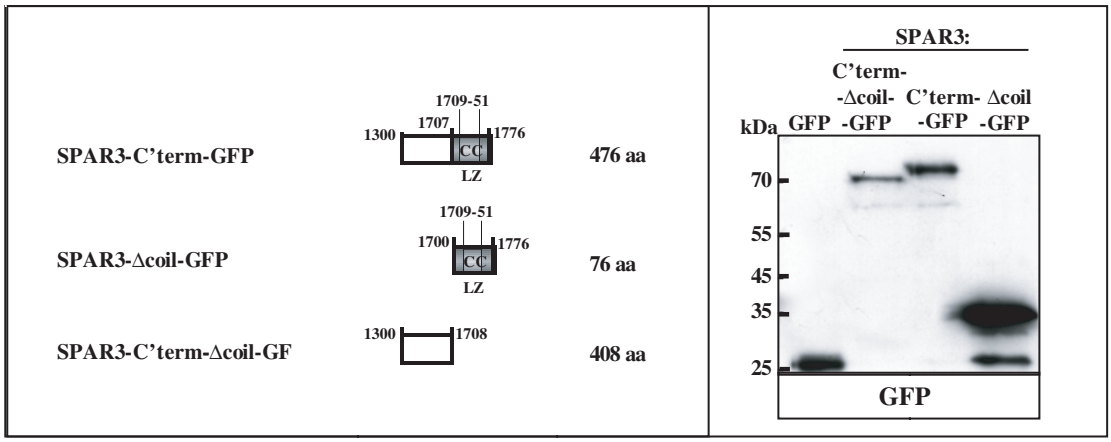

Figure 4.28: Truncated forms of Spar3 C'terminus used for additional targeting experiments. The domain structure (**A**) and visualization on a Western blot (**B**) the overexpressed in Cos–7 Spar3 truncated forms. **B**. The GFP–tagged truncated forms of Spar3 were overexpressed in Cos–7 and probed with anti-GFP AB (1:3000). All constructs migrated on Western as expected. GFP was applied on blot as a control.

4.20 Identification of putative interaction partners for Spar3

A yeast–two–hybrid system was used to identify proteins that interact with Spar3. A rat brain cDNA library was screened with the C-terminal 476 aa as a bait. This part of Spar3 has a coiled coil domain with a leucine zipper motif which is involved in protein-protein interactions. Besides, the entire construct $1300-1776$ aa of Spar3 (*i.e.*, not fragments of it) was targeted to spines. The C'terminus of Spar3 was cloned into the vector pAS2-1, containing the GAL4 DNA-binding domain. The yeast–two–hybrid screen was performed as described in section 3.13. Out of 1.1×10^6 yeast transformants screened 72 positive clones were isolated and analyzed for the $\beta-$galactosidase activity by a filter–lift experiment. After preliminary analysis by digestion with Eco RI/XhoI 25 clones were chosen for sequencing. Seven independent clones encoded members of the Fezzin family: ProSAPiP1/LZTS3, LAPSER1/LZTS2 and PSD-Zip70/LZTS1 (table 4.1). Those proteins, first described as tumor suppressors in the cell lines and as adaptor molecules in brain, are now shown to play a role in $\beta-$catenin/NF–kB signaling (Cho et al., 2008).

Obtained clone (prey)	**Name**	**Num. of clones found**	**Short characteristics of putative interactors**	**Domain structure of the shortest clone of prey**
NM_172022.2	ProSAPiP1/-LZTS3	3 #12, #27, #56	Protein of PSD; described as an adaptor protein, recruiting Spar to the scaffold protein ProSAP2 (Wendholt et al., 2006).	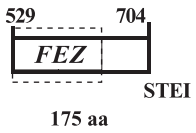
DQ_176638.1	LAPSER1/-LZTS2	3 #2, #4, #5	First described as a tumor suppressor protein, which interacts with $\beta-$catenin and supresses the $\beta-$catenin-dependent transcription (Thyssen et al., 2006). Enriched in PSDs. Interacts with ProSAP (Schmeisser, 2007).	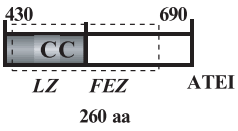

NM_153470.1	PSD-Zip70/-LZTS1	1 #25	Regulator of cell growth and tumor suppressor protein, later described as a component of PSDs and dendritic rafts, recruiting Spar to spines (Vecchione et al., 2002; Konno et al., 2002; Maruoka et al., 2005)	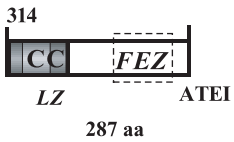
AY043226	Spar/-SerSAP1	2 #34, #54	RapGAP (GTPase activating protein for Rap2A) found in the complex with PSD–95 in spines. Overexpression of Spar caused enlargement of spines (Pak et al., 2001).	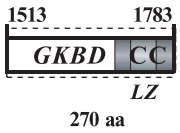
NM_017344	GSK3α (Glycogen synthase kinase 3 alpha)	2 #20, #45	Serine/threonine protein kinase (S_TK), which regulates the level and transcriptional activity of $\beta-$catenin. GSK3α phosphorylates tau protein (Asuni et al., 2006) and is necessary for the axon formation (Garrido et al., 2007). It regulates the production of Alzheimer's disease amyloid-β peptides (Phiel et al., 2003).	
AB_006461	Neurochond–rin/NORBIN	1 #51	Negative regulator of the Ca^{2+}/calmodulin–dependent kinase II phosphorylation. Is important for the spatial learning. Knock–out of the gene in nervous system caused epileptic seizures (Dateki et al., 2005). Obtained clone contained leucine-rich region (leu–rich).	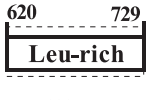
BC062075	Calcium binding atopy-related autoantigen 1	1 #59	contains Ca^{2+}–binding EF-hands (EFh). Might belong to the signaling molecules (InterPro Scan). Function is not known.	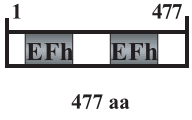

NM_001017477	G protein pathway suppressor 2	1 #14	Predicted (InterProScan) regulatory molecule of JNK and MAPKKK cascade. Function is not known.	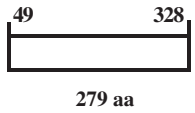

Table 4.1: The summary of prey clones obtained in the yeast–two–hybrid screen with the C'terminus of Spar3 as a bait

Two obtained clones coded for Spar. Possibly, Spar and Spar3 are able to form heterodimers. The other two clones were identified as glycogen synthase kinase 3 α (GSK3-α), one of the regulators of the $\beta-$catenin transcription (Asuni et al., 2006). One revealed clone coded for neurochondrin/NORBIN, a signaling leucine–rich molecule, regulating Ca^{2+}/calmodulin-dependent kinase II (CaMKII) phosphorylation. The function of several other found proteins, listed in the table below, was not clear.

4.21 Spar3 interacts with ProSAPiP1

A clone of Spar was obtained in a yeast–two–hybrid screen of rat brain cDNA library with ProSAPiP1 as a bait (Wendholt et al., 2006). It was no surprise that by screening of the same cDNA library *vice versa* with the C'terminus of Spar3 as a bait (s. section 4.16) several clones of ProSAPiP1 were found. The shortest "prey" clone coded for the C'terminus of ProSAPiP1 with two thirds of the FEZ domain ($529-704$ aa). The other two clones were similar and both had a coiled coil and a FEZ domain (Fig. 4.29).

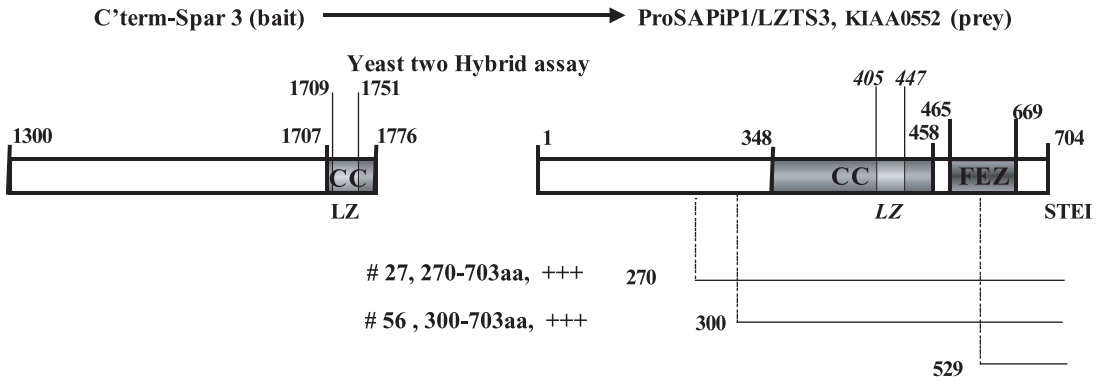

Figure 4.29: Scheme of yeast two–hybrid screen with the rat brain cDNA library. The Spar3 bait is depicted on the left. The obtained clones of ProSAPiP1 and its domain structure are designated on the right, with the longest clone coding for 434 aa and the shortest – for 175 aa of the C'terminus. CC – a coiled coil domain, LZ – a leucine zipper motif, FEZ – a F37/Esophageal cancer-related gene coding leucine zipper motif 1, STEI – a PDZ–binding motif of 4 aa.

For the verification of the Spar3–ProSAPiP1 interaction, an overlay-experiment was carried out. The overlay-assay is based on the ability of denaturated proteins immobilized on a membrane to recruit the interaction partners from brain lysate (Rosenbluh et al., 2006). The Spar3–GFP, the truncated Spar3–GFP constructs and an empty EGFP vector (control) were overexpressed in the Cos–7 cells and applied to Western blot. A part of the membrane was probed with GFP AB to control the overexpression level and migration of the GFP–tagged proteins. The other part of the membrane containing the immobilized proteins was thoroughly blocked, incubated with a rat brain lysate, extensively washed with PBS and probed with anti–ProSAPiP1 AB. Full size immobilized Spar3–GFP binds and retains ProSAPiP1 from the brain lysate, while GFP does not (Fig. 4.30, **A**). The recruited protein was detected at an approximate molecular weight of about 220 kDa, which differs from that of ProSAPiP1–GFP at about 90 kDa and from ProSAPiP1 expressed in brain, 75 kDa (Wendholt et al., 2006). The C'terminus of Spar3 alone also binds ProSAPiP1 from the brain lysate efficiently (Fig. 4.30, **B**). Spar3 lacking the C'terminus fails to bind ProSAPiP1. Therefore, Spar3 interacts with ProSAPiP1 and the C'terminus of Spar3 ($1300 - 1776$ aa) is responsible for this interaction.

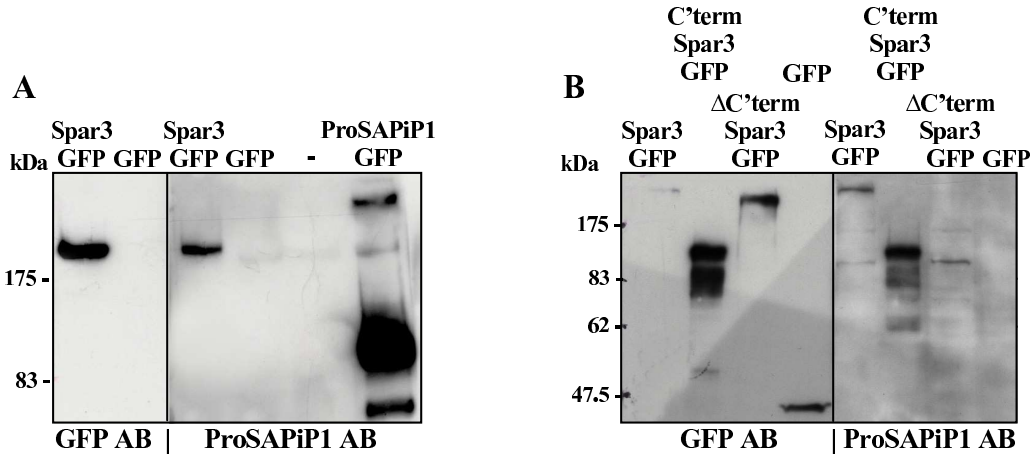

Figure 4.30: Overlay assay illustrating the interaction of Spar3 and ProSAPiP1. The Spar3–GFP (**A**) and the truncated Spar3–GFP constructs overexpressed in Cos–7 (**B**) were subjected to Western blot analysis. The GFP was co-probed as a control of the non-specific binding. The ProSAPiP1–GFP clone was applied on Western blot as reference. A part of the membrane (A,B, on the right) with immobilized proteins was incubated with brain lysate, washed and probed with ProSAPiP1 AB (1:2000) for bound proteins. Another part was incubated in PBS and then with anti–GFP AB (1:3000) to visualize the overexpressed proteins. ProSAPiP1 is recruited from brain lysate and is detected at an approximate molecular weight of Spar3–GFP, 220 kDa, compared to ProSAPiP1–GFP migrating at 90 kDa. The upper bands of the ProSAPiP1–GFP lane correspond to di– and trimeres formed by the protein ($\approx$ 180, 270 kDa), described in Wendholt et al. (2006)

The pull-down assay was performed to confirm additionally the ProSAPiP1 and Spar3 interaction. The Spar3–C'terminus 1300 – 1776 aa–GST–fusion protein was expressed in *E.coli*, strain BL21, and purified on a glutathione-sepharose column. After dialysis 0.1 mg of the purified protein was coupled to brom–cyan–(Br–CN)–sepharose and incubated with brain lysate. The column was washed. Precipitated ProSAPiP1 was detected by Western blot analysis (Fig. 4.31). The control aliquot of sepharose, without Spar3–C'terminus–GST, did not precipitate ProSAPiP1.

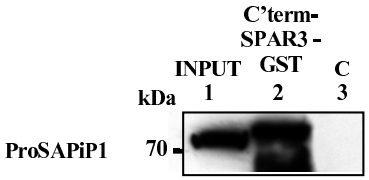

Figure 4.31: Precipitation of ProSAPiP1 by the Spar3–C'terminus–GST in the pull–down assay. ProSAPiP1 is detected in the input (lane 1). Spar3–C'terminus-GST precipitates ProSAPiP1 from rat brain lysate (lane 2). ProSAPiP1 is not precipitated in the control (C) by sepharose beads alone (lane 3).

The C'terminus of Spar3 forms fibers similar to intermediate filaments after transfection in Cos–7 cells (s. section 4.9). The cotransfection of ProSAPiP1–RFP together with the C'–terminus-Spar3–GFP disrupts the fiber-pattern observed in single–transfected cells and brings C'term–Spar3 to the clusters of ProSAPiP1 protein (Fig. 4.32).

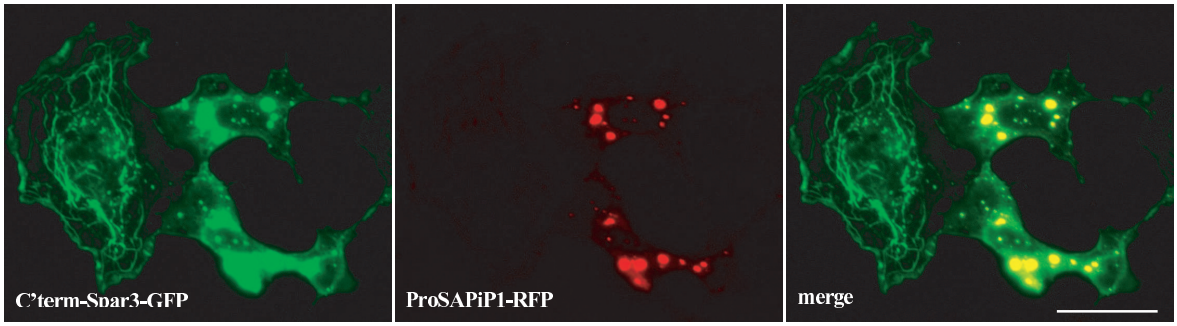

Figure 4.32: Cotransfection of the C'–terminus of Spar3–GFP and ProSAPiP1–RFP in Cos–7 cells. The C'-terminus of Spar3–GFP completely overlaps with ProSAPiP1-RFP in cotransfected cells. Scale bar 20 μm.

To verify the interaction Spar3-ProSAPiP1 in hippocampal neurons, the culture was transfected with Spar3–GFP and stained with ProSAPiP1 AB (Fig. 4.33). Endogenous ProSAPiP1 is often present in spines which are filled with Spar3–GFP.

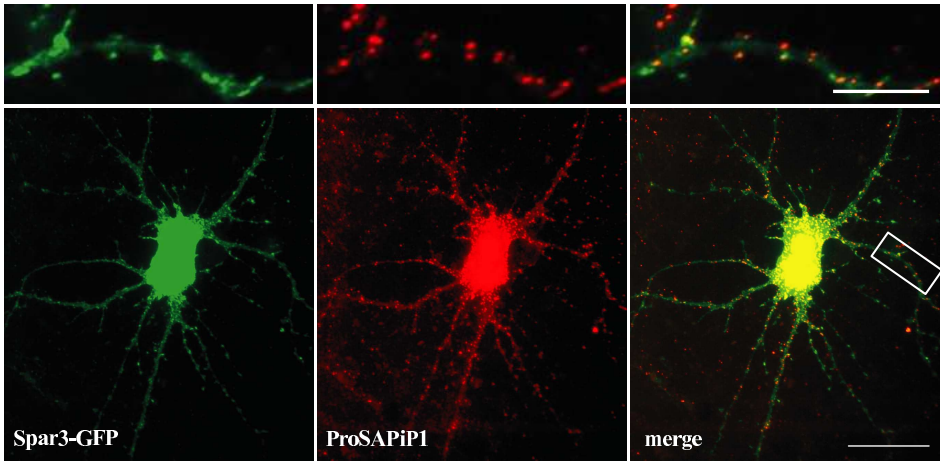

Figure 4.33: Colocalization of endogenously expressed ProSAPiP1 and overexpressed Spar3–GFP in cultured hippocampal neurons 16 DIV. The neurons were transfected with the Spar3–GFP construct and stained with affinity purified anti–ProSAPiP1 AB (1:100). Scale bar 30 μm (overview), 10 μm (insert).

4.22 Spar3 interacts with LAPSER1, another member of Fezzin family

As indicated in section 4.20, three independent clones of LAPSER1 were obtained by screening of the cDNA rat brain library with the C'terminus of Spar3 (1300−1776 aa) in the yeast–two–hybrid system. One clone contained a full size cDNA of LAPSER1, two clones had a partial cDNA of LAPSER1, corresponding to 314−690 aa and 430−690 aa. All found clones of LAPSER1 contained a coding region for the FEZ (F37/Esophageal cancer-related gene coding leucine zipper motif 1) domain (Fig. 4.34).

To verify that Spar3–LAPSER1 interaction occurs in brain, a pull–down assay was carried out. The Spar3–C'terminus, 1300–1776aa–GST–fusion protein, was coupled to the column, as described in section 4.21. The beads, coupled with the fusion protein were incubated with rat brain lysate. As a control, uncoupled sepharose beads were incubated with brain lysate. Both probes were washed. Bound proteins were eluated and probed with AB to LAPSER1 on Western blots.

On Fig. 4.35 a 70 kDa band characteristic for LAPSER1 is detected in brain lysate (input, lane 1). The same 70 kDa band is pulled–down by the Spar3–C'terminus (lane 2) as well as LAPSER1 migrating at 90 kDa. This upper band possibly represents a phosphorylated form of the protein (as observed by Schmeisser M., personal communication). Several bands downstream around 35 − 55 kDa might be a result of protein degradation during the experiment. No LAPSER1 was detected in the eluate after the

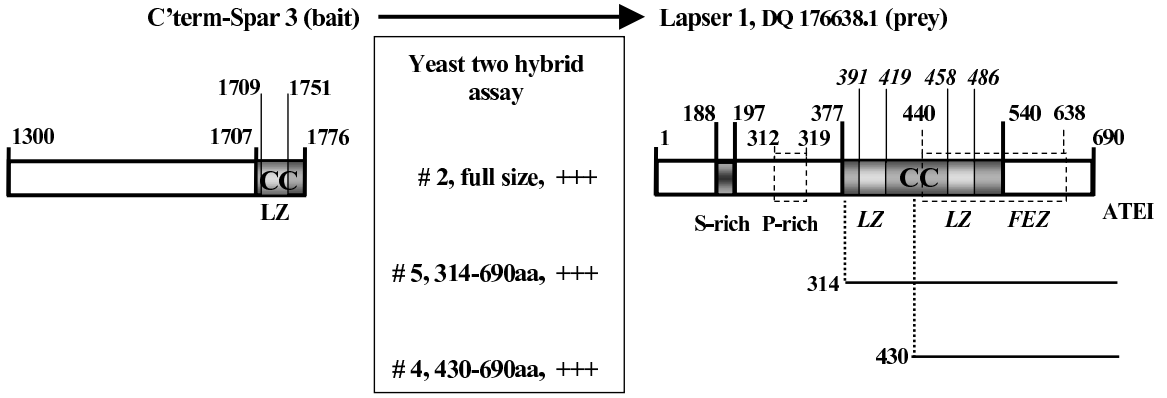

Figure 4.34: Schematic view of LAPSER1–clones found by the screen in the yeast–two–hybrid system. The Spar3–bait used in screen is shown on the left. On the right the domain structure of LAPSER1 is depicted. CC – a coiled coil domain, LZ – a leu–zipper, P-rich – a prolin–rich motif, S-rich – a serine rich motif, FEZ – a F37/Esophageal cancer–related gene coding leucine zipper motif 1, ATEI – 4 aa motif responsible for the binding of the PDZ domain.

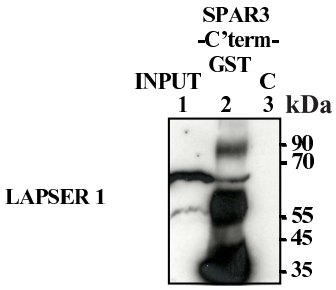

Figure 4.35: Precipitation of LAPSER1 by the C'terminus of Spar3–GST in pull–down assay. Brain lysate was incubated with the C'term–Spar3–GST–fusion protein (1300 – 1776 aa) immobilized on Br–CN–sepharose. The first lane shows the rat brain lysate used for the pull-down assay (input), the second lane displays the eluate from the beads, coupled with the C'term–Spar3–GST–fusion protein (1300 – 1776 aa), the third lane represents the eluate from glutathione–sepharose incubated only with the brain lysate as a control.

incubation of the brain lysate with beads without bound Spar3–C'terminus.

To examine if LAPSER1 is associated with Spar3 *in vivo*, a rat brain lysate was subjected to immunoprecipitation with anti-LAPSER1 AB and immunoblotted with anti-Spar3 and *vice versa* (Fig. 4.36). The respective AB were coupled to protein A coated magnetic beads, incubated with brain lysate, washed thoroughly and then immunoblotted for bound proteins. As a control AB-free beads were incubated with brain lysate, washed and analyzed on Western blots. Spar3 AB precipitate the typical double 70 – 90 kDa forms of LAPSER1 from brain lysate (lane 3, 4, **A**). In spite of the low concentration of the Spar3 protein in the input, it has been precipitated from

brain lysate (lane 2, **B**). The results of immunoprecipitations indicates that Spar3 and LAPSER1 occur in the brain as complexes.

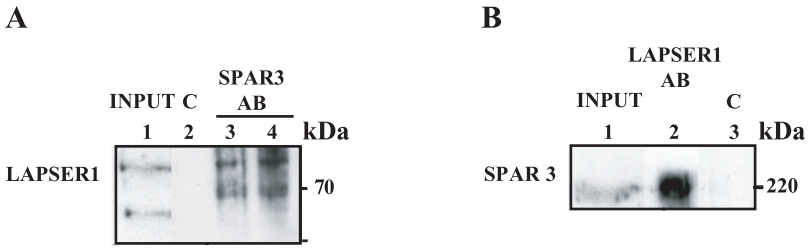

Figure 4.36: Coimmunoprecipitation of Spar3 and LAPSER1. **A** Brain lysate was immunoprecipitated with anti–Spar3 AB and immunoblotted with LAPSER1 AB (lanes 3, 4, different concentration of SPAR3 AB was applied). No signal is detected in the control. **B** Brain lysate was immunoprecipitated with anti–LAPSER1 AB and immunoblotted with Spar3 AB (lane2). The input and the control are at lines 1 and 3.

Immunocytochemical studies on HeLa cells support the idea of Spar3–LAPSER1 interaction. In double–transfected cells the overexpressed proteins Spar3–GFP and LAPSER1–RFP show a complete colocalization. The typical small–sized grains of LAPSER1 protein (seen on top of Fig. 4.37, **A**) are not observed in the double–transfected cells. LAPSER1–RFP is recruited to bigger clusters of Spar3–GFP. According to the results of the two–hybrid screen and pull-down assay, the C'terminus of Spar3 can interact with LAPSER1. This interaction might be mediated by the coiled-coil domain containing leucine–zipper in Spar3 and by the FEZ–domain in LAPSER1 (Schmeisser, 2007). The N'terminus of Spar3 ($1 - 500$ aa) should not interact with LAPSER1. As expected no overlapping of the signals is observed by co–transfection of the N'terminus of Spar3–GFP and LAPSER1–RFP (Fig. 4.37, **B**). On the contrary, the C'terminus of Spar3–GFP is recruited to the grains of LAPSER1–RFP and looses its filamentous structure, typical for the single transfected cells (Fig. 4.37, **C**).

Finally, Spar3–GFP and LAPSER1-RFP were co-transfected in hippocampal neurons. Spar3 is completely recruited to the sites of the LAPSER1 expression. Moreover, the double–transfected neurons acquire a special phenotype, different from a Spar3–single transfected cell (compare Fig. 4.38 **A** and **AA**). Interestingly, the other member of the SPA family, Spar–GFP, localizes to the LAPSER1 aggregates. But the colocalization is not as complete as in the case of Spar3 (Fig. 4.38, **B**). The various extent of recruitment of Spar and Spar3 to LAPSER1 might reflect the difference in affinity of the interactions Spar1–LAPSER1 and Spar3–LAPSER1.

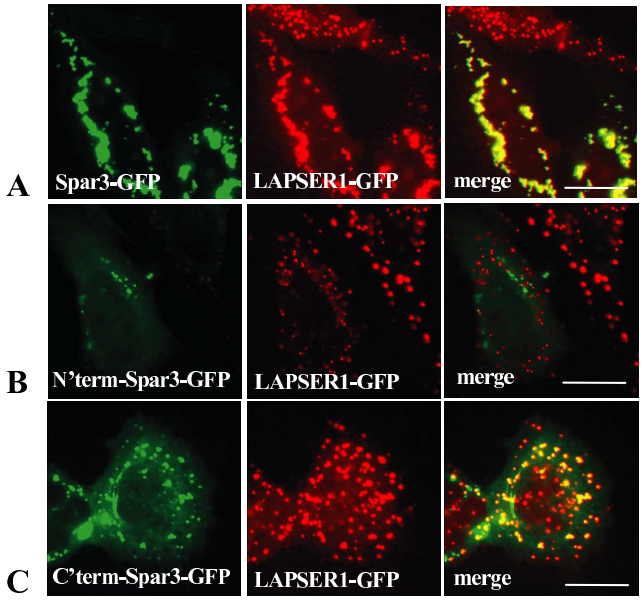

Figure 4.37: The interaction Spar3–LAPSER1 is verified by transfection in HeLa cells. **A**. When overexpressed in HeLa cells Spar3 and LAPSER1 form a stable complex. The signals from both proteins completely overlap. In the presence of Spar3 the clusters of LAPSER1 are bigger unlike the protein aggregates in a single–transfected cell. **B** The N'terminus of Spar3–GFP is co–transfected with LAPSER1 as a control. No colocalization of proteins is observed. **C**. In contrast, the C'terminal part of Spar3 with the coiled coil domain is localized to the LAPSER1–RFP clusters. Scale bar 20 μm.

4.23 Coexpression of LAPSER1 and ProSAPiP1 in hippocampal neurons

The ability of Fezzins for forming of homo- and heterodimeres was already demonstrated at a biochemical level and in cell lines (Wendholt et al., 2006). To verify the interaction of the proteins in the hippocampal culture ProSAPiP1–GFP and LAPSER1–RFP were cotransfected in neurons. As expected ProSAPiP1 formed complexes with LAPSER1 and the signals from both fluorescent proteins colocalized significantly (Fig. 4.39, **A**). Note, that the ProSAPiP1/LAPSER1 double–transfected cells display a distinct phenotype, different from ProSAPiP1 single transfected neurons (Fig. 4.39, **A**, **AA**).

4.24 Spar3 is in a complex with $\beta-$catenin

Thyssen et al. working on the human colon cancer cells SW 480, described LAPSER1 as a novel $\beta-$catenin-interacting protein, which retained $\beta-$catenin in the cytoplasm of cells and suppressed $\beta-$catenin-mediated transcription (Thyssen et al., 2006). The

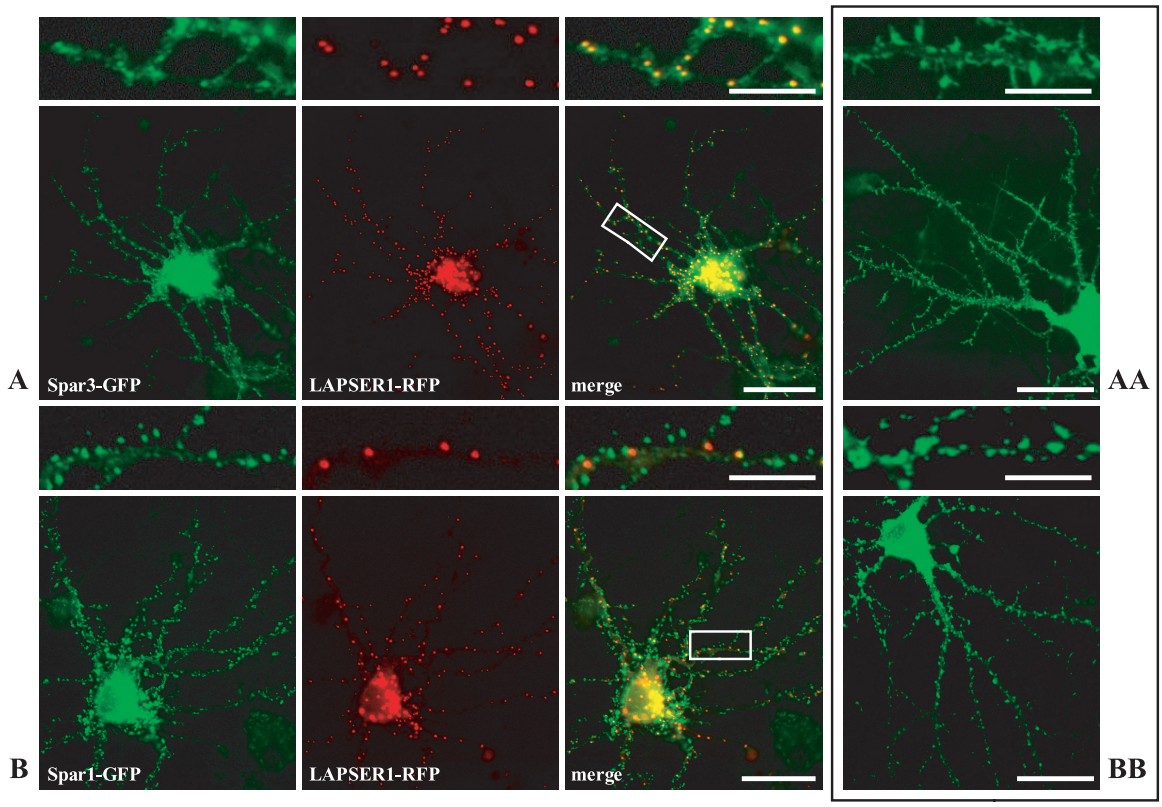

Figure 4.38: Recruitment of Spar3– and Spar–GFP to the LAPSER1–RFP–clusters in hippocampal neurons, 17 DIV. Hippocampal neurons are cotransfected with Spar3- or Spar–GFP together with LAPSER1–RFP, respectively. **A**. Spar3 is fully localized to LAPSER1. **B**. Cotransfection of Spar–LAPSER1. Note, that Spar localizes to LAPSER1, but with a less affinity in comparison to Spar3. Not every signal of Spar overlaps with LAPSER1. **AA**, **BB**: Single transfected neurons 16 DIV with Spar3–GFP (**AA**) and Spar–GFP (**BB**) display another phenotype as double transfected cells. Scale bar 30 μm (overview), 10 μm (insert).

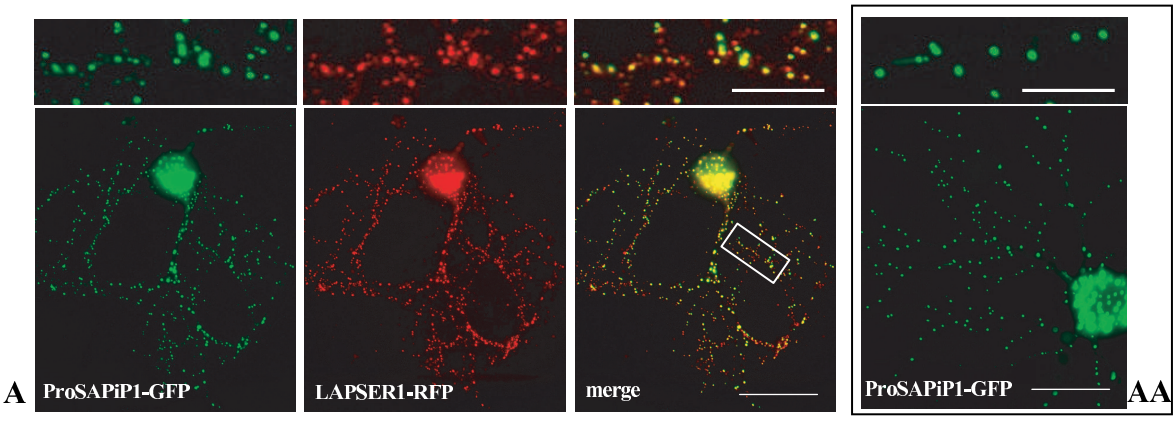

Figure 4.39: Double transfection of hippocampal cells with Fezzins. **A**. When overexpressed in the hippocampal neurons ProSAPiP1–GFP and LAPSER1–RFP form a complex and the signals from both proteins overlap. The double transfected neurons differ from single transfected cells (compare with the ProSAPiP1-transfected neuron on **AA**). Scale bar 30 μm (overview), 10 μm (insert).

interaction LAPSER1–β−catenin was also confirmed in our lab in hippocampal neurons (Schmeisser, 2007). Spar3 interacts with LAPSER1 *in vivo*, as it is shown in the previous chapter. To examine the possibility that Spar3 occurs in a complex with β−catenin, coimmunoprecipitation of the Spar3–β−catenin complex was performed. From rat brain lysates β−catenin is precipitated by Spar3 AB probably indirectly as a complex (Fig. 4.40, **A**). No signal is detected in control probes. *Vice versa*, β−catenin AB are also able to precipitate Spar3 from brain lysates (Fig. 4.40, **B**). Thus, Spar3 is found in the complex with β−catenin in the rat brain. Interestingly, the Fezzins PSD–Zip70 and ProSAPiP1 show high identity with LAPSER1 in the C'terminus (447−669 aa), which is responsible for the LAPSER1–β−catenin interaction (Thyssen et al., 2006). On the other hand, the Fezzins are able to form heterodimers (Wendholt et al., 2006). Hence, it is not surprising, that PSD-Zip70 and ProSAPiP1 AB precipitate β−catenin from the brain lysate (Fig. 4.40, **C**).

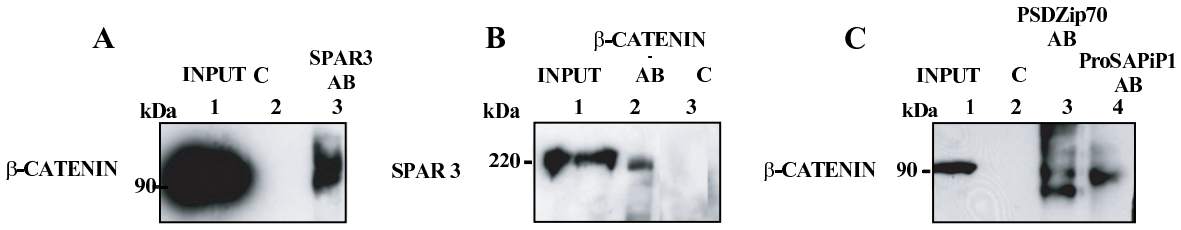

Figure 4.40: Coimmunoprecipitation of β−catenin and Spar3; coimmunoprecipitation of β−catenin with the Fezzins PSD-Zip70 and ProSAPiP1. **A**. β−catenin is highly concentrated in brain lysates (lane 1). Spar3 AB precipitate β−catenin from lysates (lane 3). As a control, magnetic beads were incubated with the brain lysate and the eluate was analysed with β−catenin AB (lane 2). **B**. β−catenin AB precipitate Spar3 from the brain lysate (lane2). Spar3 was detected in the brain lysate used for coimmunoprecipitation (lane 1). The control incubation of magnetic beads with the brain lysate displayed no binding to Spar3 (lane 3). **C**. PSD-Zip70 and ProSAPiP1 precipitate β−catenin (lane 3 and 4, respectively). The brain lysate used as input and control incubation are presented at lanes 1 and 2.

To verify the Spar3–β–catenin interaction in a cell system, the hippocampal neurons were transfected with Spar3–GFP and stained with β–catenin AB. The significant part of β−catenin is recruited to the spine protrusions filled with overexpressed Spar3 (Fig. 4.41).

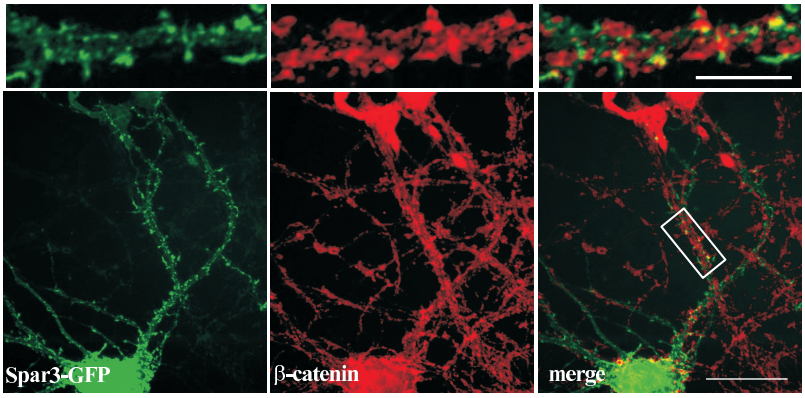

Figure 4.41: Recruitment of intrinsic $\beta-$catenin to the sites of Spar3 overexpression. The Spar3–GFP transfected neurons DIV16 are immunostained for $\beta-$catenin (1:100, ms). The transfected neurons display considerable overlapping of Spar3–GFP and $\beta-$catenin signals. Scale bar 30 μm (overview), 10 μm (insert).

4.25 Spar3 interacts with another component of Wnt-pathway – GSK3α

Recently serin–threonine protein kinase GSK3α was described as a constituent of the axin-$\beta-$catenin complex, which negatively regulates $\beta-$catenin mediated transcription (Asuni et al., 2006). Two GSK3α clones were obtained in the yeast–two–hybrid screen with the C'terminus of Spar3. To examine if the interaction Spar3–GSK3α occurs *in vivo*, GSK3 was precipitated with Spar3 AB. The AB used for the detection of GSK3 were specific for the two known isoforms of GSK3, α and β, respectively. In brain lysates (input) two bands, 51 kDa (α) and 47 kDa (β), are clearly seen. Various Spar3 AB precipitate only the α isoform, corresponding to the upper band of 51 kDa (Fig. 4.42).

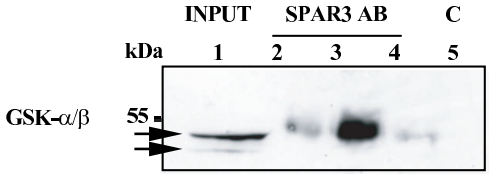

Figure 4.42: Coimmunoprecipitation of GSK3α/β and Spar3. Arrows show the double band in input, 51 and 47 kDa, for α and β isoform of the kinase respectively (lane1). Spar3 AB (lane 2 – AB generated against Spar3 peptides, lane 3 – AB generated in rabbit against C'term–GST fusion protein, lane 4 – AB generated in guinea pig against C'term–GST fusion protein) precipitate GSK3α. The control probe of beads without AB (C) does not display any signal.

Staining of Spar3–GFP overexpressing neurons with GSK3α/β AB indicates, that

the spines, filled with Spar3–GFP often display GSK3 staining (Fig. 4.43). The results of yeast–two–hybrid screen, coimmunoprecipitation and immunostaining indicate that Spar3 is in the complex with GSK3α *in vivo*.

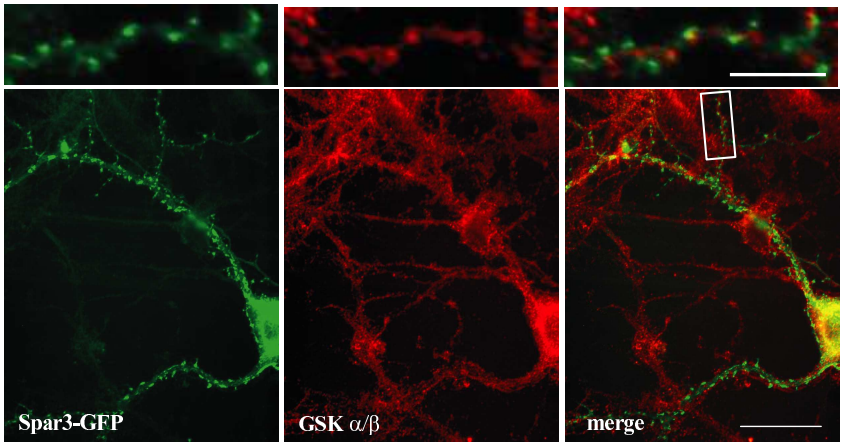

Figure 4.43: An endogenous GSK3α/β is found at the sites of Spar3–GFP overexpression. The Spar3–GFP transfected neurons (DIV 16) were stained for GSK3α/β (1:100) Scale bar 30 μm (overview), 10 μm (insert).

4.26 Spar3 is a constituent of the cell adhesion complex

Neuroligin 1 is a part of the cell-adhesion complex, which links pre– and postsynaptic compartments in excitatory synapses together. A yeast–two–hybrid screen with the C'terminus of neuroligin 1 as a bait containing a type I PDZ-binding motif resulted in the detection of a number of interaction partners and among them Spar (Meyer et al., 2004). The PDZ domains of Spar3 and Spar show 87% identity on aa level (Spilker et al., 2008). Hence, it was interesting to examine if Spar3 might be in the complex with neuroligin. Coimmunoprecipitations with brain lysate confirmed the results of the two–hybrid yeast assay. The only commercially available AB specific for neuroligins 1-3 precipitated Spar3 from the brain lysate and *vice versa* (Fig. 4.44, **A**, **B**).

4.27 The Spar3 knock–out mouse

Mutations of specific genes in living animals provide us with an insight into gene function *in vivo*. A novel method to obtain knock–out mice is the use of murine embryonic

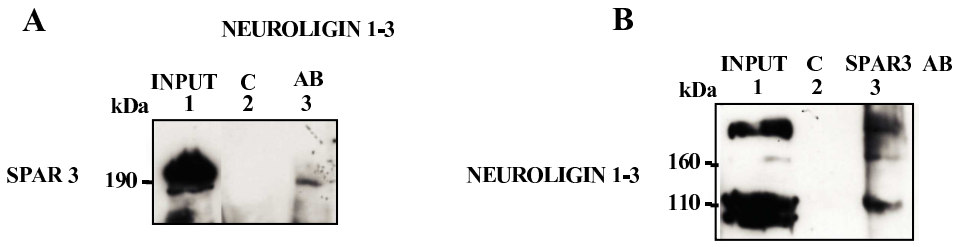

Figure 4.44: Coimmunoprecipitation of Spar3 and neuroligins 1–3. **A**. Brain lysate was immunoprecipitated with neuroligin 1–3 AB and probed with Spar3 AB on blot (lane 3). A specific signal was detected in the input (lane 1) and in the precipitate (lane 3), but not in the control (lane 2). **B**. Spar3 AB precipitate neuroligins 1–3 from the brain lysate (lane 3). Input and control probes are presented at lanes 1 and 2, respectively.

stem cells (ES) where the gene of interest is mutationally inactivated. Inactivation of the gene is achieved by the insertion of a gene trap vector. The project of random mutagenesis of the mouse genome by gene trap vectors is run by Wellcome Trust Sanger Institute. The gene trap vector pGT0Ixf RC consists of a splice acceptor site, a portion of the $\beta-$galactosidase gene fused to a modified neomycin–resistance protein and a polyadenylation site of the Simian virus to terminate the transcription. The insertion occurs randomly in the genome. The modified cells are selected by exposure to neomycin and can be controlled by visualization of $\beta-$galactosidase activity. The position of the insert is identified by sequencing starting from the insert in 5'–direction, so that an exon upstream of the gene trap insertion is identified and entered into the database (Hicks et al., 1997; Jackson, 2001).

The search of the database of the Sanger Institute Gene Trap Resource (SIGTR) showed the availability of the cell line XT0120, where an insert was mapped to the chromosome 7:29094816-29094875. The site of the insert corresponded to the locus containing the Spar3 gene (NM_001081028, 7:29029138–29214220 according the Mouse Genome Database Project), which was reported as 'similar to signal–induced proliferation associated 1 like 3' gene in *Mus musculus*. The alignment of the Spar3 transcript with the mouse genome contig revealed a different location of the Spar3 gene sequence in the genome 7:27105397–27290479 (NCBI database), which was taken as a basis for the further mapping of the insert location. The targeted ES cells were obtained from SIGTR and sent to the University of Muenster for injection into blastocytes. The obtained chimeric offsprings were subjected to genotyping and breeding.

4.27.1 Mapping of the position of the gene trap vector in the mouse genome

According to the data from SIGTR the gene trap vector pGT0Ixf RC consists of 8660 bp. The insertion of this sequence occurred within the intron between exons 5 and 6 (Fig. 4.45). The exact location of the insert within the intron was not known.

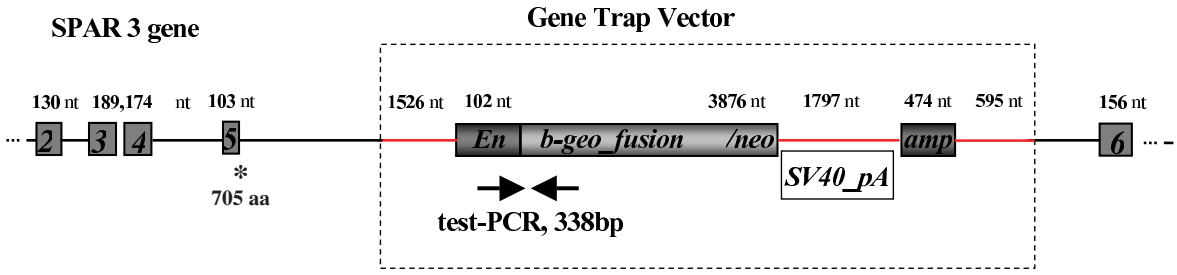

Figure 4.45: Knock–out strategy at the genomic level. Optimization of genotyping for the preliminary selection of vector targeted mice (test PCR). The trap vector is located within the intron between exons 5 and 6. En2 – coding leader sequence, b–geo fusion/neo – fusion of β–galactosidase and neomycin transferase coding sequences, SV40_pA – Simian virus 40 polyadenylation signal, amp – ampicillin resistance coding sequence. The introns of the gene trap vector are marked in red. Spar3 exons 1–5 code for 1–705 aa.

Genomic DNA was isolated from the tails of chimeric mice and tested for the presence of the gene trap vector by PCR. The combination of sense and anti–sense primers for the test-PCR was designed for a coding part of the gene trap vector (the En2-coding leader sequence and b-geo-fusion gene):

$$5' - \text{ACGCAGATCGCATCGATAAC} - 3'$$

and

$$5' - \text{TAACCGTGCATCTGCCAGTT} - 3'.$$

The PCR product migrated in the gel at about 338 bp. As a negative control of the reaction genomic DNA of wild type mice was subjected to the reaction with the same primers. On Fig. 4.46 is shown an example of the positive PCR with the corresponding control reaction.

The genomic DNA of animals, where the gene trap vector was detected, was taken for the subsequent analysis. The intron 5/6 consists of 2698 bp. To identify the exact location of the pGT0Ixf RC vector in the genome, several sense and anti–sense primers were chosen within the intron. Simultaneously, the sense and anti–sense primers were designed for 5' and 3' ends of the trap vector (Fig. 4.47, **A**, **C**). Different primer combinations were tested to amplify PCR fragments that allow to verify the exact

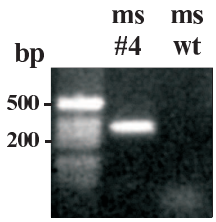

Figure 4.46: Example of a test PCR for the detection of the gene trap vector. Genomic DNA #4 (ms#4, lane 1) gave a positive PCR with primers, specific for the gene trap vector. PCR with a control DNA from wild type mouse (ms wt, lane 2) was negative.

transition between genomic and vector DNA. The sizes of the obtained fragments were about 800 bp less than expected for the reaction A and approximately 1000 bp less for the reaction B. But the PCR products migrated in the gel step–like and with predicted distances (Fig. 4.47, **B**). Therefore, PCR A and PCR B products were amplified in a preparative scale and sequenced.

A

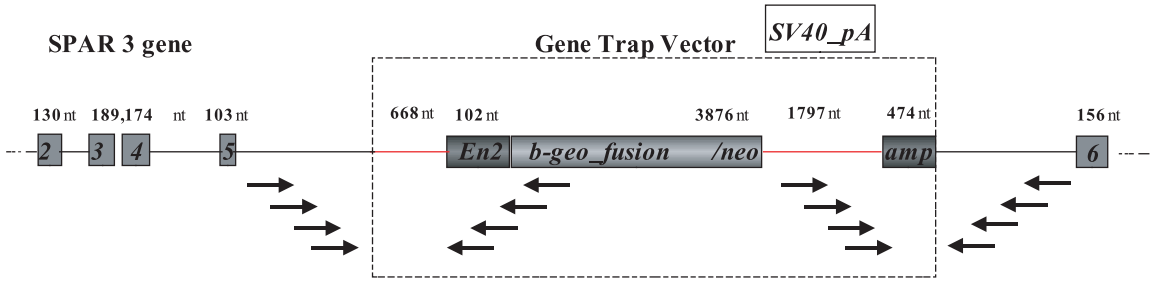

B



C

PCR	5′–sense primer–3′	5′–anti–sense primer–3′
A 01	TGCTTGCTGTGTGAGCTCAGGAC	TTCAGTCTTCCTGTCCAGGA
A 02	–	AACTTGAGGCTGGACATGTG
B 01	TGCTTAATCAGTGAGGCACC	CAAGAGAGGGAGCTGTCACA
B 02	–	GTGGCAGTGACTCATTTGAC
B 03	–	GTATGACACCACGTAGATGC

Figure 4.47: Detection of the gene trap vector insertion in the murine genomic DNA. **A**. Scheme of PCRs. **B**. Several combinations of primer sequences in the intron 5/6 and the gene trap vector gave specific products. **C**. The primer combinations, which amplified the specific products, are presented in the table.

The sequencing revealed that the gene trap vector was inserted in chromosome 7 at the position 7:27169159–98. The targeting vector replaced 27 nucleotides in the intron 5/6 of mouse genome: 7:27169160–97. When the insertion into genome occurred, 861 nucleotides from the 5' splice acceptor site and 988 nucleotides from the 3' flanking sequence of the vector downstream of SV40 polyadenylation signal were deleted. One novel nucleotide was inserted upstream from the vector and four novel nucleotides downstream, between the intron sequence and the vector. The final sequence of the area containing the insert is presented on Fig. 4.48.

4.27.2 Genotyping of Spar3 knock–out mice

After mapping of the gene trap vector in the genome of chimeric mice, two reactions were optimized for the rapid genome screening of mice (PCR 1, PCR 2, Fig. 4.49, **A**). The first primer combinations

$$5' - \text{CGGCTCCAGATTTATCAGCA} - '3$$

and

$$5' - \text{GGACCCCAACTTGATTTTGA} - '3$$

amplified a 275 bp band from the modified allele (3' piece of the vector and intron 5/6 downstream of the vector as it is shown on Fig. 4.49). The second pair of primers

$$5' - \text{CAAGAACATCGGCATCAGAA} - '3$$

and

$$5' - \text{GGACCCCAACTTGATTTTGA} - '3$$

was used to amplify 309 bp of the non-modified region of intron 5/6. In case of a trap vector insertion (6811 nt) in both chromosomes of homozygotic animals, the PCR 2 would give no product, as illustrated in Fig. 4.49, **B**.

4.27.3 Analysis of mRNA expression in Spar3 knock–out mouse

The insertion of the gene trap vector in the intron 5/6 on the genomic level should result in the production of a truncated Spar3 mRNA. The mRNA exons 1-5 of Spar3 is fused with the En2-leader coding sequence and the b–geo/neomycin exon of the vector. The location of the polyadenylation site of the Simian virus 40 (SV40_pA) in the gene trap sequence immediately after b-geo exon induces the premature termination of transcription. The theoretical scheme of the Spar3 RNA in knock–out mice is presented on Fig. 4.50, **A**.

EXON 5
GACTCCACGGGGACCCACTCCCTCTACACGACGTACCAGGACTACGAGATCATGTTCCACGTCTCCACCTTGCTCCC
TTACACTCCCAACAACAGGCAGCAGGTCAGTGGTCCCCAGCTGGGGCACAGTTAGTCCCTAAGCTTTCACTCTTCTC
AAGACTGGTGGCCATCAGCCAGGCCATCTGCCCAGGGATGGCGGAGATGCGCCCCACAGTCAGTGCTCTTGTCCCA
CCATTCAGAGGAAAGCGACTGGGCCTGAATGAAATACGTGGCCATCCTGGAAAGGGTGAATGGTTTAGGGGCCAGG
TGCTGGGAGATAACAGTAGACACCTATGGCCAGGGGGCTGCAGGAGACTGCAGATGTGACAGCTCCCTCTCTTGGG
CACAGCAGGCCAACTGAGCCAGCAGGACAGTGGGACTACTTTCTGGTGGGTAGGAACCCAGAGTGCTAAGAATTTAG
AACATAGGTTTATGGTTTTGTTTTGTTGTTGTTTGGTTTTGGGAGGTTTTTTGTTGTTGTTGTTGTTGTGGTT
TTGATTTTGTTTTTTTTCATTTGTTAGGACAGATCACAATATAGTCTCAGTAGGCCAAAACTAGTCAAAATACAGGCC
ATTTCCTAAGGATATCCTAATAACACACTCTCAAGAACATCGGCATCAGAATTAAACATAAGTTTGAGCTCTTTGCCC
CTGCTTGCTGTGTGAGCTCAGGACAGTGAAGGCACCTCTCTAGGCCACAGGTCCTTCCTCCACACATGGGCAGCATG
GTCCTGATGGATGCTGCATGGGTACTAGAAAAGATACTTGCTTCCATGCGCAGGCCCTGAGCACCAGGCAGCCAATA
CTTTTAGGAAGCAGGAGCCTGCTGCTGCGTACCAGGACCTCCACACTTGCCCCAAACACTGCCAACTATGTAGGAGG
AAGGGGTTGGGACTAACAGAAGAACCCGTTGTGGGGAAGCTGTTGGGAGGGTCACTTTATGTTCTTGCCC--------
---- ---------- **6811 bp (TRAP VECTOR)** ----------
------CTTAATCAGTGAGGCACCTATCTCAGCGATCTGTCTATTTCGTTCATCCATAGTTGCCT GACTCCCCGTCGTG
TAGATAACTACGATACGGGAGGGCTTACCATCTGGCCCCAGTGCTGCAATGATACCGCGAGACCCACGCTCACCGGC
TCCAGATTTATCAGCAATAAACCAGCCAGCCGGAAGGGCCGAGCGCAGAAGTGGTCCTGCAACTTTATCCGCCTCCA
TCCAGTCTATTAATTGTTGCCGGGAAGCTAGAGTAAGTAGTTCGCCAGTTAATAGTTTGCGCAACGTTGTTGCCATTG
CTACAGGCATCGTGGTGTCACGCTCGTCGTTTGGTATGGCTTCATTCAGCTCCGGTTCCCAACGATCAAGGCGAGTTA
CATGATCCCCCATGTTGTGCAAAAAAGCGGTTAGCTCCTTCGGTCCTCCGATCGTTGTCAGAAGTAAGTTGGCCGCAG
TCCTGCAAAATCAAAATCAAGTTGGGGTCCCACCCTTTTGCCTTCATTCTTGTAGGACAGAAGGCAGGTCACTTTTAG
TTTCTCTGAACCAAGTTTTCCCATCCTTTGAAAAGCAGTCAAATGAGTCACTGCCACTCAGGGTTTGGGGAAGGTTCA
GCAAGGTCACGAATTTAAGATATGACTGGGAGGTAGGCCTCATATGGGGTCAGCCACAGGAAGCAATTCTTGTAACT
TCATTTGTACAGTTCAGATGCATAAAAGCTAGAGAGCTAACAGGCCCAGGGCTGGAGTGACAACTCAGAGCTCAAGC
GCACTGGCTGCTGTTCCAAAAGACCCAGGTTCAATTCCCAGCATCTACGTGGTGTCATACAACTGTCTAACTCCAGTC
CCAGGGGATCTGATACCTTCTTCTGGCCTCTGAGGGCACTTGGCACACACATAGTATACAGATGTGCATGCAGGCAA
AACACACATGCACATAAAAATAAAAAAATTAAAAGTCTTTGGTGCTATACTTGGCAGCACATGCCTTTAACCCCAACA
CTAGAGTCACAGAAGCAGGTGAATGGATCTCTGCTAGTTCTAGACTGTGGTCTACTGCAGGACTTCCAGAATAGTCA
GAGCTACATAGATGATCCTGTTCCAGAATAAACAAATGAAAAAGAACTAGCAGGCTGGATAAAGTAGTTCAAGCAGG
AGATTGCCCAGTTTGGTGGTTTCAGGCCAGTCTGGGCAATTTAGGAAAGCTGTCTCAAATTAAATAGTTAAGAACAAA
ACAGAACTCAGCTGTGGTGACCAGCTCCCTTTGTTGGATCAAGAGTAAGAGATCGGGCTGGTGAGATGGCTCAGTGG
GTAAGAGCACCCGACTGCTCTTCCAAAGGTCTGGAGTTCAAATCCCAGCAACCACATGGTGGCTCACAACCATCCGTA
ACGAGATCTGACTCCCTCTTCTGGAGTGCCTGAAGACAACTACAGTGTACTTACATATAATGAATTAAAAAAAAAAAA
AAAGTAAGAGATCATGCTGAGCTGTTTACTGAGTCTGGGTCCTAGCCTGGGCTGTGTGAGACCTGTCTTCCCTGCCCT
CCAGAAAAGAACAAAAGGTGTGGGGGATGTCAGTTGTAGTCTTGTCGAATAAAGAAGATACCATGAAGACACCCATTC
TGGAGATGGAAGCAGGGGGCATGGCTCCCAGGAGTGCAGGAGAGAGAGCCTCCTAGCATGGGCCCTACCTGTGCATC
CTGGTCAGATTCTGCCATTGTCCATATGGCCTGCGCAGGTCCAAGGTCTCCCACATGGGTCCTCCTGCAGTAAATATG
ATTTGCCAAGCACTCCAGTTTATCAAGATCTTTGCTAGGAACTAAGGGACTGATACAGGCAACAGTCAAAACAATGTC
CCATTTTCTCATCACTGACAACCTGAATGGGAAGAGATAAATGAGGAACAGGGAGGGAGAGCCTCTGTGTGCAAAAT
GTGGGCATAAATATCAGATAAGGAATAGGAAAAGGCAAAGAAAGGCATGCTGGGGCAGGACAGATCTCAGATTTGCT
GTGGGTGACAGAAATCCCTCCAAGGAGGAAGGAGCAGCAGGGACAGCCATTCCCACTGTTTGCAAGAGGAAGGCTTT
CCTGGAATGCTTGAAGAGCATCCGGGCAGGTGTGGGAGGAGAACAGGCTGTGTCAGAGGCTGGGGGGTCCCATGTG
GGGCCTTCTTGGCTTTGTCCATTCCTCTGGAGTGAGAAGGAGCCAGAAGGGCTCTGAGCTTCCAGGGACTAGGCCTG
ACTCCGGCGCTCACATGCGCCCTCTGCTGGTAGTGGGCATGGGAAGCCAGCAAGGCAGTCTGGGTAGGATTCTTAGA
GCTGACCTGTGACCCTTCCCTCCTCCCTCTCTGCTTCCAGCTGCTGAGGAAGAGGCACATAGGGAATGACATCGTGA
CGATCATCTTCCAGGAGCCCGGCGCCTTACCTTTCACCCCTAAGAACATCCGCTCGCACTTCCAGCACGTCTTCATCA
TCGTCCGAGTCCACAACCCCTGCACTGAGAATGTCTGCTATAG
EXON 6

Figure 4.48: Modified genomic DNA in the Spar3 knock–out mouse with the inserted gene trap vector into intron 5/6. The exon sequences are shown in red. The sequence of the intron 5/6 is marked in grey and the trap vector sequence – in green. Nucleotides, which did not belong to the intron or vector sequence are presented in dark blue.

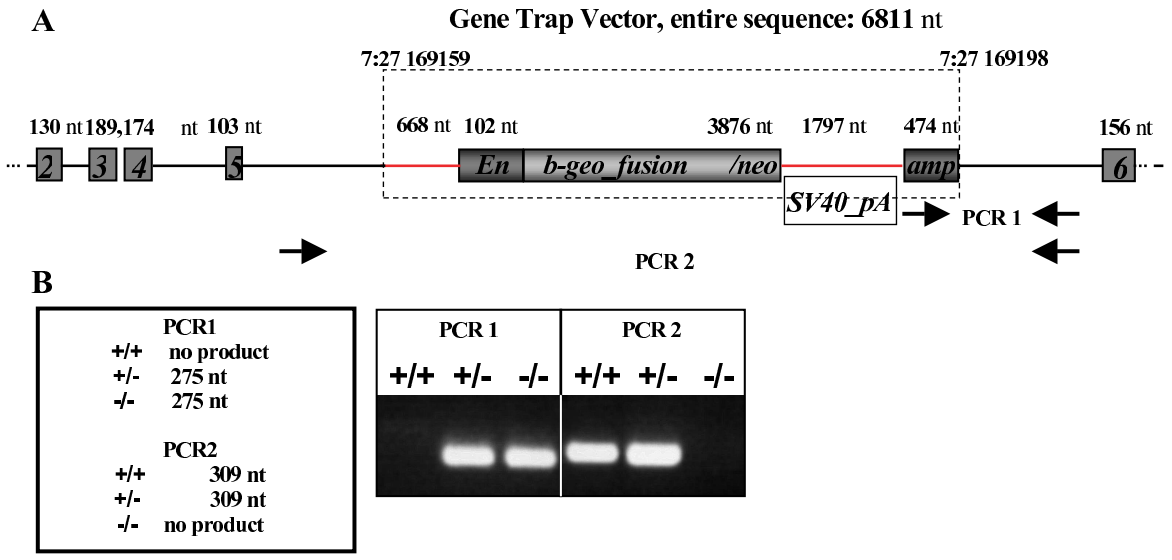

Figure 4.49: Genotyping of Spar3 knock–out mice. **A**. A scheme of the genomic DNA with the designed primers. **B**. Summary of the expected PCR products for different genotypes and an example of the PCR for genotyping.

To confirm the insertion of the vector on the RNA level, total RNA was extracted from brain homogenates of Spar3 knock–out and wild type mice. The cDNA syntheses were carried out with the M–MVL reverse transcriptase using random hexamere primers as described in the methods. The obtained cDNA was used as a template for PCR with the sense primer from exon 2 and the corresponding primers in b–geo fusion exon of the vector to amplify the transition between exon 5 of Spar3 and the gene trap vector (Fig. 4.50, **A**, **C**) . The similar PCRs were performed using sense primers in exon 3 and exon 4 with the same set of anti–sense sequences.

The RT–PCR products migrated in the gels step–like and had the predicted size (Fig. 4.50, B). The bands were cut out and sent for sequencing. In knock–out mice a PCR amplifying the exon 8 unexpectedly gave a product (Fig. 4.50 **B**, lane C on the left). The band was very weak in comparison to the RT-PCR product with the cDNA of wild type animals (Fig. 4.50 **B**, lane C on the right). Exon 8 should not be present in knock–out animals. To explain this result additional experiments were performed (section 4.28).

As a negative control the cDNA of wild type mice was subjected to the same set of PCRs A, B, D (Fig. 4.50 **B**, on the left). No bands were detected on the gels, except the positive control reaction, amplifying the exon 8 in the cDNA of wild type animals.

The sequencing of RT–PCR products confirmed the expression of a truncated form of the Spar3 mRNA. The exons 2, 3, 4 and 5 appear as in the wild type cDNA of

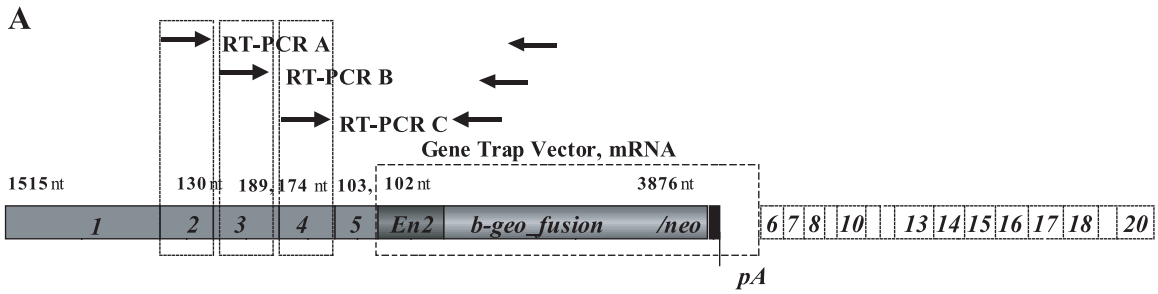

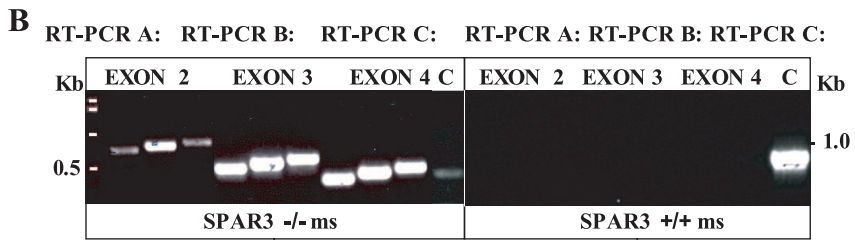

C

RT–PCR groups	sense primer	anti–sense primer
PCR A (EXON 2)	CCAATTACTTTGGCGTGGAT exon2 sense	GATCCTCTAGAGTCCAGATC b–geo 1 as
–	–	GGCGATTAAGTTGGGTAACG b–geo 2 as
–	–	TCTTCGCTATTACGCCAGCT b–geo 3 as
PCR B (EXON 3)	ACATCCATTGCTTGCGTCTG exon3 sense	GATCCTCTAGAGTCCAGATC b–geo 1 as
–	–	GGCGATTAAGTTGGGTAACG b–geo 2 as
–	–	TCTTCGCTATTACGCCAGCT b–geo 3 as
PCR C (EXON 4)	AGCTCAGAGGAGGAGATGTA exon2 sense	GATCCTCTAGAGTCCAGATC b–geo 1 as
–	–	GGCGATTAAGTTGGGTAACG b–geo 2 as
–	–	TCTTCGCTATTACGCCAGCT b–geo 3 as
C (control PCR)	GGCGACAAGGTCTGTCTGAAG exon 8 sense	CCATCGTACTTCACGTGGAA exon 8 as

Figure 4.50: A verification of the gene trap vector insertion in the mRNA of Spar3 by RT–PCR. **A**. Scheme of the RT–PCR A, B, C with primers designed to confirm the fusion of the exons 1–5 of Spar3 with the vector. The missing exons are shown in dotted lines. **B**. RT–PCR detection of the truncated Spar3 mRNA by PCR A, B and C. **C**. Primer sequences used in RT-PCRs for amplifying of Spar3 exon 5–gene trap vector transition.

Spar3. Exon 5 is fused to nucleotide 1530 of the vector sequence, coding for the En2 leader sequence of the gene trap cassette. The En2–leader coding region is followed by the b–geo-neomycin fusion sequence. Thus, the insertion of the vector led to the expression of a chimeric truncated Spar3 mRNA (Fig. 4.51).

EXON 2
GATGAAAAGCTGGGGCCCGTGGCCGTGAGCATCAAGCGGGAGAAGCTGGAGGACCATAAGGACCACGGACCTCAGTA
CCAGTACAGAATCATCTTCCGGACTCGTGAGCTCATCACGCTTCGGGGCTCCATTCTCGAGGATGCCACTCCTACGGC
CACCAAGCACGGGACAGGGCGGGGCCTACCCCTGAAGGATGCTCTGGAGTACGTCATCCCAGAGCTCAACATCCATTG
CTTGCGTCTGGCTCTCAACACTCCCAAAGTCACAGAGCAGCTGCTGAAGCTCGATGAGCAAGGGCTGTGCCGCAAGCA
CAAGGTCGGCATCCTGTACTGCAAGGCGGGCCAGAGCTCAGAGGAGGAGATGTACAACAACGAGGAAGCCGGCCCTG
CCTTCGAGGAGTTCCTGGACCTCTTGGGCGACAAGGTCTGTCTGAAGGGCTTCACCAAGTATGCCGCGCAGCTGGATG
TCAAGACGGACTCCACGGGGACCCACTCCCTCTACACGACGTACCAGGACTACAGATCATGTTCCACGTCTCCACCTTG
EXON 5 **TRAP VECTOR nt Nr. 1530: En 2 coding leader sequence (green), B-GEO (dark green)**
CTCCCTTACACTCCCAACAACAGGCAGCAGGTCCCAGGTCCCGAAAACCAAAGAAGAAGAACGCAGATCGCATCGATA
ACTTCGTATAGCATACATTATACGAAGTTATCGCAGATCTGGACTCTAGAGGATCCCGTCGTTTTACAACGTCGTGACT
GGGAAAACCCTGGCGTTACCCAACTTAATCGCCTTGCAGCACATCCCCCTTTCGCCAGCTGGCGTAATAGCGAAGAGG
CCCGCACCGATCGCCCTTCCCAACAGTTGCGCAGCCTGAATGGCGAATGGCGCTTTGCCTGGTTCCGGC----

Figure 4.51: Nucleotide sequence of the RT–PCR product illustrating the transition of exon5 of Spar3–gene trap vector at RNA level. Exons 2 and 4 of Spar3 are shown in blue, exons 3 and 5 of Spar3 – in red. The leader coding sequence is marked in bright green and b–geo fusion region – in dark green.

4.28 An unexpected splice event

The control reactions in Spar3 knock–out mice gave a weak signal (Fig. 4.50, lane C). To differentiate between an unspecific signal and a possible splice event, the cDNA synthesis was performed with the M–MVL reverse transcriptase using a primer annealing in exon 20 of the Spar3 gene to specifically amplify the rare Spar3 sequences of the knock–out mouse. The total brain RNA of a wild type mouse was taken as a control. The obtained cDNA was used as a template for PCR with the sense primer from exon 4 and primers in exons 7, 8, 9 and so on up to 17 of Spar3 (Fig. 4.52, **A**).

The set of reactions had to be positive for wild type and negative for knock–out mice. The control reactions included (1) the amplifying of exon 1, thus a positive control (P–C) both for wild type and knock–out; (2) a vector-control (V–C) reaction, amplifying the transition between exon 5 of Spar3 and the gene trap vector, positive solely for knock–out mice; (3) a negative control for transgenic animals, two reactions specifically detecting exons 17–19 and 17–20. The primer combinations used in RT-PCRs "spanning the trap vector" are listed in the table 4.2. All controls except the negative control for knock–out mice gave a predicted result (Fig. 4.52, **B**, **C**). The reactions for exons 17–19 and 17–20 in knock–out mice were positive. Similarly, the RT–PCR 'over the gene trap vector' from exon 4 to exons 7, 8, 9, 10 unexpectedly

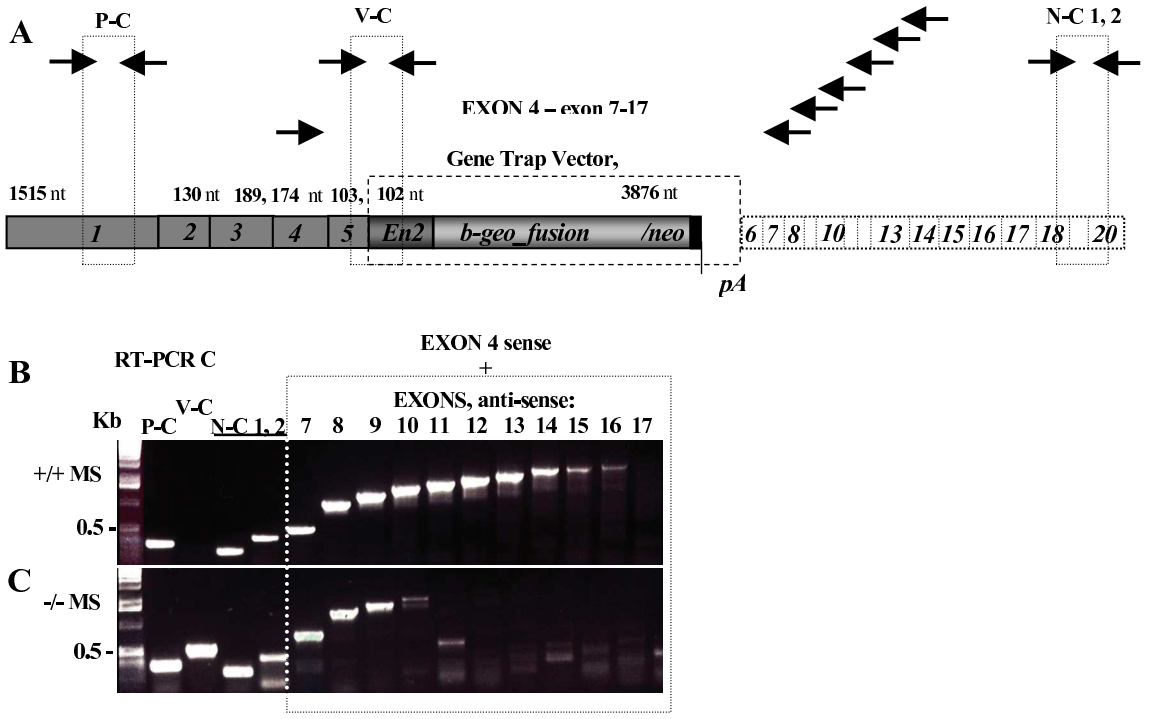

Figure 4.52: Control RT-PCR "over the gene trap vector", amplifying Spar3 exon 4-exons 7–17. **A**. The scheme of RT–PCR . P–C – positive control for both wild type and Spar3 knock–out mouse. V-C – vector control, reaction, positive only for knock–out mouse. N-C – negative control, negative for knock–out and positive for wild type animals. **B**. RT-PCR with cDNA from wild type mouse (+/+ ms) **C**. RT–PCR with cDNA from Spar3 knock–out mouse (-/- ms).

produced bands. The comparison of RT–PCR band profiles of knock–out with wild-type revealed the difference: the RT-PCR products of knock–out mice migrated at a higher molecular weight than products from control PCRs with cDNA of wild type mice. The PCR product exon 4 – exon 7 from knock–out mouse cDNA was sent for sequencing.

The sequencing of the RT–PCR product of exon 4–exon 7 showed the existence of an alternatively spliced form of the Spar3 mRNA (Fig. 4.53). In this case the gene trap vector was not spliced to the En2 leader coding sequence but to the nucleotide number 7268 of the ampicillin resistance gene downstream the SV40–pA signal. This leads to the generation of an mRNA containing the exons 1–5, followed by the short fragment of gene trap cassette (7268–7469 bp) directly fused to the exons 6 – 20. The analysis of this transcript revealed the premature termination of translation by the stop–codon in the ampicillin resistance gene. The translation of this chimeric mRNA containing all exons of Spar3 does not lead to the production of a Spar3 protein.

RT–PCR groups	5'–sense primer–'3	5'–anti–sense primer–'3
P–C (positive control)	AGAACCTCGGTGAGCTCCTGC 3 sense (exon 1)	AAGCTCTTCTGGCAGACCCAT 3 anti–sense (exon 1)
V-C (vector control)	ACATCCATTGCTTGCGTCTG exon3a sense	GATCCTCTAGAGTCCAGATC b–geo 01as
N-C 1 (negative control)	TGGTCTTGAATGGTCCAGCT exon 17 sense	GTACACCTTGCCTGTCAGAT exon 19 anti–sense
N-C 2 (negative control)	TGGTCTTGAATGGTCCAGCT exon 17 sense	CTGAAGAGCTCTGCGAACTT exon 20 anti–sense
Exon 4–exon 7 (over trap vector)	AGCTCAGAGGAGGAGATGTA exon4a sense	GGATTTGTGAGCAGCGTTCT exon 7 anti–sense
Exon 4–exon 8	–	CCATCGTACTTCACGTGGAA exon 8 anti–sense
Exon 4–exon 9	–	CTTGGGTTCCGAAGCATTCA exon 9 anti–sense
Exon 4–exon 10	–	GGTGTTTCTGGGAAACTGAC exon 10 anti–sense
Exon 4–exon 11	–	CAAACGACAGCAGAGGGTGT exon 11 anti–sense
Exon 4–exon 12	–	GATGCTTGCTGCCAATGCTT exon 12 anti–sense
Exon 4–exon 13	–	GGAGGTGTAGAGCGTGGTAT exon 13 anti–sense
Exon 4–exon 14	–	AGAAGAAAGACTTGGGGACG exon 14 anti–sense
Exon 4–exon 15	–	ACGTTCTTTGCGTTGGTGTC exon 15 anti–sense
Exon 4–exon 16	–	AGGCTCTCATCTGACAGTGT exon 16 anti–sense
Exon 4–exon 17	–	AGCTGGACCATTCAAGACCA exon 17 anti–sense

Table 4.2: Primer combinations for control RT–PCR amplifying Spar3 exons 4–exons 7–17. Combinations of primers used for RT–PCR "over gene trap vector" and for control reactions (s. explanation in text) are presented in the table.

4.28.1 Control of the Spar3 gene expression by *in situ* hybridization in Spar3 knock–out mice

Spar3 mRNA expression was controlled in brain sections of Spar3 knock–out and wild type mice. In Spar3 knock–out animals the transcription of Spar3 ends at exon 5. The control hybridizations with oligos specific for exons 1 and 3

$$3' - \text{CACCCTGTTGGCCGCTGACTCGTTGAGGTCGAACAG} - '5$$

and

$$3' - \text{CTCTGGGATGACATACTCCAGGGCATCCTTCAGGGG} - '5$$

A

EXON 4
TGCCTTCGAGGAGTTCCTGGACCTCTTGGGCGACAAGGTCTGTCTGAAGGGCTTCACCAAGTATGCCGCGCAGCTGG
A F E E F L D L L G D K V C L K G F T K Y A A Q L
ATGTCAAGACGGACTCCACGGGGACCCACTCCCTCTACACGACGTACCAGGACTACGAGATCATGTTCCACGTCTCC
D V K T D S T G T H S L Y T T Y Q D Y E I M F H V S
EXON5 TRAP VECTOR nt 7268-7469
ACCTTGCTCCCTTACACTCCCAACAACAGGCAGCAGTTGCCTGACTCCCCGTCGTGTAGATAACTACGATACGGGAGG
T L L P Y T P N N R Q Q L P D S P S C R *
GCTTACCATCTGGCCCCAGTGCTGCAATGATACCGCGAGACCCACGCTCACCGGCTCCAGATTTATCAGCAATAAACC
AGCCAGCCGGAAGGGCCGAGCGCAGAAGTGGTCCTGCAACTTTATCCGCCTCCATCCAGTCTATTAATTGTTGCCGG
GAAGCTAGACTGCTGAGGAAGAGGCACATAGGGAATGACATCGTGACGATCATCTTCCAGGAGCCCGGCGCCTTACC
TTTCACCCCTAAGAACATCCGCTCGCACTTCCAGCACGTCTTCATCATCGTCCGAGTCCACAACCCCTGCACTGAGAA
TGTCTGCTATAGCATGGCTGTGACCCGATCCAAAGATGCGCCTCCCTTTGGCCCCCCAATCCCTAACGGAACCACATT
CCGCAAGTCTGATGTCTTCAGAGACTTTTTGCTAGCCAAGGTAATTAATGCTGAGAACGCTGCCAACAA
EXON 6

B

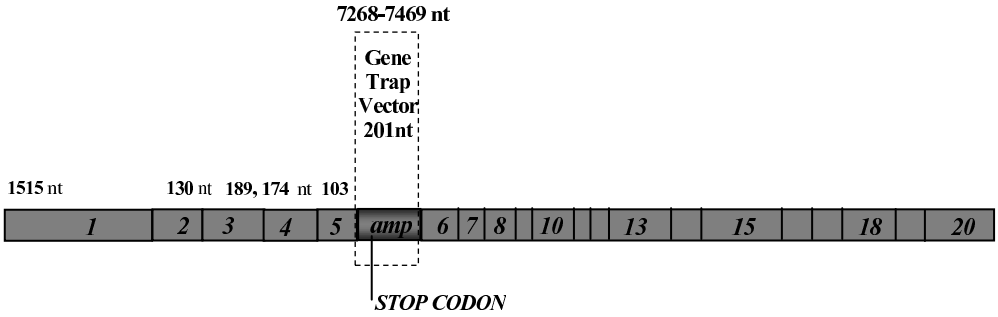

Figure 4.53: Nucleotide sequence (**A**) and scheme (**B**) of an alternatively spliced chimeric mRNA consisting of Spar3 and the gene trap vector. **A**. Exon 4 is shown in blue, the exons 5 and 6 – in red. The vector sequence is marked in green. The translated aa sequence is depicted in black. **B**. amp – ampicillin resistance sequence.

were positive both for Spar3 knock–out and wild type mice. They also revealed the typical pattern of the Spar3 expression with a major signal in hippocampus and cerebellum (Fig. 4.54). The detection of mRNA with oligos, specific for the exons downstream of the gene trap vector, 17 and 18

$$3' - \text{CCGTCCATCAGCCAGTGAGAGCTCCGAGGCTGAGAT} - '5$$

and

$$3' - \text{CAGATGGCTGTGCACAGGGCTGTGTGCAGGAGGGAT} - '5,$$

revealed characteristic pattern of the Spar3 expression only in sections of wild type mice and not in Spar3 knock–out animals.

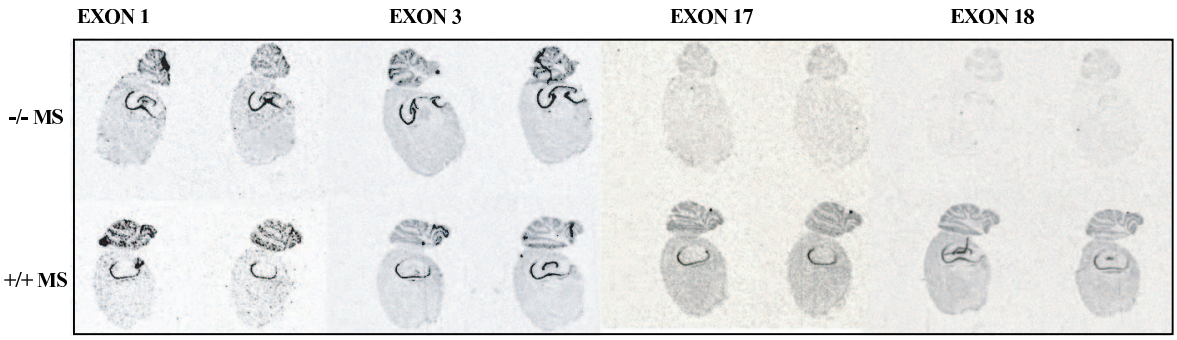

Figure 4.54: Visualization of Spar3 mRNA expression in Spar3 knock–out (−/−MS) and wild type (+/+MS) mice. The oligos chosen for the exons 1 and 3 of Spar3 reveal Spar3 mRNA in both Spar3 knock–out and in wild type mouse in hippocampus and cerebellum. Oligos, specific for the exons 17 and 18 of Spar3, hybridize only in sections of wild type mice. No hybridization occurred in sections of Spar3 knock–out mice. Scale bar 6 mm.

4.28.2 Visualization of the β–galactosidase expression in brains of Spar3–knock–out mice

The gene trap vector codes for the functional $\beta-$galactosidase fusion protein. The expression of this enzyme is under control of the endogenous promotor of the targeted gene and reflects its expression pattern. To ensure that the expression of the truncated Spar3 corresponds to the expression profile of wild type Spar3, the cryo-sections of brains of knock–out mice were incubated with the substrate of $\beta-$galactosidase, X–gal (Fig. 4.55). No staining was observed in wild type animals. In contrast, in brain sections of Spar3 knock–out mice the hippocampus was specifically stained. In the cerebellum a slight staining was detected. This pattern of staining corresponds to the expression profile of the Spar3 mRNA.

4.28.3 Detection of the Spar3 truncated protein

The truncated protein of Spar3 consists of 705 aa coded by the exons 1–5 of Spar3 and 1324 aa coded by the gene trap vector. The fusion Spar3–b–geo protein has a predicted molecular weight of 222 kDa. It does not contain the C'terminal epitope recognized by the anti–Spar3 AB but codes for the $\beta-$galactosidase. Therefore, the protein was visualized in the brain homogenate of Spar3 knock–out mice by anti-beta-galactosidase AB. The homogenate of a wild type mouse was used as a control. A very strong signal was found in Spar3 knock–out mice at about 220 kDa (Fig. 4.56).

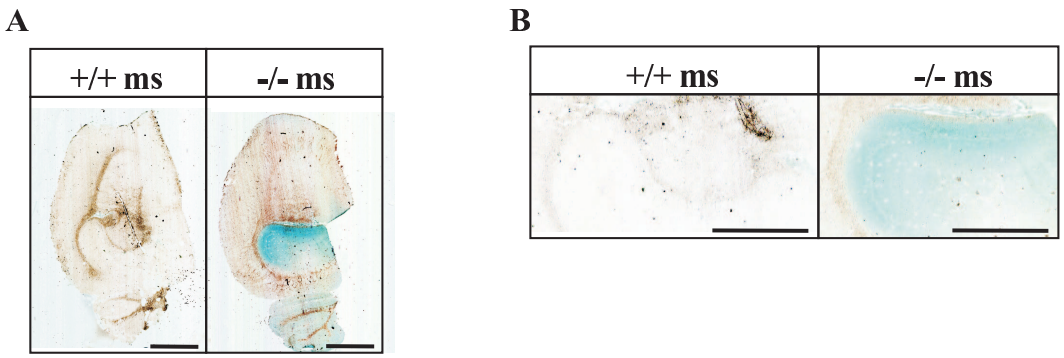

Figure 4.55: X–gal staining of brain sections. The cryosections of wild type and Spar3–knock–out mice were tested for β–galactosidase activity. **A**. Overview of the brain sections of wild type (+/+ ms) and Spar3 knock–out (−/− ms) mice. No β−galactosidase activity was detected in sections of the wild type animals. The brain section of Spar3-knock–out mouse displays specific staining in hippocampus area and, slightly, in cerebellum. **B**. Enlarged view of hippocampus of wild type (+/+ ms) and Spar3 knock–out (−/− ms) mice. Scale bar 3 mm (**A**), 1.8 mm (**B**)

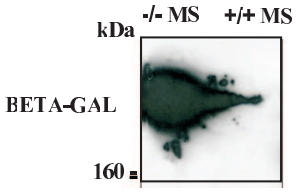

Figure 4.56: Detection of the Spar3 truncated protein with β−galactosidase AB. The truncated form of Spar3 is detected as expected at about 220 kDa in brain homogenates of Spar3 knock–out mice. β–gal − β–galactosidase AB. +/+ MS − wild type mouse; −/−MS / Spar3 knock–out mouse.

4.29 Spar3 knock–out mice display cataract

The Spar3 −/− mice are viable. Preliminary analysis showed, that the Spar3 knock–out animals displayed no obvious abnormalities, except a congenital cataract (Fig 4.57). The ocular phenotype of Spar3 knock-out mice is represented at Fig. 4.57 **B** and **BB** (compare with a wild-type counterpart at Fig. 4.57 **A**, **AA**).

Normally the lens consists of highly elongated fiber cells and germinative zone at the the lens equator (de Iongh et al., 2005). This is clearly seen at Fig. 4.58 **A**–**AAA**. The histological analysis of the eyes of trangenic animals revealed the changes, typical for the cataract. The cataract is characterized by the epithelial–mesenchimal transition of epithelial cells. Morphologically it is manifested in the disruption of differentiation of epithelial cells to fiber cells and formation of the subcapsular plaques, consisting of fibroblastic cells (de Iongh et al., 2005). The fibroblastic cells penetrating the fiber mass, are clearly seen in the lens of trangenic mouse (Fig. 4.58 **B**–**BBB**).

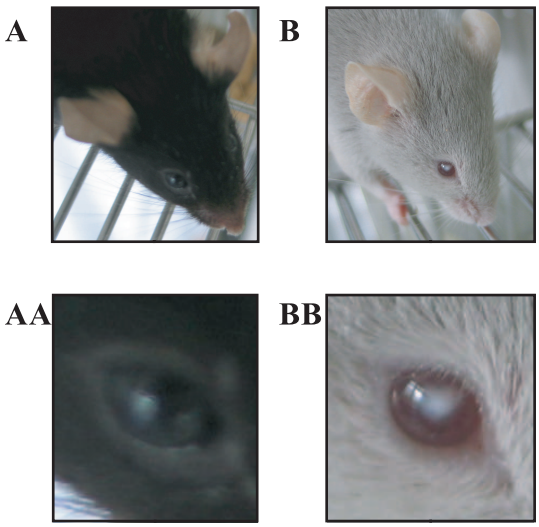

Figure 4.57: Macroscopical representation of wild type (**A**) and Spar3 knock–out mice (**B**). The lens opacity is clearly visible in the eye of adult trangenic mice (**BB**) compared to the clear lens of wild–type (**AA**).

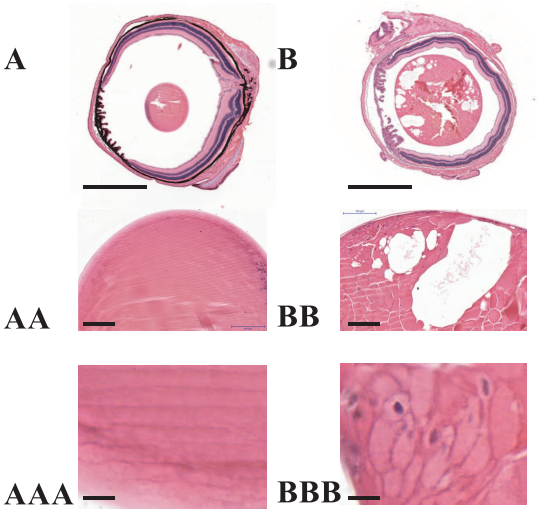

Figure 4.58: Hematoxylin–eosin staining of sections of wild type (**A**–**AAA**) and Spar3 (**B**–**BBB**) knock–out mice. The fiber cells are seen in the lens of wild–type mice (**A**–**AAA**). The plaques, consisting of fibroblastic cells are found in the transgenic mice (**B**–**BBB**). Scale bar 1 mm (**A**, **B**), 100 μm (**AA**, **BB**), 17 μm (**AAA**, **BBB**).

Chapter 5

Discussion

The "electron–dense thickening" of the postsynaptic membrane, the PSD, is a characteristic part of excitatory synapses. The PSD is a complex proteinaceous structure made of hundreds of proteins and specialized for the postsynaptic signal transduction. A striking diversity of components from different signaling pathways are present in the PSD. To those molecules belong protein kinases, phosphatases, small GTPases and their regulators. Although the first biochemical isolations of PSD were successfully accomplished in 1970's, the structure and composition of the PSD are still not fully understood (Sheng and Hoogenraad, 2007; Cotman and Taylor, 1972).

Many major PSD components are already identified and characterized. However, many new PSD molecules are reported each year. One of the methods, utilized for the detection of novel PSD proteins is the yeast–two–hybrid screen with major PSD players. One of the molecules organizing PSD is ProSAP2/Shank3. ProSAP2 is a large scaffold molecule, which clusters various receptor complexes, adhesion molecules and signaling molecules in the PSD. Therefore, ProSAP2 is called the master organizer of the PSD: the ProSAP molecules build a platform via self–association or association with other ProSAP proteins (Boeckers, 2006; Gundelfinger et al., 2006).

A yeast–two–hybrid screen was performed with the PDZ domain of ProSAP2/-Shank3. It resulted in the finding and the characterization of two members of the Fezzin family, namely ProSAPiP1 and LAPSER1. A further screening with a full–size ProSAPiP1 resulted in the identification of the SPA–family members, Spar, Spar2 and Spar3 (Wendholt et al., 2006; Wendholt, 2006). This study is directed towards the characterization of the novel protein, Spar3.

5.1 Characterization of Spar3 adds a new member to the SPA–family

The Spar3 molecule contains four known structural domains. Two of them, PDZ and coiled coil, might mediate the protein-protein interactions. The next two domains, RapGAP and serine–rich stretch, are characteristic for signaling proteins. A database search and a sequence analysis showed, that Spar3 belongs to the SPA–family of proteins. The other SPA family members have the same principal domain structure as Spar3. Together with Spar3 two other members of the family, Spar and Spar2, are expressed in the brain (Spilker et al., 2008; Pak et al., 2001). The fourth member, SPA–1, is non–neuronal and is the shortest protein of the family. It contains 1040 aa (Kurachi et al., 1997). The "neuronal" Spars are large proteins and consist of 1722 aa (Spar2), 1776 aa (Spar3) and 1783 aa (Spar), respectively. The analysis of the phylogenic tree of the SPA–family revealed, that Spar3 is evolutionary close to the non–neuronal SPA–1 (section 4.3). The comparison of the Spar proteins, expressed in nervous system, illustrates, that the proteins display a high homology of aa within the RapGAP ($85-89\%$), the PDZ ($83-91\%$) and coiled coil ($53-65\%$) domains (Spilker et al. (2008), Table 5.1). The coiled coil domain of all members including SPA–1 is characterized by a conserved leucine zipper-like motif ($Lx_6Lx_6Lx_6Ex_6Lx_6Lx_6Lx_6$). The regions between the mentioned domains are, however, less homologous. The comparison of aminoacid sequences of the N'-terminus or the C'-terminus of Spar molecules showed a lower homology ($31-51\%$) (Spilker et al., 2008). However, the high homology of the protein sequences found within the PDZ and coiled coil domains raises the possibility that the Spar proteins might share common interacting partners.

% identity within domains	RapGAP	PDZ	coiled coil	entire sequence
Spar : Spar2	89	91	62	54
Spar : Spar3	85	87	53	50
Spar2 : Spar3	87	83	65	49

Table 5.1: Results of the alignment of the SPA–family members, expressed in the brain (adapted from Spilker et al. (2008))

5.2 Spar3 mRNA is widely expressed in brain

An analysis of the gene expression of Spar proteins revealed significant differences in their expression pattern. According to results of *in situ* hybridization in rat brain sec-

tions, Spar3 is widely expressed. The transcript is detected in cortex, all hippocampal regions and in the cerebellum. The level of Spar3 mRNA is constantly increasing in the hippocampus during development. In cerebellum and cortex the level of Spar3 mRNA is increasing during the first three weeks of life and then slightly decreases. The other Spar genes display a more distinct expression pattern in the brain.

In situ hybridizations revealed, that Spar mRNA is highly expressed in the cortex and all regions of the hippocampus. An extremely low, almost undetectable level of Spar mRNA is found in the cerebellum. Spar2 mRNA has an even more restricted pattern of expression. It is almost exclusively detected in granule cells of the hippocampus and the cerebellum (Spilker et al., 2008). In the adult rat brain the distribution of mRNA of Spar family members overlap in some brain regions. The mRNA of all three Spars is only co-expressed in the dentate gyrus of the hippocampus. Spar and Spar3 are expressed in CA1, CA2 and CA3 of the hippocampus and in the cortex. Spar2 and Spar3 mRNAs are found in the cerebellum, whereas Spar2 is restricted to granule cells. Thus, in most neurons, except a restricted area in the hippocampus, only two transcripts can be detected: Spar-Spar3, Spar2–Spar3. This differential expression of mRNAs of different members of the SPA–family in the brain might contribute later on to the heterogeneity of the protein composition between different brain regions and cell types.

5.3 Thw peak of the Spar3 expression coincides with the active spino– and synaptogenesis

Western blot analysis confirmed the expression of Spar3 protein in brain and in retina. In adult animals Spar3 is detected at moderate levels in the cortex, the cerebellum and at high levels in the hippocampus, the thalamus and the hypothalamus. The examination of the protein level during development showed, that the peak of the Spar3 expression in all tested regions of brain falls on the first postnatal week. This period is characterized by the establishment of synaptic contacts and the active formation of dendritic spines and synapses (Ethell and Pasquale, 2005). This is accompanied by the protrusion of multiple filopodia. Filopodia are very dynamic actin-rich structures, that are thought to be the precursors of spines (Yuste and Bonhoeffer, 2004). This suggests that the function of Spar3 is associated with the establishment of contacts. The protein might play a role in immature unstable contacts and in the formation of new synapses. SPA–1, evolutionary most similar to the Spar3 protein, is highly ex-

pressed in hematopoetic progenitor cells of the bone marrow. With time, as the cells differentiate, it is gradually replaced by Rap1GAP. The mature myeloid cells express low levels of SPA–1. Both proteins, Rap1GAP and SPA–1, downregulate the activity of the Rap1 GTPase to the same extent *in vitro*. It is still unclear, why one RapGAP protein is replaced by a similar one during maturation. This replacement is, however, important: SPA–1 knock–out mice develop myeloproliferative disorders after a long latent period (Kometani et al., 2004). On the other hand it is known that the expression level of Spar, another member of the family, increases significantly during development (Pak, 2007). Spar is present in mature spines. The overexpression of Spar in hippocampal neurons leads to an enlargement and maturation of spines with concomitant decrease in the number of filopodia–like structures (Pak et al., 2001). One can suggest that the maturation and stabilization of synapses in some brain regions, *e.g.*, in the hippocampus, is associated with the Spar3–Spar transition in protein expression.

5.4 Regulation of the Spar3 protein level

A comparison of *in situ* hybridizations and Western blots reveals a discrepancy in the dynamics of Spar3 mRNA and the corresponding level of protein expression during development. In the hippocampus, the level of Spar3 transcript is constantly increasing with age (Fig. 4.8). On protein level the highest expression was detected on embryonic day 18 and in the first postnatal week (Fig. 4.19). A difference between high mRNA and lower protein level might be the result of post–transcriptional regulation of Spar3. Western blots of brain homogenates with Spar3 AB reveal two, sometimes three distinct bands with difference in the molecular mass of approx. $15 - 20\,\mathrm{kDa}$ (Fig. 4.5 **A**, Fig. 4.12, Fig. 4.19). Additionally, the analysis of Spar3 expression in the cultured hippocampal neurons of different age clearly shows that Spar3 migrates in the gel differently (Fig. 4.20). Again, the overexpressed Spar3–GFP has other mobility in polyacrylamide gel, as expected (Fig. 4.5). Last, a Western blotting with the separately cloned and overexpressed in Cos–7 serine–rich domain of Spar3 revealed a similar shift in protein migration. In Fig. 4.17 the Act–GFP construct is detected as expected at 60 kDa (predicted weight), but also multiple bands are seen at $75 - 90\,\mathrm{kDa}$. This difference in migration might be explained by protein modification. According to the sequence analysis, the cloned construct contained a serine stretch which might be phosphorylated by CK1 or GSK3 kinases. The phosphorylation event might, in turn, influence the protein stability. The regulation of the protein level by phosphorylation, that is followed by ubiquitination and proteosome–dependent degradation is common

for many signaling molecules. Thus, the level of $\beta-$catenin, a central effector of the Wnt pathway to the nucleus, is constitutively kept at low levels in the cytoplasm in the absence of the Wnt signal (Seidensticker and Behrens, 2000). Pak D. et al. (2003) demonstrated that the Spar level in neurons is controlled by neuronal activity. Spar is phosphorylated by activity induced SNK-kinase, ubiquitinated and then undergoes proteosome–mediated proteolysis. The degradation of Spar (as well as RNAi knock-down of Spar) leads to synapse destabilization. The activity–dependent regulation of Spar in spines contributes to the homeostatic regulation of the synaptic strength (Pak and Sheng, 2003; Seeburg and Sheng, 2008). A potential candidate protein which phosphorylates Spar3 is GSK3 kinase, which will be discussed later (section 5.14). Possibly, the levels both of Spar and Spar3 are controlled by phosphorylation within different signaling pathways.

5.5 Spar3 is a component of the PSD

The PSD contains glutamate receptors, signaling complexes, cytoskeletal proteins and adhesion molecules. All these different components are assembled by scaffold molecules in an organized dense "cytomatrix". A typical PSD consists of hundreds of proteins (Boeckers, 2006; Sheng and Hoogenraad, 2007). Biochemical fractionation revealed the enrichment of Spar3 along with the postsynaptic marker protein ProSAP2/Shank3 in the PSD fraction (Fig. 4.12). The same amount of Spar3 was also found in the soluble fraction S2. Electron microscopy confirmed the presence of Spar3 in PSDs. This result adds Spar3 to a long list of proteins present in the PSD. In the PSD Spar3 might associate with the central scaffold protein ProSAP2/Shank3 via the adaptor proteins ProSAPiP1 or LAPSER1 (Wendholt, 2006; Schmeisser, 2007). It might also be in complex with the adhesion molecule neuroligin (section 4.26). Spar3 contains structural domains, important for the assembly of protein complexes, and regions, characteristic for signaling molecules. It interacts with central components of signaling pathways, *e.g.*, $\beta-$-catenin and GSK–3, and might recruit them to the PSD scaffold (section 4.24, 4.24, 4.26). On the other hand, Spar3 contains a RapGAP domain and might downregulate some GTPases, present in the PSD.

Also, the presence of a pool of Spar3 in the soluble fraction is quite intriguing. Electron microscopy confirmed the existence of a second pool of Spar3 beyond the PSD, in the cytoplasm of spines. The proteinaceous composition of the PSD is a subject to regulation. The molecular matrix of the PSD is changed during development and by different forms of synaptic activity (Okabe, 2007). Recent live imaging studies fur-

ther demonstrated the dynamic structure of the PSD. ProSAP2/Shank3, a prominent scaffold protein and component of the PSD cytomatrix, was continuously redistributed between different PSDs in cultured living neurons (Tsuriel et al., 2006). CaMKII is very abundant in the PSD fraction, but the pool of CaMKII is present in the cytoplasm of dendritic spines in association with F–actin. In response to glutamate stimulation CaMKII translocates to the PSD and its content in the PSD increases up to five times. This translocation of kinase subunits leads to a two-fold increase of the PSD thickness (Okabe, 2007). As it follows from experiments in cell culture (Fig. 4.14, 4.16, Fig. 4.23, **A**) Spar3 most probably associates in spines with actin fibers. The presence of comparable amounts of Spar3 in the PSD and soluble fractions raise the possibility, that the Spar3 content in the PSD might also be regulated similarly to the CaMKII kinase. The pool of Spar3, present in spines, might therefore integrate in the PSD depending on activity.

5.6 Domains of Spar3 that are required for spine targeting

Staining of cultured hippocampal neurons with Spar3 AB revealed a dotted pattern of the Spar3 localization. Double staining for Spar3 and synaptophysin showed that Spar3 was juxtaposed to this presynaptic marker (Fig. 4.21). These results indicate that Spar3 is targeted to the dendritic spines. Spines are tiny morphological specializations of neurons, which function as small biochemical compartments. The sorting and specific localization of different synaptic proteins to those structural microdomains are crucial for synaptic transmission and plasticity (Sorra and Harris, 2000).

To determine which domains of the protein are required for the targeting to the dendritic spines, Spar3 and different Spar3–truncated GFP–tagged constructs were transfected in cultured hippocampal neurons. Overexpressed Spar3 specifically accumulated in spines. The deletion of the C'terminal part of the protein (last 476 aa) greatly impaired the targeting. All N'terminal constructs with this deletion were distributed diffusely in dendritic shafts with no enrichment in spines. These data indicate, that the PDZ domain and the binding partners of the PDZ domain, *e.g.*, neuroligin, are not essential for the accumulation of Spar 3 in spines.

Accordingly, the C'terminus of Spar3 ($1300-1776$ aa) was sufficient for enrichment in spines. We supposed, that the coiled coil domain with leucine-zipper motif, highly conserved in the SPA–family, might be responsible for Spar3 targeting. However, nor

the coiled coil domain alone neither the C'terminus of Spar3, lacking the coiled coil were accumulated in spines. Thus, both the coiled coil domain and an unknown targeting element in the stretch of $1300 - 1700$ aa are necessary for a localization of Spar3 to spines. A similar strategy of the targeting by a bipartite signal located in the C'terminus was already reported for scaffold molecules of the PSD, ProSAP1/Shank2 and ProSAP2/Shank3. The bipartite signal consisted of 65 aa (with a mapped dynamin binding site) and a SAM domain. Those two sequences are separated by a stretch of 300 aa. Interestingly, the third member of the family, ProSAP3/Shank1, utilizes a different mechanism of accumulation in spines, which is only mediated by the PDZ domain (Boeckers et al., 2005).

5.7 Spar and Spar3 are recruited to the spines in a different way

Spar was also described as a protein, specifically concentrated in spines. The targeting of Spar to spines was evaluated by transfecting of hippocampal neurons with various mutant constructs as in this work. The C'terminus of Spar, the GKBD domain ($1506 - 1783$ aa), or longer C'terminal constructs were not targeted to spines. A deletion of the GKBD domain did not influence the accumulation of Spar in spines. This is quite surprising, since this part of the protein is responsible for the direct interaction with an abundant scaffold protein of the PSD, PSD–95. The interaction was examined in yeast and biochemically confirmed in other systems (Pak et al., 2001). The results of the targeting examination of Pak D. et al. (2001) are not in line with a later work of Maruoka et al. (2005). The group characterized one more binding partner for the C'terminus of Spar, PSD–Zip70. This interaction is mediated by GKBD of Spar and coiled coil domain of PSD–Zip70. By RNAi knock–out of PSD–Zip70 or overexpression of mutant PSD–Zip70 Spar lost its localization in spines. Maruoka H. et al. (2005) suppose, that this Fezzin is responsible for the Spar targeting to spines.

Interestingly, Spar recruitment to spines was mediated by the N'terminal sequence $1 - 628$ aa, designated as Act1 domain for its ability to reorganize the actin cytoskeleton. In spite of similar actin reorganizing properties, the analogous N'-terminal sequence of Spar3, $1 - 500$ aa is not targeted to spines. Moreover, in neurons it induces the formation of filopodia–like protrusions in association with a decrease in mushroom–like spines. Probably, this difference in targeting and effects on spine morphology is due to a low identity of the aa sequences in the N'terminal region. The mechanism of

specific targeting of Spar to spines is still to be clarified. Act1 does not contain any specific motifs (*e.g.*, SAM–domain) and no interaction partner is known for that part of the protein, which can bring Spar to spines (Pak et al., 2001). It could be speculated, that different mechanisms are involved in the targeting of Spar and Spar3 to spines. The differences in the targeting mechanism would enable a fine regulation of the Spar and Spar3 presence in spines and PSDs.

5.8 Association with the actin cytoskeleton

A major component of spines, actin, provides a basis for the shape of spines. Changes in the dynamics and rearrangement of actin underly changes in the morphology of spines. Many actin-binding proteins control or modulate the actin organization in spines (Ethell and Pasquale, 2005). Spar was described as a protein, which binds and reorganizes actin filaments. Overexpressed Spar caused the transformation of actin fibers in aggregates ("clumps") in Cos-7 cells. In neurons the overexpression of Spar led to spine enlargement and irregular shaped spines. Two regions, Act1 and Act2, which are responsible for this effect and for the association with actin were mapped in the protein (see also Fig. 1.4). Act1 and Act2 domains do not contain any similar motifs within their sequences and, as Pak D. et al. suggested, associate with F–actin via different mechanisms (Pak et al., 2001). Spar2, on the contrary, does not bind actin. Small clusters of overexpressed Spar2 are diffusely distributed in Cos-7 cells and do not affect the actin cytoskeleton (Spilker et al., 2008). As shown in another study, SPA–1 interacts with an actin-bundling protein, $\alpha-$actinin (Harazaki et al., 2004). In non–activated T-lymphocytes the protein, as Spar2, is diffusely distributed in the cytoplasm. By interaction with an antigen-presenting cell, SPA–1 is recruited to "immunological synapses", where it associates with actin via $\alpha-$actinin (Harazaki et al., 2004). Therefore, it would be very interesting to test if the actin-binding properties of other members of SPA–1 family might be modulated, *e.g.*, by neuronal activity.

Overexpressed Spar3 associates to actin fibers, but this association is not as distinctive, as in the case of Spar. In neurons, Spar3 colocalizes with actin in spines. In Cos-7 cells the N'terminus of Spar3, $1-500$ aa (corresponding to Act1 of Spar) reorganizes the F–actin, as Spar does. The middle part of Spar3, $548-1300$ aa, shows a very precise association with actin fibers (Fig. 4.16, **C**). This part of the protein contains RapGAP, PDZ and serine-rich domains and does not include Act1 and Act2 regions, described for Spar. The only part of Spar3, which does not associate with actin is the C'terminus, $1300-1776$ aa. The Spar proteins do not contain any known motifs, re-

sponsible for actin binding. The proteins also show some variations in the aa sequence between conservative domains (Spilker et al., 2008). Most probably, Spar and Spar3 bind to the actin cytoskeleton indirectly via different interaction partners, in the same way like SPA–1 localizes to actin via $\alpha-$actinin. As Spar and Spar3 proteins are part of the PSD, one might suggest that they provide a link between PSD scaffold proteins and the actin cytoskeleton.

5.9 Association of the C'terminus of Spar3 with intermediate filaments

The C'terminus of Spar3, $1300-1776$ aa, does not associate with actin fibers. Overexpressed in Cos-7 cells the Spar3 C'terminus formed a network of filaments (Fig. 4.16, **D**, Fig. 4.18, **A**). The staining revealed a complete colocalization of vimentin and filaments formed by the C'terminus of Spar3. In neurons the C'terminal construct also built a similar filament network and an especially strong GFP signal was found in the axon (Fig. 4.22, **D**). However, the truncated construct was targeted to dendrites and dendritic spines, too. Interestingly, tuberin, a specific brain expressed GAP for Rheb and Rap1 was also found in a complexes with intermediate filaments in the neurons. Tuberin associates indirectly via hamartin with a light chain of neurofilaments in the neuronal growth cone (Haddad et al., 2002). The last study of Spar revealed, that this protein, initially described as a component of the PSD–95–NMDA receptor complex, is also present in growth cones of the axons (Richter et al., 2007). There Spar, via its PDZ domain, interacted with the C'terminus of the EphA4 receptor. The interaction was responsible for ephrin-dependent inactivation of Rap1 GTPase. This resulted in the downregulation of adhesion and was followed by a growth cone collapse. The signaling via EphA4 receptor is very important for the axon guidance (Richter et al., 2007). It would be interesting to examine the Spar3 expression in young neuron cultures and to check if Spar3 might be an integrator of intermediate filaments and actin cytoskeleton in growth cones.

5.10 Overexpression of Spar3 in neurons

Spar was described as a regulator of the spine morphology. Spar was present not in all spines: approx. 45% of small spines did not contain Spar. On the contrary, the protein was present in almost all large mushroom–like spines. The overexpression of

Spar lead to an enlargement and maturation of spines. Concomitantly, the neurons displayed less filopodia–like protrusions. The effect of the protein on spine morphology was dependent on the RapGAP activity and on GKBD and Act2 domains (Pak et al., 2001).

Spar and Spar3 have the same principle structure and display a high homology on the protein level within RapGAP, PDZ and coiled coil domains. However, overexpression of Spar3 did not affect the ratio of mature/stubby/filopodia–like spines. But the neurons displayed additional actin-rich, filopodia–like structures, which were not associated with the presynaptic marker bassoon. The effect can not be described as "opposite to Spar", since there was no significant reduction in mature spines. As the peak of Spar3 expression falls into the first postnatal week *in vivo*, one can speculate, that the overexpression of Spar3 in mature neurons activates spinogenesis or dendritogenesis. The fine filopodia in young immature neurons are continuously added and retracted. Some protrusions are stabilized and transformed into spines. Some filopodia are stabilized, extended and transformed into dendritic branches. Both dendrites and spines arise from filopodia, mostly composed of actin and its regulatory proteins (Govek et al., 2005; Ethell and Pasquale, 2005).

Spar influences the spine morphology through downregulation of Rap1 and Rap2 GTPases and reorganization of actin (Pak et al., 2001; Singh et al., 2003; Spilker et al., 2008). Spar2 does not bind to actin, but downregulates Rap1 and Rap2 GTPases, although with a GTPase activation 20% weaker than Spar. However, overexpressed, Spar2 did not influence the spine morphology in neurons (Spilker et al., 2008). Spar3 associates with actin. The N'terminus reorganizes F–actin in the same matter, as Spar does. The middle part of the protein RapGAP-PDZ associates with actin with a high affinity (Fig. 4.16 **B**, **C**). Spilker C. et al.(2008) have tested the isolated GAP domain of Spar3 in an *in vitro* assay for small GTPases. They found, that Spar3 does not display any GAP specificity for Rap1A, Rap1B, Rap2A, Rap2B, Rap2C or for Ras (Spilker C., Gundelfinger E., unpublished data). This finding might explain in part, why overexpressed Spar3 does not contribute to spine maturation. But it can not account for the formation of new filopodia–like structures. SynGAP, previously described solely as a Ras–GAP, in the GAP test as a full–size molecule showed dual specificity for Ras and Rap GTPases (Pena et al., 2008). It might be possible, that Spar3 shows specificity for some Rap isoforms, when tested in assay as a full size protein. Possibly, the protein might have also a specificity to other small GTPases. A possible candidate could be RhoA: downregulation of the GTPase facilitates the extension of filopodia and promotes the formation of fine filopodia branches. Inhibition of Rho by

C3 exoenzyme increases filopodia density in some types of neurons in culture and slices (Govek et al., 2005; Ethell and Pasquale, 2005).

5.11 ProSAPiP1, a PSD scaffold protein, interacts with Spar3

This study demonstrates that Spar3 interacts with ProSAPiP1/LZTS3, a scaffold molecule of the PSD. Three independent clones of ProSAPiP1 were obtained in the yeast–two–hybrid screen with the C'terminal $1300 - 1776$ aa of Spar3, which implies a direct interaction of two proteins. The shortest clone of ProSAPiP1 contained only a part of the FEZ domain, $529 - 704$ aa. The alignment of the FEZ domain sequences of LAPSER1, ProSAPiP1 and PSD–Zip70 showed, that the overall homology of FEZ domain is not high, only 32% in case of LAPSER1–ProSAPiP1 and 40% in case of LAPSER1–PSD–Zip70. But FEZ domains of all mentioned proteins contain two conservative stretches (29 aa in the N'terminal part and 34 aa in the C'terminal part of the domain), where the overall identity is high, approx. 85%. For ProSAPiP1 these stretches are mapped to $468 - 497$ aa and $627 - 661$ aa. The second conservative region is present in the shortest ProSAPiP1 clone, obtained in yeast–two–hybrid screen. It is tempting to speculate, that the second conservative region $627 - 661$ aa, present with little variations also in other Fezzins, is responsible for the interaction with Spar proteins.

In an overlay assay, the C'terminus of Spar3 precipitated ProSAPiP1 from brain lysate. On the contrary, truncated Spar3 protein, lacking $1300 - 1776$ aa, did not show any interaction with ProSAPiP1 (section 4.21). Based on these data, the sequence, which is responsible for the interaction with ProSAPiP1 must be located within $1300 - 1776$ aa of Spar3. The C'terminus of Spar3 contains the coiled coil domain with a leucine zipper motif, which might, in part, mediate such interaction. As the coiled coil domain alone is not targeted to spines, one can suggest, that a longer stretch might be responsible for that interaction.

ProSAPiP1, as Spar3, is widely expressed in brain. The distribution of both proteins overlap in neurons of the cortex, hippocampus and cerebellum. ProSAPiP1 is enriched in the PSD fraction. ProSAPiP1 is tightly connected to the postsynaptic cytomatrix and is not solubilized in Triton X-100 solutions (Wendholt, 2006). The synaptic targeting element in Spar3, that is necessary for the synaptic localization, are 476 aa of the C'terminus. The same Spar3 region contains a sequence, responsible for

the interaction with ProSAPiP1. Therefore, ProSAPiP1 might be considered as an anchoring protein, which mediates the targeting of Spar3 to PSDs. Spar and Spar2 were also characterized as ProSAPiP1 interactors (Wendholt, 2006; Spilker et al., 2008). Depending on the brain region, Spar or Spar2 might compete with Spar3 for the interaction with ProSAPiP1.

The C'terminal motif of ProSAPiP1 binds with high specificity to the PDZ domains of the central PSD-player, ProSAP2/Shank3. ProSAP/Shank proteins "hold together" NMDA-, AMPA- and mGluR receptor complexes and facilitates the crosstalk between different signaling pathways, bringing many molecules together (Boeckers, 2006; Sheng and Kim, 2000; Wendholt, 2006). The interaction with ProSAPiP1 might bring Spar3 in complex with this major scaffold molecule of the PSD. Moreover, the coiled coil domains of the Fezzins bind each other in a homomeric and heteromeric fashion. Fezzins build homo– and heteromeric complexes, which contributes to the assembly of the scaffold backbone of the PSD (Wendholt, 2006). The dimerization of Fezzins rise the possibility, that several Spar proteins might be brought to a complex with one molecule of ProSAP2/Shank3.

5.12 Spar3 interacts with LAPSER1

This study identified LAPSER1 as an interaction partner of Spar3. The interaction was identified in a yeast–two–hybrid screen, and confirmed in pull–down assay, coimmunoprecipitation and in cell culture (section 4.22). The interaction is mediated by the C'terminus of Spar3 ($1300 - 1776$ aa), as in case with ProSAPiP1. Interestingly, LAPSER1 also interacts with Spar (Schmeisser, 2007). Comparison of double transfections, Spar3-LAPSER1 and Spar-LAPSER1, revealed, that Spar3 is recruited to LAPSER1 with much higher affinity than Spar in hippocampal neurons (Fig. 4.38). Potentially, it would mean, that Spar3 might successfully compete with Spar for binding to the corresponding interaction site and might be found more often in complexes with LAPSER1 in brain.

LAPSER1/LZTS2 was first described as a tumor suppressor and a cell growth regulator. It was not expressed in many samples of prostata tumor tissues. Overexpressed in the cultures of transformed cells LAPSER1 inhibited cell growth (Cabeza-Arveliaz et al., 2001). Further studies showed, that LAPSER1 interacts with $\beta-$catenin and affects its subcellular localization. Overexpression of LAPSER1 repressed $\beta-$catenin-mediated transcription in human colon cancer cell line SW40 (Thyssen et al., 2006). Moreover, LAPSER1 is one of the proteins, which mediates the crosstalk between

$\beta-$catenin and NF$-\kappa$B pathways. NF$-\kappa$B inhibits the expression of LAPSER1, which leads to the translocation of $\beta-$catenin to the nucleus and the activation of the Tcf promoter (Cho et al., 2008).

In one day old animals, LAPSER1 is already expressed at high levels in the cerebellum. The high expression persists in the cerebellum throughout development. In older animals LAPSER1 is transcribed in cortex and hippocampus, but at a moderate level in comparison to the cerebellum. The LAPSER1 expression pattern completely overlaps with that of Spar3 and in part with Spar. This, together with other data obtained, implies that proteins interact *in vivo* (section 4.22). LAPSER1 is also enriched in the PSD. As ProSAPiP1, it specifically binds with its C'terminal motif to the PDZ domain of ProSAP2/Shank3. The interaction of LAPSER1 with $\beta-$catenin was confirmed for neurons (Schmeisser, 2007). It is likely that Spar3 might be recruited to the PSD backbone molecules ProSAP/Shank via LAPSER1 as well. In the same way, Spar3 might also be recruited to $\beta-$catenin, where Spar3 might have unknown specific functions, *e.g.*, modulation of the $\beta-$catenin-dependent transcription.

5.13 PSD–Zip70 is a possible interaction partner of Spar3

PSD–Zip70 is another member of the Fezzin family and is structurally similar to ProSAPiP1 and LAPSER1. A clone of PSD–Zip70 was obtained in a yeast–two–hybrid screen with the C'terminus of Spar3 ($1300 - 1776$ aa) as a bait. Recently PSD–Zip70 was described as an interaction partner of Spar (Maruoka et al., 2005). This Fezzin has a more restricted pattern of expression as ProSAPiP1 and LAPSER1. In adult brain PSD–Zip70 was only found in cortex, hippocampus, olfactory bulb, striatum and pons. In the cerebellum PSD–Zip70 has a very similar developmental expression, like Spar2. Hardly detected in the cerebellum of new-born animals, PSD–Zip70 has a peak of expression in week 1–3 of development and later on is downregulated to undetectable level. In the cerebellum Spar2 is highly expressed exactly at the same time, d8–d16. Spilker et al. (2008) suppose that this might point at the interaction Spar2-PSD–Zip70 and special functions of the proteins by maturation of cerebellum. Spar3 and PSD–Zip70 are coexpressed in hippocampus and cortex. PSD–Zip70 has the same conserved regions in the FEZ domain like LAPSER1 and ProSAPiP1. This, together with the results of the yeast–two–hybrid screen, implies the possibility, that Spar3 might also interact with PSD–Zip70.

5.14 Spar3 and the Wnt pathway

Wnt's are a family of secreted glycoproteins with distinct expression patterns, that coordinate gene expression. In embryogenesis different Wingless (Wnt) pathways regulate many key events: *i.e.*, in the specification of body axis, polarity of cell division, cell migration, cell fate and growth. In the adult organisms Wnt signaling is involved in cell cycle control, cell differentiation, changes in adhesion and cell polarity. The results of coimmunoprecipitation and immunostaining indicated that Spar3 is in a complex with at least two components of the Wnt pathway: $\beta-$catenin and GSK3α (sections 4.24, 4.25). The involvement of Spar proteins in the non-canonical Wnt-pathway by embryogenesis in *Xenopus* was already reported. There Spar is regulated by Wnt8 via casein kinase I epsilon (CKIε), which binds, phosphorylates and, therefore, influences the stability of Spar. Spar, in turn, controls the activity of the Rap1 GTPase, which contributes to proper axis formation (Tsai et al., 2007).

$\beta-$catenin is a regulatory protein, which binds to transcription factors such as T–cell factor (Tcf) and induces the transcription of the Wnt target genes (Seidensticker and Behrens, 2000). Since $\beta-$catenin is a central component of the Wnt-signal transmission to the nucleus, the level of this protein is strictly controlled. In the absence of the Wnt signal $\beta-$catenin is constitutively recruited to the multiprotein "$\beta-$catenin destruction complex". The complex consists of the scaffold protein axin, which simultaneously binds to adenomatous polyposis coli protein (APC), GSK3β and $\beta-$catenin. GSK3β phosphorylates $\beta-$catenin, that leads to its ubiquitination and degradation by proteosome, keeping the level of free $\beta-$catenin in the cell low (Seidensticker and Behrens, 2000). Binding of a secreted Wnt to cell surface receptors leads to the inactivation of "$\beta-$catenin destruction complexes" by inhibiting of the GSK3β activity. $\beta-$catenin accumulates in the cytosol and translocates to the nucleus, where it activates the transcription (Jozwiak and Wlodarski, 2006; Seidensticker and Behrens, 2000).

Coimmunoprecipitations and stainings of hippocampal neurons revealed the interaction between Spar3 and $\beta-$catenin (sections 4.24, 4.25). Possibly, the interaction is indirect and might be mediated by other proteins, *e.g.*, by LAPSER1. In neurons, a pool of $\beta-$catenin is present in the synapses, in association with the transmembrane adhesion molecules N-cadherins. In mature synapses N–cadherins are localized to distinct regions, bordering the active zone and the PSD, called the *puncta adherentia*. There, $\beta-$catenin forms a complex with catenin p120 and $\alpha-$catenin, which connects the whole adhesion complex to the actin cytoskeleton (Arikkath and Reichardt, 2008,

in press; Mulholland et al., 2005; Jozwiak and Wlodarski, 2006). Spar was already found at cell–cell borders in association with $\beta-$catenin in heart and epithelial cells of the esophagus (Roy et al., 1999). Like Spar3, Spar can precipitate $\beta-$catenin and *vice versa* (Schmeisser, 2007). Interestingly, electron microscopy revealed, that PSD–Zip70 is often present in the perisynaptic region, which might also be an area of the *puncta adherentia* (Konno et al., 2002). Other Fezzins have not been examined in this respect. This raises the possibility, that Spar and Spar3 might be constituents of this adhesion complex, where they can modulate the adhesion. During development N–cadherins and $\beta-$catenin are found diffusely distributed in the motile dendritic filopodia. In young neurons, upon contact with an axon, cadherin complexes are concentrated at the point of contact. The disruption of N-cadherins affects to a greater extent younger neurons, which display a delay in synaptic assembly. In mature neurons the disruption of cadherin complexes causes a loss of spines and filopodia–like protrusions (Gerrow and El-Husseini, 2006). Spar3 is highly expressed in the brain of young animals. The overexpression of Spar3 in mature cultured neurons leads to the formation of filopodia–like structures. One might speculate that Spar3 is involved in synaptic adhesion and dynamic processes, mediated by N-cadherins.

Two independent clones of GSK3α were obtained in a yeast–two–hybrid screen of a rat brain library with the C'terminus of Spar3. The interaction was confirmed by coimmunoprecipitation and in cell culture. GSK3α and GSK3β share 97% identity within the kinase domains. Recently, GSK3α was shown to regulate the level of $\beta-$catenin in the same manner as GSK3β at least in a model using Wnt–1 and Dvl–1 (Phiel et al., 2003; Asuni et al., 2006). RapGAP proteins are often targeted for proteosomal turnover: Rap1GAP is phosphorylated by GSK3β, Spar by SNK kinase, tuberin by Akt kinase (Tsygankova et al., 2004; Pak and Sheng, 2003; Manning et al., 2002). Most probably, GSKα phosphorylates Spar3 within the serine-rich region, and this event might trigger the degradation of Spar3. This supports the idea of the important regulatory role of the RapGAPs in the cells.

The other possibility, which explains Spar3–GSK3 interaction, is the presence of Spar3, GSK3α and $\beta-$catenin in "$\beta-$catenin destruction complex". This idea needs further investigation, *e.g.*, precipitation with AB to the main scaffold element of the complex, Axin. It would then be interesting to check if Spar3 might influence the $\beta-$catenin-dependent transcription.

5.15 Spar3 knock–out mouse

A Spar3 knock–out mouse was generated within this project to better investigate the function of Spar3 (section 4.27). Spar3 homozygotic mice are viable, and do not display any obvious abnormalities except a cataract. The homozygotes have a congenital cataract or develop cataract early in the development. The main cause of cataract is the epithelial–mesenchymal transition (EMT) in the lens cells. The signaling pathways, mediating EMT are currently under investigation. It was shown, that EMT is caused by changes in growth factors and cytokines in ocular media. The best studied factor, mediating EMT, is the transforming growth factor beta (TGFβ). TGFβ induces the upregulation of numerous extracellular matrix proteins (collagens, fibronectin, proteoglycans), expression of integrins and mesenchymal marker molecules ($\alpha-$smooth muscle actin, desmin). Simultaneously, it downregulates epithelial markers, *e.g.*, E-cadherins, zona occludens–1 protein (ZO–1), $\alpha-$crystallin. The changes are mediated via TGF$\beta-$Smad3. Recently, it was shown, that the TGFβ signal can be transmitted in lens cells via Ras/MAPK, RhoA and PI3K/Akt pathways. As already mentioned, Spar is found in association with the junctional protein ZO–1 and $\beta-$catenin (Roy et al., 1999). SPA–1, evolutionary the closest family member to Spar3, is found in tight junctions. SPA–1 directly binds afadin (AF–6), which was shown to be involved in the organization of cell junctions during human embryogenesis. AF-6 specifically binds to the tight junction protein ZO–1, actin, profilin and brings signaling molecules to junctional complex, *e.g.*, Rap1 GTPase and Eph-related receptor tyrosine kinases (EphA7, EphB2, EphB3, EphB5 and EphB6). Via afadin SPA–1 is directly connected to a tight junction protein ZO–1. This raises the possibility, that Spar3 is also present in junctional complexes and in association with E–cadherin. One can suggest, the knock–out of Spar3 negatively influences the stability or expression of junctional complexes in the lens. Another possibility could be the activation of RhoA in the lens in the absence of Spar3. The overexpression of Spar3 in cultured neurons lead to a phenotype, similar to the downregulation of this GTPase. The activation of RhoA together with the activation of Smad3 by TGFβ is necessary for EMT and cataract induction. Further investigations are necessary to understand how the knock–out of Spar3 induces the cataract. The analysis of the mouse model as an *in vivo* model of cataract might contribute to further understanding of cataract mechanisms and might be used for the identification of potential therapeutic strategies.

5.16 Model of the PSD with a newly characterized Spar3

The novel protein, Spar3, is a member of the SPA–family of RapGAPs. All members of the family have the same principal domain structure and are characterized by a RapGAP domain, a PDZ domain and a coiled coil domain with a leucine zipper. The detailed characterization of Spar3 and the comparison of Spar proteins showed, that they produce different effects on neurons.

Spar3 is widely expressed in the brain. In neurons Spar3 is located to spines and targeted to the PSD. The structural domains, *e.g.*, the PDZ and the coiled coil, mediate the recruitment of Spar3 to different protein complexes. To those proteins belong ProSAPiP1 and LAPSER1. These proteins are part of the PSD scaffold platform, formed by ProSAP/Shank proteins (Fig. 5.1). Via its PDZ domain Spar3 is also recruited to adhesion molecules, spanning the synaptic cleft and anchored in the PSD, the neuroligins. In most brain regions according to the data of *in situ* hybridizations Spar3 is coexpressed together with Spar or with Spar2 (section 5.2). The high homology of the domains within this protein family raises the possibility, that Spar proteins compete for the limited number of binding sites. It is known, that Spar interacts with ProSAPiP1, LAPSER1 and PSD–Zip70 (Wendholt, 2006; Schmeisser, 2007; Maruoka et al., 2005). Spar3, in addition to LAPSER1 and ProSAPiP1, might also interact with PSD–Zip70 (s. data from yeast–two–hybrid screen, section 4.20). Although only the binding to ProSAPiP1 was described for Spar2, it is very probable, that Spar2 interacts with the other two Fezzins (Spilker et al., 2008). The brain regions differ in the expression of Fezzins. Therefore, Fezzins might interact with Spar family members with different affinities (section 4.22). This implies the possibility, that the content and composition of Spar proteins in the PSD might be regulated by the Fezzins.

Spar3 was found in complexes with $\beta-$catenin. Therefore, Spar3 might be associated with cadherins, and act downstream, modulating the adhesion (Fig. 5.1).

From other Spar proteins it is known, that the overexpression of Spar causes maturation and enlargement of spines. On the contrary, overexpressed Spar2 does not influence the spine morphology. Under the same conditions Spar3 induces the formation of additional filopodia–like structures and possibly initiates some dynamic processes in neurons. In the row Spar–Spar2–Spar3 the GAP activity to Rap GTPases decreases from functional Spar to unfunctional RapGAP Spar3. It might be possible, that Spar3 is specific for other GTPases. This must be further investigated and the study of the generated Spar3 knock-out mouse would help to answer this question.

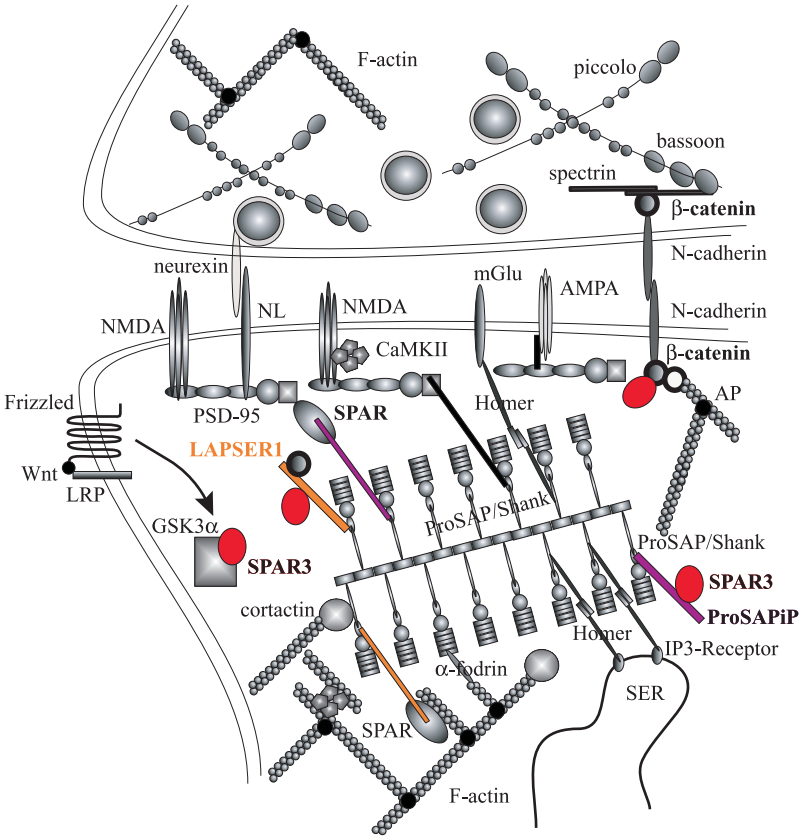

Figure 5.1: Model of the PSD, with the newly characterized Spar3. This scheme is a composite of the published material Boeckers (2006); Ziv and Garner (2004) and the conclusions of this thesis. Spar3 is recruited by the Fezzins ProSAPiP1 and LAPSER1 to the stacks of ProSAP/ Shank molecules, present in the deeper layer of the PSD. Via the platform of ProSAP/Shank proteins Spar3 might be connected to receptor complexes. Moreover, Spar3 might link PSD components to the actin cytoskeleton. Spar3 might be also present in complexes with $\beta-$catenin in *puncta adherentia* and might modulate the cadherin adhesion complexes. The level of Spar3 might be controlled by GSK3α, which activity, in turn, is controlled by the Wnt pathway.
AMPA, $\alpha-$amino–3–hydrohy–5–methyl–4–isoxazoleproprionic acid receptor, AP, adaptor protein, CaMKII, calcium/calmodulin dependent protein kinase, F–actin, filamentous actin, GSK3α, glycogen synthase kinase alpha, IP3–Receptor, inositol–1,4,5–triphosphate receptor, LRP, low density lipoprotein related protein 1, mGlu, metabotropic glutamate receptor, NMDA, N–methyl–D–aspartat receptor, NL, neuroligin, ProSAP/Shank, prolin rich synapse associated protein/SH3 and multiple ankyrin repeats domains protein, PSD–95, postsynaptic density–95 protein, SER, smooth endoplasmic reticulum, SPAR, spine associated RapGAP, ProSAPiP1, ProSAP interacting protein1, Wnt, wingless.

Chapter 6

Summary

The postsynaptic density (PSD) is a characteristic component of excitatory synapses. The PSD is a complex proteinaceous structure specialized for the postsynaptic signal transduction. Partial clones of novel proteins belonging to the SPA–family were obtained in a yeast–two–hybrid screen with the molecule ProSAPiP1, which is a part of the PSD scaffold. One member of this family, Spar3, has been further characterized. Spar3 is a 1776 aa protein that codes for a PDZ, a RapGAP and a coiled coil domain. The Spar3−ProSAPiP1 interaction is mediated by a leucine zipper containing coiled coil region of Spar3 as revealed by blot–overlay assays, pull–down and cotransfection experiments. Spar3 is widely expressed in the brain with high transcript levels in hippocampus, cortex and cerebellum. In adult animals Spar3 protein expression could be confirmed for those brain regions, and was also found in thalamus and hypothalamus.

The light and electron microscopy showed that the protein is localized at dendritic spines. The C–terminal part of Spar3 ($1300 - 1776$ aa) is critically involved in this synaptic targeting. The biochemical fractionation revealed that Spar3 is enriched in the PSD along with a major PSD scaffold protein ProSAP2/Shank3. The highest level of Spar3 protein expression was found in the hippocampus, cerebellum, cortex at E18 and in the first week of development, which coincides with high level of synaptogenesis. During development the Spar3 protein level decreases gradually. In cultured neurons overexpression of Spar3 induces other effects on neurons as already described for the other family members Spar and Spar2. It causes the formation of filopodia–like structures, which are not associated with the presynaptic marker protein bassoon. Spar3 associates with, but does not reorganize F–actin. The transfection of different parts of Spar3 in Cos–7 cells showed, that the only Spar3 region, which does not associate with F–actin is the C'terminus ($1300 - 1776$ aa).

A yeast–two–hybrid screen using the C'terminal part of Spar3 as a bait resulted in the identification of three of four members of the Fezzins family: ProSAPiP1/LZTS3, LAPSER1/LZTS2 and PDZ–Zip70/LZTS1. Coimmunoprecipitations, pull–down assays with the C–terminal part of Spar3 and cotransfection experiments of LAPSER1 and Spar3 in hippocampal neurons confirmed that the interaction between those two proteins occurs *in vivo*. However, in cultured neurons cotransfected with the Spar–LAPSER1 and Spar3–LAPSER1 interaction seems to be different with respect to affinity. Both ProSAPiP1 and LAPSER1 bind to the PDZ domain of ProSAP2/Shank3 and should connect Spar3 to the master scaffold molecule of the PSD.

Moreover, two independent clones of GSKα were obtained in the yeast–two–hybrid screen with Spar3. Spar3 builds a complex with several components of the Wnt–pathway. The coimmunoprecipitation and stainings of hippocampal neurons revealed, that Spar3 is found in complex with $\beta-$catenin and GSKα.

Spar3 knock-out mice were generated to understand the function of the protein. The initial characterization of Spar3 mice revealed, that the mice are viable and display no visible neuroanatomical abnormalities, except an early onset cataract.

The characterization of Spar3 adds a new member to the growing list of PSD signaling molecules at spines and synapses. This new molecule might therefore be important for the structural remodeling of spines and PSDs.

Appendix A

Alignment of the SPA–family

Alignment of the SPA–family members expressed in brain: Spar, Spar2, Spar3. High consensus aa (identical in all three proteins) are shown in red. Low consensus aa (identical in two out of three proteins) are shown in blue. Non-conservative residues are shown in black. Dashed line illustrates gaps in the alingment. At alignment are shown: a Rap-GTPase activating protein domain (Rap–GAP), a PDZ (PSD–95/Discs Large/Zona occludens) – domain, a serine-rich motif (Ser–rich), a coiled coil (CC). The frames in the coiled coil domain mark a conserved leucin zipper motif, characteristic for the SPA-family: ($Lx_6Lx_6Lx_6Ex_6Lx_6Lx_6Lx_6$).

```
            1                                                  50
Spar        MTSLKRSQTE RPVTADRASV VSTDGTPKVH TDDFYMRRFR SQNGSLGSSV
Spar3       MTTYRPLPND GVDLATSCGA RSTDILPGPH PGDYTPMGFW AQSGSMSQPL
Spar2       MSDPRPSQAE KHKLG-RAAS KFKDPSRAMQ SDDYFARKFK AINGSMGPAT
Consensus   Mt..rpsq.# ...la.ra.. .stD..p..h .dD%..r.F. aqnGS$g...

            51                                                 100
Spar        MAAVGPPR SEGPHHITST PGVPKMGVRA RIADWPPRKE NVKESSRSSQ
Spar3       GES---PA AATTRPSPTT PAMPKMGVRA RVADWPPKRD ALREQSNPSP
Spar2       LNTSSLSEGG GGGGGPANGT PAVPKMGVRA RVSEWPPKKD CSKDLACKTL
Consensus   ....s...p...g..p...T PavPKMGVRA R!a#WPPkk# ..k#.s..s.

            101                                                150
Spar        EIETSSCLES LSSKGSPVSQ GSSVSLNSND SAMLKSIQNT LKNKTGPAES
Spar3       SQDTDGVKTT KVAHSMRNLQ NGQLPSSTPA SSGSRAFHRL SRRRSKDVEF
Spar2       WESRSQSSYE SATSIIQNGQ NDQVDRQQEE QLDLDFVE-- AKYTIGDI--
Consensus   ...ts..........n.Q n.qv.....s..l.....k...gd.e.

            151                                                200
Spar        MDSRFLMPEA YPSSPRKALR RIRQRSNSDI TISELDVDSF DECISPTYKS
Spar3       QDG-------- WPRSPGRAFL PLRHRSSSEI TLSECDVEEP GDPRGTRHPG
Spar2       ---------- FVHSPQRGLH PIRQRSNSDI TISDIDTEDV LDQHAVNPNT
Consensus   .d........p.SP.ral. piRqRSnS#I TiS#.Dv#... #........
```

```
           201                                                                 250
Spar       GPSLHREYGS TSSIDKQGTS GESFFGLLKG YKDDRADRGP TPTKLSDFLI
Spar3      VLPLFREYGS TSSIDVQGVP EQSFFDILNE FRSEQPEARG SQN-LGELLR
Spar2      GAALHREYGS TSSIDRQGLS GENVFAMLRG YRIESYDPKV TSSFGFPDFF
Consensus  g..LhREYGS TSSID.QG.s g#sfF..L.g %r.#..#... t...l...l.

           251                                                                 300
Spar       TGGGKGSGFS LDVIDGPISQ R------ENL RLFKEREK-- --PLKRRSKS
Spar3      VDPGALSGGS CGAKGDPRNG QPTKDSLQSL QPLKEKEKAR KKPVRGLGSG
Spar2      PCDTAISPSL HAAAQISRGE FVRISGLDYM DGGLLMGRDR DKPFKRRLKS
Consensus  ...ga.Sg.s..a...pr.....l#.$...ke.ek.r.kP.krr.ks

           301                                                fl       350
Spar       ETGDSSIFRK LRNAKGE-EL GKS-SDLEDN RSE-DSVRPW TCPKCFAHYD
Spar3      DTVDSSIFRK LRSSKPEGEV GRPLGETEEG RSPPEASRPW VCQKSFAHFD
Spar2      ESVETSLFRK LRTVKSEHET FKFTSDLEEG RLD-RGIRPW SCQRCFAHYD
Consensus  #tv#sSiFRK LR..K.E.E. gk..s#lE#g Rs.....RPW .CqkcFAH%D

           351                                                                 400
Spar       VQSILFDLNE AIMNRHNVIK RRNTTTGASA AAVASLV--- SGPLSHSTSF
Spar3      VQSMLFDLNE SAANRVSVAQ RRNTTTGASA ASAASAMVAL TASRAHSLGT
Spar2      VQSILFNINE AMATRASVGK RKNITTGASA ASQTPV---- --PVGPAGGC
Consensus  VQSiLF#INE a.anR.sV.k RrNtTTGASA As.as..... ..p..hs.g.

           401                                                                 450
Spar       SSP-MGSTED FNSKGSLGMD QGDDKSNELV MSCPYFRNEI GGEGERKISL
Spar3      LDPTTFTSTED LNCKENLEQD LGDDNSNDLL LSCPHFRNEI GGERERNVSF
Spar2      ESP-LGSKED LNAKENPDAD EGDGKSNDLV LSCPYFRNET GGEGDRRIAL
Consensus  .sP..gStED lN.KenI..D .GddkSN#Lv $SCPyFRNEi GGEg#R.!sl

           451                                                                 500
Spar       SKSNSGSFSG C-ESTSFESA LSSHCTNAGV AVLEVPKESL MLHLDRVRRY
Spar3      SRASVGSPGG SSEAHMAEPA LSTHRTNASI SVLEVPKEQQ RTQ-SRPRQY
Spar2      SRANSASFSS G-ESCSFESS LSSHCTNAGV SVLEVPRENQ PIHREKVKRY
Consensus  SransgSfsg ..Es.sfEsa LSsHcTNAg! sVLEVPkE.q ..h..rvrrY

           501                                                                 550
Spar       TVEHVDLGAY YYRKCFYQKE HWNYFGADEN LGPVAVSIRR EKPEDMKE-N
Spar3      SIEHVDLSAR YYQDYFVGKE HANYFGVDEK LGPVAVSIKR EKLEDHKD-H
Spar2      IIEHVDLGAY YYRKFFYGKE HQNYFGIDEN LGPVAVSIRR EKVEDPREKE
Consensus  .!EHVDLgAy YYrk.FygKE H.NYFG.DEn LGPVAVSIrR EK.ED.k#..

           551                                                                 600
Spar       GSPYNYRIIF RTSELMTLRG SVLEDAIPST AKHSTARGLP LKEVLEHVIP
Spar3      GPQYQYRIIF RTRELITLRG SILEDATPTA TKHGTGRGLP LKDALEYVIP
Spar2      GSQFNYRVAF RTSELTTLRG AILEDAVPST ARHGTARGLP LKEVLEYVIP
Consensus  Gsq%#YR!iF RTsEL.TLRG s!LEDA.Pst akHgTaRGLP LK#vLEyVIP

           601                                                                 650
Spar       ELNVQCLRLA FNTPKVTEQL MKLDEQGLNY QQKVGIMYCK AGQSTEEEMY
Spar3      ELNIHCLRLA LNTPKVTEQL LKLDEQGL-- --------CR ----------
Spar2      ELSIPCLRQA ANSPKVPEQL LKLDEQGLSF ---------- ----------
Consensus  ELn!.CLRIA .NtPKVtEQL $KLDEQGL.. .........c ..........
```

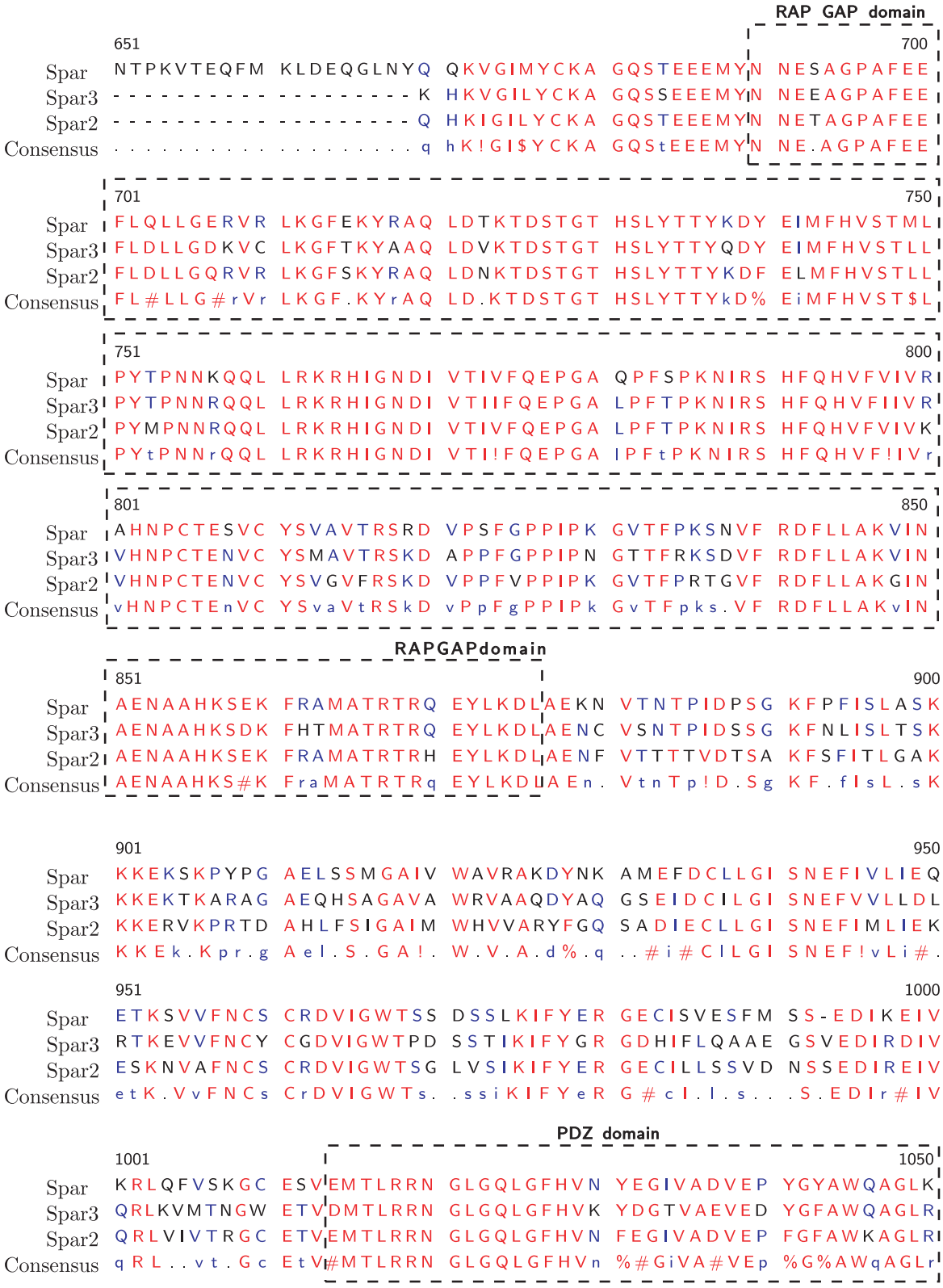
RAP_GAP_domain
651
700
Spar NTPKVTEQFM KLDEQGLNYQ QKVGIMYCKA GQSTEEEMYN NESAGPAFEE
Spar3 ---------- ---------- K HKVGILYCKA GQSSEEEMYN NEEAGPAFEE
Spar2 ---------- ---------- Q HKIGILYCKA GQSTEEEMYN NETAGPAFEE
Consensus .... q hK!GI$YCKA GQStEEEMYN NE.AGPAFEE
701
750
Spar FLQLLGERVR LKGFEKYRAQ LDTKTDSTGT HSLYTTYKDY EIMFHVSTML
Spar3 FLDLLGDKVC LKGFTKYAAQ LDVKTDSTGT HSLYTTYQDY EIMFHVSTLL
Spar2 FLDLLGQRVR LKGFSKYRAQ LDNKTDSTGT HSLYTTYKDF ELMFHVSTLL
Consensus FL#LLG#rVr LKGF.KYrAQ LD.KTDSTGT HSLYTTYkD% EiMFHVST$L
751
800
Spar PYTPNNKQQL LRKRHIGNDI VTIVFQEPGA QPFSPKNIRS HFQHVFVIVR
Spar3 PYTPNNRQQL LRKRHIGNDI VTIIFQEPGA LPFTPKNIRS HFQHVFIIVR
Spar2 PYMPNNRQQL LRKRHIGNDI VTIVFQEPGA LPFTPKNIRS HFQHVFVIVK
Consensus PYtPNNrQQL LRKRHIGNDI VTI!FQEPGA IPFtPKNIRS HFQHVF!IVr
801
850
Spar AHNPCTESVC YSVAVTRSRD VPSFGPPIPK GVTFPKSNVF RDFLLAKVIN
Spar3 VHNPCTENVC YSMAVTRSKD APPFGPPIPN GTTFRKSDVF RDFLLAKVIN
Spar2 VHNPCTENVC YSVGVFRSKD VPPFVPPIPK GVTFPRTGVF RDFLLAKGIN
Consensus vHNPCTEnVC YSvaVtRSkD vPpFgPPIPk GvTFpks.VF RDFLLAKvIN
RAPGAPdomain
851
900
Spar AENAAHKSEK FRAMATRTRQ EYLKDLAEKN VTNTPIDPSG KFPFISLASK
Spar3 AENAAHKSDK FHTMATRTRQ EYLKDLAENC VSNTPIDSSG KFNLISLTSK
Spar2 AENAAHKSEK FRAMATRTRH EYLKDLAENF VTTTTVDTSA KFSFITLGAK
Consensus AENAAHKS#K FraMATRTRq EYLKDUAEn. VtnTp!D.Sg KF.fIsL.sK
901
950
Spar KKEKSKPYPG AELSSMGAIV WAVRAKDYNK AMEFDCLLGI SNEFIVLIEQ
Spar3 KKEKTKARAG AEQHSAGAVA WRVAAQDYAQ GSEIDCILGI SNEFVVLLDL
Spar2 KKERVKPRTD AHLFSIGAIM WHVVARYFGQ SADIECLLGI SNEFIMLIEK
Consensus KKEk.Kpr.g Ael.S.GA!. W.V.A.d%.q ..#i#CILGI SNEF!vLi#.
951
1000
Spar ETKSVVFNCS CRDVIGWTSS DSSLKIFYER GECISVESFM SS-EDIKEIV
Spar3 RTKEVVFNCY CGDVIGWTPD SSTIKIFYGR GDHIFLQAAE GSVEDIRDIV
Spar2 ESKNVAFNCS CRDVIGWTSG LVSIKIFYER GECILLSSVD NSSEDIREIV
Consensus etK.VvFNCs CrDVIGWTs. .ssiKIFYeR G#cI.l.s...S.EDIr#IV
PDZ_domain
1001
1050
Spar KRLQFVSKGC ESVIEMTLRRN GLGQLGFHVN YEGIVADVEP YGYAWQAGLK
Spar3 QRLKVMTNGW ETVIDMTLRRN GLGQLGFHVK YDGTVAEVED YGFAWQAGLR
Spar2 QRLVIVTRGC ETVIEMTLRRN GLGQLGFHVN FEGIVADVEP FGFAWKAGLR
Consensus qRL..vt.Gc EtVI#MTLRRN GLGQLGFHVn %#GiVA#VEp %G%AWqAGLr

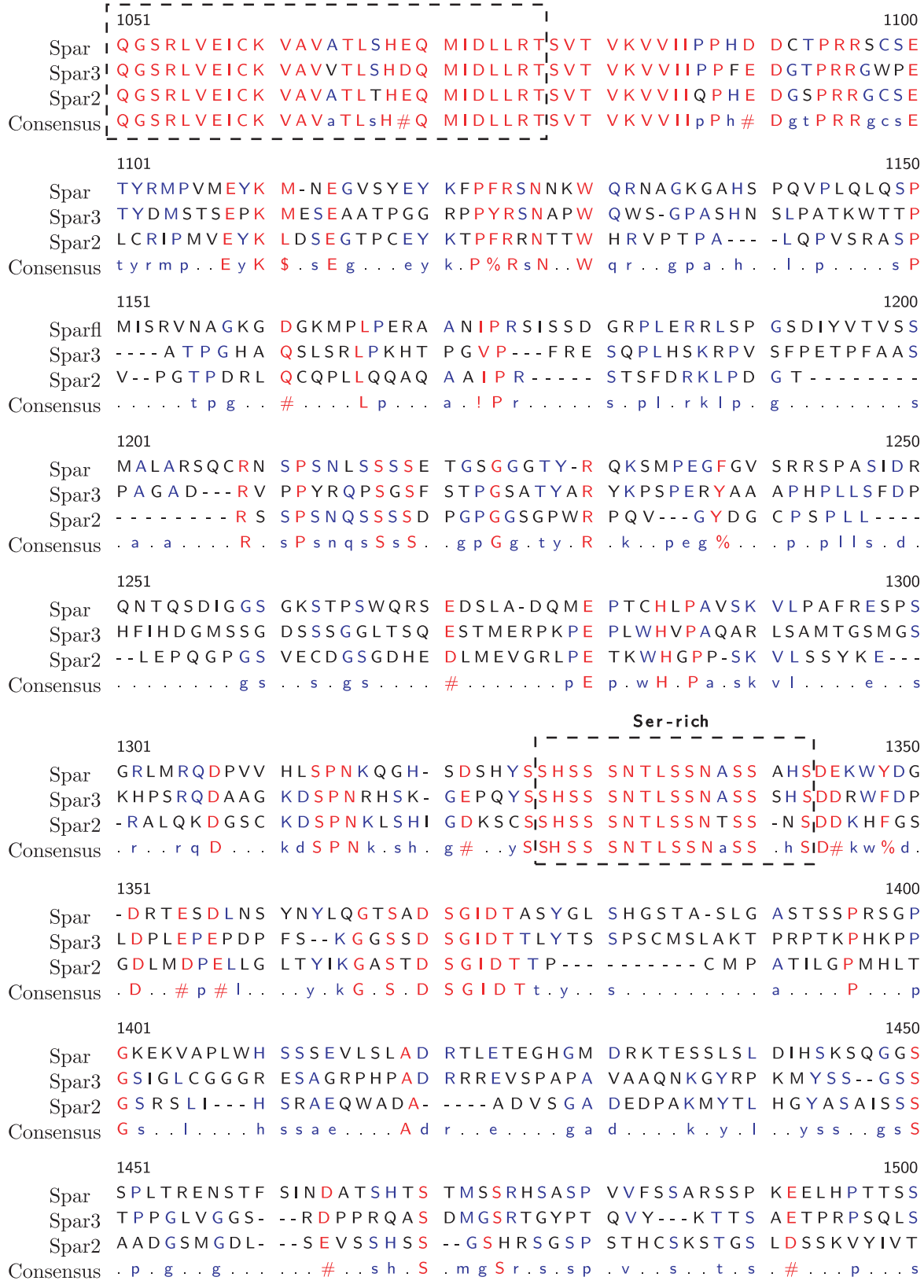
1051 1100
Spar QGSRLVEICK VAVATLSHEQ MIDLLRTSVT VKVVIIPPHD DCTPRRSCSE
Spar3 QGSRLVEICK VAVVTLSHDQ MIDLLRTSVT VKVVIIPPFE DGTPRRGWPE
Spar2 QGSRLVEICK VAVATLTHEQ MIDLLRTSVT VKVVIIQPHE DGSPRRGCSE
Consensus QGSRLVEICK VAVaTLsH#Q MIDLLRTSVT VKVVIIpPh# DgtPRRgcsE
1101 1150
Spar TYRMPVMEYK M-NEGVSYEY KFPFRSNNKW QRNAGKGAHS PQVPLQLQSP
Spar3 TYDMSTSEPK MESEAATPGG RPPYRSNAPW QWS-GPASHN SLPATKWTTP
Spar2 LCRIPMVEYK LDSEGTPCEY KTPFRRNTTW HRVPTPA--- -LQPVSRASP
Consensus tyrmp..EyK $.sEg...ey k.P%RsN..W qr..gpa.h. .l.p....sP
1151 1200
Sparfl MISRVNAGKG DGKMPLPERA ANIPRSISSD GRPLERRLSP GSDIYVTVSS
Spar3 ----ATPGHA QSLSRLPKHT PGVP---FRE SQPLHSKRPV SFPETPFAAS
Spar2 V--PGTPDRL QCQPLLQQAQ AAIPR----- STSFDRKLPD GT--------
Consensus .....tpg.. #....Lp... a.!Pr..... s.pl.rklp. g.......s
1201 1250
Spar MALARSQCRN SPSNLSSSSE TGSGGGTY-R QKSMPEGFGV SRRSPASIDR
Spar3 PAGAD---RV PPYRQPSGSF STPGSATYAR YKPSPERYAA APHPLLSFDP
Spar2 --------RS SPSNQSSSSD PGPGGSGPWR PQV---GYDG CPSPLL----
Consensus .a....R.sPsnqsSsS. .gpGg.ty.R .k..peg%.. .p.pll s.d.
1251 1300
Spar QNTQSDIGGS GKSTPSWQRS EDSLA-DQME PTCHLPAVSK VLPAFRESPS
Spar3 HFIHDGMSSG DSSSGGLTSQ ESTMERPKPE PLWHVPAQAR LSAMTGSMGS
Spar2 --LEPQGPGS VECDGSGDHE DLMEVGRLPE TKWHGPP-SK VLSSYKE---
Consensus ....gs ..s.gs.... #.......pE p.wH.Pa.sk vl....e..s
Ser-rich
1301 1350
Spar GRLMRQDPVV HLSPNKQGH- SDSHYSSHSS SNTLSSNASS AHSDEKWYDG
Spar3 KHPSRQDAAG KDSPNRHSK- GEPQYSSHSS SNTLSSNASS SHSDDRWFDP
Spar2 -RALQKDGSC KDSPNKLSHI GDKSCSSHSS SNTLSSNTSS -NSDDKHFGS
Consensus .r..rqD... kdSPNk.sh. g#..ySSHSS SNTLSSNaSS .hSD#kw%d.
1351 1400
Spar -DRTESDLNS YNYLQGTSAD SGIDTASYGL SHGSTA-SLG ASTSSPRSGP
Spar3 LDPLEPEPDP FS--KGGSSD SGIDTTLYTS SPSCMSLAKT PRPTKPHKPP
Spar2 GDLMDPELLG LTYIKGASTD SGIDTTP--- -------CMP ATILGPMHLT
Consensus .D..#p#l.. ..y.kG.S.D SGIDTt.y.. s.........a....P...p
1401 1450
Spar GKEKVAPLWH SSSEVLSLAD RTLETEGHGM DRKTESSLSL DIHSKSQGGS
Spar3 GSIGLCGGGR ESAGRPHPAD RRREVSPAPA VAAQNKGYRP KMYSS--GSS
Spar2 GSRSLI---H SRAEQWADA- ----ADVSGA DEDPAKMYTL HGYASAISSS
Consensus Gs..l....h ssae....Ad r..e....ga d....k.y.l ..yss..gsS
1451 1500
Spar SPLTRENSTF SINDATSHTS TMSSRHSASP VVFSSARSSP KEELHPTTSS
Spar3 TPPGLVGGS- --RDPPRQAS DMGSRTGYPT QVY---KTTS AETPRPSQLS
Spar2 AADGSMGDL- --SEVSSHSS --GSHRSGSP STHCSKSTGS LDSSKVYIVT
Consensus .p.g..g.....#..sh.S .mgSr.s.sp .v..s..t.s .#...p...s

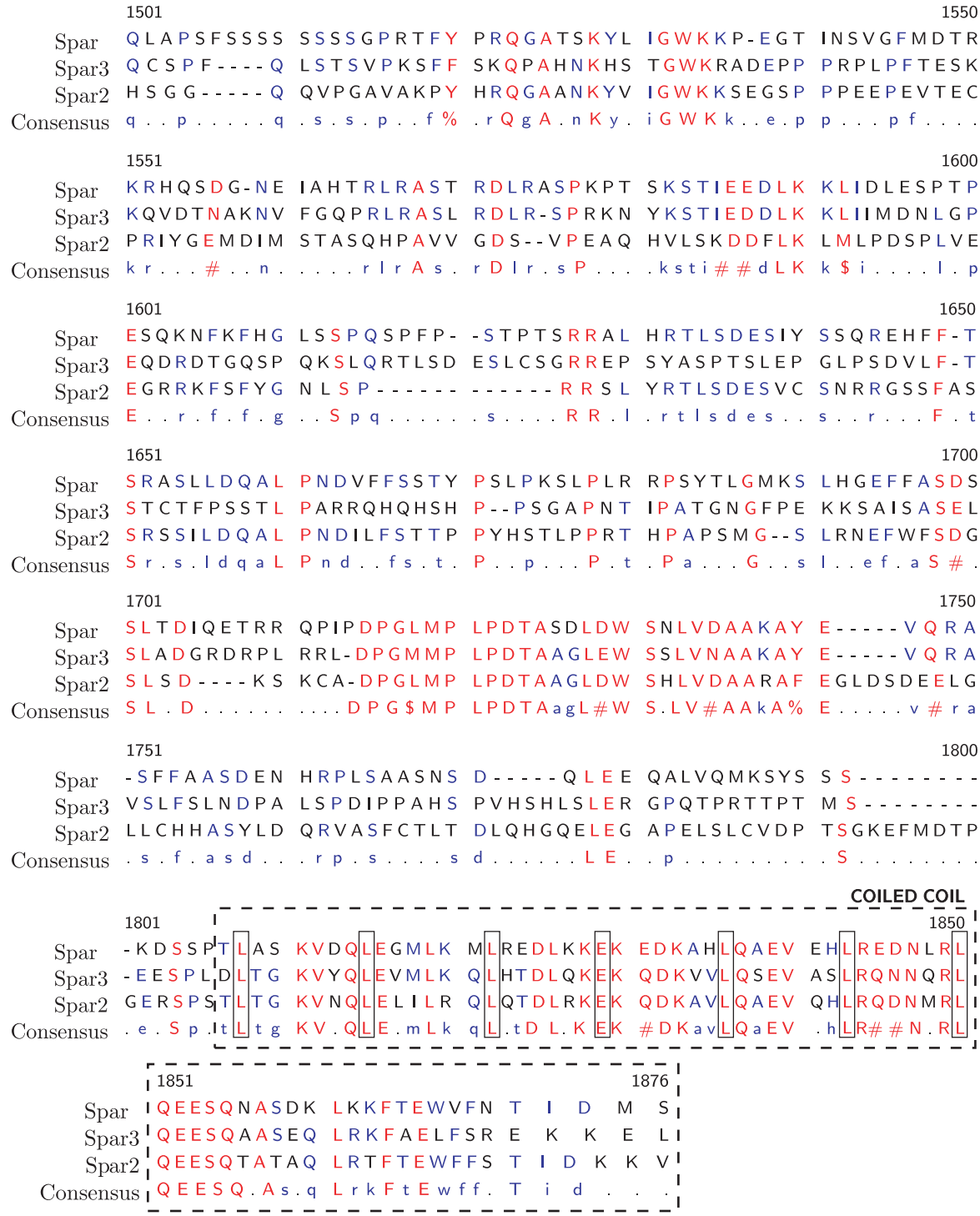
1501 1550
Spar QLAPSFSSSS SSSSGPRTFY PRQGATSKYL IGWKKP-EGT INSVGFMDTR
Spar3 QCSPF----Q LSTSVPKSFF SKQPAHNKHS TGWKRADEPP PRPLPFTESK
Spar2 HSGG-----Q QVPGAVAKPY HRQGAANKYV IGWKKSEGSP PPEEPEVTEC
Consensus q..p.....q .s.s.p..f% .rQgA.nKy. iGWKk..e.p p...pf....
1551 1600
Spar KRHQSDG-NE IAHTRLRAST RDLRASPKPT SKSTIEEDLK KLIDLESPTP
Spar3 KQVDTNAKNV FGQPRLRASL RDLR-SPRKN YKSTIEDDLK KLIIMDNLGP
Spar2 PRIYGEMDIM STASQHPAVV GDS--VPEAQ HVLSKDDFLK LMLPDSPLVE
Consensus kr...#..n.....rlrAs.rDlr.sP....ksti##dLK k$i....l.p
1601 1650
Spar ESQKNFKFHG LSSPQSPFP- -STPTSRRAL HRTLSDESIY SSQREHFF-T
Spar3 EQDRDTGQSP QKSLQRTLSD ESLCSGRREP SYASPTSLEP GLPSDVLF-T
Spar2 EGRRKFSFYG NLSP------ ------RRSL YRTLSDESVC SNRRGSSFAS
Consensus E..r.f.f.g..Spq.....s....RR.l.rtlsdes..s..r...F.t
1651 1700
Spar SRASLLDQAL PNDVFFSSTY PSLPKSLPLR RPSYTLGMKS LHGEFFASDS
Spar3 STCTFPSSTL PARRQHQHSH P--PSGAPNT IPATGNGFPE KKSAISASEL
Spar2 SRSSILDQAL PNDILFSTTP PYHSTLPPRT HPAPSMG--S LRNEFWFSDG
Consensus Sr.s.ldqaL Pnd..fs.t. P..p...P.t.Pa...G..sl..ef.aS#.
1701 1750
Spar SLTDIQETRR QPIPDPGLMP LPDTASDLDW SNLVDAAKAY E-----VQRA
Spar3 SLADGRDRPL RRL-DPGMMP LPDTAAGLEW SSLVNAAKAY E-----VQRA
Spar2 SLSD----KS KCA-DPGLMP LPDTAAGLDW SHLVDAARAF EGLDSDEELG
Consensus SL.D..... ....DPG$MP LPDTAagL#W S.LV#AAkA% E.....v#ra
1751 1800
Spar -SFFAASDEN HRPLSAASNS D-----QLEE QALVQMKSYS S---------
Spar3 VSLFSLNDPA LSPDIPPAHS PVHSHLSLER GPQTPRTTPT MS--------
Spar2 LLCHHASYLD QRVASFCTLT DLQHGQELEG APELSLCVDP TSGKEFMDTP
Consensus .s.f.asd..rp.s....sd.....LE..p.........S........
COILED COIL
1801 1850
Spar -KDSSPTLAS KVDQLEGMLK MLREDLKKEK EDKAHLQAEV EHLREDNLRL
Spar3 -EESPLDLTG KVYQLEVMLK QLHTDLQKEK QDKVVLQSEV ASLRQNNQRL
Spar2 GERSPSTLTG KVNQLELILR QLQTDLRKEK QDKAVLQAEV QHLRQDNMRL
Consensus .e.Sp.ItLtg KV.QLE.mLk qL.tDL.KEK #DKavLQaEV .hLR##N.RL
1851 1876
Spar QEESQNASDK LKKFTEWVFN T I D M S
Spar3 QEESQAASEQ LRKFAELFSR E K K E L
Spar2 QEESQTATAQ LRTFTEWFFS T I D K K V
Consensus QEESQ.As.q LrkFtEwff. T i d . . .

Bibliography

B. Alberts, A. Johnson, J. Lewis, M. Raff, K. Roberts, and P. Walter. Molecular Biology of the Cell, Garland Science. *New York*, 1463, 1991.

J. Arikkath and L. F. Reichardt. Cadherins and catenins at synapses: roles in synaptogenesis and synaptic plasticity. *Trends Neurosci*, 2008, *in press*.

A.A. Asuni, C. Hooper, C.H. Reynolds, Lovestone S., B.H. Anderton, and R. Killick. GSK3α exhibits β–catenin and tau directed kinase activities that are modulated by Wnt. *Eur J Neurosci*, 24:3387–3392, 2006.

M. K. Baron, T. M. Boeckers, B. Vaida, S. Faham, M. Gingery, M. R. Sawaya, D. Salyer, E. D. Gundelfinger, and J. U. Bowie. An architectural framework that may lie at the core of the postsynaptic density. *Science*, 311:531–535, 2006.

H. C. Birnbaum and J. Doly. A rapid alkaline extraction procedure for screening recombinant plasmid DNA. *Nucleic Acids Res*, 7:1513–1523, 1979.

T. M. Boeckers, J. Bockmann, M. R. Kreutz, and E. D. Gundelfinger. ProSAP/Shank proteins - a family of higher order organizing molecules of the postsynaptic density with an emerging role in human neurological disease. *J Neurochem*, 81:903–910, 2002.

T.M. Boeckers. The postsynaptic density. *Cell Tissue Res*, 326:409–422, 2006.

T.M. Boeckers, T. Liedke, C. Spilker, T. Dresbach, J. Bockmann, M.R. Kreutz, and E.D. Gundelfinger. C–terminal synaptic targeting elements for postsynaptic density proteins ProSAP1/Shank2 and ProSAP2/Shank3. *J Neurochem*, 92:512–524, 2005.

J. L. Bos. All in the family? New insights and questions regarding interconnectivity of Ras, Rap1 and Ral. *EMBO J*, 17:6776–6782, 1998.

W.O. Bullock, J.M. Fernandez, and J.M. Short. XL 1-Blue: A high efficiency plasmid transforming recA *Escherichia coli* strain with beta-galactosidase selection. *Biotechniques*, 5:376–379, 1987.

B. C. Roy, K. Kohu, K. Matsuura, H. Yanai, and T. Akiyama. SPAL, a Rap-specific GTPase activating protein, is present in the NMDA receptor-PSD-95 complex in the hippocampus. *Genes to Cells*, 7:607–617, 2002.

Y. Cabeza-Arveliaz, T.C. Thompson, J.L. Sepulveda, and A.C. Chinault. LAPSER 1: a novel candidate tumor suppressor gene from 10 q 24. 3. *Oncogene*, 20:6707–6717, 2001.

B. Calabrese, M.S. Wilson, and S. Halpain. Development and regulation of dendritic spine synapses. *Physiology*, 21:38–47, 2006.

C.M. Carlin, L.J. Kepley, and A.J. Bard. Polymer Films on Electrodes. *J Electrochem Soc*, 132:353, 1985.

Y. Chen, P.Y. Wang, and A. Ghosh. Regulation of cortical dendrite development by Rap1 signaling. *Mol Cell Neurosci*, 28:215–228, 2005.

H.H. Cho, H.J. Joo, J.S. Song, Y.C. Bae, and J.S. Jung. Crossregulation of $\beta-$catenin/Tcf pathway by nf-κb is mediated by LZTS2 in human adipose tissue-derived mesenchymal stem cells. *Biochim Biophys Acta*, 1783:419–428, 2008.

G.L. Collingridge, J.T.R. Isaac, and Y.T. Wang. Receptor trafficking and synaptic plasticity. *Nat Rev Neurosci*, 5:952–962, 2004.

C.W. Cotman and D. Taylor. Isolation and structural studies on synaptic complexes from rat brain. *J Cell Biol*, 55:696–711, 1972.

M. Dateki, T. Horii, Y. Kasuya, R. Mochizuki, Y. Nagao, J. Ishida, F. Sugiyama, K. Tanimoto, K. Yagami, H. Imai, and A. Fukamizo. Neurochondrin negatively regulates CaMKII phosphorylation, and nervous system–specific gene disruption results in epileptic seizure. *J Biol Chem*, 280:20503–20508, 2005.

K.M.T. de Bruyn, S. Rangarajan, K.A. Reedquist, C.G. Figdor, and J.L. Bos. The small GTPase Rap1 is required for Mn2+-and antibody-induced LFA-1-and VLA-4-mediated cell adhesion. *J Biol Chem*, 277:29468–29476, 2002.

RU de Iongh, E. Wederell, FJ Lovicu, and JW McAvoy. Transforming growth factor-β-induced epithelial-mesenchymal transition in the lens: A model for cataract formation. *Cells Tissues Organs*, 179:43–55, 2005.

O. El Far and H. Betz. Synaptophysins: vesicular cation channels? *J Physiol*, 539:332, 2002.

J.A. Esteban. AMPA receptor trafficking: a road for synaptic plastisity. *Molecular Interventions*, 3:376–385, 2003.

I.M. Ethell and E.B. Pasquale. Molecular mechanisms of dendritic spine development and remodelling. *Progress in Neurobiology*, 75:161–205, 2005.

A. Farina, M. Hattori, J. Qin, Y. Nakatani, N. Minato, and K. Ozato. Bromodomain protein Brd4 binds to GTPase-activating SPA-1, modulating its activity and subcellular localization. *Mol Cell Biol*, 24:9059, 2004.

S. Fields and O. Song. A novel genetic system to detect protein–protein interactions. *Nature*, 340:245–246, 1989.

Z. Fu, S.H. Lee, A. Simonetta, J. Hansen, M. Sheng, and D.T.S. Pak. Differential roles of Rap1 and Rap2 small GTPases in neurite retraction and synapse elimination in hippocampal spiny neurons. *J Neurochem*, 100:118, 2007.

Q. Gao, S. Srinivasan, S.N. Boyer, D.E. Wazer, and V. Band. The E6 oncoproteins of high–risk pappillomaviruses bind to a novel putative GAP protein, E6TP1, and target it for degradation. *Mol Cell Biol*, 19:733–744, 1999.

J.J. Garrido, D. Simón, O. Varea, and F. Wandosell. GSK3 alpha and GSK3 beta are necessary for axon formation. *FEBS Letters*, 581:1579–1586, 2007.

K. Gerrow and A. El-Husseini. Cell adhesion molecules at the synapse. *Front Biosci*, 11:2400–2419, 2006.

Y. Gluzman. SV40-transformed simian cells support the replication of early SV40 mutants. *Cell*, 23:175–82, 1981.

E.E. Govek, S.E. Newey, and L. Van Aelst. The role of the Rho GTPases in neuronal development. *Genes & Dev*, 19:1, 2005.

E.D. Gundelfinger and S. tom Dieck. Molecular organization of excitatory chemical synapses in the mammalian brain. *Naturwissenschaften*, 87:513–523, 2000.

E.D. Gundelfinger, T.M. Boeckers, M.K. Baron, and J.U. Bowie. A role for zinc in postsynaptic density asSAMbly and plasticity? *Trends Biochem Sci*, 31:366–373, 2006.

L.A. Haddad, N. Smith, M. Bowser, Y. Niida, V. Murthy, C. Gonzalez-Agosti, and V. Ramesh. The TSC1 tumor suppressor hamartin interacts with Neurofilament-L and possibly functions as a novel integrator of the neuronal cytoskeleton. *J Biol Chem*, 277:44180–44186, 2002.

M. Harazaki, Y. Kawai, L. Su, Y. Hamazaki, T. Nakahata, N. Minato, and M. Hattori. Specific recruitment of SPA-1 to the immunological synapse: involvement of actin-bundling protein actinin. *Immunol Lett*, 92:221–226, 2004.

J.W. Harper, G.R. Adami, N. Wei, K. Keyomarsi, and S.J. Elledge. The p 21 Cdk-interacting protein Cip 1 is a potent inhibitor of G 1 cyclin-dependent kinases. *Cell*, 75:805–816, 1993.

M. Hattori, N. Tsukamoto, M. Nur-e Kamal, B. Rubinfeld, K. Iwai, H. Kubota, H. Marute, and N. Minato. Molecular cloning of a novel mitogen-inducible protein with a Ran–GTPase–activating domain that affects cell cycle progression. *Mol Cell Biol*, 15:552–560, 1995.

H. Hering and M. Sheng. Dendritic spines: structure, dynamics and regulation. *Nat Neurosci*, 2:880–888, 2001.

G.G. Hicks, E-G. Shi, X-M. Li, C.-H. Li, Pawlak M., and Ruley E.H. Functional genomics in mice by tagged sequence mutagenesis. *Nat Genet*, 16:338–344, 1997.

N. Honkura, M. Matsuzaki, J. Noguchi, G.C.R. Ellis-Davies, and H. Kasai. The subspine organization of actin fibers regulates the structure and plasticity of dendritic spines. *Neuron*, 57:719–729, 2008.

A. Y. Hung, K. Futai, C. Sala, J. G. Valtschanoff, J. Ryu, M. A. Woodworth, F. L. Kidd, C. C. Sung, T. Miyakawa, M. F. Bear, R .J. Weinberg, and M. Sheng. Smaller dendritic spines, weaker synaptic transmission, but enhanced spatial learning in mice lacking Shank1. *J Neurosci*, 28:1697–1708, 2008.

I.J. Jackson. Mouse mutagenesis on target. *Nat Genet*, 28:198–200, 2001.

P. James, J. Halladay, and E.A. Craig. Genomic libraries and a host strain designed for highly efficient two-hybrid selection in yeast. *Genetics*, 144:1425–1436, 1996.

J. Jozwiak and P. Wlodarski. Hamartin and tuberin modulate gene transcription via β-catenin. *J Neurooncol*, 79:229–234, 2006.

H. Jung Chung, Y. Nung Jan, and L.Y. Jan. Polarized axonal surface expression of neuronal KCNQ channels is mediated by multiple signals in the KCNQ2 and KCNQ3 C–terminal domains. *Proc Natl Acad Sci USA*, 103:8870–8875, 2006.

K. Katagiri, M. Hattori, N. Minato, and T. Kinashi. Rap1 functions as a key regulator of T-cell and antigen-presenting cell interactions and modulates T-cell responses. *Mol Cell Biol*, 22:1001, 2002.

K. Kometani, D. Ishida, M. Hattori, and N. Minato. Rap1 and SPA-1 in hematologic malignancy. *Trends Mol Medicine*, 10:401–408, 2004.

D. Konno, J.-A. Ko, S. Usui, K. Hori, H. Maruoka, M. Inui, T. Fujikado, Y. Tano, T. Suzuki, K. Tohyama, and K. Sobue. The postsynaptic density and dendritic raft localization of PSD-Zip70, which contains an N-myristoylation sequence and leucine-zipper motifs. *J Cell Sci*, 115:4695–4706, 2002.

M.R.H. Kooistra, N. Dube, and J.L. Bos. Rap1: a key regulator in cell-cell junction formation. *J Cell Sci*, 120:17, 2007.

H. Kurachi, Y. Wada, N. Tsukamoto, M. Maeda, H. Kubota, M. Hattori, K. Iwai, and N. Minato. Human SPA–1 gene product selectively expressed in lymphoid tissues is a specific GTPase–activating protein for Rap1 and Rap2. *J Biol Chem*, 272: 28081–28088, 1997.

U.K. Laemmli. Cleavage of structural proteins during the assembly of the head of bacteriophage T4. *Nature*, 227:680–685, 1970.

R. Lujan, R. Shigemoto, and G. Lopez-Bendito. Glutamate and GABA receptor signalling in the developing brain. *Neuroscience*, 130:567–580, 2005.

M.A. Lynch. Long-term potentiation and memory. *Physiol Rev*, 84:87–136, 2004.

D.J. Mackay and A. Hall. Rho GTPases. *J Biol Chem*, 273:20685–20688, 1998.

R. Malenka and M. Bear. LTP and LTD: An embarrasment of riches. *Neuron*, 44:5–21, 2004.

B.D. Manning, A.R. Tee, M.N. Logsdon, J. Blenis, and L.C. Cantley. Identification of the Tuberous Sclerosis Complex-2 Tumor Suppressor Gene Product Tuberin as a Target of the Phosphoinositide 3-Kinase/Akt Pathway. *Molecular Cell*, 10:151–162, 2002.

H. Maruoka, D. Konno, K. Hori, and K. Sobue. Collaboration of PSD–Zip70 with its binding partner, SPAR, in dendritic spine maturity. *J Neurosci*, 25:1421–1430, 2005.

G. Meyer, F. Varoqueaux, A. Neeb, M. Oschlies, and N. Brose. The complexity of PDZ domain–mediated interactions at glutamatergic synapses: a case study on neuroligin. *Neuropharmacology*, 47:724–733, 2004.

M. Migaud, P. Charlesworth, M. Dempster, L.C. Webster, A.M. Watabe, M. Makhinson, Y. He, M.F. Ramsay, R.G.M. Morris, and J.H. Morrison. Enhanced long-term potentiation and impaired learning in mice with mutant postsynaptic density-95 protein. *Nature*, 396:433–439, 1998.

A. Morozov, I.A. Muzzio, R. Bourtchouladze, N. Van-Strien, K. Lapidus, D.Q. Yin, D.G. Winder, J.P. Adams, J.D. Sweatt, and E.R. Kandel. Rap1 couples cAMP signaling to a distinct pool of p42/44MAPK regulating excitability, synaptic plasticity, learning, and memory. *Neuron*, 39:309–325, 2003.

S.J. Moss and T.G. Smart. Constructing inhibitory synapses. *Nat Rev Neurosci*, 2: 240–250, 2001.

D. J. Mulholland, S. Dedhar, G. A. Coetzee, and C. C. Nelson. Interaction of nuclear receptors with the Wnt/β-catenin/Tcf signaling axis: Wnt you like to know? *Endocrine Rev*, 26:898–915, 2005.

Y. Noda and S. Sasaki. Trafficking mechanism of water channel aquaporin-2. *Biol Cell*, 97:885–92, 2005.

Y. Noda, S. Horikawa, T. Furukawa, K. Hirai, Y. Katayama, T. Asai, M. Kuwahara, K. Katagiri, T. Kinashi, M. Hattori, N. Minato, and S. Sasaki. Aquaporin-2 trafficking is regulated by PDZ-domain containing protein SPA–1. *FEBS Letters*, 568: 139–145, 2004.

S. Okabe. Molecular anatomy of the postsynaptic density. *Mol Cell Neurosci*, 34: 503–518, 2007.

D. Pak, 2007. personal communication.

D. Pak, S. Yang, S. Rudolph-Correia, E. Kim, and M. Sheng. Regulation of spine morphology by Spar, a PSD–95–associated RapGAP 2. *Neuron*, 31:169–171, 2001.

D.T.S. Pak and M. Sheng. Targeted protein degradation and synapse remodeling by an inducible protein kinase. *Science*, 302:1368, 2003.

V. Pena, M. Hothorn, A. Eberth, N. Kaschau, A. Parret, L. Gremer, F. Bonneau, M. R. Ahmadian, and K. Scheffzek. The C2 domain of SynGAP is essential for stimulation of the Rap GTPase reaction. *EMBO Rep*, 9:350–355, 2008.

CJ Phiel, CA Wilson, VMY Lee, and PS Klein. GSK-3α regulates production of Alzheimer's disease amyloid-beta peptides. *Nature*, 423:435–439, 2003.

M. Richter, K.K. Murai, C. Bourgin, D.T. Pak, and E.B. Pasquale. The EphA4 receptor regulates neuronal morphology through SPAR-mediated inactivation of Rap GTPases. *J Neurosci*, 27:14205, 2007.

J. Rosenbluh, A. Kapelnikov, D.E. Shalev, M. Rusnati, Bugatti, and A. A. Loyter. Positively charged peptides can interact with each other, as revealed by solid phase binding assays. *Anal Biochem*, 352:157–168, 2006.

G. Roussignol, F. Ango, S. Romorini, J. C. Tu, C. Sala, P. F. Worley, J. Bockaert, and L. Fagni. Shank expression is sufficient to induce functional dendritic spine synapses in aspiny neurons. *J Neurosci*, 25:3560–3570, 2005.

B.C. Roy, T. Kuroda, S. Mori, K. Kohu, T. Akiyama, and T. Senda. Localization of a novel GAP family protein SPAL in the rat esophagus and heart. *Med Electron Microsc*, 32:20–24, 1999.

J. Sambrook, EF Fritsch, and T. Maniatis. Molecular Cloning: A Laboratory Manual. *Cold Springs Harbor Laboratory, Cold Springs Harbor, NY*, 1989.

W.F. Scherer, J.T. Syverton, and G.O. Gey. Studies on the propagation *in vitro* of Poliomyelitis visuses IV. Viral multiplication in a stable strain of human malignant epithelial cells (strain HeLa) derived from an epidermoid carcinoma of the cervix. *J Exp Med*, 97:695–710, 1953.

M. Schmeisser. personal communication. 2007.

S. Schoch and E.D. Gundelfinger. Molecular organization of the presynaptic active zone. *Cell Tissue Res*, 326:379–391, 2006.

V. Schubert and C.G. Dotti. Transmitting on actin: synaptic control of dendritic architecture. *J Cell Sci*, 120:205–212, 2007.

J. Schultess, O. Danielewski, and A.P. Smolenski. Rap1GAP2 is a new GTPase-activating protein of Rap1 expressed in human platelets. *Blood*, 105:3185, 2005.

J.C. Schwamborn and A.W. Pueschel. The sequential activity of the GTPases Rap 1 B and Cdc 42 determines neuronal polarity. *Nat Neurosci*, 7:923–929, 2004.

D.P. Seeburg and M. Sheng. Activity-induced Polo-like kinase 2 is required for homeostatic plasticity of hippocampal neurons during epileptiform activity. *J Neurosci*, 28:6583, 2008.

M.J. Seidensticker and J. Behrens. Biochemical interactions in the Wnt pathway. *BBA Mol Cell Res*, 1495:168–182, 2000.

M. Sheng and C. C. Hoogenraad. The postsynaptic architecture of excitatory synapses: a more quantitative view. *Annu Rev Biochem*, 76:823–847, 2007.

M. Sheng and E. Kim. The Shank family of scaffold proteins. *J Cell Sci*, 113 (Pt 11): 1851–1856, 2000.

L. Singh, Q. Gao, A. Kumar, T. Gotoh, D.E. Wazer, H. Band, L.A. Feig, and V. Band. The high-risk human papillomavirus type 16 E6 counters the GAP function of E6TP1 toward small Rap G proteins. *J Virol*, 77:1614, 2003.

W.C. Skarnes, H. von Melchner, W. Wurst, G. Hicks, A.S. Nord, T. Cox, S.G. Young, P. Ruiz, P. Soriano, M. Tessier-Lavigne, et al. A public gene trap resource for mouse functional genomics. *Nat Genetics*, 36:543–544, 2004.

P.K. Smith, R.I. Krohn, G.T. Hermanson, A.K. Mallia, F.H. Gartner, M.D. Provenzano, E.K. Fujimoto, N.M. Goeke, B.J. Olson, and D.C. Klenk. Measurement of protein using bicinchoninic acid. *Anal Biochem*, 150:76–85, 1985.

K.E. Sorra and K.M. Harris. Overview on the structure, composition, function, development, and plasticity of hippocampal dendritic spines. *Hippocampus*, 10:501–511, 2000.

C. Spilker, G.A. Acuna Sanhueza, T.M. Boeckers, M.R. Kreutz, and E.D. Gundelfinger. Spar2, a novel SPAR-related protein with GAP activity for Rap1 and Rap2. *J Neurochem*, 104:187–201, 2008.

E.N. Star, D.J. Kwiatkowski, and V.N. Murthy. Rapid turnover of actin in dendritic spines and its regulation by activity. *Nat Neurosci*, 5:239–246, 2002.

F.W. Studier, A.H. Rosenberg, J.J. Dunn, and J.W. Dubendorff. Use of T7 RNA polymerase to direct expression of cloned genes. *Methods Enzymol*, 185:60–89, 1990.

L. Su, M. Hattori, M. Moriyama, N. Murata, M. Harazaki, K. Kaibuchi, and N. Minato. AF-6 controls integrin-mediated cell adhesion by regulating Rap1 activation through the specific recruitment of Rap1GTP and SPA-1. *J Biol Chem*, 278:15232–15238, 2003.

Y. Takai, T. Sasaki, and T. Matozaki. Small GTP–binding proteins. *Physiol Rev*, 81: 153–189, 2001.

G. Thyssen, T.H. Li, L. Lehmann, M. Zhuo, M. Sharma, and Z. Sun. LZTS2 is a novel β–catenin–interacting protein and regulates the nuclear export of β–catenin. *Mol Cell Biol*, 26:8857–8867, 2006.

IC Tsai, JD Amack, ZH Gao, V. Band, HJ Yost, and DM Virshup. A Wnt-CKIε-Rap1 pathway regulates gastrulation by modulating SIPA1L1, a Rap GTPase activating protein. *Dev Cell*, 12:335–47, 2007.

N. Tsukamoto, M. Hattori, H. Yang, J.L. Bos, and N. Minato. Rap1 GTPase-activating protein SPA-1 negatively regulates cell adhesion. *J Biol Chem*, 274:18463–18469, 1999.

S. Tsuriel, R. Geva, P. Zamorano, T. Dresbach, T.M Boeckers, E.D. Gundelfinger, C.C. Garner, and N.E. Ziv. Local sharing as a predominant of synaptic matrix molecular dynamics. *PLoS Biol*, 4:271, 2006.

O.M. Tsygankova, E. Feshchenko, P.S. Klein, and J.L. Meinkoth. Thyroid-stimulating Hormone/cAMP and Glycogen Synthase Kinase 3 β Elicit Opposing Effects on Rap1GAP Stability. *J Biol Chem*, 279:5501, 2004.

W.J. Tyler and L. Pozzo-Miller. Miniature synaptic transmission and BDNF modulate dendritic spine growth and form in rat CA1 neurones. *J Physiol*, 553:497–509, 2003.

L. E. Vazquez, H. J. Chen, I. Sokolova, I. Knuesel, and M. B. Kennedy. SynGAP regulates spine formation. *J Neurosci*, 24:8862–8872, 2004.

A. Vecchione, H. Ishii, G. Baltasarre, P. Bassi, F. Trapasso, H. Alder, F. Pagano, L.G. Gomella, C.M. Croce, and R. Baffa. FEZ1/LZTS1 is down-regulated in high-grade bladder cancer, and its restoration suppresses tumorigenicity in transitional cell carcinoma cells. *Am J Pathol*, 160:1345–1352, 2002.

C. Verderio, S. Coco, E. Pravettoni, A. Bacci, and Matteoli. Synaptogenesis in hippocampal cultures. *Cell Mol Life Sci*, 55:1448–1462, 1999.

D. Wendholt. *ProSAPiP1, ein neues Protein der Postsynaptischen Dichte (PSD)*. PhD thesis, Muenster, 2006.

D. Wendholt, C. Spilker, A. Schmitt, A. Dolnik, K-H. Smalla, Proepper, J. C., Bockmann, K. Sobue, E.D. Gundelfinger, M.R. Kreutz, and T.M. Boeckers. ProSAP-interacting Protein 1 (ProSAPiP1), a novel protein of the postsynaptic density that links the Spine-associated Rap-Gap (SPAR) to the scaffolding protein ProSAP2/Shank3. *J Biol Chem*, 281:13805–13816, 2006.

Z. Xie, R.L. Huganir, and P. Penzes. Activity-dependent dendritic spine structural plasticity is regulated by small GTPase Rap1 and its target AF-6. *Neuron*, 48: 605–618, 2005.

R. Yuste and T. Bonhoeffer. Genesis on dendritic spines: insights from ultrustructural and imaging studies. *Nat Neurosci*, 5:24–34, 2004.

G.R. Zhai and H.J. Bellen. The architecture of the active zone in the presynaptic nerve terminal. *Physiology*, 19:262–270, 2004.

Y. Zhang, X. Gao, L.J. Saucedo, B. Ru, B.A. Edgar, and D. Pan. Rheb is a direct target of the tuberous sclerosis tumour suppressor proteins. *Nat Cell Biol*, 5:578–581, 2003.

J.J. Zhu, Y. Qin, M. Zhao, L. Van Aelst, and R. Malinow. Ras and Rap Control AMPA Receptor Trafficking during Synaptic Plasticity. *Cell*, 110:443–455, 2002.

Y. Zhu, D. Pak, Y. Qin, S.G. McCormack, M.J. Kim, J.P. Baumgart, V. Velamoor, Y.P. Auberson, P. Osten, and L. van Aelst. Rap2-JNK removes synaptic AMPA receptors during depotentiation. *Neuron*, 46:905–916, 2005.

N.E. Ziv and C.C. Garner. Cellular and molecular mechanisms of presynaptic assembly. *Nat Rev Neurosci*, 5:385–99, 2004.

Ackowledgements

This study has been performed in the Institute of Anatomy and Cell Biology, at the University of Ulm. I would like to sincerely thank Prof. Dr. T. M. Boeckers for providing facilities for this research, for giving me a freedom to work independently and guidance during those years. I also deeply appreciate the given possibility to experience the Neuroscience conferences.

I am especially grateful to PD Dr. J. Bockman for supervision, introduction in the biochemical methods and great help in work with knock–out animals. I deeply appreciate support in troubleshooting, especially in the first year of my work.

I am very grateful to Dr. C. Proepper for interest in my project, for fruitful discussions, for providing me new ideas for my research and for help in troubleshooting.

I would like to thank Renate Zienecker for performing *in situ* hybridizations, for sharing experiences in fixations and providing protocols for immunohistochemistry.

I cordially thank Dr. B. Vaida for providing the protocols for EM and for the patience by helping me to adapt to local electron microscopes. It was really a great help. We also have been a great "prep–team".

I thank Janine Dahl for fractionation experiments, which were started at her initiative. It was really a fun to perform the PSD preparations together.

I would like to thank Dr. D. Wendholt for providing ProSAPiP1 constructs and AB. I deeply appreciate also the support in the lab, which Doreen provided me especially during the first monthes of my work. I thank Dr. A. Schmitt for providing a LAPSER1–RFP construct and sharing an expertise in AB purification at any time of the day. I thank Michael Schmeisser for providing of LAPSER1–specific AB for my experiments. I thank Dr. S. Liebau for sharing his expert knowledge in the cell culture. I thank Dr. K. Langer and Dr. S. Liebau for help by live imaging experiments.

I wish to thank Andreas Grabrucker, Michael Schmeisser, Janine Dahl for help in preparations, for cooperation and great time we spent together in the lab.

I deeply appreciate sharing of experiences and support of Nicola Martin in the cell cultures and great help in correcting of this manuscript. My very special thank is to

Natalie Damm for sharing the experiences in molecular biology, great help and constant support over those years.

I am grateful to Ursula Pika–Hartlaub for the support, especially by the start of my work and readiness to help. I would like to thank Maya Manz for support and help, especially by ordering. I also would like to thank all collegues and all PhD students in the department.

I cordially thank Prof. Dr. Olga Podgornaya from Sankt–Petersburg, who directed me on the way of science. Very deeply and sincerely I thank Eric Sträng for a great help in correction, formating of manuscript and for constant support over those years. I am very grateful to my parents, Dina and Veniamin Dolnik, to whom I dedicate this work.